Promoting Central Nervous System Regeneration by Targeting Intracellular Pathways

Veselina Petrova

Hughes Hall

2nd April 2019

This dissertation is submitted for the degree of Doctor of Philosophy.

DECLARATION

1. Declaration

This dissertation is the result of my own work carried out under the supervision of Prof. James Fawcett and Dr Richard Eva at the Cambridge Centre for Brain Repair, University of Cambridge.

This thesis has not been submitted in whole or in part for any degree, diploma or qualification at any other university and includes nothing which is the outcome of work done in collaboration except the following:

1. Optic nerve crush model in *Chapter 4* – optic nerve crush experiments were carried out at the National Institutes of Health, Bethesda, UK by Craig Pearson and Andrea Soleano in Prof. Herbert Geller's laboratory

2. Rat glaucoma model in *Chapter 4* were carried out in collaboration with Dr Tasneem Khatib in Prof. Keith Martin's laboratory at the John van Geest Centre for Brain Repair, University of Cambridge

3. Blind quantification analysis of Brn3a-positive staining in the retina after glaucoma induction in *Chapter 4* were carried out by Yusuf Mushtaq.

4. Rab7 staining and quantification experiments in *Chapter 5* were carried out by Dr Jared Ching.

2. Word Count

This dissertation of a total word count of 56 483 does not exceed the limit of 60 000 words set by the Degree Committee for the Faculties of Clinical Medicine and Veterinary Medicine.

3. Funding

PhD funding for this work has been provided by the Gates Cambridge Trust.

Research funding was received by the Christopher Reeve Foundation and the Medical Research Council.

ACKNOWLEDGEMENTS

I would like to first and foremost thank Prof. James Fawcett for his enthusiasm and continued support during my PhD. He helped me get exposure to some of the most current research and encouraged me to network with numerous other researchers in the field which benefited my project enormously. Also a huge thanks to other members of our laboratory: to Dr Richard Eva who advised my work on live cell imaging and axotomy as well as for his support throughout my degree; to Bart Nieuwenhuis who advised me on my molecular cloning work and provided me with unconditional support at all times and who proved to be the best conference buddy one can ask for; to Dr Barbara Haenzi for her help with mutagenesis and cloning and for her contribution to making sure that I become a good and thorough scientist; to Dr Hiroaki Koseki who gave me guidance on the technique of culturing primary cortical neurons, shared his unpublished RNA sequencing data with me and helped me settle into the lab; and to Dr Elise Laperrousaz for her advice and guidance as well as for testing my hypothesis after spinal cord injury.

I would like to thank Dr Evan Reid for providing me with the initial protrudin DNA constructs and for sharing his expertise with me throughout my PhD. I would like to also thank Dr Craig Person, Dr Andrea Soleano and Prof. Herb Gellar for helping create the protrudin viruses and for performing the optic nerve crush experiments at the National Institute of Health, Bethesda, US. Special thanks to Tasneem Khatib and Prof. Keith Martin for encouraging me to put my ideas into practice and helping me design and execute the chronic glaucoma experiment in rats.

I would also like to thank all staff and students at the John van Geest Repair Centre who made my time in Cambridge one of the most memorable in my life. I would also like to thank my boyfriend, Stuart Few for being the most patient and encouraging during this difficult process. Last but not least, I would like to thank my family for always being there for me – in particular, I would not have been able to do this without unstoppable support, motivation and unconditional love from my mother – Natalia, my sister – Plamena and my grandparents. This thesis is dedicated to you all!

Summary

Adult central nervous system neurons regenerate poorly after injury. One reason for this regenerative failure is that a developmental change occurs where essential growth-molecules become excluded from axons with maturation. In this thesis, two strategies were employed in order to improve axon regeneration: 1) restoring the axonal transport of growth-molecules in mature axons via manipulation of transport machinery; 2) reverting mature neurons to an earlier developmental state where growth-molecules are abundant in the axon.

In order to restore axon transport of growth-molecules, protrudin - a membrane-associated protein involved in directional membrane trafficking, was studied. Phosphorylated protrudin preferentially binds Rab11, a small GTPase involved in axon transport of growth receptors. This association is required for neurite outgrowth and for anterograde movement of this complex. We found that endogenous protrudin is excluded from mature axons similar to other growth-related machinery and cargo. It was hypothesised that introducing a phosphomimetic form of protrudin to mature cortical neurons, could increase the phospho-protrudin/Rab11 interaction resulting in improved anterograde transport of growth-molecules and enhanced axon regeneration. We found that overexpression of two constitutively phosphorylated forms and also wild-type protrudin increased the proportion of regenerating axons after *in vitro* laser axotomy. Furthermore, overexpression of wild-type and phospho-protrudin in the retina resulted in enhanced axon regeneration in a mouse model of optic nerve crush 2 weeks after injury. Live-cell imaging experiments revealed that this increased regenerative ability is accompanied with increased transport of Rab11 endosomes as well as growth receptors into the axon. Importantly, by further studying protrudin's mechanisms of action, we identified novel players in the process of axon regeneration, including an exciting new role for the endoplasmic reticulum. In summary, protrudin is a promising intervention which improves axon regeneration *in vitro* and *in vivo* and due to its participation in multiple molecular pathways, new targets for aiding and understanding axon regeneration could be uncovered.

Another approach to aid axon regeneration is to rejuvenate mature neurons. We hypothesised that overexpressing different combinations of transcription factors that are developmentally down-regulated could bring neurons to an earlier developmental stage. Four maturity markers were identified – doublecortin as an early maturity marker and 68-kDa neurofilament, calcitonin, tubulin-4a as late maturity markers. Some transcription factors showed promising results in rejuvenating primary cortical neurons. Further studies are needed to identify correct combinations of transcription factors to achieve maximum effect and to examine the effects of this treatment on axon regeneration.

CONTENTS

ABBREVIATIONS

CNS – central nervous system

PNS – peripheral nervous system

chABC – chondroitinase ABC

ARSB – arylsulfatase B

CST – corticospinal tract

IOP – intraocular pressure

HSP – hereditary spastic paraplegia

ALS – amyotrophic lateral sclerosis

SCI – spinal cord injury

CSPG – chondroitin sulfate proteoglycan

GAG – glycosaminoglycan

MAG – myelin-associated glycoprotein

OMgp – oligodendrocyte myelin glycoprotein

NGF – nerve growth factor

PTEN – phosphatase and tenasin homolog

mTOR – mammalian target of rapamycin

SOCS3 – suppressor of cytokine signalling 3

RGC – retinal ganglion cell

PI3K – phosphoinositide 3-kinase

DRG – dorsal root ganglion

RhoA – Ras homologue gene family, member A

DIV – days in vitro

dpi – days post injury

HSP – hereditary spastic paraplegia

AIS – axon initial segment

GTP – guanosine triphosphate

GDP – guanosine diphosphate

MAPK – mitogen-activated protein kinase

AAV – adeno-associated virus

VAP-A – VAMP-associated protein A

VAP-B – VAMP-associated protein B

Surf4 – Surfeit 4

RTN3 – Reticulon 3

GEF – guanine nucleotide exchange factor

GAP – GTPase-activating protein

Rab – Ras-related in brain

ARF – ADP ribosylation factor

TrkB – tropomyosin receptor kinase B

BDNF – brain-derived neurotrophic factor

IGF – insulin growth factor

IGFR1 – insulin growth factor receptor 1

GFP – green fluorescent protein

RFP – red fluorescent protein

ATF3 – activating transcription factor-3

CGRP – calcitonin-gene related protein

NPY – neuropeptide Y

CA – constitutively active

DN – dominant negative

ER – endoplasmic reticulum

MT – microtubules

GAG – glycosaminoglycan

KLF – Kruppel-like transcription factor

LE – late endosome

RE – recycling endosome

RAG – regeneration associated gene

ONC – optic nerve crush

TM – transmembrane domain

FYVE – Fab 1, YOTB, Vac 1, and EEA1 domain

FFAT – two phenylalanines in an acidic tract domain

CC – coiled-coiled domain

FASN – fatty acid synthase

CMV – cytomegalovirus promoter

SYN – synapsin promoter

CAG – CMV early enhancer/chicken β-actin promoter

SFFV – spleen focus-forming virus promoter

CHAPTER I: INTRODUCTION

I. Introduction

1. The burden of spinal cord injury and glaucoma

Injuries to the central nervous system (CNS) can often lead to permanent disability and reduced quality of life for the affected individuals and their families. Spinal cord injury (SCI), for example, is a devastating condition which affects more than 50 000 people in the UK and Ireland (*What is spinal cord injury?|Spinal Research*, 2018). SCI results from damage to the nerve cells connecting the brain and the spinal cord to the rest of the body's organs, limbs and muscles. Full or partial paralysis is the most common outcome of SCI; however, the condition is also associated with a high risk of developing secondary symptoms such as urinary incontinence, depression, sleep disturbance, chronic pain and in some severe cases, respiratory failure. Currently there are several treatments on the market which ameliorate some of the symptoms of this complex condition, but no cure exists to repair the damaged nerves.

Glaucoma is another condition which features sustained damage to the optic nerve – the nerve which transmits visual information from the eye to the brain in order to process an image. The highest risk for developing glaucoma is increased intraocular pressure (IOP) due to ineffective drainage of intraocular fluid. When persistent, IOP results in neuronal cell loss from the retina, optic nerve damage and vision impairment. Glaucoma is the second leading

cause of blindness around the world and currently there is no treatment for protecting the cells of the retina or for repairing the damaged nerves (*Glaucoma Facts and Stat |Glaucoma Research Foundation*, 2018). The limited number and quality of treatments for both SCI and glaucoma emphasise the pressing need to understand more about the biology of CNS neurons and their loss of regenerative ability with ageing in order to design innovative therapies and to improve the quality of life of patients and their families.

2. Regeneration in the adult mammalian central nervous system

Axons of immature CNS and adult peripheral nervous system (PNS) neurons readily regenerate after injury (Nicholls and Saunders, 1996; Huebner and Strittmatter, 2009). In contrast, mammalian CNS axons lose their regenerative capabilities with maturity (Bradke and Marín, 2014). For centuries, many scientists believed that adult CNS neurons simply do not regenerate after injury (Illis, 2011). Ramon y Cajal first described the swollen ends of injured axons as “dystrophic endballs” which are incapable of regeneration (Ramon y Cajal, 1928). Seminal studies over the past few decades, however, have challenged this long-standing dogma. In a series of pioneering experiments, Aguayo and colleagues showed that injured adult spinal cord or brain axons are, in fact, capable of regenerating through a peripheral nerve graft where the extracellular environment is more growth-permissive (Richardson, McGuinness and Aguayo, 1980; David and Aguayo, 1981; Benfey and Aguayo, 1982). These findings demonstrated for the first time that adult mammalian CNS neurons retain some intrinsic ability for regeneration and identified the non-permissive CNS extracellular environment as a key determinant of the CNS regenerative failure.

2.1 Extrinsic Factors

2.1.1 Chondroitin sulphate proteoglycans

Several extracellular processes have been associated with the regenerative failure in adult CNS axons. Firstly, after injury to the CNS axons, a complex cascade of molecular and cellular events is triggered leading to the formation of a glial scar. The glial scar is a dynamic structure with different cell types (astrocytes, oligodendrocytes, immune cells) arriving at

different times and performing a variety of functions attempting to repair the damaged axons (Fawcett and Asher, 1999). While initially these cells are protective and aiding repair, sustained activation results in the secretion of numerous inhibitory molecules which oppose regeneration and remyelination. For example, reactive astrocytes secrete extracellular matrix molecules such as chondroitin sulphate proteoglycans (CSPGs) after injury which are restrictive to growth (Shen *et al.*, 2009; Fisher *et al.*, 2011). CSPGs contain a single protein core to which glycosaminoglycan (GAG) chains are attached. Treatment with chondroitinase ABC (ChABC), an enzyme which severs the GAG chains of the proteoglycans or with arylsulfatase B (ARSB), an enzyme which changes the sulfation pattern of GAGs to a more permissive one, result in improved regeneration after optic nerve crush (Pearson *et al.*, 2018). ChABC treatment also leads to improved regeneration proximal to the lesion site and sprouting which are accompanied by partial functional recovery after spinal cord injury (Moon *et al.*, 2001; Bradbury *et al.*, 2002; Barritt *et al.*, 2006).

2.1.2 Myelin-derived inhibitors

Other inhibitory molecules present in the extracellular milieu after injury originate from the myelin debri around the injury site. Some examples include NoGo (neurite outgrowth inhibitor), myelin-associated glycoprotein (MAG) and oligodendrocyte myelin glycoprotein (OMgp)(Yiu and He, 2006). The use of antibodies sequestering NoGo-A, genetic ablation of the NoGo gene, or interfering with its receptor NR1, have all been useful methods of improving the regenerative response and in aiding functional recovery after injury mostly by increasing neuronal sprouting and plasticity (GrandPré, Li and Strittmatter, 2002; Kim *et al.*, 2003, 2004; Liebscher *et al.*, 2005; Freund *et al.*, 2006). In 2011, anti-NoGo antibodies successfully passed Phase I clinical trials in paraplegic and tetraplegic patients with acute injuries and Phase II is now underway to examine the efficacy of this therapy (Zörner and Schwab, 2010). Furthermore, treatment combining anti-NoGo antibodies and chABC has been shown to be more effective than single treatments in stimulating sprouting and functional recovery after spinal cord injury in rats, suggesting that a combinational approach might be the way forward (Zhao *et al.*, 2013). Interfering with MAG has not resulted in axon regeneration in the corticospinal tract (CST) up to date in animal models (Bartsch *et al.*, 1995). In a recent study, transgenic mice lacking NoGo, MAG and OMgp were examined for

synergistic effects compared to single treatments. A modest effect was observed on sprouting but no improved spinal axon regeneration or functional recovery was recorded suggesting that while these inhibitors might have a role in sprouting, they are not the main players in the regenerative failure in CNS axons (Lee *et al.*, 2010).

2.1.3 Growth factors signalling

One further obstacle to axon regeneration after injury is the supply of growth factors and their receptors to injured cells. Growth factors such as nerve growth factor (NGF), brain-derived neurotrophic factor (BDNF) and Neurotrophin-3 have all been associated with aiding neuronal survival, neurite outgrowth, plasticity and neurotransmission in development and after injury in the PNS (Jones *et al.*, 2001). In the CNS, the expression of several of these factors decreases with maturation and their upregulation after injury is very limited which could further complicate the process of axon regeneration (Schwab and Bartholdi, 1996). Recent attempts focused at delivering these growth factors to the injury site in spinal cord injury and optic nerve crush models - indeed many of them showed promising results in aiding sprouting and axon regeneration (Tuszynski *et al.*, 1996; Menei *et al.*, 1998; Zhang *et al.*, 2000; Blesch and Tuszynski, 2003; Blesch *et al.*, 2004; Wong *et al.*, 2014).

Many of the studies described above, do indeed show promising results in aiding neuronal sprouting and plasticity as well as in improving functional recovery. Some of them even report enhanced axon regeneration near the lesion site. In most cases, however, the axons grow proximal to the lesion site and very rarely through the injury. Also, the extent of growth seen in these animal models would be negligible if translated to the human situation. These observations suggest that rendering the environment more permissive for growth is one step forward in the right direction – however, in order to observe true, long-range, translatable axon regeneration, the intrinsic ability of adult CNS neurons to grow must also be considered.

2.2 Intrinsic Factors

In addition to the non-permissive extracellular environment after injury, intrinsic neuronal factors also play an important role in axon regeneration (He and Jin, 2016; Tedeschi and Bradke, 2017). Aguayo and colleagues showed that only a subset of neurons is capable of re-growing through a peripheral nerve graft whereas others such as descending CST axons have lost this ability even if the environment is permissive (Aguayo, David and Bray, 1981; Richardson, Issa and Aguayo, 1984). This discovery opened a new avenue for boosting regeneration – modulating the intrinsic ability of adult neurons to re-grow after injury.

2.2.1 PTEN and PI3K pathways

One approach includes stimulating pathways, essential for neuronal growth and survival. For example, PTEN (phosphatase and tensin homologue), an inhibitor of the mammalian target of rapamycin (mTOR) pathway was initially identified as a negative regulator axon growth as it opposes the actions of phosphoinositide 3-kinase (PI3K). The PI3K pathway is an essential cellular pathway involved in cell survival, metabolism and growth processes (*Fig. 1.1)*. Knocking down PTEN resulted in robust long-range retinal ganglion cell (RGC) regeneration after optic nerve crush (Park *et al.*, 2008). In addition, deletion of PTEN improved sprouting of uninjured axons and aided regeneration at short distances past the lesion site of some injured CST neurons *in vivo* – this effect was attributed to upregulation of mTOR pathway (Liu *et al.*, 2010). The mTOR pathway is highly active during early development but is diminished with maturation in the CNS and PNS. Its activation, however seemed to specifically be involved in CNS and not PNS regeneration as blocking the pathway by rapamycin reduced the regenerative potential of immature cortical neurons but not that of adult PNS neurons (Huang *et al.*, 2017). The effect of PTEN deletion was further enhanced by a combination with another deletion – suppressor of cytokine signalling 3 (SOCS3), a negative regulator of Janus kinase/signal transducers and activators of transcription (JAK/STAT) pathway. A combination of two separate intracellular pathways activation - mTOR and JAK/STAT, resulted in an additive effect on RGC survival and a robust long-range retinal ganglion cell regeneration after optic nerve crush (Smith *et al.*, 2009; Sun *et al.*, 2011). PTEN, however also acts as tumour

suppressor so deletion of this gene is not a reliable therapeutic approach to improve axon regeneration.

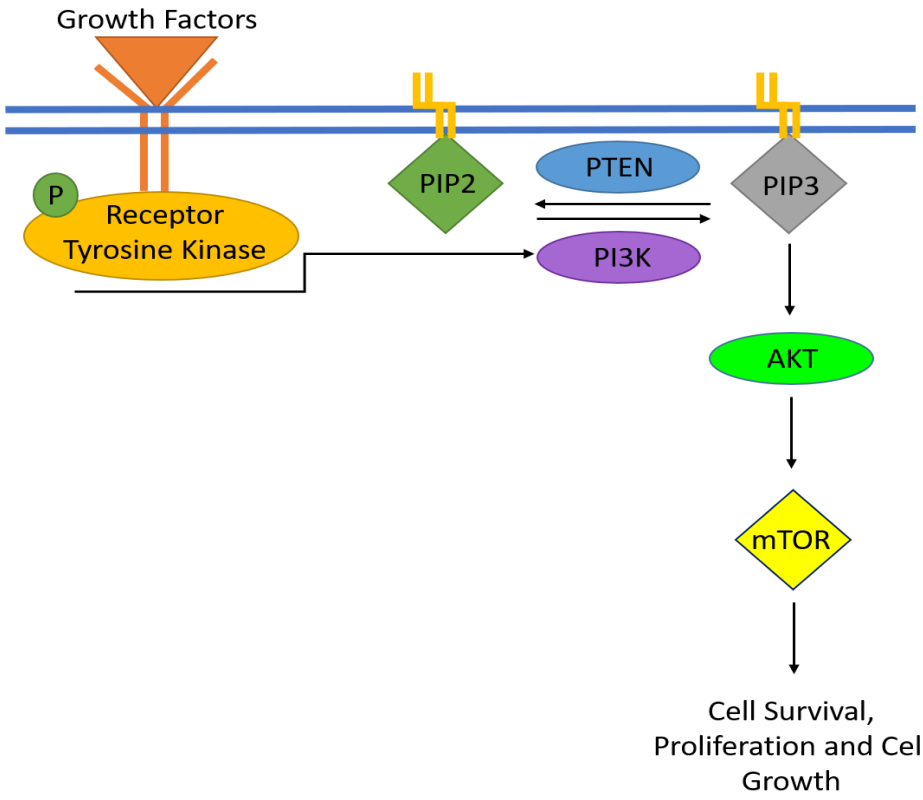

Figure 1.1 A schematic diagram to illustrate the PI3 Kinase Signalling Pathway. Insulin or growth factors from outside the cell bind to receptor tyrosine kinases and activate them which in turn, activate PI3K. PI3K then converts phosphatidylinositol-4,5-bisphosphate (PIP2) to phosphatidylinositol (3,4,5)-trisphosphate (PIP3). PIP3 acts as an effector which triggers numerous downstream intracellular cascades, one of which is the activation of Protein Kinase B (or also known as AKT) and subsequently of mTOR ultimately leading to cellular events which support cell survival, proliferation and growth.

Other strategies, however, such as manipulating PI3K instead could prove to be more effective in the clinic in the future. PI3K activation has so far been achieved through potentiating the insulin growth factor 1 receptor (IGF1R) which is upstream of PI3K signalling. IGF1 expression peaks during development and falls gradually during adult life (Wrigley, Arafa and Tropea, 2017). Combinational viral delivery of the IGF1 receptor (IGF1R) and osteopontin – an enhancer of neuronal response to IGF1R activation, results in improved axon regeneration in RGCs after optic nerve crush (Duan *et al.*, 2015) and in sprouting, short-range axon regeneration and some functional recovery in CST neurons after T10 spinal cord hemi-section (Liu *et al.*, 2017). These findings highlighted the potential of modulating neuronal intrinsic pathways in order to promote some therapeutically relevant functional recovery after

spinal cord injury. Despite that, long-range axon regeneration of the CST was not achieved and most of the functional recovery observed was due to sprouting.

2.2.2 Other intracellular pathways

Recently, another intracellular signalling molecule – Cacna2d2, a gene encoding for voltage-gate calcium channel units, has been shown to restrict axon growth and regeneration. In fact, using a pharmacologically available antagonist – pregabalin, to block this channel resulted in improved regeneration in adult mice after spinal cord injury (Tedeschi *et al.*, 2016). Improving adult neuronal sensitivity to growth factors such as BDNF by overexpressing its receptor - the TrkB receptor has also proved to be beneficial for axon growth and regeneration and revealed new pathways involved – such as the ERK/MAPK pathway (Hollis *et al.,* 2009). Other intracellular pathways involved are the RhoA/ROCK pathway. Ras homolog gene family, member A (RhoA) is a small GTPase which is downstream of many pathways activated by extracellular inhibitory factors such as MAG, OMgp and CSPGs (Hu and Selzer, 2017). Inactivation of RhoA by C3 transferase enzyme was first shown to improve axon regeneration of the optic nerve and neuronal survival after an optic nerve crush (Lehmann *et al.*, 1999; Koch *et al.*, 2014). Inhibition of RhoA with C3 transferase or with a pharmacological inhibitor was later showed to result in increased axon regeneration and sprouting as well as in improved motor behaviour in mice with partial spinal cord injury (Dergham *et al.*, 2002). These effects, however seem to result from benefits in sprouting and survival instead of long-range regeneration to initial muscle targets (Tuszynski and Steward, 2012). Many other intercellular molecules such as cyclic AMP, GSK3 and others have been targeted to improve axon growth, regeneration and survival after injury (Qiu *et al.*, 2002; Leibinger *et al.*, 2017) . No intracellular manipulations to date however, have resulted in long-range axon regeneration of injured CNS axons back to their original target cells to form functional synapses.

So far, one of the most robust axon regeneration improvements observed *in vivo* has been in the peripheral nervous system where overexpression of activated growth-promoting receptor - integrin alpha9 - resulted in robust regeneration (more than 25mm in length) and in functional recovery after dorsal root crush (Cheah *et al.*, 2016). This study was the first of

its kind to highlight the importance of transport and trafficking of growth-promoting molecules such as integrins to the tip of regenerating neurons as another intrinsic process key for regeneration in addition to the activation of intracellular signalling cascades. Intracellular trafficking and transport and their involvement in axon regeneration are discussed in detail in *Section 3.*

2.3 Gene expression changes and epigenetics

While targeting individual intracellular pathways or molecules did show some promising effects in aiding axon sprouting and short-range regeneration past the lesion site, all studies described so far, highlight the importance of targeting a global set of intracellular events in order to trigger more robust axon growth. PNS neurons upregulate a particular set of genes after injury in order to enable axon regeneration – a response that is only partially present in the CNS (Neumann and Woolf, 1999; Plunet, Kwon and Tetzlaff, 2002; Hoffman, 2010). Recent efforts have been concentrated on altering intrinsic factors on a more global level by neutralising inhibitory transcription factors such as KLF4 or by overexpressing developmentally down-regulated and growth-associated transcription factors such as ATF3 and KLF7 – all leading to increased expression of pro-regenerative genes and enhanced regeneration (Seijffers, Mills and Woolf, 2007; Moore *et al.*, 2009; Blackmore *et al.*, 2012a; Fagoe *et al.*, 2015; Wang *et al.*, 2015). A detailed review of the most recent studies in which transcription factors are used as a tool to target multiple growth-related genes at once is provided in *Chapter 6.* Despite the promising initial results that these studies yielded, there seemed to be other mechanisms in the CNS such as epigenetic changes which do not allow for PNS-like regeneration to be observed (Trakhtenberg and Goldberg, 2012; Venkatesh *et al.*, 2016; Wang *et al.*, 2017). PCAF, for example, is a histone acetyltransferase which associates with the promoters of known pro-regenerative genes and drives their expression (Puttagunta *et al.*, 2014). PCAF is highly active in PNS neurons after injury to induce axon growth and its overexpression in CNS non-regenerative neurons is sufficient to promote axon regeneration after spinal cord injury (Puttagunta *et al.*, 2014). Other epigenetic factors and their use to improve axon regeneration are reviewed in *Chapter 6, Section 1*.

In addition, many of the studies mentioned above show that numerous aspects of neuro-regeneration recapitulate development and that both processes share similar molecular players (Harel and Strittmatter, 2006; Hilton and Bradke, 2017). In this sense, understanding the transition from early to late neuronal development might be essential to identifying factors contributing to the regenerative failure of mature neurons.

2.4 Regeneration Capacity Declines with Maturation

Research over the past few decades has shown that the regenerative abilities of immature and mature neurons can be very different, with young neurons readily regenerating after injury and mature neurons failing to re-grow their injured axons (Nicholls and Saunders, 1996). Regeneration of some adult CNS axons which have lost their regenerative ability could be partially improved by grafting embryonic spinal cord or PNS tissue which provide more permissive environment (Vidal-Sanz *et al.*, 1987; Mori *et al.*, 1997). Despite that, even in neurons capable of regeneration such as those of the PNS, the regenerative response is delayed and less effective in aged compared to younger animals (Verdú *et al.*, 2000).

2.4.1 In vitro studies

In the CNS, the effects of maturation are even more pronounced with strongly diminished regenerative ability in mature neurons. As adult CNS regeneration rarely occurs *in vivo,* some *in vitro* models could prove valuable to test different strategies to improve axon regeneration (Bradke, Fawcett and Spira, 2012). Recently, Koseki and colleagues showed that the maturational state of cultured rat cortical neurons negatively correlates with their regenerative abilities whereby less than 10% of neurons aged 23-30 DIV (days *in vitro*) regenerate compared to 70% of 3-5 DIV neurons (Koseki *et al.*, 2017). This failure of regeneration in mature CNS neurons was attributed to an intrinsic change because when young neurons were cultured in an aged environment (24-day-old cultures), they retained their regenerative ability. Another change that accompanied the regenerative failure was exclusion of Rab11-positive endosomes from axons but not from dendrites in aged neurons, implicating axonal transport as a possible mechanism by which maturation can affect

regeneration (Koseki *et al.*, 2017). The maturational change in cultured primary cortical neurons was further confirmed by RNA sequencing studies which showed extensive changes in gene expression with upregulation of genes involved in synapse formation and function, and downregulation of genes important for growth and development (Koseki *et al.*, 2017).

Other *in vitro* studies showed that retinal ganglion cells (RGCs) show similar age-dependent decline - RGCs lose their regenerative ability shortly after birth and have reduced growth potential when cultured *in vitro* whether grown on neonatal (unmyelinated) or adult (myelinated) optic nerve sections (Goldberg *et al.*, 2002). In contrast, dorsal root ganglion (DRG) neurons isolated from the PNS retain their intrinsic ability to grow on either of these substrates suggesting that they have a preserved intrinsic ability to regrow (Shewan, Berry and Cohen, 1995). Furthermore, embryonic RGCs were better regenerators compared to adult RGCs when grown on laminin and injured (Verma *et al.*, 2005). This was not the case for PNS neurons where the majority of injured axons formed a growth cone and regenerated irrespective of their maturational stage (Verma *et al.*, 2005).

2.4.2 In vivo studies

Ageing and maturation are complex processes which can affect the regenerative abilities of axons through different pathways, hence studying their effects *in vivo* has proven to be rather challenging. The lack of true regeneration in aged animals also complicates this study. Early studies showed that the developmental decline in regenerative ability is triggered by intracellular events rather than ageing of the environment or influences from surrounding glia. For example, the majority of neonatally-derived retinal axons lose their ability to re-innervate their target brain region (the tectum) even when presented with an embryonic target or when oligodendrocyte inhibitory proteins are neutralised (Chen, Jhaveri and Schneider, 1995). On the contrary, embryonic retinal explants are capable of extending long axons to immature or mature tectum (Chen, Jhaveri and Schneider, 1995). Similar observations were made in entorhinal-hippocampal slices where “old” entorhinal axons are not able to project to “old” or “young” hippocampal areas whereas more immature entorhinal axons are able to extend connections to any target (Li, Field and Raisman, 1995). These studies

were seminal in establishing that the critical factor for the maturational decline in regenerative ability is the age of the projecting neurons.

Recent studies in Caenorhabditis elegans (*C. elegans)* showed similar results to the ones Koseki and colleagues obtained *in vitro* with 65% of GABA motor neurons regenerating after single-neuron laser axotomy in young adult worms (1 day post the final larval stage) compared to only 28% of aged neurons (5 days post the final larval stage) regenerating (Byrne *et al.*, 2014). The current study was also able to attribute this decline specifically to the intrinsic ability of aging neurons to regenerate rather than to secondary processes occurring in the ageing organism or to the length of the worm's lifespan (discussed by Belin, Norsworthy and He, 2014). Further studies in *C. elegans* where laser axotomy was performed on various neuronal cell types at different stages of development, revealed that regenerative ability is highly dependent on neuronal cell type, developmental stage and signalling from molecules in the surrounding environment (Wu *et al.*, 2007).

The regenerative ability with maturation was also studied in more complex organisms. Opossums, for example, are marsupials which are born immature and complete their nervous system development after birth. Their spinal cord neurons are capable of axon regeneration until they are 9–12 postnatal days old for cervical segments, and 17 days old in lumbar segments (Varga *et al.*, 1995). This critical period of developmental regenerative decline coincides with upregulation of myelination and the secretion of myelin inhibitors in the extracellular environment as well as with downregulation of cAMP and other growth-associated pathways (Mladinic and Wintzer, 2002; Mladinic, 2007; Mladinic *et al.*, 2010). In this sense, the opossum CNS provides a model where axon regeneration declines both temporally and spatially.

In mammals, an early study of the effects of neuronal maturation on regeneration was carried out in organotypic slice cultures of auditory gerbil neurons where P7 cultures showed robust regeneration which was not observed in P12 cultures (Hafidi, Lanjun and Sanes, 1999). In hamsters, injured as infants there was a greater axon regeneration and functional recovery of hindlimb function after lesion to the medullary pyramidal tract compared to animals injured

as adults (Kalil T., 1979; Keifer and Kalil, 1991). Examining the regenerative potential in chicks shows that maturation results in 55% reduction in regeneration potential of spinal cord neurons and in 90% reduction in hindbrain neurons (Blackmore and Letourneau, 2006). Furthermore, transplanting embryonic neurons into the adult spinal cord allows for robust axon growth whereas adult neurons do not grow well even when plated on permissive substrates again highlighting the importance of the intrinsic ability of axons to grow in axon regeneration (Blackmore and Letourneau, 2006).

The most comprehensive study so far about the effects of ageing of regeneration used a model for regeneration in adult CNS neurons *in vivo*. As mentioned above, in previous reports PTEN deletion was shown to promote axon regeneration in retinal ganglion cells and corticospinal tract neurons after injury in young adult mice (Park *et al.*, 2008; Liu *et al.*, 2010). Geoffroy and colleagues recently expanded on these findings and examined the effects of ageing on the efficacy of PTEN deletion to promote axon regeneration in CST neurons (Geoffroy *et al.*, 2016). Ageing did not reduce the positive effects of the PTEN deletion on improving the intrinsic neuronal ability to regenerate proximally to the spinal cord injury. In contrast, ageing greatly reduced the axonal regeneration normally seen in young adult animals distal to the injury and resulted in increased inflammatory markers expression at the injury site (Geoffroy *et al.*, 2016). This study suggests that the ability of injured axons to regenerate at long distances diminishes with ageing.

In summary, it has been long known that younger neurons have enhanced regenerative abilities compared to their older counterparts (Ramon y Cajal, 1928). Despite the enormous advancement in our understanding of the extrinsic and intrinsic processes that contribute to the regenerative failure with maturation, most studies to date which aimed at manipulating these factors only achieved modest axon regeneration and insignificant functional recovery. Improving axonal transport of various growth and regeneration-related molecules in adult neurons has recently come to the forefront of regeneration research as a strategy to improve delivery of receptors to newly formed growth cones in order to achieve better guided and more robust axon regeneration.

3. Axon Transport in Development and Regeneration

3.1 What is Axon Transport?

The transport of molecules, organelles and other cellular components along the axon is required for proper functioning of the cell. The great length of axons (some can reach up to 1m in length) requires tight spatial and temporal regulation of axonal transport. Long-range axon transport and trafficking is mediated by motor proteins which move along microtubule tracts which enable high velocity movement. Microtubules in axons have homogenous organisation with all minus ends pointing towards the cell body and all plus ends pointing towards the tip of the axons. In contrast, in dendrites mixed polarity microtubule structures are present (Yau *et al.*, 2016; Tas *et al.*, 2017). There are two types of active transport in axons at all times – retrograde (towards the cells body and the minus end of microtubules) mediated by dyneins and anterograde transport (towards the tip of growing neurites and the plus end of microtubules) mediated by kinesins (*Fig. 1.2).* In addition, transport involving the actin cytoskeleton and myosin motors allows for slower, more flexible transport beyond the rigid skeleton of the microtubule network. Proteins and cellular components are usually enclosed in membrane structures which connect to the correct motor proteins via adaptor proteins.

3.2 Control of membrane axon transport – ARF6 and Rab11

Research from the past few decades revealed that two small GTPases – Ras-related in brain (Rab, in particular Rab11) and ADP ribosylation factor (ARF, in particular ARF6), play key roles in controlling the transport of recycling endosomes along the axon (Salminen and Novick, 1987; D'Souza-Schorey and Chavrier, 2006; Stenmark, 2009). These small G proteins alternate between a GDP- and a GTP-bound state which regulates their binding to various adaptor proteins (Bos, Rehmann and Wittinghofer, 2007). The GDP-GTP cycle is highly regulated by guanine nucleotide exchange factors (GEFs) which release GDP to be replaced by GTP and by GTPase-activating proteins (GAPs) which stimulate hydrolysis of GTP to GDP. The spatial and temporal availability of GEFs and GAPs regulate the rate of GTP-to-GDP cycling in Rab11 and ARF6 which in turn influences the directionality and speed of axon transport.

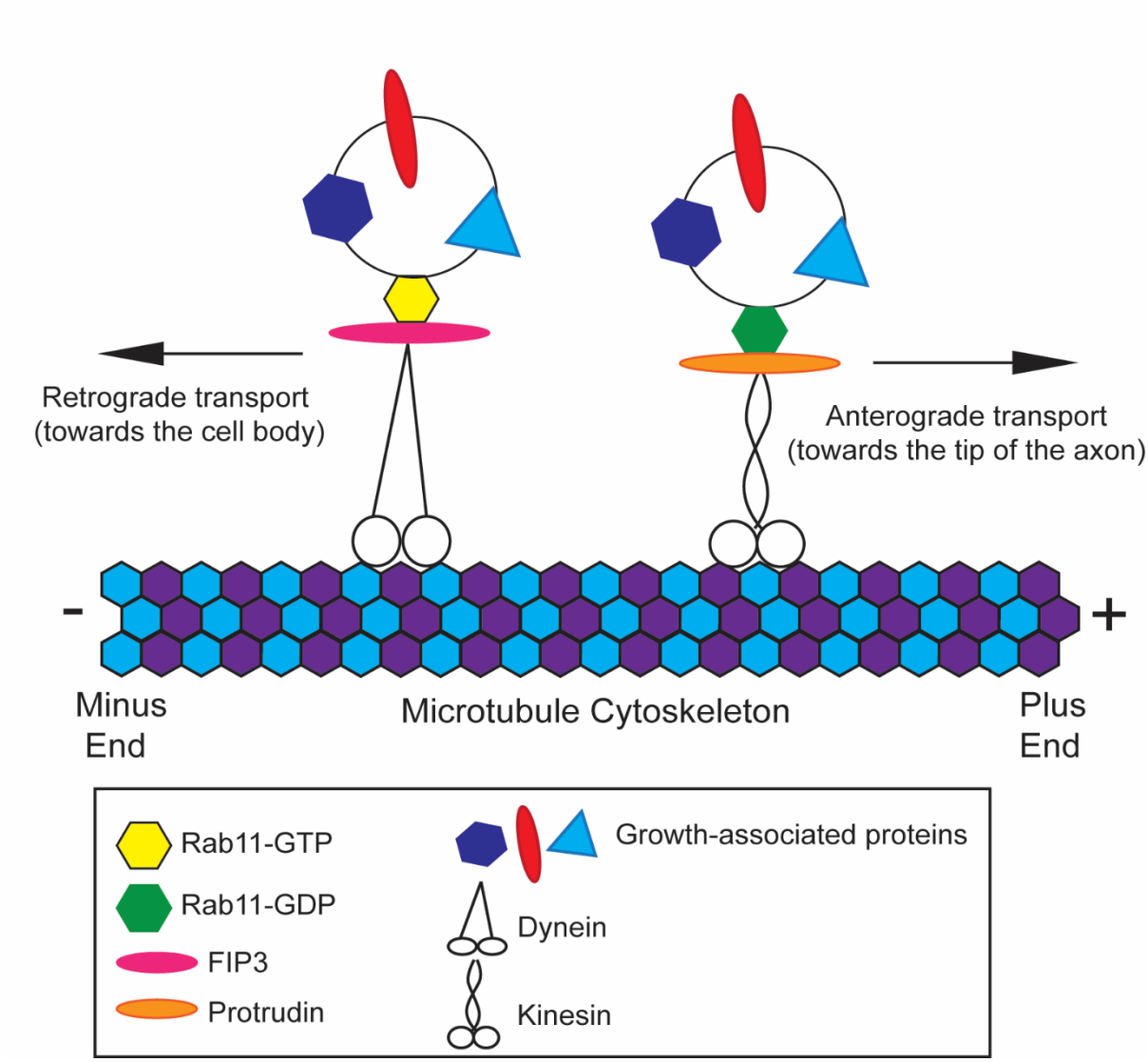

Figure 1.2 A schematic diagram to illustrate the bidirectional movement of recycling endosomes along microtubule tracts in the axon. Motor proteins such as dyneins and kinesins associate with adaptor proteins such as FIP3 and protrudin which in turn interact with Rab11-tagged recycling endosomes carrying various cargo molecules such as integrins and other growth-associated receptors. The activational state of Rab11 is thought to influence which type of adaptor proteins it associates with. Dyneins transport cargo towards the minus end of microtubules, i.e. towards the cell body – this movement is also referred to as retrograde transport. Kinesins such as KIF5 transport cargo towards the positive end of microtubules i.e. to the tip of processes, also referred to as anterograde transport (modified from Welz, Wellbourne-Wood and Kerkhoff, 2014).

Previous studies show that Rab11 is involved in exocytosis as well as in the insertion of various proteins in the plasma membrane. For example, Rab11 is essential for the membrane recycling of receptors such as the transferrin receptor (Ullrich *et al.*, 1996; Ren *et al.*, 1998), β2 adrenergic receptor (Parent *et al.*, 2009), AMPA receptors (Park *et al.*, 2004; Correia *et al.*, 2008; Esteves da Silva *et al.*, 2015), toll-like receptors (Husebye *et al.*, 2010), fibroblast growth factor receptor 4 (Haugsten *et al.*, 2014), tropomyosin receptor kinase B (TrkB) (Lazo *et al.*, 2013; Sui *et al.*, 2015; Song *et al.*, 2015) and the integrin receptor (Powelka *et al.*, 2004; Caswell *et al.*, 2008; Eva *et al.*, 2010). Interestingly, Rab11 and ARF6 both regulate the vesicular transport of integrins – growth-associated receptors which are involved in axon guidance, extension and migration. ARF6, similarly to Rab11 cycles between an active (GTP-bound) and an inactive form (GDP-bound form) whereby the active form in the axon favours retrograde axonal transport and the inactive form supports anterograde transport (Eva *et al.*, 2012). In summary, Rab11 and ARF6 act in co-ordination along the axon and control membrane-dependent recycling and exocytosis with their activation states and adaptor binding being key to these processes (Welz, Wellbourne-Wood and Kerkhoff, 2014).

3.3 Developmental decline in regeneration-associated axon transport

It has been widely known that axon transport is essential for successful regeneration after injury and many groups have focused their efforts in understanding the differences in axon transport in regenerating vs. non-regenerating neurons and in immature vs. mature axons.

During development, neurons are fully equipped with the growth machinery they need to extend long axons, reach their target cells and form functional connections. Once these connections have been established, the elongation capacity of neurons declines dramatically. One reason why adult CNS axons have poor regenerative capabilities might be that a developmental change occurs where essential growth molecules are no longer transported to the tip of axons given they are no longer needed there. Instead, the transport of synapse-associated cargoes becomes priority over the transport of growth-associated molecules (Bonanomi *et al.*, 2008; Tedeschi *et al.*, 2016). Axon transport has been

shown to change with maturation and there are also stark differences between transport in the adult PNS and in the CNS which might be responsible for the differential regenerative abilities of these neurons.

Early studies have shown that PNS and CNS axonal transport of some essential cytoskeletal proteins in rats declines with age – between 1 and 6 months of age (McQuarrie, Brady and Lasek, 1989). Recently, Milde and colleagues (2015) were able to identify some specific developmental changes in both CNS and PNS axon transport using single-axon fluorescence live imaging of acute tissue explants of mice aged between 1.5 and 24 months. They observed two major periods of axonal transport decline of two specific cargoes – a neuronal survival factor NMNAT2 and mitochondria. Initial decline in axonal transport was observed for both cargoes in PNS and CNS neurons between 1.5 and 6 months of age and a later drop in the number of particles transported along the axon was observed in sciatic and optic nerve but not in hippocampal axons at 24 months (Gilley *et al.*, 2012; Milde *et al.*, 2015). Interestingly, peripheral nerve crush induced an increase in the axonal transport of mature axons in an ageing environment (24-month-old mice) – there were more anterogradely moving particles containing NMNAT2 and mitochondria at rates similar to young mice. Retrograde transport was unaffected (Milde *et al.*, 2015). These studies support previous findings that a balance between a retrograde and an anterograde transport is needed for axon growth and extension, whereas predominant retrograde movement is restrictive to growth (Hollenbeck and Bray, 1987; Hollenbeck, 1993). These findings further highlight that enhanced anterograde transport is need for axon regeneration after peripheral nerve injury.

One reason for the change in axonal transport with maturation in CNS neurons could be that the axon initial segment (AIS) forms. The AIS acts as a molecular barrier which can enable or restrict the transport of specific cargos along the axon (Song *et al.*, 2009; Rasband, 2010) . For example, in multipolar hippocampal neurons, cargo specific to the somatodendritic compartment is excluded from axons by the AIS, which at the same time selectively permits axon-specific cargo to pass through to the distal axon (Song *et al.*, 2009). Our group has shown that an activator of ARF6 – EFA6 is localised within the AIS where it regulates directional transport in the axon (Eva *et al.*, 2017). Interfering with EFA6 resulted

in enhanced anterograde transport of growth-associated molecules in the axon which in turn results in improved regeneration after laser axotomy in primary cortical neurons (Eva *et al.*, 2017). This finding suggests that molecules in the AIS could be targeted in order to improve axonal transport of growth-related molecules. A similar mechanism has recently been described in sensory DRG neurons whereby microtubule-associated protein 2 – MAP2 has a strict somatodendritic and proximal axon distribution *in vitro* and *in vivo* regardless of age of the neurons (Gumy *et al.*, 2017). This distribution plays a role in the balance between two motor adaptor proteins – KIF5 and KIF1 which in turn regulates the entry of specific axonal cargo into axons as well as axonal growth (Gumy *et al.*, 2017).

Cytoskeletal re-arrangement and the proper formation of a growth cone are some of the requirements for successful axon regeneration (Bradke, Fawcett and Spira, 2012). Early studies identified that the transport of cytoskeletal proteins such as growth-associated protein 43 – GAP43, is rapidly upregulated in the optic nerve in the CNS of neonatal rabbits after injury to aid regeneration – an effect which declined steadily in the adult (Skene and Willard, 1981). In contrast, the transport of GAP43, was highly upregulated in the readily regenerating neurons of hypoglossal nerve in the PNS in the adult (Skene and Willard, 1981). This upregulation in GAP43 in regenerating immature and adult PNS axons after injury was also shown to be co-ordinated with an increase in the transport of other cytoskeletal elements such as beta tubulin (Hoffman *et al.*, 1983). In the adult, the trafficking of cytoskeletal elements along the axon was also shown to slow down during maturation of motor neurons and retinal ganglion cells (Hoffman *et al.*, 1983; McQuarrie, Brady and Lasek, 1989). Furthermore, enhanced regeneration after a conditioning lesion in the PNS or axon growth of RGCs into a peripheral graft both resulted in enhanced axon transport of cytoskeletal elements such as microtubules and neurofilaments (McQuarrie and Grafstein, 1982; Oblinger and Lasek, 1988; McKerracher, Vidal-Sanz and Aguayo, 1990; McQuarrie and Jacob, 1991). Recently, the axon transport of other regeneration-associated molecules such as 14-3-3 proteins and the RhoA inhibitor – RhoGDI, as well as membranous structures such as lysosomes, synaptophysin and APP vesicles was also found to be upregulated in the central branch of DRG neurons upon a peripheral branch conditioning lesion (Mar *et al.*, 2014). This study suggests that global axon transport changes take place after a conditioning lesion to allow for axon regeneration.

In summary, the experiments described above point towards a global decline in the axonal transport with maturation, and to an increase in trafficking of growth-associated molecules and cellular components during enhanced regeneration in immature and adult PNS neurons. Some of the most pronounced changes in the distribution and the axon transport of growth and regeneration-associated proteins, organelles and mRNAs in adult CNS neurons are described below. These changes could be in the epicentre of the regenerative failure observed in mature neurons and restoring axon transport of these components could prove a valuable tool to aid targeted axon regeneration.

3.3.1 Developmental decline in the axon transport of growth molecules

3.3.1.1 Integrins

The distribution of surface receptors along the axon and their insertion into the growth cone membrane triggers a cascade of molecular and cellular events which result in the cytoskeletal re-arrangement and the improved axon transport that are necessary for enhancing axon regeneration. Integrins are large family of cell surface receptors, which are essential for neuronal survival, growth cone formation and axon elongation in the developing CNS and in the PNS after injury (Nieuwenhuis *et al.*, 2018). In PNS neurons, integrins are found abundant in axons, dendrites and growth cones and they are transported in recycling endosomes to a similar extent in the retrograde and in the anterograde direction along axons (Eva *et al.*, 2010, 2012). Overexpression of alpha9 integrin showed increased neurite outgrowth in sensory DRG neurons *in vitro* and *in vivo* and had a modest effect on axon regeneration and functional outcome on sensory axons after rhizotomy and spinal cord injury (Andrews *et al.*, 2009). Interestingly, AAV-mediated expression of activated α9-integrin in the dorsal root ganglion promoted long-range axon regeneration of sensory neurons into the non-permissive environment of the spinal cord as well as functional recovery after a dorsal root crush (Cheah *et al.*, 2016). This effect was likely observed as anterograde transport of integrins into PNS axons is possible, but this strategy would likely fail in descending CNS axons because their anterograde transport of growth-associated molecules seems to be compromised.

In contrast to the PNS, integrins become excluded from CNS axons both *in vitro* and *in vivo* as neurons mature resulting in decreased axonal regeneration (Andrews *et al.*, 2009, 2016; Franssen *et al.*, 2015). In CNS axons, there is a developmental change in the transport of integrins such that retrograde trafficking increases in cortical neurons *in vitro* as observed by live cell imaging of integrins at 3 DIV (35%) and 10 DIV (57%) (Franssen *et al.*, 2015). This change in the direction of axonal transport coincides with the exclusion of integrins from the mature axon and with decreased regenerative ability (Franssen *et al.*, 2015; Koseki *et al.*, 2017). Allowing more integrins to enter the axon by either interfering with the AIS or changing the direction of integrin transport from predominantly retrograde to anterograde resulted in increased neurite outgrowth and improved regenerative ability in primary cortical neurons *in vitro* (Franssen *et al.*, 2015; Eva *et al.*, 2017; Koseki *et al.*, 2017). It is yet to be tested whether increasing integrin amount in CNS axons *in vivo* can promote neurite outgrowth and axon regeneration similar to previous studies in the PNS (Cheah *et al.*, 2016).

3.3.1.2 Rab11 endosomes

The absence of integrins from mature CNS axons is accompanied by absence of their carriers – Rab11-positive endosomes too. Previous reports show that Rab11 vesicles are excluded selectively from axons but not dendrites both *in vitro* (Franssen *et al.*, 2015; Koseki *et al.*, 2017) and *in vivo* (Sheehan *et al.*, 1996). In another report, the failure of regeneration in mature CNS neurons coincided with the time point of exclusion of Rab11-positive vesicles from axons (Koseki *et al.*, 2017). Similar to integrin transport, Rab11-positive vesicles are also trafficked predominantly retrogradely in mature axons – a phenomenon localised to the axon but not dendrites where bidirectional movement was observed (Koseki *et al.*, 2017). Restoring Rab11 to axons by overexpressing it in mature cortical neurons *in vitro* resulted in improved regeneration which was accompanied in with an increase in the amount of axonal integrins (Koseki *et al.*, 2017). Interestingly, this phenomenon was also observed in human ESC-derived dopaminergic neurons. Rab11-tagged endosomes are known to transport a variety of growth-promoting receptors as discussed above which are important during the developmental stage

of neuronal maturation. Their absence of the mature axon could instead be reflecting a change in the requirements for recycling within the axon.

3.3.1.3 TrkB and IGFR1

The availability of growth factors and growth factor receptors after injury is also an essential requirement for successful regeneration. Growth receptor activation at the growth cone is associated with enabling an array of downstream intracellular pathways involved in growth and survival, but also with sensing the environment and sending retrograde signals to the cell body to alter gene expression, transport and cell function (Bhattacharyya *et al.*, 1997; Cosker, Courchesne and Segal, 2008). Two growth receptors, in particular, are well-studied in this regard - tropomyosin receptor kinase B (TrkB) and insulin-growth factor receptor 1 (IGFR1) which are activated by two growth factors – brain-derived neurotrophic factor (BDNF) and insulin growth factor (IGF), respectively (Lu and Tuszynski, 2008; Hollis *et al.*, 2009a; Hollis *et al.*, 2009b; Duan *et al.*, 2015; Liu *et al.*, 2017).

Both IGFR1 and TrkB receptors play an important role in developmental axon growth and survival. IGFR1 activation acting through the PI3K pathway has recently been implicated in the axon specification and initial growth in hippocampal neurons (Sosa *et al.*, 2006; Dupraz *et al.*, 2009). This effect was preceded by IGFR1 accumulation in the newly forming axonal process by means of selective transport – a critical step for axon outgrowth. Furthermore, IGFR1 signalling is required in the initial axonal outgrowth of retinal ganglion cells *in vitro* (Dupraz *et al.*, 2013) and of CST neurons *in vivo* (Özdinler and Macklis, 2006). Similarly, neuron-specific mouse knockout of TrkB displayed reduced survival and attenuated axon growth both *in vitro* and *in vivo* (Gates, Tai and Macklis, 2000).

Intracellularly, the IGFR1 and TrkB undergo dynamic recycling and were both shown to co-localise with Rab11-positive recycling endosomes (Romanelli *et al.*, 2007; Ascano *et al.*, 2009; Huang *et al.*, 2013; Lazo *et al.*, 2013). These observations suggest that similarly to integrins and Rab11, IGFR1 and TrkB might be present at very low levels in the mature axon which could in addition contribute to the regenerative failure. Indeed, IGFR1 and TrkB were shown to be

excluded from the mature axon in CST neurons of the spinal cord (Hollis *et al.*, 2009a; Hollis *et al.*, 2009b). TrkB was also excluded from axons of rubrospinal neurons (Kwon *et al.*, 2004).

Given their effects on axon growth, overexpression of IGF1 or TrkB in mature neurons was expected to improve axon growth after injury. Applying IGFR1, however, to the injured CST only improved neuronal survival but did not aid axon regeneration (Hollis *et al.*, 2009a). When IGFR1 activation is combined with osteopontin (a potent growth activator which interacts with integrins), enhanced sprouting as well as partial functional recovery in two different models of CST injury was observed (Liu *et al.*, 2017). This effect was further strengthened by electrical stimulation highlighting the therapeutic relevance of proper receptor functioning and distribution in the axon as well as of rehabilitation through electrical stimulation as key for improving function after injury. Knockout of the TrkB receptor significantly reduced the amount of regeneration whereas the use of TrkB agonists promoted structural and functional repair of peripheral nerves after injury (English *et al.*, 2013). Strikingly, CST neurons show abundant TrkB receptor distribution in their soma and dendrites. CST axons, however, had very little TrkB present which correlated closely with their inability to regenerate after injury (Lu, Blesch and Tuszynski, 2001). In contrast, motor neurons contained axonal TrkB and were, therefore, able to regenerate past the lesion. These findings point towards a key role for axonal TrkB in stimulating axon growth after injury (Lu, Blesch and Tuszynski, 2001). It is no surprise then that when overexpressed TrkB improved the regeneration capacity of corticospinal neurons after a CST lesion (Hollis et al., 2009b). Importantly, abundance of BDNF at the growth cone stimulated enhanced anterograde transport of the TrkB receptor suggesting that signalling at the distal axon can enhance growth-promoting mechanisms by a feedforward mechanism (Cheng *et al.*, 2011).

In summary, essential growth-associated receptors (integrins, IGFR1 and TrkB) as well as their trafficking machinery (Rab11), seem to be evolutionary removed from the fully-grown mature axon and to adopt a more somatodendritic distribution. Their absence from developed axons could contribute to the regenerative failure after injury and their transport back into the axon could improve axon regeneration and functional outcome to some extent.

3.3.2 *Developmental decline in the axon transport of organelles*

The axon transport of organelles is another cellular process which also varies noticeably with maturation and that could further contribute to reduced regenerative ability in mature axons after injury.

3.3.2.1 *Mitochondria*

The dynamics and direction of mitochondrial axonal transport as well as their morphology change dramatically with CNS maturation. Early on in development, mitochondria adopt shortened morphology to aid their highly mobile nature and bidirectional movement along the axon (Chang and Reynolds, 2006). While functionally similar, in the mature, synaptically active neuron, mitochondria acquire an elongated form and their axonal movement slows down (Chang and Reynolds, 2006). This study, however, together with many others measured the bulk mitochondrial transport down the axon. Only recently with the advance of imaging technology, the specifics of individual mitochondrion axonal movement could be studied. Tracking individual mitochondrial particles, Lewis and colleagues observed that in immature cortical neurons (3-7 DIV) mitochondria are very mobile whereas in more mature neurons (10+ DIV), up to 95% of all axonal mitochondria become stationary by 28 DIV (Lewis *et al.*, 2016). This change in mitochondrial dynamics coincides with their localisation to the pre-synapse and with reduced regenerative ability. The authors also examined the transport of mitochondria in anaesthetised or awake, behaving animals using two-photon imaging. More than 90% of mitochondria in distal axons of cortical neurons were shown to be of stationary nature (Lewis *et al.*, 2016). Furthermore, a recent study identified one reason why mitochondria are less mobile in mature neurons - they become docked to the axon by a protein called syntaphilin (Kang *et al.*, 2008). Interestingly, syntaphilin knockout mice showed increased mitochondrial dynamics in the distal axon which resulted in improved axon regeneration after a sciatic nerve crush (Zhou *et al.*, 2016). Enhancing mitochondrial mobility by overexpression of Armcx1 – a mitochondrial-related protein involved in axon regeneration, again resulted in improved axon growth *in vitro* and in enhanced axon regeneration *in* vivo after optic nerve crush (Cartoni *et al.*, 2016). Taking into account that the unmet energy

demands after axonal injury are speculatively one reason why mature axons do not regenerate well, improving anterograde axonal transport of functional mitochondria could be key for regeneration.

3.3.2.2 Proteasome

The ubiquitin-proteasome system (UPS) is essential for the clearance of damaged and misfolded proteins. Similar to mitochondria, the axonal transport of proteasomes seems to be affected by the process of neuronal maturation. Proteasome activity drastically declines during normal ageing in the brain (Keller, Huang and Markesbery, 2000). Furthermore, impairments in UPS have been shown to result in protein aggregation and deficits in axonal transport (Otero *et al.*, 2018). In hippocampal neurons, at very early stages of development (1 DIV) there is a bidirectional movement of proteasomes along neurites (Hsu *et al.*, 2015). After axon specification at 3 DIV, however, there is an enhanced retrograde movement of proteasomes in the axon. Anterograde transport, on the other hand, remains unaffected suggesting that retrograde transport increases with axon length and development (Hsu *et al.*, 2015). In a different study, 10 DIV hippocampal neurons were shown to exhibit fast axonal transport when associated with membranous vesicles and certain motor proteins (Otero *et al.*, 2014). The majority of proteasomal transport, however, was found to be random and diffuse which only small proportion being long-range active transport (Otero *et al.*, 2014).

In regenerative PNS neurons, ligation of the sciatic nerve causes proteasome accumulation both at the proximal and distal site of the ligation, with the proximal being predominant (Otero *et al.*, 2014). This study points out that anterograde axonal transport of proteasomes plays a crucial role in the regenerative response mounted by PNS neurons. Importantly, a conditioning lesion further enhanced the amount of proteasomal machinery both *in vivo* and *in vitro* suggesting that improved regeneration is associated the delivery of more proteasomes into the axons of regenerating neurons (Verma *et al.*, 2005). This form of active anterograde axonal transport of proteasomes upon injury and even during development was not observed in adult CNS neurons (Verma *et al.*, 2005). Furthermore, blockade of UPS by lactacystin or N-acetyl-Nor-Leu-Leu-Al resulted in reduced ability of

injured axons to form a growth cone and therefore, impaired regeneration (Verma *et al.*, 2005).

The most current view on the role of the proteasome after injury is that the oxidative stress caused by the injury damages axonal proteasomes resulting in the accumulation of ubiquitinated proteins which in turn is deleterious to axon regeneration (Gong *et al.*, 2016). Taking into account that the dynamic balance between local protein synthesis and protein degradation is essential for axon regeneration after injury (Gumy, Tan and Fawcett, 2010), axonal redistribution of proteasomes with development and upon injury might play a crucial role in defining the regenerative response of an adult neuron.

3.3.2.3 Autophagosome

Autophagy plays a crucial role in the recycling of dysfunctional organelles and aggregated proteins (Kulkarni, Chen and Maday, 2018). In neurons, the majority of autophagy takes place in the soma. Therefore, retrograde axonal transport of autophagosomes (double-membranous structures enwrapping cellular components targeted for degradation) from the distal axon to the cell body is essential for neuronal homeostasis in both PNS and CNS axons (Hollenbeck, 1993; Maday, Wallace and Holzbaur, 2012; Maday and Holzbaur, 2014). Defective transport of autophagosomes has previously been associated with a number of neurodegenerative diseases such as Alzheimer's disease, Huntington's disease and amyotrophic lateral sclerosis (ALS) (Fu, Nirschl and Holzbaur, 2014). Fusion of autophagosomes with late endosomes in the distal axons triggers the recruitment of dynein motors which in turn transport the whole complex retrogradely (Cai *et al.*, 2010; Cheng *et al.*, 2015). During this trafficking event, autophagosomes fuse with lysosomes to form auto-lysosomes. The lysosomal acidic environment ensures that the cellular contents are degraded and recycled for further use. In order to ensure continuous retrograde transport of autophagosomes, a scaffold protein - JIP1, interacts with the autophagosome adaptor – LC3 to simultaneously activate dyneins and dephosphorylate kinesins (Fu, Nirschl and Holzbaur, 2014). This study reveals for the first time some of the tightly regulated mechanism behind distributing autophagosomes to the correct cellular compartments in

neurons. Interestingly, autophagosomal axon transport dynamics are not altered in a neurodegenerative model of protein aggregation in DRG neurons which possibly suggests that post-mitotic mature neurons are less efficient at upregulating this process after insult (Maday, Wallace and Holzbaur, 2012).

In the contest of injury, some autophagy markers were previously shown to be upregulated *in vivo* after peripheral and central nerve injury (Hou *et al.*, 2013; Liu *et al.*, 2015; Bisicchia *et al.*, 2017). In a recent study, activation of autophagy by the addition of a specific autophagy-inducing peptide – Tat-Bec or two other autophagy-inducing agents – rapamycin or spermidine in 1 DIV cortical neurons, enhanced axon growth and counteracted the negative influence of myelin when neurons were grown on a myelin substrate (He *et al.,*2016). This increase in neurite outgrowth was accompanied by increased microtubule stabilisation due to the degradation of microtubule-severing protein SCG10 as a result of increased autophagy. Microtubule stabilisation had previously been reported to be involved in axon regeneration as low doses of microtubule-stabilising drugs such as taxol, epothilone B or epothilone D result not only in attenuated fibrosis after injury, but also in improved axon growth and regeneration as well as in functional recovery (Erturk *et al.*, 2007; Hellal *et al.*, 2011; Ruschel *et al.*, 2015; Ruschel and Bradke, 2018). Furthermore, administration of the Tat-Bec peptide to a mouse model of spinal cord injury reduced the retraction of corticospinal neurons after injury and promoted the regeneration of another type of descending axons (serotonergic neurons) which resulted in mild functional recovery (He *et al*., 2016). The majority of autophagosomes in this system were found in the axon, so the inability of this treatment to promote regeneration of CST neurons after injury, might be a result of differential axonal transport, distribution and clearance.

Controversial to these findings, in a different study suppression of autophagy (by silencing ATG7 – autophagy-related gene 7) resulted in an increased neurite outgrowth in primary cortical neurons (Ban *et al.*, 2013). These discrepancies could be due to the duration and the timing of autophagy induction as well as differential targeting and transport of auto-phagosomes in CNS and PNS axons. For example, autophagy biogenesis was 4 times slower in the distal axon of hippocampal neurons compared to DRG neurons – a possible contributing factor for the differential regenerative ability of these two types of neurons (Maday and

Holzbaur, 2016). Interestingly, neuronal autophagy was found to be constitutively active unlike in other cell types where it is induced by starvation suggesting that it plays a role in balancing the protein synthesis and degradation (Maday and Holzbaur, 2016). Autophagosomes have also been reported to contain BDNF/TrkB signalling elements which are transported back from the distal axon to the cell soma in order to enhance survival and prevent neurodegeneration as well as to promote neuronal complexity in hippocampal neurons (Kononenko *et al.*, 2017).

Autophagosomes were also thought to interact with other membranous structures such as recycling endosomes and lysosomes near the growth cone (Farías *et al.*, 2017). Taking into account that some lysosomes were found to lack an acidic environment near the growth cone (Farías *et al.*, 2017). These findings suggest that autophagosomes might not necessarily only have a degradative function in the axon but might also be involved in the recycling of materials and membranes at the growth cone – an essential process during the remodelling of the growth cone and initiation of axon regeneration. Further studies are needed to clarify whether there is a developmental change in the transport and distribution of autophagosomes and their derivatives along axons with differential regenerative capacity.

3.3.3 Developmental decline in the axon transport of mRNAs

Over past several decades local axonal translation has been implicated as key for axonal growth and regeneration (Gumy, Tan and Fawcett, 2010). In order for neurons to produce a timely response to injury or any external cues, their axons need to have a continuous supply of mRNAs which can then be translated in a swift manner to produce the proteins needed for an appropriate response (Twiss *et al.*, 2000; Zheng *et al.*, 2001; Holt and Schuman, 2013; Terenzio *et al.*, 2018). Furthermore, additional evidence such as the quick formation of a growth cone in some regenerative axons *in vivo* (quicker than protein synthesis in the cell body and transport to the site of injury) (Pan *et al.*, 2003), the formation of growth cones in axons which have been disconnected from the cell body (Shaw and Bray, 1977; Verma *et al.*, 2005) and the presence of various translational machinery and mRNAs in the axon (Bleher and Martin, 2001; Jung, Yoon and Holt, 2012), point towards an essential role of this

process in the initiation of axon regeneration. Indeed, blockade of protein synthesis with inhibitors (anisomycin or cycloheximide) resulted in reduced ability of normally regenerative neurons such as embryonic sensory neurons to re-grow their axons but had little effect on weak regenerators such as adult RGC neurons after *in vitro* injury (Verma *et al.*, 2005). Many mRNAs have been detected in axons so far and their importance in growth cone formation and turning as well as in axon elongation and regeneration has been elucidated. For example, the axonal abundance and translation of beta-actin mRNA is required for successful axon regeneration of DRG neurons after *in vitro* axotomy as suppression of this mRNA by RNAi resulted in failure of growth cone regeneration (Vogelaar *et al.*, 2009). Other mRNAs such as importins, vimentin, STAT3A and KIF3C mRNAs are also essential for successful axon regeneration (Gumy, Tan and Fawcett, 2010; Gumy *et al.*, 2013).

mRNAs are produced in the nucleus where they bind to RNA-binding proteins (RBPs). RBPs are then packaged in glanular-like particles to be transported along the microtubule tracts to distant locations in the axon (Xing and Bassell, 2013). A recent study revealed some of the main molecular players in this process in retinal ganglion cells – mRNA-containing particles associated with Rab7-positive late endosomes which transported them and docked them to mitochondria (Cioni *et al.*, 2019). Late endosomes then acted like hotspots for *de novo* protein synthesis of mitochondrial proteins. This process was highly reliant on targeted transport along the axon and when Rab7 was mutated, protein synthesis in the axon was impaired resulting in mitochondrial defects and reduced cell viability (Cioni *et al.*, 2019). The study further supports the hypothesis that constitutive, targeted transport of mRNAs for local axonal protein synthesis is essential for survival, and possibly for regeneration.

Several studies recently provided evidence that the transport, distribution and function of mRNAs along the axons might differ in immature vs. mature neurons. Embryonic and adult DRG neurons which importantly have different regenerative capabilities, display the presence of different repertoires of mRNAs in their axons. One mRNA in particular – tubulin-beta3 (Tubb3) – encoding an essential-for-regeneration cytoskeletal protein was shown to be only present and locally translated in axons of immature DRG neurons (Gumy *et al.*, 2011). Tubb3's abundance and function in mature DRG neurons is entirely dependent on anterograde transport of the protein to growing axons (Gumy *et al.*, 2011). Furthermore,

higher abundance of ribosomal components and translational machinery before and after injury was observed in DRG neurons compared to RGCs both *in vivo* and *in vitro* suggesting that regenerative DRGs have increased capacity for local protein synthesis (Verma *et al.*, 2005). Anterograde transport of specific mRNA transcripts encoding cytoskeletal proteins was shown to be elevated after NGF or BDNF treatment in DRG neurons suggesting that axonal transport can be altered by signalling from external factors (Willis *et al.*, 2007). Another example is the enhanced anterograde transport of an ion channel involved in pain sensing (Trpv1) mRNA upon inflammatory response in the periphery (Tohda *et al.*, 2001). Interestingly, some mRNAs such as Creb mRNAs are specifically enriched in a particular type of neurons – sensory peripheral neurons but not in central neurons (Cox *et al.*, 2008).

Apart from very a specific spatial distribution throughout the cell, mRNAs also undergo temporal control. In an attempt to unravel the differences in mRNA transcripts over time, Zivraj and colleagues performed laser capture microdissection of growth cones in Xenopus either during their immature, growing state or in their synaptically-mature state (Zivraj *et al.*, 2010). They found that mRNA transcripts could be specifically target to the soma, the axon or the growth cone itself suggesting that there are active targeting mechanisms taking place. Moreover, they showed that some mRNAs such as EphB4 (ephrin B4 receptor) that are enriched at the growth cone in mature neurons, are actually abundant in both younger and older somas suggesting that there is a developmental regulation of these transcripts' transport down the axon (Zivraj *et al.*, 2010). Recently, mRNAs from mature and regenerating hippocampal neuron axons were isolated and 866 mRNAs were found to differentially distributed upon injury (Taylor *et al.*, 2009). This study also identified major differences in the mRNA transcripts present in regenerating axons after injury in the PNS and in the CNS (Taylor *et al.*, 2009). A key question remains: Does injury reactivate a developmental growth programme in the neuron instructed by changes in gene expression or does it simply cause changes in mRNAs axonal transport? In summary, the transport of mRNAs down the axon is a dynamic process with changes with development and after injury – tight regulation of this transport is essential for proper functioning and successful regeneration.

3.4 The virtuous cycle of axon growth

Over the past few decades, it has become clear that intrinsic mechanisms play an essential role in the regenerative failure observed in mature CNS neurons. As described above, a developmental change in CNS neurons exists whereby there is a reduced abundance and transport of growth-promoting molecules, organelles and mRNAs as well underactive signalling pathways accompanied by altered gene expression as a result of epigenetic modifications. We recently described the concept of the "virtuous cycle of axon growth" in a review paper elaborating on the possible mechanisms behind low regenerative CNS ability (Petrova and Eva, 2018). We speculated that at all times in neurons, there exists a cycle whereby changes in gene expression could activate growth-promoting pathways but also improve axonal transport of regeneration-associated cargo. Once this cargo reaches the growth cone, its interaction with the extracellular environment is enabled which in turn, results in retrograde signalling to the soma. These signals can then lead to a further enhancement of the growth-promoting program by amplification of transcription, translation and axon transport – a cycle which promotes virtuous axon growth (*Fig. 1.3).* We also proposed that this cycle of events could be targeted at any one point in order to enhance axon growth and regeneration after injury.

In this thesis, "the virtuous cycle of axon growth" is targeted at the level of anterograde axon transport of growth-promoting cargo to the tip of axons by activating the transport machinery involved in the process – in this case the adaptor protein protrudin (discussed below). A second strategy is to trigger gene expression changes in the nucleus with the use of transcription factors which could lead to enhanced regenerative program activation (discussed in detail in Chapter 6). Both strategies show promising results for enhancing axon regeneration in adult CNS neuron.

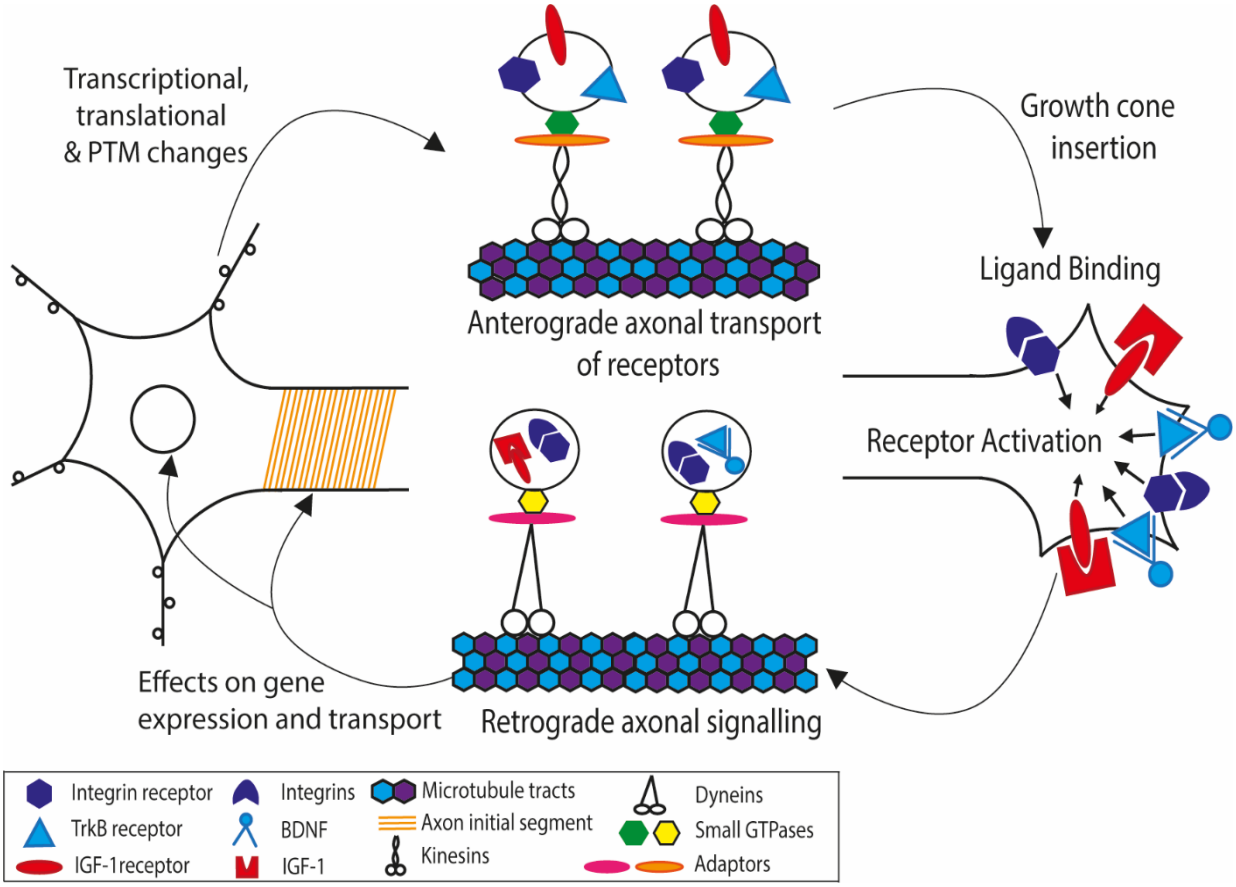

Figure 1.3 The "virtuous cycle of axon growth". A schematic diagram illustrating the cycle of events within a neuron which can enable growth and regeneration. For example, increasing the transport of growth-associated receptors in recycling endosomes facilitates their insertion in the growth cone, ligand binding and intracellular signalling cascades. Activated growth cone receptors triggers retrograde signalling in signalling endosomes to the cell body. A response is then evoked in the cell body resulting in gene expression changes and protein translation favouring a growth-promoting program. Retrograde signals from growth factor receptors can also stimulate anterograde transport (adapted from Petrova and Eva, 2018).

4. Protrudin – the linker

4.1 The protrudin protein and its domains

Protrudin, encoded by the ZFYVE27 gene is a member of the ZFYVE family of zinc-binding proteins. Protrudin is a peripheral membrane protein which contains several binding domains. The protein contains a Rab11-binding domain (RBD), 2 hydrophobic domains (TM-1 and TM-2), FFAT motif important for ER localisation, a coiled-coiled domain (CC) and a FYVE domain (a phosphoinositide-binding domain) (*Fig. 1.4A).* The protrudin protein is membrane-bound and could be found in endosomes, the endoplasmic reticulum (ER) or the plasma membrane. It has also been shown that the protrudin protein oligomerises in order to perform some of its main functions such as to aid neurite outgrowth (Pantakani *et al.*, 2011).

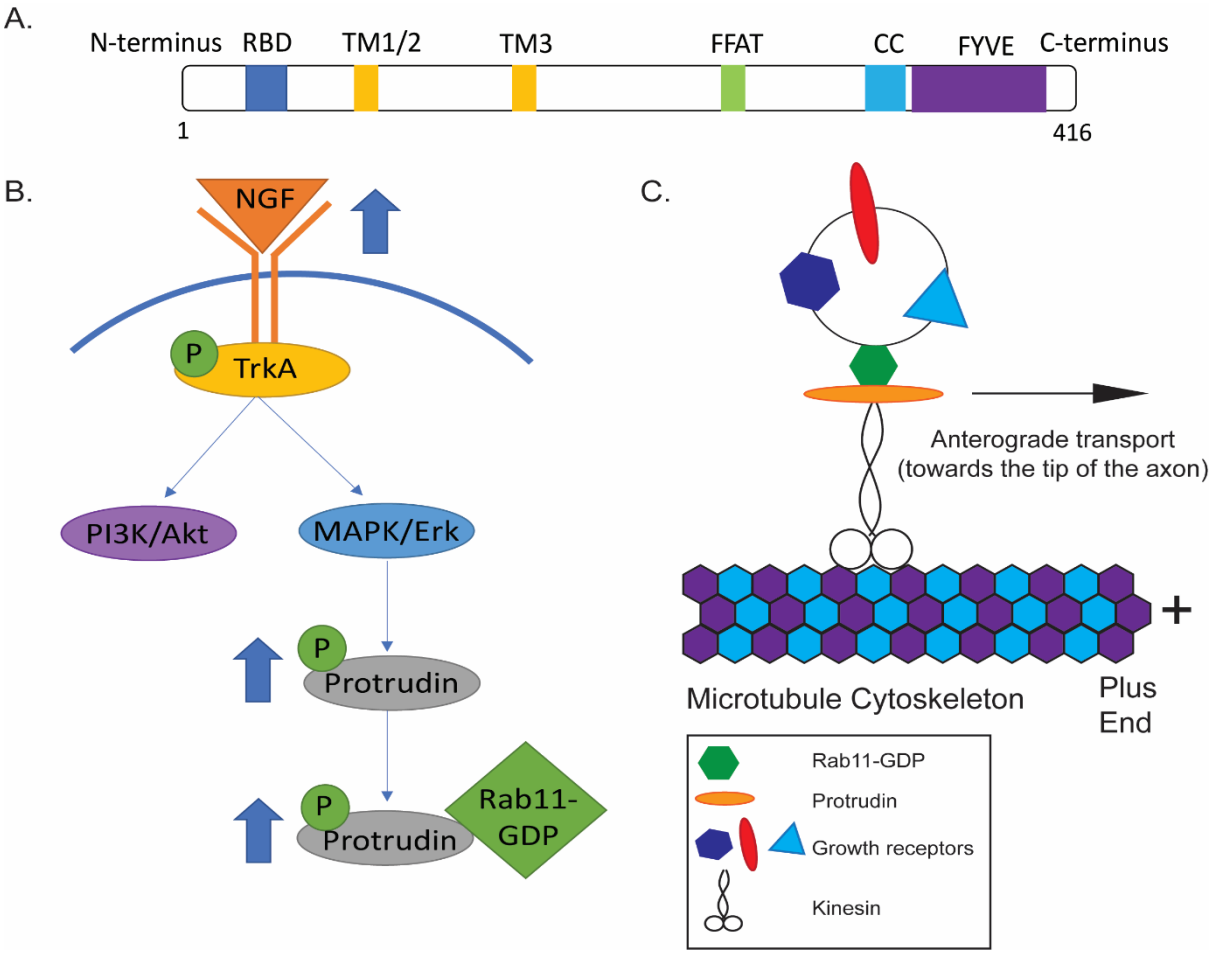

Figure 1.4 Figure summarising key features of the protrudin protein. A. Schematic diagram of the human protrudin protein domains. B. Schematic diagram showing the molecular pathway through which protrudin is phosphorylated in PC12 cells upon the addition of nerve-growth factor. Phosphorylation through the MAPK/ERK pathway leads to enhanced interaction of protrudin with Rab11-GDP specifically. C. Protrudin acts as a linker between motor proteins (kinesin 1) and Rab11-GDP-tagged endosomes carrying growth-associated molecules such as integrins and other growth receptors anterogradely towards the tip of neurites (modified from Welz, Wellbourne-Wood and Kerkhoff, 2014).

4.2 Protrudin's role in endoplasmic reticulum shaping and morphology

Protrudin is a membrane-bound molecule and possesses three transmembrane, hydrophobic domains (TM-1, TM-2 and TM-3) which allow its interaction with the lipid layer in cellular membranes. Two of protrudin's transmembrane domains are located close together (amino acids 67-87 and 89-109 in the human gene) and the third one (amino acids 180-214 with a Pro200 hairpin residue) suggesting that the protein forms hairpin structures in the membrane (Chang, Lee and Blackstone, 2013). Protrudin is a resident ER protein (Gil *et al.*, 2012) and was also found to localise with other tubular ER markers such as calnexin, REEP5 and atlastin proteins but not with sheet ER markers such as CLIMP-63 (Chang, Lee and Blackstone, 2013). Interestingly, deletion of all three transmembrane domains (ΔTM1-3) but not TM1 and TM2 or TM3 on its own results in translocation of the protrudin protein from the ER structures to the cytoplasm. Furthermore, depletion of protrudin by siRNA results in altered ER morphology with predominant sheet-like rather than tubular appearance – this phenotype was rescued by expressing siRNA-resistant wild-type protrudin but not a protrudin construct lacking the three transmembrane regions (Chang, Lee and Blackstone, 2013) once again emphasising the role of protrudin in ER morphology and shaping.

Another domain important for the interaction of protrudin with ER protein - VAP-A is the FFAT motif which represents two phenylalanine amino acids in an acidic tract. The FFAT domain (amino acid sequence of EFFDA***X***E, where ***X*** is any amino acid) is originally thought to act as an ER-targeting signal and is also found in other proteins which play a role in the transfer of lipids between the ER and other organelles such as the Golgi apparatus (Kawano *et al.*, 2006). The interaction between protrudin and VAP-A was initially identified in a proteomics study (Saita *et al.*, 2009) and was shown to be facilitated specifically by protrudin's FFAT domain as when the domain is fully deleted or mutated (D294A) at a residue important for protein interaction, the protrudin-VAP-A interaction is greatly reduced (Saita *et al.*, 2009).

4.3 Protrudin binding to phospholipids

As a member of the ZFYVE-family of membrane-binding proteins, protrudin contains a FYVE (Fab 1, YOTB, Vac 1, and EEA1) domain. However, unlike other proteins which contain a typical FYVE domain specifically binding phosphatidylinositol 3-phosphates (PtdIns(3)P), protrudin's FYVE domain preferentially binds phosphatidylinositol 4,5-bisphosphate (PtdIns(4,5)P_2), phosphatidylinositol 3,4-bisphosphate (PtdIns(3,4)P_2), and phosphatidylinositol 3,4,5-trisphosphate (PtdIns(3,4,5)P_3) (Gil *et al.*, 2012). Also contrary to typical FYVE domains which are localised to endosomes, protrudin's FYVE domain was found to be localised at the plasma membrane. Two cationic residues were shown to be particularly important for protrudin's specificity to vesicles containing the lipids listed above – lysine 367 and arginine 369 (Gil *et al.*, 2012). When mutated to aspartic acid, they result in the protrudin protein being removed from the plasma membrane. In addition, 3-phosphorylated phosphatidylinositol phosphates (PtdIns(3,4)P_2, PtdIns(3,4,5)P_3) were specifically shown to be involved in protrudin's recruitment to the plasma membrane, whereas PtdIns(4,5)P_2 played a role in its localisation to endosomes (Gil *et al.*, 2012). Interestingly, full deletion of the FYVE domain resulted in protrudin's localisation to the ER suggesting that this process is driven by protein interaction rather than lipid interaction.

In summary, the presence of all of the above domains in the protrudin protein suggests that protrudin's physiological function most likely revolves around the process of membrane trafficking and recycling.

4.4 Protrudin and spastin in disease

A protrudin mutation (p.G191V) was recently identified in a single German family with a high incidence of autosomal dominant hereditary spastic paraplegia (HSP), a condition characterised by a progressive distal axonopathy (Mannan *et al.*, 2006). Interestingly, another protein - spastin (a microtubule-severing protein) which is also a binding partner of protrudin is the most commonly mutated protein in HSP (Martignoni, Riano and Rugarli, 2008) . The mutation of protrudin identified in HSP (p.G191V) is located near the third transmembrane domain and was functionally studied by creating the same mutant protrudin in the form of a

DNA construct and introducing it to HeLa cells. In that case, the missense mutation caused abnormal interaction with spastin and protrudin's localisation to abnormal tubular structures around the cell (Mannan *et al.*, 2006). The overexpression of the same construct in PC12 cells, did not however, compromise protrudin's effects on neurite outgrowth upon NGF treatment (Zhang *et al.*, 2012). In addition, injection of mutant protrudin into zebrafish embryos resulted in altered distribution and some defects in the yolk sac expansion but there was no effect on developmental axon growth in this model or in PC12 cells (Zhang *et al.*, 2012). Mutant protrudin was also not found to alter protrudin's preferential binding to Rab11-GDP and its ability to induce neurite outgrowth when overexpressed in HeLa cells. These findings suggested that the mutation does not result in a loss of function of the protein (Martignoni, Riano and Rugarli, 2008). The same mutation was also previously identified as a single nucleotide polymorphism present in the general population which is not pathogenic (Martignoni, Riano and Rugarli, 2008). Therefore, protrudin's involvement in human HSP is yet to be elucidated.

In a recent paper, a novel role for protrudin as a central network protein involved in ALS disease pathogenesis was identified (Dervishi *et al.*, 2018). In this study, ingenuity pathway analysis was performed on genes whose mutations have previously been identified as causative or disease-modifying in ALS and their known binding partners in mammalian CNS neurons. 1105 proteins were identified from this screen which allowed for the discovery of upstream regulators. Protrudin was identified as a key upstream regulation of this network and was found to be aberrantly upregulated in the soma of Betz cells from ALS patient brains (Dervishi *et al.*, 2018). In these cells, protrudin accumulated in the cytoplasm and was no longer associated with the ER, which the authors speculate could contribute to ER dysfunction and ER stress which is one of the main causes for neuronal cell death in ALS motor neurons (Dervishi *et al.*, 2018). In summary, this paper suggests that protrudin might be a core protein linking dysfunctional ER dynamics and protein trafficking and could be a potential target for improving motor neuron viability.

4.5 Protrudin's role in neurite outgrowth and directional trafficking

Endogenous protrudin readily interact with endogenous Rab11 in PC12 cells and the two proteins colocalise 6 hours post nerve growth factor (NGF) treatment in the tip of growing neurites (Shirane and Nakayama, 2006). Although protrudin contains a Rab11-binding domain, this domain is not conserved for binding to Rab11-GTP (guanosine triphosphate). On the contrary, it contains amino acid sequences very similar to GDI-α and GDI-ß, both of which readily interact with Rab11-GDP (guanosine diphosphate). Immunoprecipitation experiments using mutant forms of Rab11 such as Q70L (GTP-bound form due to interrupted GTPase activity) and S25N (GTP-binding deficient) revealed that although protrudin binds to wild-type Rab11, it preferentially binds to Rab11-GDP demonstrated by enhance interaction with S25N mutant (Shirane and Nakayama, 2006). Furthermore, this interaction was potentiated by the addition of NGF or by constitutively activating the mitogen-activated protein kinase (MAPK) pathway, suggesting the phosphorylation of protrudin is essential for its interaction with Rab11-GDP (*Fig. 1.4B, 1.4C).* Indeed, when putative MAPK phosphorylation sites on the protrudin molecule were mutated so they could not be phosphorylated the interaction between Rab11-GDP and protrudin was markedly reduced (Shirane and Nakayama, 2006). These findings suggest a role of protrudin in directional membrane trafficking in growing processes.

One of protrudin's functions in the cell is to aid neurite outgrowth. When FLAG-protrudin is overexpressed in HeLa cells, 5-30% of cells form growing protrusions highly resembling ruffling lamellipodia (Shirane and Nakayama, 2006)s. Furthermore, when exogenous protrudin is applied to rat hippocampal neurons at 1 DIV, the neurons extend longer neurites 48 hours post transfection. As mentioned above, when NGF is applied to PC12 cells, it results in phosphorylation of protrudin, which in turn leads to increased interaction with Rab11-GDP and protrudin's redistribution from the somatodendritic compartment to the tip of growing neurites, carrying important cargos such as NgCaM (a cell adhesion molecule) with it (*Fig. 1.4C)* (Shirane and Nakayama, 2006). Downregulation of protrudin expression by RNAi in either cortical neuronal cultures or PC12 cells prevents the extension of long neurites (Shirane and Nakayama, 2006). This suppression could be rescued by administering the wild-type form of the protein but not a mutant form where the Rab11-binding domain is deleted

suggesting that the interaction between protrudin and Rab11-GDP is essential for neurite extension. Interestingly, FKBP38 (a member of the immunophilin protein family) acts as an inhibitor of protrudin phosphorylation and hyperphosphorylation of protrudin in FKBP38-/- mice resulted in abnormal extension of nerve fibres (Shirane *et al.*, 2008).

Transport mechanisms of cargo are tightly regulated in order to ensure proper functioning of the cells and successful neurite outgrowth. In the above experiments, the protrudin-Rab11 complex was shown to move anterogradely towards the tip of growing neurites suggesting that protrudin might be interacting with proteins from the kinesin family. Indeed, recent proteomics studies have identified KIF5A, a member of the Kinesin 1 family of motor proteins which is also involved in anterograde transport of membrane-associated vesicles, as another binding partner of protrudin (Matsuzaki *et al.*, 2011). Rab11, KIF5 and protrudin have all been shown to colocalise at the tip of growing processes in HeLa cells. Matsuzaki *et al.,* 2011 showed that protrudin actually serves as an adaptor protein which links KIF5A to Rab11-bound recycling endosomes and that proper functioning of the KIF5-Protrudin-Rab11-GDP complex results in displacement of cargo molecules to the tip of growing neurites. Suppressing KIF5 in HeLa cells using shRNA approach, inhibit the protrusion-forming functions of protrudin suggesting the KIF5 is necessary for protrudin's function in neurite outgrowth (Matsuzaki *et al.*, 2011). A mutant form of protrudin that lacks amino acids 324–344 and does not bind to KIF5A, did not promote the binding of Rab11-GDP to KIF5A and resulted in reduced neurite outgrowth. Furthermore, this inhibition results in the accumulation of protrudin and Rab11 but also of other proteins involved in the complex such as reticulon 3, VAP-A, VAP-B and Surf4 in the soma of cultured hippocampal neurons (Matsuzaki *et al.*, 2011). These experiments suggest that protrudin docks Rab11-associated vesicles transporting all sorts of molecules along neurites to anterograde motor proteins (in this case, KIF5) in order to ensure their transport to the tip of growing process and to aid neurite outgrowth.

Furthermore, protrudin's effect on neurite outgrowth seems to be facilitated not only by directional trafficking but also by several other processes. Some of the domain mutants mentioned above have been shown to affect neurite outgrowth. For example, if FFAT mutants (either missing the whole domain or the D294A mutant) are overexpressed in HeLa cells, the

percentage of cells extending neurites is significantly reduced compared to the overexpressing the wild-type (Saita *et al.*, 2009). Similarly, if VAP-A is depleted by shRNA in PC12 cells, protrudin-induced neurite outgrowth is suppressed and this also resulted in failure of protrudin translocation from the somatodendritic compartment normally seen upon NGF addition (Saita *et al.*, 2009). These studies suggest that VAP-A has an effect on protrudins localisation and that the VAP-A protrudin interaction is necessary for neurite outgrowth. In addition, mutations in the FYVE domain at two critical residues (K367 and R369) or deletion of the whole FYVE domain which result in decreased affinity for lipids, prevent the enhancement of neurite outgrowth normally seen with wild-type protrudin in primary hippocampal neurons (Gil *et al.*, 2012). In another report, however, after a series of rescue experiments with different mutants of protrudin, the N-terminus of protrudin was pointed out as essential for its neurite outgrowth properties and not the FYVE domain (Zhang *et al.*, 2012). This discrepancy leaves the involvement of the FYVE domain in protrudin's neurite outgrowth function still elusive.

Another important interaction of protrudin which is further required for its properties on neurite outgrowth is its interaction with the microtubule-severing protein – spastin. Co-expression of spastin and protrudin had an even more pronounced effect on driving neurite outgrowth, than protrudin on its own (Zhang *et al.*, 2012). While protrudin alone or protrudin and spastin overexpression rescued neurite outgrowth upon NGF treatment in PC12 cells which have been depleted of the two proteins, spastin was unable to do so. These experiments suggest that spastin might help promote protrudin-driven neurite outgrowth in the cells.

In summary, the protrudin protein plays an important role in membrane transport and trafficking as well as in neurite outgrowth in several cellular models. In this thesis, the interaction of protrudin with Rab11-positive endosomes is studied as a novel mechanism to enhance regenerative ability of CNS axons by delivering growth molecules to the distal axon. Phosphorylated protrudin has been shown to be particularly important for the anterograde movement of this complex which is the basis for our *Hypothesis* below.

II. Aims and Hypothesis

Hypothesis

Constitutive phosphorylation of protrudin will result in increased association with Rab11-GDP which in turn will increase anterograde axon transport. When applied to primary cortical neurons, this system will result in more growth-associated cargo being transported to the tip of injured axons, subsequently resulting in improved regeneration.

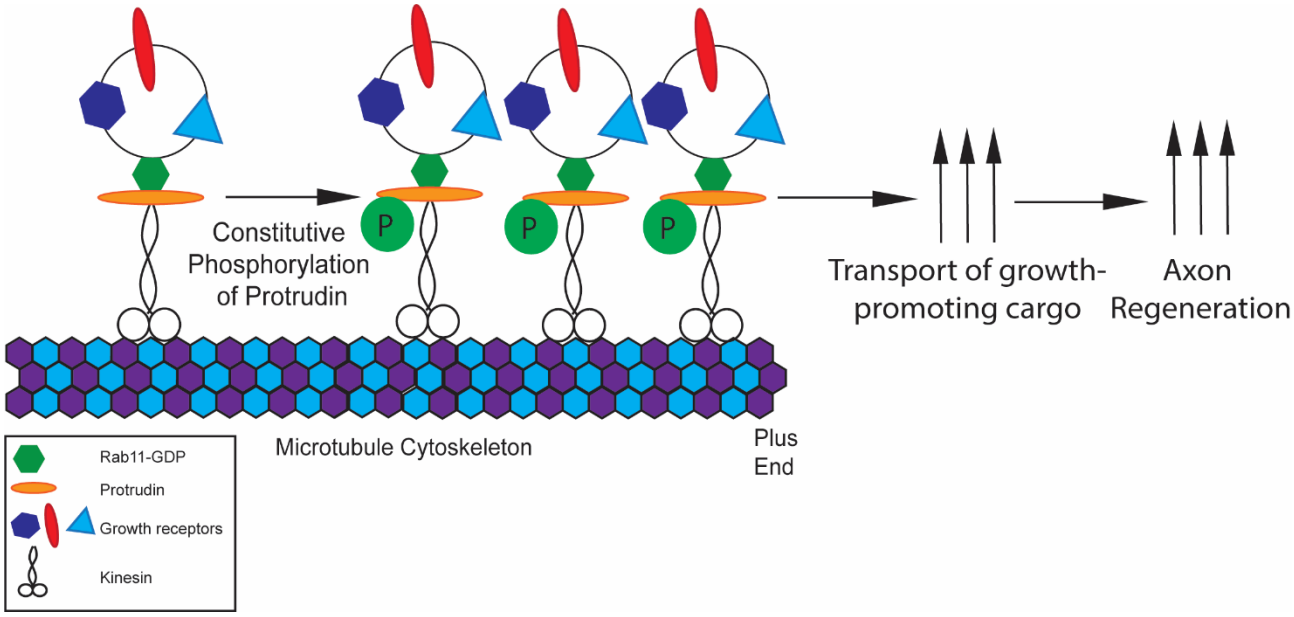

Aims

1. To investigate protrudin's localisation in developing neurons and upon injury
2. To create constitutively activated phosphomimetic forms of protrudin by altering amino acids at six putative ERK-phosphorylation sites.
3. To investigate the effects of constitutively active protrudin on Rab11-mediated transport into axons, and whether these can serve to improve axon regeneration after injury in primary cortical neurons *in vitro* and in an *in vivo* model of optic nerve crush
4. To investigate the neuroprotective effects of protrudin in a chronic model of glaucoma in rats
5. To investigate the mechanisms of protrudin action on axon regeneration

CHAPTER II: METHODS

1. Plasmids, antibodies and reagents

1.1 Plasmid constructs

Protrudin constructs (in pmCherry-C1 and pEGFP-C1 vectors) were a kind donation by Dr Evan Reid, Cambridge Institute for Medical Research. The control GFP plasmid was pHR-sinUbEM-GFP with GFP under SFFV promoter and Emerald under ubiquitin promoter. The control mCherry plasmid was pmCherry-C1 empty plasmid vector. CMV-Rab11-GFP construct was kind donation from Dr Jim Norman, Beatson Institute, Cancer Research UK. CMV-integrin-alpha9-GFP constructs were purchased from Addgene, deposited by Dean Sheppard (University of California, San Francisco, CA). Viral vector plasmid backbones (AAV2-sCAG-GFP) and CRISPR-backbone plasmid (pAAV-SYN-SaCas9-hU6-sgRNA) were a kind donation by Prof. Joost Verhaagen, The Netherlands Institute for Neuroscience. CRISPR sgRNA sequences against rat protrudin were designed by Bart Nieuwenhuis, Cambridge Centre for Brain Repair (*Table 2.1*). 4 unique 29-mer shRNA constructs (*Table 2.1*) against rat protrudin in retroviral vector with GFP tag were purchased from OriGene (catalogue number: TG713727).

Name	Sequence
Protrudin-1 sgRNA	GATGCAGTCTTCGGATCGGGAC
Protrudin-2 sgRNA	GGTACAGGGCTTGTCTGCAGCG
Protrudin-3 sgRNA	GGGCGGATGAGCCCCAAGCAGG
TG713727A (shRNA_A)	GTGTGCCTCCTGTAATCAGACCTTGAGCA
TG713727B (shRNA_B)	TACCACAGCGTGCGGCAGGAAGACCTGCA
TG713727C (shRNA_C)	TTCAACCTGGTTCTGTCCTACAAGAGGCT
TG713727D (shRNA_D)	CAACATCTTGTTCCTCACTCTGAATGAGG

Table 2.1 A table showing the target shgRNA sequences in CRISPR constructs (Protrudin-1 sgRNA, Protrudin-2 sgRNA, Protrudin-3 sgRNA and target shRNA sequences for shRNA constructs (TG713727A, TG713727B, TG713727C, TG713727D).

Transcription factor constructs were kindly provided by Prof. Joost Verhaagen, The Netherlands Institute for Neuroscience (ATF3, CEBP, Sox11, Egr constructs), Dr Lawrence Moon, King's College London (pCMV-SPORT6-sox4 construct) and Prof. Vance Lemmon and Prof. John Bixby, University of Miami (STAT3ACA constructs). REST transcription factor construct (pHR'-NRSF-CITE-GFP construct) was obtained from AddGene (plasmid #21310). Pou6f1 construct was obtained (Myc-DDK-tagged) was purchased from OriGene.

1.2 Antibodies

1.2.1 Primary antibodies

Rabbit polyclonal anti-ZFYVE27 (ProteinTech, 126801-AP, 1:500), rabbit polyclonal anti-tropomyosin-1 (Abcam, ab55915, 1:100); chicken polyclonal anti-68kDa-neurofilament (Abcam; ab134460, 1:1000); rabbit polyclonal anti-MAP1A (Abcam, ab89648, 5mg/µL), rabbit polyclonal anti-doublecortin (Abcam, ab18723, 5mg/µL); rabbit monoclonal anti-TUBA4A (Abcam, ab177479, 1:100); rabbit polyclonal anti-tropomyosin 4 (EMD Millipore, AB5449, 1:500); rabbit polyclonal anti-REEP5 (ProteinTech, 14643-1-AP, 1:100); chicken polyclonal anti-MAP2 (Abcam, ab5392, 1:800); mouse monoclonal pan-neurofascin (NeuroMab, 75/12 AR-18, 1:100); mouse monoclonal anti-CGRP (Abcam, ab81887, 1:100); rabbit polyclonal anti-OMgP (Abcam, ab101567, 1:1000); rabbit polyclonal anti-Vangl2 (Merck, ABN373, 1:500); mouse monoclonal anti-mCherry (Clontech, 632543, 1:250); rabbit polyclonal anti-ATF3

(SantaCruz, Sc-188, 1:500), mouse monoclonal anti-spastin [Sp 6C6] (Abcam, ab77144, 1:500); rabbit polyclonal anti-Rab11 (ThermoFisher Scientific, 71-5300, 1:50), rabbit polyclonal anti-integrin alpha 5 (Chemicon International, AB1928, 1:500), rabbit polyclonal anti-GFP CHIP grade (Abcam, ab290, 1:1000), rabbit polyclonal anti-mCherry (Abcam, ab167453, 1:800); rabbit polyclonal anti-v5 tag (Bioss, bs-2109R, 1:200); rabbit polyclonal anti-v5-647 conjugated (Bioss, bs-2109R-A647, 1:200); mouse monoclonal anti-HA tag (BioLegend, 901501, 1:200), goat polyclonal anti-Brn3a (C-20) (Santa Cruz, sc-31984, 1:200).

1.2.2 Secondary antibodies

Goat anti-rabbit Alexa®Fluor 488 (Abcam, ab150077, 1:800), donkey anti-rabbit Alexa®Fluor 568 (Life Technologies, A10042, 1:800), goat anti-rabbit Alexa®Fluor 647 (Life Technologies, A27040, 1:800), goat anti-mouse 405 (Life Technologies, A31553, 1:200), donkey anti-mouse Alexa®Fluor 488 (Life Technologies, A21202, 1:800), goat anti-mouse Alexa®Fluor 568 (Life Technologies, A11004, 1:800), goat anti-mouse Alexa®Fluor 660 (ThermoFischer Scientific, 10103852, 1:200), goat anti-chicken Alexa®Fluor 488 (Life Technologies, A11039, 1:800), goat anti-chicken Alexa®Fluor 647 (Abcam, ab150171, 1:800), mouse monoclonal anti-beta actin (C4) HRP conjugated (Santa Cruz, sc-47778, 1:5000), goat anti-mouse IgG HRP conjugated (Sigma, A9917, 1:80000), goat anti-rabbit IgG HRP conjugated (Sigma, A4914, 1:80000), mouse monoclonal Living Colours anti-mCherry (Takara, 632543, 1:250), mouse monoclonal Living Colours anti-dsRed (Takara, 632392, 1:250), donkey anti-rabbit IgG biotinylated (GE Healthcare, RPN1004V, 1:500), streptavidin Alexa®Fluor 647 (ThermoFischer Scientific, S21374, 1:200).

1.3 Reagents and materials

1.3.1 Media and Solutions

The following media was used: Hank's Balanced Salt Solution (HBSS) without Ca^{2+} and Mg^{2+} (Gibco, 14170-088), Dulbecco's Modified Eagle Medium (DMEM) (Gibco, 41966-029), MACS Neurobasal Media (Miltenyi Biotech, 130-093-570, RPMI 1640 media (with sodium bicarbonate, without L-glutamine) (Sigma, R0883).

1x phosphate buffered saline (PBS) was made from communal 10x PBS lab stock and filter sterilised (pH=7.4). 1x Tris non-saline buffer (TNS) (pH=7.6) was prepared from 10x TNS stock (30g Trizma-base in 500 mL ddH20). 1x Tris buffered saline with Tween 20 (TBST) (pH=7.5) was prepared from 10x TBS stock (24.23g Trizma-base, 87.66g sodium chloride in 1L ddH20) with the addition of 0.5 mL of Tween 20. Mild glycine stripping buffer (pH=2.5) was prepared by dissolving 7.509g of glycine in 500 mL ddH20 and adding 0.25 mL of Tween 20. 0.1M borate buffer contained 2.48 g boric acid and 3.8g sodium tetraborate decahydrate, dissolved in 800 mL of ddH20 (pH=8.5).

1.3.2 Chemical reagents

Collagen Type IV from human placenta (Sigma Aldrich, C5533-5MG) was dissolved in 10 mL ddH20 containing 25 µL of acetic acid, and was then filter sterilised and kept at 4°C. Foetal Bovine Serum (FBS) (Biosera, FB1280/500, French Origin) was used in PC12 cells culture media. Foetal Bovine Serum (Invitrogen, 10500064) was used for all other experiments. Nerve growth factor (NGFß from rat) (Sigma, N2513-0.1MG) was reconstituted with sterile PBS containing 0.1% bovine serum albumin (BSA) to a final concentration of 1 mg/mL. DNAase (Sigma Aldrich, D5025) was diluted to 0.01% solution in HBSS without Ca^{2+} and Mg^{2+}. Poly-D-lysine (Sigma, D1149-100MG) was dissolved in ddH20 to stock concentration of 2 mg/mL.

A list of other reagents which did not require reconstitution: 0.05% Trypsin-EDTA (Fischer Scientific, 11580626); magnetofection transfection reagents (Neuromag, NM50200); GS21 neuronal supplement (AMSBIO, gsm.3100), Papain (Warthington, LK003178, 5 vials); Glutamax supplement (Thermofisher Scientific, 3505-060); HEPES (Sigma Aldrich, 15630-056, 1M); SOC Media (Thermofisher Scientific, 15544-034); DMSO (Sigma Aldrich, D5879), Geneticin (Gibco, G418); Penicillin/Streptomycin/Fungiezone (PSF) (Life Technologies, 15240-062); L-Glutamine (200mM, ThermoFischer Scientific, 25030081); Triton X-100 (Sigma Aldrich, X100); Kanamycin (Sigma Aldrich, K0254), Ampicillin (Sigma Aldrich, A5354); 36% paraformaldehyde (TAAB Laboratories).

1.3.3 Materials

Cell strainers (40 µm) (Falcon, 352340) were used for primary cortical culture. Primary neuronal cultures were grown on CELLView glass-bottom culture dishes (Greiner Bio-One,

627860). 18mm coverslips were used for mounting of live cell imaging dishes (MatTek Coorporation, PCS-0-18).

2. Cell Culture and Transfections

2.1 Primary Cortical Neurons

Cortical neurons were dissected from E18 Sprague Dawley rat embryos and plated on imaging dishes or on acid-washed glass coverslips at the following densities: $1x10^5$cells/dish for immunocytochemistry, $2x10^5$ for axotomy or live-cell imaging and $8x10^4$cells/coverslip. All surfaces were coated with poly-D-lysine, diluted in borate buffer to a final concentration 50 µg/mL. The cells were grown in serum-free MACS Neurobasal Media supplemented with 2% GS21 and 1% GlutaMAX supplements at 37°C in 7% CO_2 incubator. The media was not changed during the incubation period.

Cortical neurons (1 DIV) on imaging dishes were transfected using lipofectamine 2000 reagent (ThermoFisher Scientific) as follows: 10.8µg of DNA plasmid were mixed with 1.2 mL NB media and 19.8 µL lipofectamine 2000. The reaction was kept for 30 minutes at room temperature and then added to the cells which were in 2 mL of freshly warmed-up NB media supplemented with GlutaMAX for 1 hour at 37°C. The transfection media was then removed, and the original media was transferred back to the imaging dishes. Plasmid reporter gene expression was observed 48 hours post-transfection. Cortical neurons (7 DIV onwards) on imaging dishes were transfected using NeuroMag magnetofection system where 7µg of DNA plasmid is mixed with 100µL NB media and 8µL of magnetic beads. The reaction was kept for 30 minutes at 37°C before adding 900µL of pre-warmed NB media to a final volume of 1 mL. The original neuronal media was removed, and 1 mL of transfection mixture was added. Dishes were then incubated at 37°C for 30 minutes on a magnetic plate before the original media was returned on the plates. Plasmid reporter gene expression was observed 48 hours post-transfection.

2.2 Pheochromocytoma cells (PC12s)

PC12 cells were maintained in T75 flasks coated with collagen type IV in RPMI-1640 media supplemented with 1% L-glutamine, 10% foetal bovine serum and PSF. The media was changed every 2 days. When 80-90% confluent, the cells were dissociated by removing the media, washing with PBS (1x) and adding 4 mL of 0.05% Trypsin-EDTA for 3-5 minutes at 37°C. The reaction was then stopped by the addition of 4 mL of warm cell culture medium. The cells were spun down at 800 rpm for 5 mins. Excess liquid was removed, and the pellet was resuspended in 5mL of cell culture media – 1 mL was plated to a newly coated flask containing warm media and the rest was frozen in 1 mL aliquots in 10% DMSO in FBS at -80°C. PC12 cells were transfected using microporator MP-100 and the Neon® Transfection System (Invitrogen) as previously described (Covello *et al.*, 2014).

2.3 HeLa cells

HeLa cells were grown in 6-well plates in DMEM media supplemented with 10% FBS and PSF. The media was changed every 2 days. When 80-90% confluent, the cells were dissociated by removing the media, washing with PBS (1x) and adding 2 mL of 0.05% Trypsin-EDTA for 3-5 minutes at 37°C. The reaction was then stopped by the addition of 4 mL of warm cell culture medium. The cells were spun down at 800 rpm for 5 mins. Excess liquid was removed, and the pellet was resuspended in 5 mL of cell culture media. Cells were frozen in 1 mL aliquots in 10% DMSO in FBS at -80°C. HeLa cells were transfected using the TransIT-HeLaMONSTER transfection kit (Mirus Bio) and the TransIT-LT1 transfection kit (Mirus Bio) following the company's protocol.

3. Cloning

3.1 Site-directed mutagenesis

The wild-type human protrudin protein (in pmCherry-C1 construct) was mutated using Quick II-Site Directed Mutagenesis kit (Agilent Technologies). Forward and reverse

mutagenesis primers containing each of the desired mutations were designed using the Agilent Technologies primer design tool. A PCR reaction was then carried out using each set of mutagenesis primers and the non-mutated protrudin construct using the PCR quantities and parameters in *Fig. 2.1*.

A.

Reagent	Quantity (µL)
10x Reaction Buffer	10
Plasmid DNA (10 ng/µL)	1
Primer 1 (100 ng/µL)	1
Primer 2 (100 ng/µL)	1
dNTP mix	1
ddH_2O	40
PfuUltra HF Polymerase (2.5U/10 µL)	1

B.

Step	Number of Cycles	Temperature (°C)	Time
1	1	95	30 sec
2	18	95	20 sec
		62	10 sec
		68	6 min
3	1	4	∞

C.

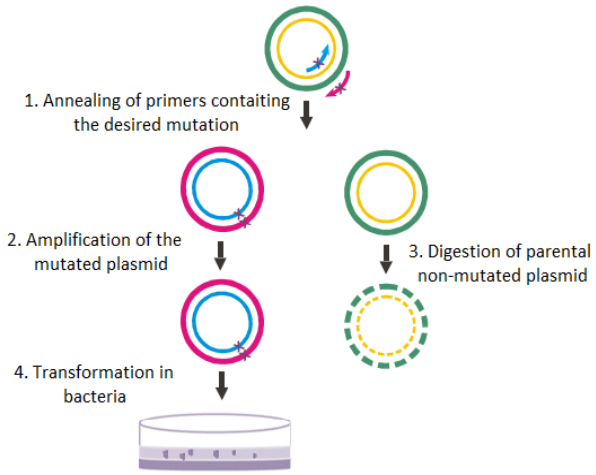

Figure 2.1 A figure outlining the mutagenesis process, the PCR parameters used and the final mutant products of the human protrudin gene. A) The quantities of PCR reagents used (in µL) for a single mutagenesis reaction. B. A table showing the cycling PCR parameters used in all reactions. C. A step-by-step schematic representation of the mutagenesis process (adapted from Agilent Technologies).

The PCR reaction was then treated with 1µL of DpnI enzyme for 1 hour at 37°C. The DpnI enzyme recognises and digests the parental methylated and non-mutated plasmid so it is able to select for the newly synthesizes mutated plasmid. Once the parental DNA is digested, 2 µL of the PCR reaction were transformed in XL-10 Gold Ultracompetent bacteria and grown on agar plates containing kanamycin (1:1000 concentration) for 18 hours overnight. Colonies were then picked and grown in LB medium containing kanamycin overnight. The plasmid DNA was purified using Qiagen Mini Prep kit and sent for sequencing. This method was used to create two constitutively phosphorylated forms of protrudin as well as the following functional mutants - ΔFYVE and ΔFFAT (*Fig. 2.2*) (described in *Chapter 3, 4 and 5*).

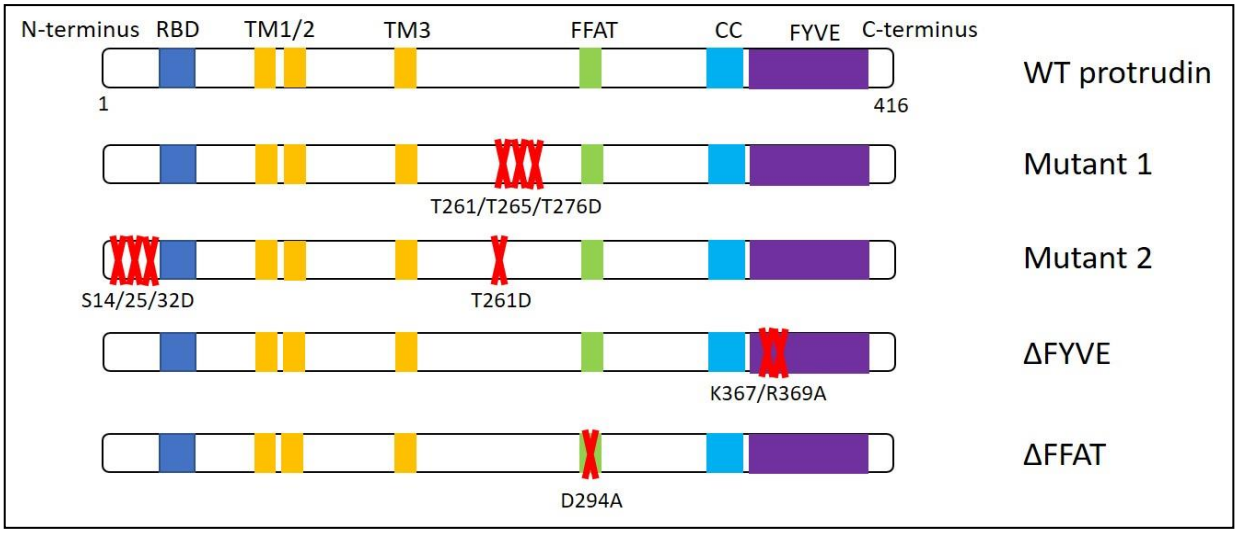

Figure 2.2 A schematic diagram of protrudin mutants created by site-directed mutagenesis. The protrudin protein contains multiple domains – RBD (Rab11-binding domain) (dark blue), TM1 and TM2 (two hydrophobic domains) (yellow), FFAT (ER-targeting domain) (green), CC (coiled-coil domain) (light blue) and FYVE (phospholipid-binding domain) (purple). Two phosphomimetic forms were created at 6 putative ERK phosphorylation sites important for its interaction with Rab11 by converting threonine and serine amino acids to aspartic acid (described in more detail in *Results*) (Shirane et al., 2006). ΔFYVE and ΔFFAT domain mutants were create by substitution of lysine (367) and arginine (369) for alanine and aspartic acid (294) for alanine respectively (Saita *et al.*, 2009; Gil *et al.*, 2012).

3.2 Gibson Assembly Cloning

Gibson assembly (GA) cloning was performed as described in (Gibson *et al.*, 2009). Cloning primers were designed using the NEBuilder Tool and the annealing temperature for pairs of primers was derived using the NEB Tm Calculator. A PCR reaction was then carried out as described (*Fig. 2.3*) and the PCR products were analysed on an agarose gel. The correct size fragments were then cut out from the gel and purified using the Wizard® SV Gel and PCR Clean-Up System (Promega, UK). The DNA fragments were then assembled using the Gibson Assembly® Master Mix (New England Biolabs, Inc.) for 1.5 hours at 50°C in the following quantities: 50ng of insert DNA was mixed with 25ng of vector DNA and 10 µL of the Master Mix and the reaction was complimented with distilled water to final volume of 20 µL. The reactions were then transformed in XL-10 Gold Ultracompetent bacteria and grown on agar plates containing kanamycin (1:1000 concentration) for 18 hours overnight at 37°C. Colonies were then picked and grown in LB medium containing kanamycin overnight. The plasmid DNA was purified using Qiagen Mini Prep kit and the sequence was confirmed by DNA sequencing.

The DNA was amplified by using Qiagen Endo-free Maxi Prep kit. This cloning method was used for several purposes (described below).

A.

Reagent	Quantity (µL)
Q5 Reaction Buffer	10
40mM dNTPs	0.25
Primer 1 (100µM)	0.25
Primer 2 (100µM)	0.25
Template DNA (200ng/µL)	0.5
Q5 DNA Polymerase	0.5
GC Enhancer	10
ddH2O	28.7

B.

Cycle number	Temperature (C)	Time Interval
1x	98	30s
35x	98	8s
	Primer specific	45s
	72	2 mins
1x	72	10 mins
1x	4	∞

C.

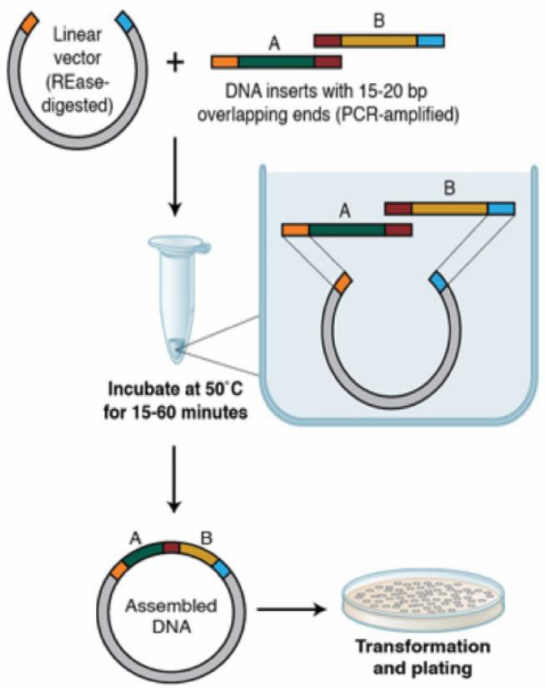

Figure 2.3 Figure outlining the Gibson Assembly cloning process and the PCR parameters used. A. The quantities of PCR reagents used (in µL) for a single mutagenesis reaction. B. A table showing the cycling PCR parameters used in all reactions. C. A step-by-step schematic representation of the cloning process (adapted from Gibson, 2011).

3.2.1 Promoter Cloning

Initially, DNA constructs contained the cytomegalovirus promoter (CMV promoter). However, after several attempts to transfect these plasmids into primary cortical neurons at 10 DIV, very low transfection rates were observed (5-10/100 000 cells). In addition, many non-neuronal cells were also transfected. Therefore, a neuron-specific promoter (synapsin) was cloned into all protrudin, Rab11 and integrin constructs to achieve better transfection efficiency and specificity of cortical neurons. Transfection efficiency was increased 10x after promoter change and very few or no non-neuronal cells were transfected.

3.2.2 Protrudin Mutants Cloning

GA cloning was also used to create ΔRBD, ΔSpastin, ΔKIF5 and ΔER domain mutants of protrudin (*Fig. 2.4)* (described in *Chapter 5*).

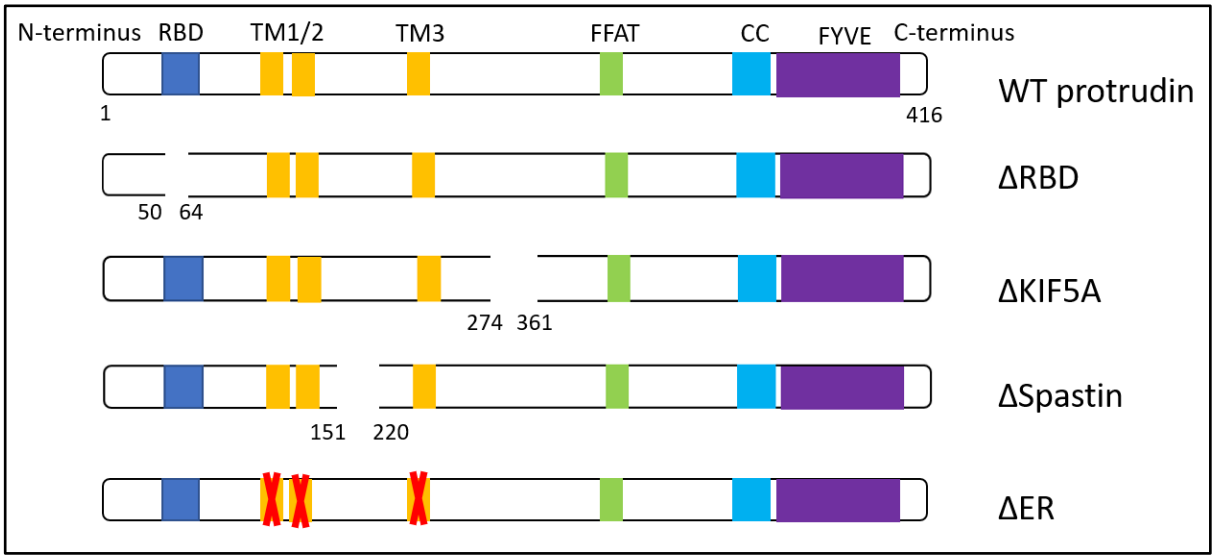

Figure 2.4 A schematic diagram of protrudin mutants created by Gibson Assembly cloning. Rab11-binding domain mutant (ΔRBD) was created by deleting amino acids 50-64 (Shirane and Nakayama, 2006). KIF5-binding mutant (ΔKIF5) lacked amino acids 274-361 (Matsuzaki *et al.*, 2011), spastin mutant protrudin (ΔSpastin) had amino acids 151 to 220 removed (Zhang *et al.*, 2012) and ER mutant protrudin where the three transmembrane domains (TM1 (67–87a), TM2 (89–109aa) and TM3 (180–214aa) are removed so protrudin cannot associate with membranes (Chang, Lee and Blackstone, 2013).

3.2.3 Viral Vectors Cloning

In order to create viruses to transform the retina and perform optic nerve crush (see *Chapter 4*), GFP-WT-protrudin or GFP-Mutant2-Protrudin were cut out from their original vector. These inserts placed in AAV2-sCAG-GFP vector which contains interval terminal repeats (ITR sites) aiding the insertion into viruses. In all examples above, the vector DNA was opened up by a PCR reaction and purified from gel. The GA method, however, also allows for the vector DNA to be cut open using restriction enzymes. In the case of viral vectors cloning, the vector was opened up by using the restriction enzyme BsrGI as described (*Fig. 2.5A*). GA primers were again designed using the NEBuilder tool with overhangs for the BsrGI enzyme and PCR was performed (*Fig. 2.5B*). The correct size GFP-protrudin (either WT or mutant2) was cut out from the gel, purified and GA ligation were performed as described above.

A.

Step 1	Reagent	Quantity	Step 2	Reagent	Quantity
Restriction Digestion	DNA Template	2µg	Treatment to reduce auto-ligation	Antarctic Buffer	5.6µL
	BsrGI Restriction Enzyme	1µL		Antarctic Phosphatase	1µL
	10x Buffer 2.1	5µL			
	ddH20	42.6µL			
		1 hour at 37C			1 hour at 37C, then 5 mins at 80C

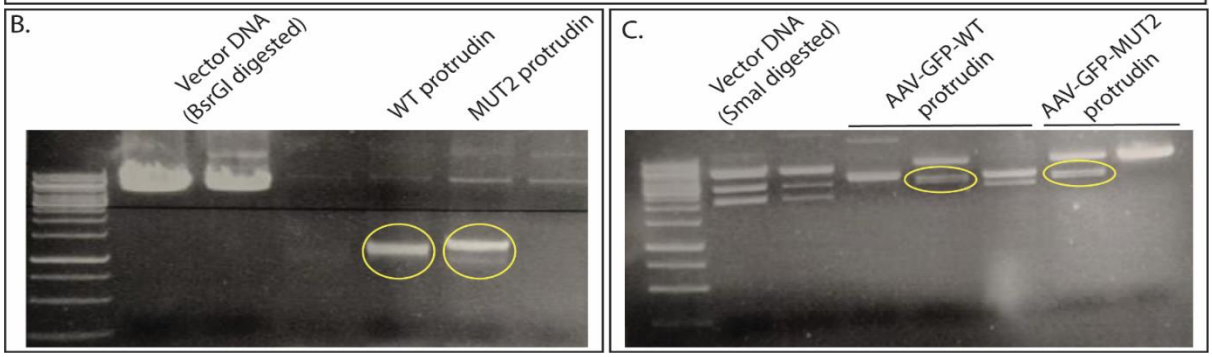

Figure 2.5 Cloning details for viral vectors. A. Table with the step-by-step restriction digestion procedure to open up the vector plasmid with BsrGI enzyme. B. Gel electrophoresis blot showing the correct size PCR products for protrudin GFP wild-type and mutant 2 which were subsequently purified from the gel and inserted into the vector digested with BsrGI. C. A gel electrophoresis blot showing SmaI digestion. SmaI restriction sites are present in both ITRs so upon digestion 2 bands of a size around 3000bp should be obtained. Many clones were tested but only the correct size ones (circled in yellow) were used for viral production.

In order to minimise sequencing waiting times, each clone was screened using the restriction enzyme BspEI to determine whether the protrudin gene was inserted. Lastly, the restriction enzyme SmaI was used to identify whether both ITR sites are present in the final cloning vectors (*Fig. 2.5C*). Once all characteristics were confirmed, vectors were sent for complete sequencing, maxi prepped and used to create AAV2 virus by Raymond Fields at the NINDS Viral Production Core Facility at the National Institutes of Health, Bethesda, Maryland, US.

4. Immunostaining

5.1 Immunocytochemistry

Cortical neurons and PC12 cells were fixed in 3% PFA for 15 minutes and then thoroughly washed and kept in PBS at 4°C. Cells were permeabilised in 3% BSA in PBS and 0.1% Triton for 5 minutes and then blocking solution was added (3% BSA in PBS) for 1 hour at

room temperature. Primary antibodies (listed in *Section 1.2.1*) were added at the correct concentration and kept overnight at 4°C. On the next day antibodies were washed 3 times in PBS for 5 minutes. Secondary antibodies (listed in *Section 1.2.2*) were applied at the correct concentration for 1 hour at room temperature in a dark chamber. The cells were then washed twice in 1xPBS and twice in 1xTNS (5-minute washes) and mounted using coverslips and Diamond anti-fade mounting agent with DAPI (Molecular Probes) or FluorSave mounting reagent (Calbiochem).

4.2 Immunohistochemistry

Mice were anesthetised using 1-2% isoflurane and rats were anaesthetised using phenobarbital, and transcardially perfused with PBS followed by 4% paraformaldehyde (PFA). Optic nerves were dissected and immersed in 4% PFA. The tissue was post-fixed overnight, then immersed in 30% sucrose for 24 h for cryoprotection. Tissue was embedded in Tissue-Tek OCT and snap-frozen for cryosectioning. 14 µm-thick longitudinal sections of the optic nerve of both groups of animals and 50 µm-thick brain slices from the rats were obtained on charged Superfrost microscope slides using a Leica CM3050 cryostat. Slides were dried and stored at -80°C. GAP-43 staining was performed as previously described (Leon *et al.*, 2000). Briefly, slides were thawed, rinsed in TBS (50 mM Tris buffer containing 8.766 g/L NaCl), washed with methanol for 10 min, and then blocked in TBS with 10% donkey serum for 1 h. GAP-43 was diluted (1:50 000) in a solution of TBS_2T (50 mM Tris buffer, 17.532 g/L NaCl, and 0.1 % Tween) containing 5% donkey serum and 2% BSA. Slides were incubated with GAP-43 overnight on a rocking platform, then washed with TBS_2T for 1 h, with TBS_2T plus 5% donkey serum and 2% BSA for 1 h, and with TBS_2T for 1 h, all on a rocking platform. The secondary antibody (donkey anti-sheep 633, Thermofisher) was diluted 1:1,000 in TBS_2T with 5% donkey serum and 2% BSA and slides were incubated for 2 h, followed by 30 min washes with TBS_2T, TBS_2T, and TBS. Slides were mounted using Fluormount and glass cover slips, and stored at 4°C for imaging. Wholemount mice retinas were also stained for retinal ganglion cell marker RBMS and the percentage of GFP-virus-positive RGC number was calculated.

Slides with rat brain sections and wholemount retinas were thawed at room temperature for 20 mins, then washed with PBS (5-minute washes) on a slow rocker. 500 µL of blocking solution/slide (PBS/2%BSA/0.3% TritonX/10% normal goat serum) was applied for

1 hour at room temperature on a slow rocker. 500 µL of primary antibodies diluted in blocking solution at the correct concentration were applied on each slide overnight at 4°C. The slides were washed on the next day with PBS three times for 15 minutes on a slow rocker. Secondary antibodies diluted in blocking solution at the correct concentration were applied for 2 hours at room temperature on a rocker. The antibodies were then washed in PBS three times for 10 minutes at room temperature on a slow rocker. Slides were then mounted with FluorSave (Calbiochem), kept at 4°C and imaged.

5. Microscopy

5.1 Confocal Microscopy

Images of immunostained cells were taken with a confocal microscope (Leica DMI 4000 B) using LAS-AF software (Leica). For protrudin localisation, a z-stack of images was obtained through each cell by taking an image at every 0.5µm thickness and an average intensity z-projection was created in Fiji software (Schindelin *et al.*, 2012). The same strategy was used for imaging Rab11 and integrin staining. All images in a particular experiment were taken using the same microscope settings. The intensity was measured by placing a line shape (usually about 50µm) on processes and taking a background intensity of the same shape immediately next to each process (*Fig. 2.6A, 2.6B*). The same procedure was used for proximal (<100 µm from cell body) and distal (>100 µm from cell body) axons as well as dendrites. The background was then subtracted from the intensity at each process. For protrudin intensity measurements in GFP-transfected neurons, regions of interest were selected in the 488 channel and a line was placed on each process and immediately next to it to measure background. This strategy immediately excludes any biases on selecting processes with higher intensity of protrudin staining. The same strategies were used for measuring Rab11 and integrin intensity. For all experiments measuring axon-to-dendrite ratio, the intensity in dendrites was an average from measurements in at least 3 dendrites where possible.

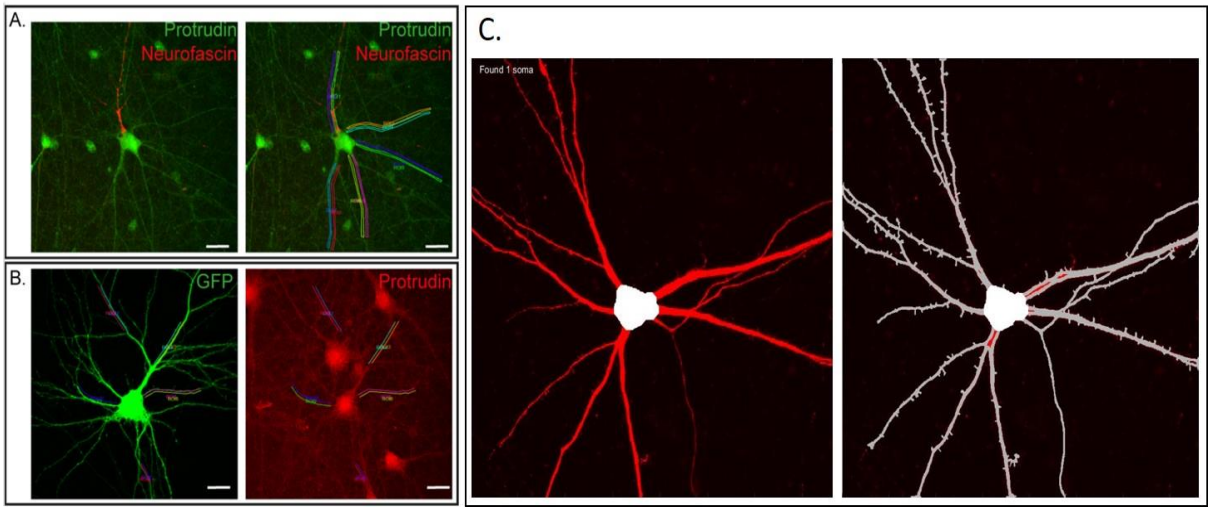

Figure 2.6 Quantification of immunocytochemistry in neurons. A. Immunofluorescent images showing the measuring strategy for protrudin intensity in neuronal process. The axon was identified by neurofascin staining (red) and a measuring line (around 50 µm) was placed on top of it as well as immediately next to it to measure background staining. Dendrites were identified by the presence of protrudin staining and the same measuring strategy was employed. The same strategy was used when measuring Rab11 and integrin intensity in the axon and dendrites. B. For cortical neurons transfected with GFP, the axon was identified by morphology and the presence of neurofascin staining (images not shown). A measuring line was drawn across the axon and immediately next to it to measure background. Dendrites were identified by the presence of GFP fluorescence and the same measuring technique was employed. C. A schematic diagram representing the strategy of identifying the cell body and tracing the neurites in the SynD software for dendritic tree analysis.

5.1.1 Morphological Analysis

Dendritic tree analysis was carried out in a semi-automated manner using a recently developed, openly available software – SynD (Schmitz *et al.*, 2011). An image of a neuron is opened in the software to begin with, and the cell body is identified (soma erode=25, morphology threshold=42). Then the neurites coming out of that cell body are traced along in radius 200 µm (max cost=0.9, filter size=2) (*Fig. 2.6C*). Sholl analysis is then applied and the dendritic complexity of different protrudin mutants' overexpression was measured. Spine morphology and number were analysed from 63x confocal images of neurons transfected with GFP as a control plasmid which diffuses in spines and protrudin mutants using Fiji software (Schindelin *et al.*, 2012).

5.1.2 Imaging and quantification of axon regeneration after optic nerve crush

Imaging was performed using a Zeiss 780 confocal microscope. Z-stacked images were collected with a z interval of 0.87 µm. CTB^+ axons were counted in ImageJ at 0.25 mm intervals starting from the lesion site. Four sections were counted for each nerve. The number of regenerating axons was then calculated at each distance using a previously developed formula (Bei *et al.*, 2016; Lim, Stafford, Nguyen, Lien, Wang, Zukor, He and Andrew D. Huberman, 2016), with the total number of axons equal to πr^2 (r being the maximum recorded radius of the optic nerve section) times the average number of counted axons, divided by the thickness of the section (14 µm).

$$\sum axons = \frac{\pi r^2 n}{t}$$

Axon counting was performed by an observer blind to the experimental conditions.

5.2 Live-cell imaging

Live-cell imaging was performed using spinning disk confocal microscopy, using an Olympus IX70 microscope with a Hamamatsu EM-CCD Image-EM camera and a PerkinElmer Ultra-VIEW scanner. Videos were taken using Meta-Morph software. Rab11 and integrin vesicle trafficking along the axon was imaged at the proximal (up to 100µm) and distal part (beyond 200µm) of axons of neurons transfected with protrudin. One image per second was obtained for 3 minutes. Kymographs were obtained by measuring as much as possible from an individual axon segment. Anterograde, retrograde, bidirectional and static modes of transport were measured. The percentage of co-localisation between integrin or rab11 and protrudin was calculated as the number of vesicles containing both was divided by the total number of vesicles. All analysis was performed using Meta-Morph software.

5.3 Tile scan imaging

Leica DMi8 tile-scan microscope was used to image the optic colliculus area of the rat brains and Brn3a staining in rat wholemount retina. CTB tracing was injected in the retina so the edges of each superior colliculus were marked using the fluorescent intensity of the CTB and a tile-scan array of images was taken at 20x. Once all images were taken, they were stitched together to form one final image (*Fig. 2.7A*). Brn3a images in retinal wholemounts (Fig. *2.7B*) were also taken at 20x, however, as single images.

5.3.1 CTB measurements and analysis

Tile-scan images of superior colliculus were uploaded on the Fiji Software and the superior colliculus was outlined using the polygon tool. Fluorescent CTB intensity, the size of the area and the integrated density were measured for each side of the brain – left and right superior colliculus. Volumetric analysis was performed as described previously (Chiasseu *et al.*, 2017) using the following formula:

$$Total\ CTB\ Area = \frac{\sum CTB\ Section\ Area}{ssf\ x\ asf\ x\ tsf}$$

Where ssf represents the number of sections used in the analysis over the total number of sections (e.g. 8/50), asf represents the areas sampled divided by the total area (1) and tsf represents the thickness of the sampled section over the total thickness over which sections were analysed (e.g.50/600).

5.3.2 Brn3a analysis

24 images of Brn3a staining were obtained from each rat retinal wholemount – 2 images in the centre of the retina, 2 in the middle and 2 in the periphery of each retinal quadrant (*Fig. 2.7B*). Automated counting of the number of Brn3a-positive cells in each image was performed using the Fiji software and an image-based tool for counting nuclei (ITCN) plugin. Blinded counts using the plugin were carried out by Yusuf Mushtaq. The final analysis was performed as the number of cells per image was divided by the area of the image in order to obtain retinal ganglion cell density per mm^2.

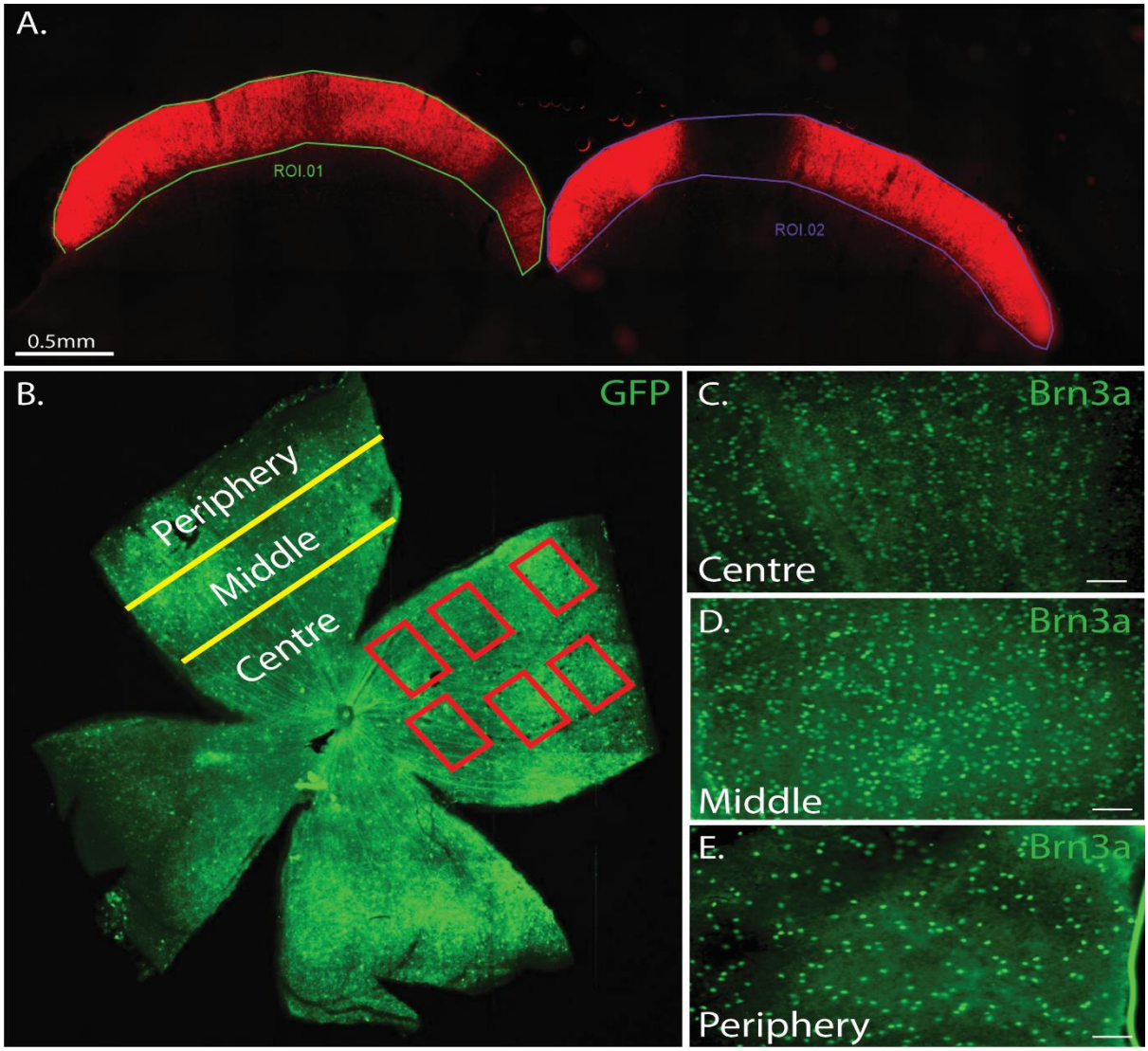

Figure 2.7 A. An example of a reconstructed image of the whole superior colliculus of a rat. ROI 0.1 and ROI 0.2 are examples of the regions of interested which were measured for the superior colliculus volume analysis. CTB staining is shown in red. Scale bar is 0.5mm. B. An example of a wholemount retina stained for GFP and the sampling method for Brn3a imaging. 24 images per retina were taken (6 images per quadrant – 2 in each area - centre, middle and periphery). C. Example images of Brn3a staining (green) from different retinal areas which were used for measuring retinal ganglion cell density. Scale bar is 50 µm.

5.4 Laser Axotomy

10 DIV neurons were transfected with various protrudin constructs using magnetofection as described above. Between 13-17 DIV, their regeneration ability was examined using the laser axotomy model described in detail in Koseki et al., 2017. Axotomy was performed by an UV Laser (355 nm, DPSL-355/14, Rapp OptoElectronic, Germany)

connected to a Leica DMI6000B (Leica Systems, Germany), and all images were taken with an EMCCD camera (C9100-02, Hamamatsu). Axons were cut at least 600 µm away from the cell body and regeneration was observed for 14 hours post injury at 30-minute intervals. If more than 50% neuronal cell death occurred in the axotomised cells, the experiment was excluded from the final analysis. The characteristics measure in each experiment are described in *Table 2.2.*

Regeneration factor	Regeneration factors were measured as below when a neuron was categorized as regeneration
Retraction distance	The length of axon that was lost between the location of axotomy and the initial retraction bulb
Regeneration percentage	The number of neurons that regenerated, over the total neurons which formed a retraction bulb
Regeneration initiation time	The time between the retraction bulb formation and the start of a steady extension lasting more than 1hr and leading to regeneration
Regeneration distance after 2 hours	The length of axon that extended within 2hrs after regeneration initiation
Total Regeneration Distance	The length of axon that extended 14 hours after axotomy
Growth cone area	The maximum growth cone area after regeneration initiation

Table 2.2 Table to explain the regeneration factors measured during laser axotomy (adapted from Koseki *et al.*, 2017).

5.5 Cellomics

In order to assess the neurite outgrowth of primary cortical neurons transfected with 9 different forms of protrudin, cortical neurons were grown in 24-well plates, transfected at 2 DIV and fixed at 4 DIV. Imaging was performed at 10x using the Cellomics ArrayScan XTI platform at the NIHR Cambridge BRC Cell Phenotyping Hub. Cells expressing the protrudin construct were identified as they were positive both for DAPI and mCherry and their cell body area was between 1 and 2000 µm^2. An algorithm was then created to trace all fluorescent processes coming out of the cell body (*Fig. 2.8A-C*) and several parameters were measured (*Fig. 2.8D*).

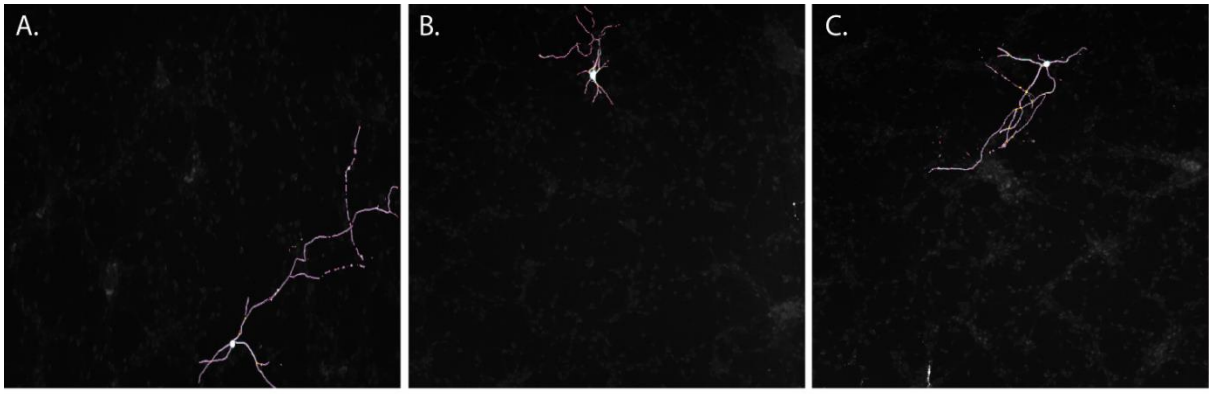

D.

Parameter	Units	Description
Cell Body Area	μm^2	Total area of individual neuronal cell body
Neurite Total Count	number	Number of neurites associated with selected cell body
Neurite Total Length	µm	Sum of lengths of all neurites associated with a particular cell body
Neurite Average Length	µm	$\frac{Neurite\ Total\ Length}{Neurite\ Total\ Count}$
Neurite Maximum Length (with branches)	µm	Length of the longest individual neurite associated with a selected cell body (plus the length of all branches associated with it)
Neurite Maximum Length (without branches)	µm	Length of the longest individual neurite associated with a selected cell body (not including the length of its associated branches)
Branch Points Count	number	The number of branches associated with the neurites from one cell body

Figure 2.8 Figure outlining some characteristics of the Cellomics paradigm. A. B. C. Example cells all treated with the same algorithm for tracing neurites. All neurites are traced (in pink) to their maximum length and no errors occurred between the different cells. The algorithm worked consistently between different cells of different shape and size. D. Table to describe some of the parameters measured in the paradigm, their units and descriptions.

6. Immunoprecipitation and Western Blots

6.1 Cell Lysis

HeLa cells were used for Rab11 and protrudin interaction detection by immunoprecipitation. PC12 cells were used for Western Blots to detect protein levels after applying shRNA against protrudin. HeLa cells and PC12 cells were transfected as described in Sections 2.2 and 2.3. 48 hours later cells were lysed using the cOmplete Lysis Kit (Roche). PBS and lysis buffer (plus proteinase inhibitor tables – 1 tablet for 10 mL of buffer) were cooled down to 4°C. The medium of each well of a 6-well plate was removed and cells were washed

with ice-cold PBS. 500 µL of pre-cooled lysis buffer was added to each well and the lysate was scraped using a cell scraper and transferred to a sterile 1.5 mL Eppendorf. The lysate was incubated on ice for 30 minutes with occasional mixing. The samples were then centrifuged at 10 000 g at 4°C for 10 minutes. The supernatant was transferred to 1.5 mL Eppendorf and the pellet was discarded. The total protein concentration was measure by BCA assay using Pierce BCA Assay Kit Protocol (ThermoFischer Scientific). The 96-well plate containing the sample lysates and BCA reagents was analysed using Gen5.1 software and concentrations were derived from a standard curve for albumin control. 15 µg of PC12 cell lysate was then treated with LDS Sample Buffer NuPAGE 4x (1:4, ThermoFisher Scientific) and Sample Reducing Agent (1:10, ThermoFisher Scientific) and were analysed by Western blot (Section 6.3). HeLa cell lysate was used for immunoprecipitation (Section 6.2).

6.2 Immunoprecipitation

Equal amounts of HeLa cell lysate between different conditions was incubated with 50 µL of GFP beads from µMACS GFP Isolation Kit (Miltenyi Biotech) for 30 mins at 4°C on a rotating wheel. Before this step 15 µg of lysate was keep aside in order to serve as an input control. In the meantime, µ columns (Miltenyi Biotech) were places on a µMACS magnetic separator. The columns were equilibrated with 200 µL of lysis buffer. Once the lysate incubation has finished, the whole lysate was applied to the column and the flow through was discarded. The columns were washed 4 times with 200 µL of Wash Buffer 1 and once with 100 µL of Wash Buffer 2. 20 µL of pre-warmed (to 95°C) elution buffer was added to the columns and incubated for 5 minutes. Any excess solution coming out of the columns was discarded. Further 30 µL of elution buffer was added and the eluate was collected in clean 1.5 mL Eppendorf tubes. The eluates were analysed on Wester Blots as described below.

6.3 Western blotting

Protein lysate samples (from PC12 cells) and IP eluates (from HeLa cells) were analysed by SDS-PAGE. Precision Plus Protein Dual Colour Standard (BioRad) was used as a ladder. Samples were run on a 4-12% gel until they reached the bottom of the gel (usually 1.5-2 hours)

at 120 V at room temperature in 40 mL Running Buffer NuPAGE (ThermoFisher Scientific) diluted in H20 to 800 mL. The gel was then transferred onto a nitrocellulose membrane (Invitrolon PDVF/Filter Paper Sandwich, ThermoFischer Scientific) for 1.5 hours at 40V at 4°C in 50 mL Transfer Buffer NuPAGE (ThermoFisher Scientific) in 100 mL methanol, topped up with ddH20 to 1 L. The membrane was then blocked either in 5% milk or 3% BSA depending on the antibody for 1 hour and incubated overnight with the primary antibody diluted the blocking solution to the right concentration at 4°C. The membrane was then rinsed three times in Tris-buffered saline with Tween 20 (TBST buffer) for 10 minutes each. The TBST buffer was removed. Secondary peroxidase-conjugated antibodies were diluted to the right concentration in blocking solution and were then added for 1 hour at room temperature. SuperSignal West Dura Extended Duration Substrate kit (ThermoFischer Scientific) and Alliance software were then used for detection.

7. Animal Studies

7.1 Animals

For optic nerve crush experiments, all procedures were performed in accordance with protocols approved by the Institutional Animal Care and Use Committee (IACUC) at the National Institutes of Health. Female C57Bl/6 mice aged 6-8 weeks (Charles River) (n=27) were housed in a pathogen free facility with free access to food and a standard 12 hr light/dark cycle. For glaucoma experiments, all procedures were performed in accordance with protocols approved by the Home Office, UK. Male Sprague-Dawley rats were house in a pathogen-free facility (n=26).

7.2 Viral Injections

Intravitreal injections of viruses (*Table 2.3*) were administered 14 days prior to optic nerve crush or laser injury. 1.5 µL of the injecting solution for mice and 5 µL for rats was drawn into a sterile 5 µL Hamilton syringe equipped with a 33-gauge removable needle. The solution was injected into the vitreous humor through the superior nasal sclera, with the needle positioned at a 45° angle to avoid the lens, external ocular muscle, and blood vessels. Before

removing the needle, a sterile 33-gauge needle was used to puncture the cornea and drain the anterior chamber, thereby reducing intraocular pressure and preventing reflux. Different needles were used for each virus to prevent contamination, and syringes were rinsed between injections with ethanol followed by sterile PBS. The same procedure was used for intravitreal viral injections of rats for glaucoma study.

Virus	Titre
AAV2-CAG-eGFP	5×10^{12} vg/mL
AAV2-CAG-protrudinWT-eGFP	2×10^{13} vg/mL
AAV2-CAG-protrudinMUT-eGFP	2×10^{13} vg/mL
AAV2-CAG-integrinα9-V5	1.2×10^{13} vg/mL

Table 2.3 A table listing all the viruses used in this research and their titres.

7.3 Optic Nerve Crush

Optic nerve crush was performed as described previously (Kevin Kyungsuk Park *et al.*, 2008). Micro-scissors were used to make an incision in the conjunctiva and expose the optic nerve. Curved forceps were then inserted below the external ocular muscle, avoiding the ophthalmic artery and retrobulbar sinus, and positioned around the exposed nerve. The nerve was crushed for 10 s approximately 1 mm behind the eye. Following the crush, eyes were observed fundoscopically for signs of ischemia, and mice were monitored for signs of intraorbital bleeding. Mice were given a subcutaneous injection of 1 mg/kg buprenorphrine as an analgesic and topical application of ophthalmic ointment to prevent corneal drying.

7.4 Laser Injury to Induce Intraocular Pressure (IOP) Rise

Ocular hypertension was induced in the left eye of rats. Rats were placed in front of a slit-lamp equipped with a 532-nm diode laser that delivers 0.7-W pulses for 0.6 seconds. Fifty to sixty laser pulses (50-µM diameter) were directed to the trabecular meshwork 360° around the circumference of the aqueous outflow area of the left eye. Animals were under general anaesthesia for the duration of the procedure - ketamine (50 mg/kg) and xylazine (10 mg/kg)

injected intraperitoneally. Afterwards, postoperative Viscotears were applied to the eye and animals recovered from anaesthesia in a warm cabinet under observation. Animals required daily lubrication with Viscotears following laser treatment. IOP was measured using a TonoLab tonometer on the day after laser injury and a week later, immediately before second injury, then again a day and a week after the second injury.

7.5 CTB Injection

Intravitreal injections of CTB (1.0 μg/μL, Sigma) were administered 2 d prior to perfusion harvest in both mice and rats. 2 μL of the solution injected as described above. The syringe was rinsed with ethanol and sterile PBS between injections.

8. Statistics

Statistical analysis was performed using GraphPad Prism 8.0 (GraphPad Software, La Jolla, CA). Each data set was individually tested for normal distribution using the D'Agostino-Pearson normality test. When data was normally distributed one-way ANOVA with multiple comparisons was used to test statistical significance between the experimental groups with Tukey's post hoc test. Several data sets were shown to be non-normally distributed. Therefore, a non-parametric Kruskal-Wallis test with multiple comparisons was used to test for significant differences across experimental groups. Dunn's multiple comparison post-hoc test was also performed. All outliers were removed after testing each set of data with the GraphPad outlier removal function. Data from different staining experiments for each experimental group were tested for statistical difference using Kruskal-Wallis test in order to determine whether values could be combined together. All statistics were carried out at 95% confidence intervals, therefore a significant threshold of $p<0.05$ was used in all analyses. For Sholl analysis, repeated measures two-way ANOVA was performed using SPSS (IBM Statistics). When comparing percentages (e.g. of regenerating cells), Fisher's exact test was performed between each two groups compared. p-values were then analysed with the "Analyse a stack of p values" function in GraphPad Prism with a Bonferroni-Dunn pairwise comparison to test for statistical significance between groups.

CHAPTER III: MUTAGENESIS OF PROTRUDIN AND ITS CELLULAR EFFECTS

Summary

This chapter explores the cellular localisation of endogenous protrudin in several cell culture paradigms and its interaction with known molecular partners. The effects of wild-type and mutant protrudin overexpression in cortical neurons are also investigated in terms of morphology, localisation and actions of the protein. Lastly, protrudin overexpression influence on neurite outgrowth in culture is also examined.

1. Introduction

1.1 Protrudin expression during development

Protrudin is an integral membrane protein, a member of ZFYVE family of zinc-binding proteins (Shirane and Nakayama, 2006). Protrudin's CNS expression during development and after injury has not been studied extensively. Despite that, protrudin expression has been

detected in several large-scale RNA sequencing studies summarised in *Fig. 3.1A*. For example, in primary rat cortical neurons protrudin's expression doubles from 1 DIV to 16 DIV (15.5 to 37.3 fragments per kilobase million (FPKM)), and then plateaus by 24 DIV (27 FPKM) (Koseki *et al.*, 2017). This expression level, however is very low compared to that of other proteins present abundantly throughout the cell such as beta-actin (1092 average FPKM) and GAPDH (285 average FPKM) or compared to other regeneration-associated scaffolding molecules such as GAP43 (628 average FPKM) and YWHAZ (14-3-3 zeta proteins) (570 FPKM) (Kaplan *et al.*, 2017; Koseki *et al.*, 2017).

In a separate RNA analysis study in DRG cultured neurons, protrudin expression is slightly increased after 36 hours in culture (from 1439 at 6 hours to 1728 normalised expression levels at 36 hours) as well as from E12.5 to E17.5 during mouse embryonic development *in vivo*, (684 to 846 normalised expression levels) but these are not considered large scale changes (Tedeschi *et al.*, 2016) (*Fig. 3.1A*). In this study, protrudin levels were again much lower than other ubiquitously expressed proteins such as beta-actin (14 020 *in vitro* and 23 153 *in vivo* average normalised expression levels). Protrudin's levels were also much lower than other regeneration-associated proteins such as GAP43 and 14-3-3s both *in vitro* (3265 and 12 320 average normalised expression levels, respectively) and *in vivo* (7853 and 12 399 average normalised expression levels, respectively) (Tedeschi *et al.*, 2016).

Overall, these two studies show that protrudin has a relatively stable expression pattern during different stages of development both *in vitro* and *in vivo* and that protrudin levels in neuronal cells, especially CNS neurons are relatively low compared to the expression of other highly abundant or regeneration-associated proteins. These studies, however focused on exploring the mRNA levels, therefore further studies are needed in order to validate the abundance of the protrudin protein in different cell types and tissues with development.

1.2 Protrudin expression after injury

The expression levels of protrudin after injury were also analysed from several different datasets. Protrudin expression in DRGs after peripheral nerve injury is slightly increased compared to sham animals (from 1692 to 2125 normalised expression values) (Tedeschi *et al.*, 2016) (*Fig. 3.1A*). However, in this paradigm, GAP43 increases from 4323 to 11 375, beta-actin from 12 585 to 17 145 and 14-3-3s from 15 605 to 16 618 normalised expression values in sham compared to injured animals (Tedeschi et al., 2016).

Furthermore, protrudin expression levels after optic nerve crush in the retinal ganglion cells (RGCs) doubled from 5.5 in uncrushed to 12 expression units 3 days post injury (3dpi) but then returned to basal level at 14dpi (5.8 expression units) (Smith et al., unpublished data). Protrudin levels are only 0.3 expression units different at 14dpi compared to uncrushed optic nerve. This change is very negligible compared to the most highly differentially expressed protein – Gm12563 where the difference between expression at 14dpi to uncrushed nerve is 298 105 expression units (Smith et al., unpublished data). Similar to during development, protrudin expression levels after optic nerve crush are, in general, very low compared to some proteins which are upregulated such as beta-actin (352 average expression units) or 14-3-3s (160 average expression units).

Lastly, the expression of protrudin in the spinal cord after a spinal cord injury remains almost unchanged 2dpi (11.35 FPKM) and 7dpi (7.12 FPKM) compared to sham control animals (11.74 FPKM) (Chen *et al.*, 2013). Again, these values are very low when compared to GAP43 (sham – 61 FPKM, 2dpi – 122 FPKM, 7dpi – 82 FPKM), GAPDH (sham – 134 FPKM, 2dpi – 202 FPKM, 7dpi – 155 FPKM), beta-actin (sham – 423 FPKM, 2dpi – 1212 FPKM, 7dpi – 1330 FPKM) and 14-3-3s (sham – 102 FPKM, 2dpi – 117 FPKM, 7dpi – 88 FRKM) (Chen *et al.*, 2013). In summary, protrudin expression levels do not change significantly after peripheral or central nervous system insult and the levels of protrudin in these cells and tissues are much lower even in the absence of injury compared to some abundantly expressed or regeneration-associated proteins.

A.

Development						Injury				
Cortical neurons *in vitro* (Koseki et al., 2017) – units (FKPM)	**DIV1**	**DIV4**	**DIV8**	**DIV16**	**DIV24**	Retinal ganglion cells after optic nerve crush (Patrice Smith, unpublished data)	**Uncrushed (mean)**	**3dpi (mean)**	**7dpi (mean)**	**14dpi (mean)**
	15.5	26.8	22.2	37.3	27.0		5.5	12.1	6.5	5.8
DRG neurons *in vitro* (Tedeschi et al., 2016) – units (normalised expression values)	**6hrs**	**12hrs**	**24hrs**	**36hrs**		DRG after peripheral nerve injury (Tedeschi et al., 2016) – units (normalised expression values)	**Sham**		**Injury**	
	1439	1540	1629	1728			1692		2125	
DRG neurons in vivo (Tedeschi et al., 2016) – units (normalised expression values)	**E12.5**		**E17.5**			Spinal cord injury (Chen et al., 2013) – units (FKPM)	**Sham**	**2dpi**	**7dpi**	
	684		864				11.7	11.3	7.1	

B.

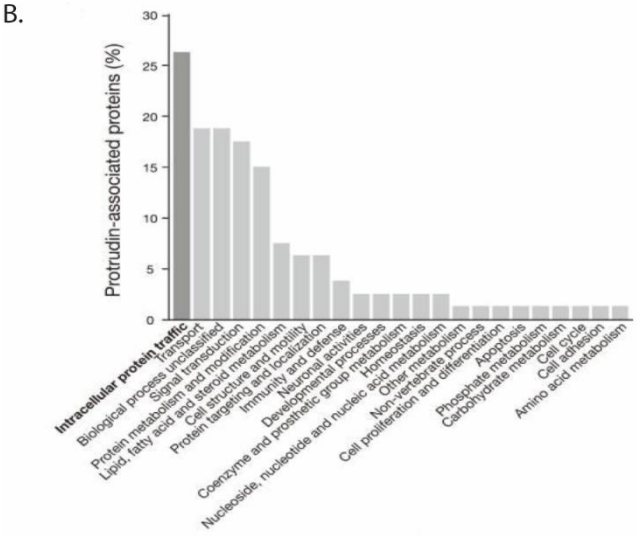

C.

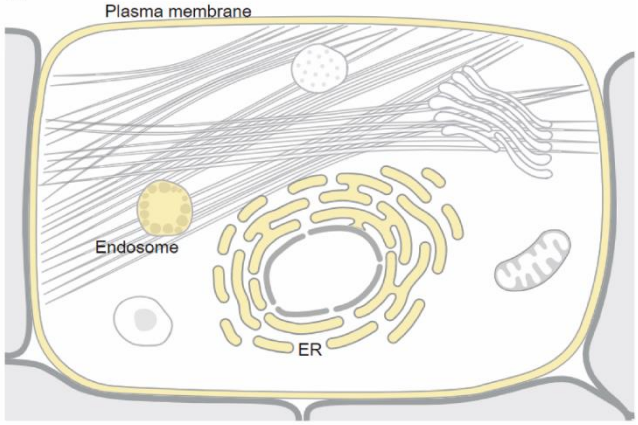

Figure 3.1 Protrudin expression levels, molecular interactions and cellular localisation. A. Table summarising the expression levels of protrudin during development in cortical neurons and peripheral nervous system neurons as well as after peripheral and central nervous system injury from several RNA sequencing studies. B. Bar graph showing the percentage of protrudin-associated protein interactions in different molecular and cellular processes derived from a large-scale proteomics study (adapted from Matsuzaki *et al.*, 2011). C. Schematic diagram showing protrudin cellular distribution which has been documented in peer-reviewed publications (adapted from uniprot.org).

1.3 Protrudin is involved in multiple molecular processes

The protrudin protein contains multiple molecular domains which mediate its interaction with other proteins and its involvement in multiple molecular mechanisms (summarised in *Introduction, Section 4*). Numerous interacting partners of protrudin were identified in a large proteomics study carried out by Matsuzaki and colleagues in 2011 including Rab11, VAP-A, VAP-B, reticulon-3, KIF5 and others. Protrudin was found to associate mostly with proteins involved in intracellular trafficking and transport, signal transduction, protein metabolism and modification and lipid, fatty acid and steroid metabolism (*Fig. 3.1B*). Our initial hypothesis was that protrudin could be used as a tool to promote Rab11 transport into the axon, leading to an increase in regenerative ability. Given that protrudin has numerous interactions, it was important to also investigate a potential role for these in the regenerative process. If protrudin could be used to stimulate regeneration, studying these component properties of protrudin could have important implications for the identification of new molecular pathways involved in the process of regeneration.

1.4 Protrudin localisation in the cell

Protrudin localisation in the cell has so far only been studied in several cancer cell types. When overexpressed in HeLa cells protrudin results in the formation of neuronal-like processes in 5-30% of cells and is enriched at the tip of growing processes (Shirane and Nakayama, 2006). In PC12 cells, in the absence of nerve growth factor (NGF), protrudin is found in a diffuse fashion throughout the cell body. After 6 hours of NGF treatment, protrudin localises to the pericentrosomal region colocalising with the endosomal marker – Rab11 (Shirane and Nakayama, 2006). Interestingly, 24 hours of NGF treatment induces the formation of long neuronal processes where protrudin re-distributes to the growing tip. Protrudin's interaction with Rab11-GDP is necessary for anterograde transport to the tip of newly growing processes (Shirane and Nakayama, 2006). The effect of protrudin overexpression on neurite outgrowth in various cell types is extensively discussed in *Introduction, Section 4.5.* These observations point towards an important role for protrudin in directional membrane trafficking in newly growing processes.

Protrudin localisation in neuronal cells is less well-studied. Protrudin overexpression in rat hippocampal neurons at 1 DIV results in increased neurite extension at 3 DIV (Shirane and Nakayama, 2006). Furthermore, protrudin was found in the soma and neurites of 1 DIV mouse primary cortical neurons and was also observed in dendrites, the axon and the growth cone of 3 DIV cortical neurons (Shirane and Nakayama, 2006). In this chapter, the localisation of endogenous protrudin in primary cortical neurons at different stages of development as they mature to become electrically active and lose their regenerative ability, is examined. One hypothesis is that protrudin may not be present in mature axons in levels that could enable protrusive growth.

In terms of organellar localisation, protrudin's association with membranes results in its localisation to membrane-bound cellular components such as the endoplasmic reticulum, the plasma membrane and recycling endosomes (*Fig. 3.1C*).

1.5 Protrudin mutagenesis

In order to test our hypothesis that enhancing the interaction between protrudin and Rab11 could improve anterograde transport and axon regeneration, two constitutively phosphorylated forms of protrudin were created as described in *Methods, Section 3.* The mutagenesis sites in the protein were selected based on previous reports. Shirane and colleagues (2006) created constitutively inactive phosphorylation mutants at various ERK phosphorylation sites in different combinations. They found that two mutants in particular (P-mut-1 and P-mut-4, mutated at S14,25,32/T265 and T265/T269/T276 respectively) dramatically reduced the interaction between protrudin and Rab11. They concluded that phosphorylation of protrudin at multiple sites by ERK is essential for its interaction with Rab11-GDP and anterograde transport to the tip of growing processes. In the paper described, the authors used a form of mouse protrudin. In our experiment, the human protrudin protein was used and was mutated at the sites equivalent to the mouse phospho-sites identified above. In addition, when FKBP38 (an interactor of protrudin) is knocked out in mice, protrudin was found to be hyperphosphorylated and to result in abnormal axon

extension in these mice (Shirane *et al.*, 2008). The constructs that are used throughout this thesis are mCherry only control plasmid (syn-mCh only), mCherry-tagged wild-type protrudin (syn-mCh-WT), mCherry-tagged mutant 1 protrudin (syn-mCh-MUT1) and mCherry-tagged mutant 2 protrudin (syn-mCh-MUT2) (see *Methods, Section 3*). All constructs were tested in PC12 cells and in primary cortical neurons in order to evaluate their effects on cell morphology, protein localisation and on neurite outgrowth.

2. Results

2.1 Protrudin is Preferentially Re-distributed to Dendrites compared to Axons as Neurons Mature in vitro

The localisation of the protrudin protein in primary cortical neuronal cultures was examined using immunocytochemistry. Firstly, neurons at different stages of development – 2-4 DIV, 7-9 DIV and 14-16 DIV were immunostained for protrudin and for neurofascin, an axon initial segment (AIS) marker to identify the beginning part of the axon (*Fig. 3.2A)*. As the AIS forms around 3-4 DIV *in vitro,* in early, 2-4 DIV neurons due to lack of neurofascin immunoreactivity, the axon was identified as the longest process. The intensity of the protrudin staining was measured in axons and dendrites as described in *Methods, Section 5.1.1.*

Our results showed that the amount of protrudin in the proximal axon declines with maturation as the intensity of protrudin staining was lower at 7-9 DIV (23 grey values) and 14-16 DIV (21 grey values) compared to 2-4 DIV (39 grey values) ($p=0.002$) (*Fig. 3.2B).* There was no statistical difference in protrudin's abundance in axons between 7-9 DIV and 14-16 DIV ($p=0.999$). This observation prompted us to examine whether protrudin might have a similar axon-to-dendrite distribution pattern as other growth-promoting and transport-related molecules such as integrins and Rab11 in aged neurons (see *Introduction, Section 3.3.1).*

When examining the amount of protrudin in dendrites, there were no significant differences with development from 2-4 DIV (49 grey values) to 7-9 DIV (52 grey values) ($p=0.91$) and then to 14-16 DIV (49 grey values) ($p=0.99$) (*Fig. 3.2C).* Finally, the relative amounts of protrudin staining intensity were used to calculate axon-to-dendrite ratio for each cell across the three different developmental stages. The results showed an increased axon-to-dendrite abundance of protrudin at earlier (2-4 DIV, ratio=1) compared to later stages of development (7-9 DIV, ratio=0.47 and 14-16 DIV, ratio=0.44) ($p<0.0001$) *(Fig. 3.2D).* There was no statistical difference in the axon-to-dendrite distribution of protrudin between 7-9 DIV and 14-16 DIV ($p=0.841$).

Interestingly, in contrast to our RNA sequencing results in primary cortical neurons where the amount of protrudin mRNA is relatively stable during development in culture (Koseki *et al.*, 2017)(see *Fig. 3.1A*), the amount of the protrudin protein in the cell body seems to decline with maturation in this paradigm. There is less protrudin in 7-9 DIV (154 grey values) and 14-16 DIV (153 grey values) compared to younger neurons at 2-4 DIV (184 grey values) (*Fig. 3.2E*). This experiment, however, had some major caveats which are explained in this chapter's *Discussion* section below.

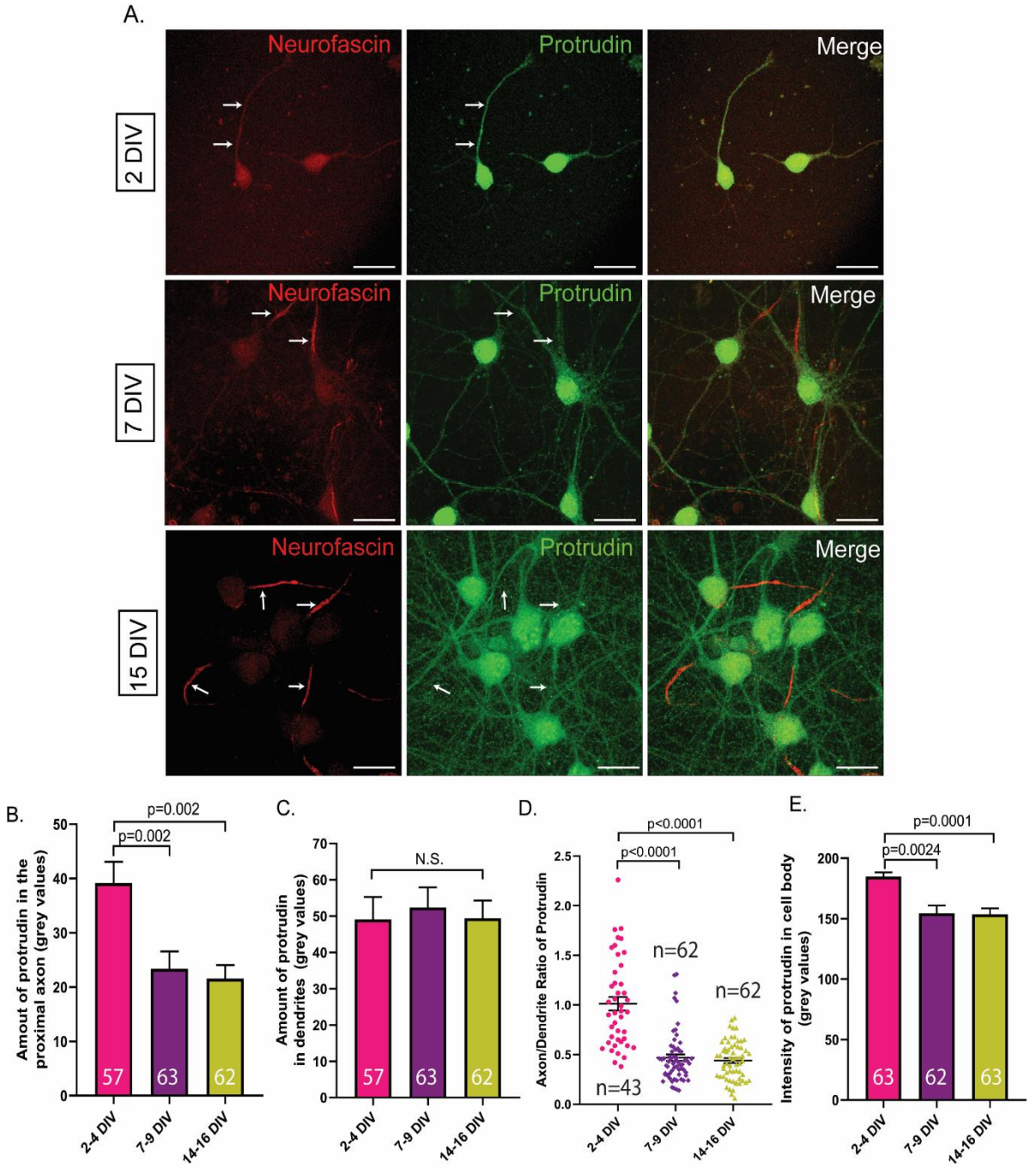

Figure 3.2 Protrudin distribution in primary cortical neurons at different stages of development. A. Immunofluorescent images of protrudin (green) and neurofascin (red) localisation at 2-4, 7-9 and 14-16 DIV taken at 63x magnification. White arrows indicate segments of the axons. Scale bars are 20 µm. B., C. Bar graphs to compare the mean protrudin intensity in axons and dendrites across the different ages. Protrudin's staining intensity is significantly higher in axons at 2-4 DIV compared to 7-9 DIV and 14-16 DIV ($p<0.0001$, Kruskal-Wallis statistic=20.82, n=4). Protrudin's abundance in dendrites does not change with development ($p=0.9816$, Kruskal-Wallis statistic=0.037, n=4). D. Scatter plot to present the axon-to-dendrite ratio of protrudin abundance across the different groups. The axon-to-dendrite ratio is higher at 2-4 DIV compared to 7-9 DIV and 14-16 DIV ($p<0.0001$, Kruskal-Wallis statistic=59.12, n=4). E. Bar graph showing the relative amount of protrudin protein in the cell body across different developmental stages. There is less protrudin in the cell body at 7-9 DIV and 14-16DIV compared to 2-4 DIV ($p<0.0001$, Kruskal-Wallis statistic=19.55, n=4). Error bars represent mean ± SEM.

The localisation experiment was refined by transfecting 1, 6 and 12 DIV neurons with a GFP-expressing construct in order to label all neuronal processes. The transfected neurons were then fixed in PFA at 4, 9 and 15 DIV and immunostained for protrudin and neurofascin (*Fig. 3.3A*). The intensity of the protrudin staining was measured in axons and dendrites as described in *Methods, Section 5.1.1.* Confirming our findings above, the amount of protrudin in proximal axons seems to decline between 4 DIV (28 grey values) and 15 DIV (18 grey values) ($p=0.004$) (*Fig. 3.3B).* However, there is no significant decline between 4 DIV and 9 DIV (23 grey values) contrary to our previous result ($p=0.114$). No significant difference was observed between protrudin levels in dendrites at 4 DIV (37 grey values), 9 DIV (46 grey values) and 15 DIV (42 grey values) ($p=0.1558$) although there is a trend towards a higher amount of protrudin at the later stage of development (*Fig. 3.3C*). Similar to our endogenous protrudin staining without GFP overexpression, the axon-to-dendrite ratio in this experiment was significantly higher at 4 DIV (ratio=0.84) compared to 9 DIV (ratio=0.52) and 15 DIV (ratio=0.49) ($p<0.0001$) but there was no difference in the axon-to-dendrite abundance of protrudin between 9 DIV and 15 DIV ($p=0.999$) (*Fig. 3.3D*).

The use of overexpressed GFP to mark the axonal processes allowed us to examine the amount of protrudin in the distal axon (600-800 µm away from the cell body) at 9 DIV and 15 DIV. Very little protrudin (<5 grey values) was observed in the distal axon of mature neurons at 9 DIV and 15 DIV (*Fig. 3.4A*). As the axons of 4 DIV neurons were mostly shorter than 600 µm, only the amount at the proximal axon was measured.

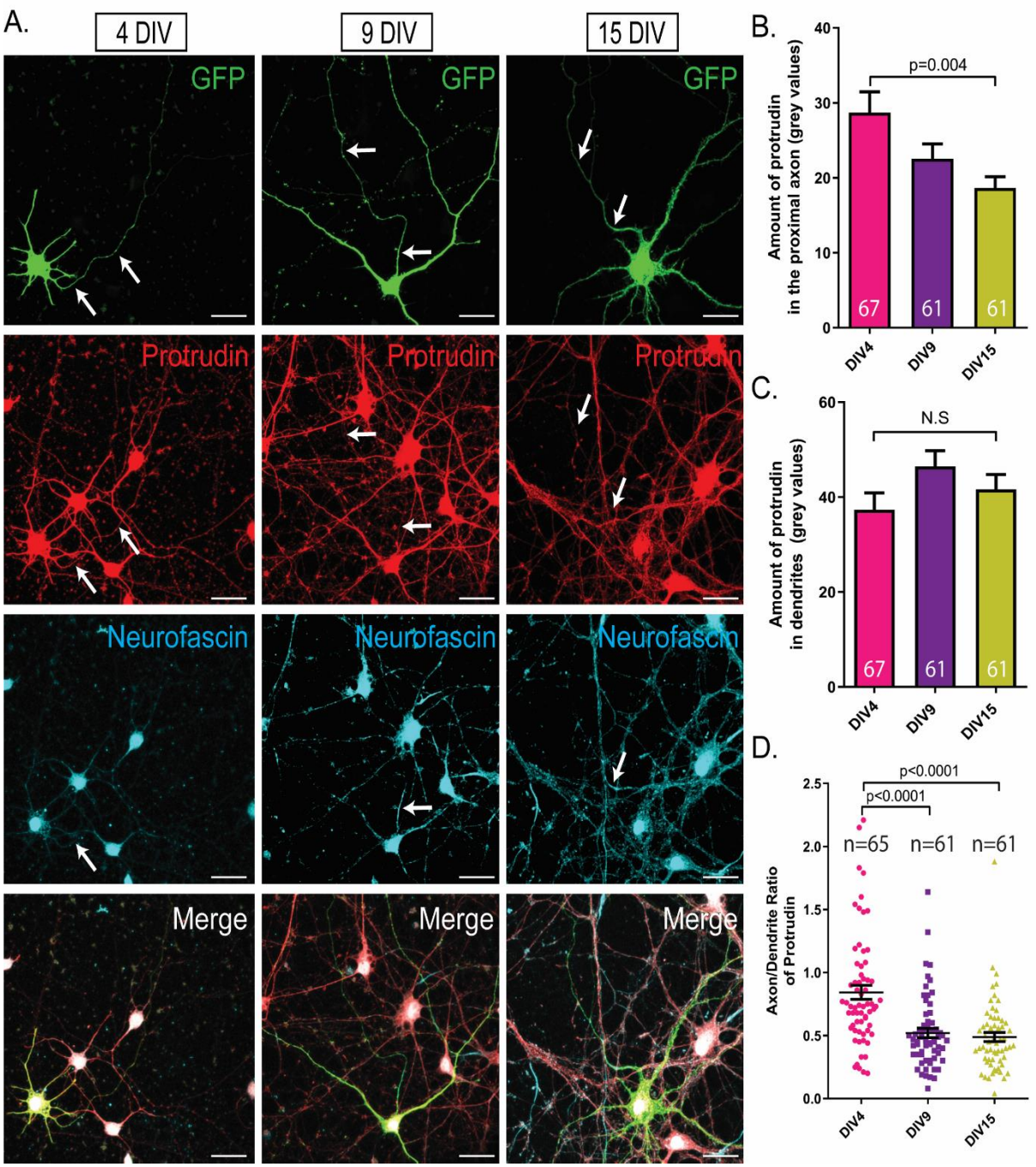

Figure 3.3 Protrudin's distribution in GFP-transfected primary cortical neurons at different stages of development. A. Immunofluorescent images of protrudin (red), GFP (green) and neurofascin (blue) localisation in the proximal axons at 4, 9 and 15 DIV taken at 40x magnification. White arrows indicate segments of the axons. Scale bars are 20 µm. B., C. Bar graphs to compare the mean protrudin intensity in axons and in dendrites across the different groups. Protrudin's staining intensity is significantly higher in proximal axons at 4 DIV compared to 15 DIV ($p=0.004$) but not compared to 9 DIV ($p=0.114$, one-way ANOVA, $n=4$). There is no difference in protrudin amount in dendrites at 4 DIV compared to 9 DIV and 15 DIV ($p=0.155$, one-way ANOVA, $n=4$). D. Scatter plot showing axon-to-dendrite ratio of protrudin. The axon-to-dendrite ratio of protrudin abundance is higher at 4 DIV compared to 9 DIV ($p<0.0001$) and 15 DIV ($p<0.0001$, Kruskal-Wallis statistic=32.22, $n=4$). All error bars represent mean ± SEM.

Last but not least, the amount of GFP fluorescence was also measured in axons and dendrites across the different developmental stages. There were no significant differences were observed in its distribution in axons at 4 DIV (82 grey values), 9 DIV (81 grey values) and 15 DIV (82 grey values) (p=0.999) (*Fig. 3.4C*). The axon-to-dendrite ratio similarly to protrudin decreased with maturation as there was more GFP in the axon compared to dendrites at 4 DIV (ratio=0.84) compared to 9 DIV (ratio=0.61) (p=0.008) and 15 DIV (ratio=0.68) (p=0.01) (*Fig. 3.4E*). Contrary to protrudin distribution though, this change in axon-to-dendrite distribution could be explained by higher amount of GFP observed in the dendrites of more mature neurons rather than a change of axonal distribution with maturation. 9 DIV (131 grey values) (p=0.0008) and 14 DIV (124 grey values) (p=0.008) neurons had more GFP in their dendrites compared to immature neurons at 4 DIV (92 grey values) (*Fig. 3.4D*). This increase in the amount of GFP in dendrites could most likely be attributed to the change in size of dendrites and the ability of more GFP to be carried in through diffusion. These results show that the reduced axon-to-dendrite ratio of protrudin with maturation is specifically a result of a reduced amount of protrudin in the axon rather than changes in its amount in dendrites.

Similar to the experiment above with no GFP, the amount of protrudin in the cell body seems to decline with maturation. There is less protrudin in 7-9 DIV (160 grey values) (p=0.027) and 14-16 DIV (157 grey values) (p=0.003) compared to younger neurons at 2-4 DIV (179 grey values) (*Fig. 3.4B)*. This result is again contradictory to our RNA sequencing results in the primary rat cortical neurons (Koseki *et al.*, 2017), but this could be attributed to the high density of the neuronal cultures with maturation and the high background staining (discussed in *Discussion*).

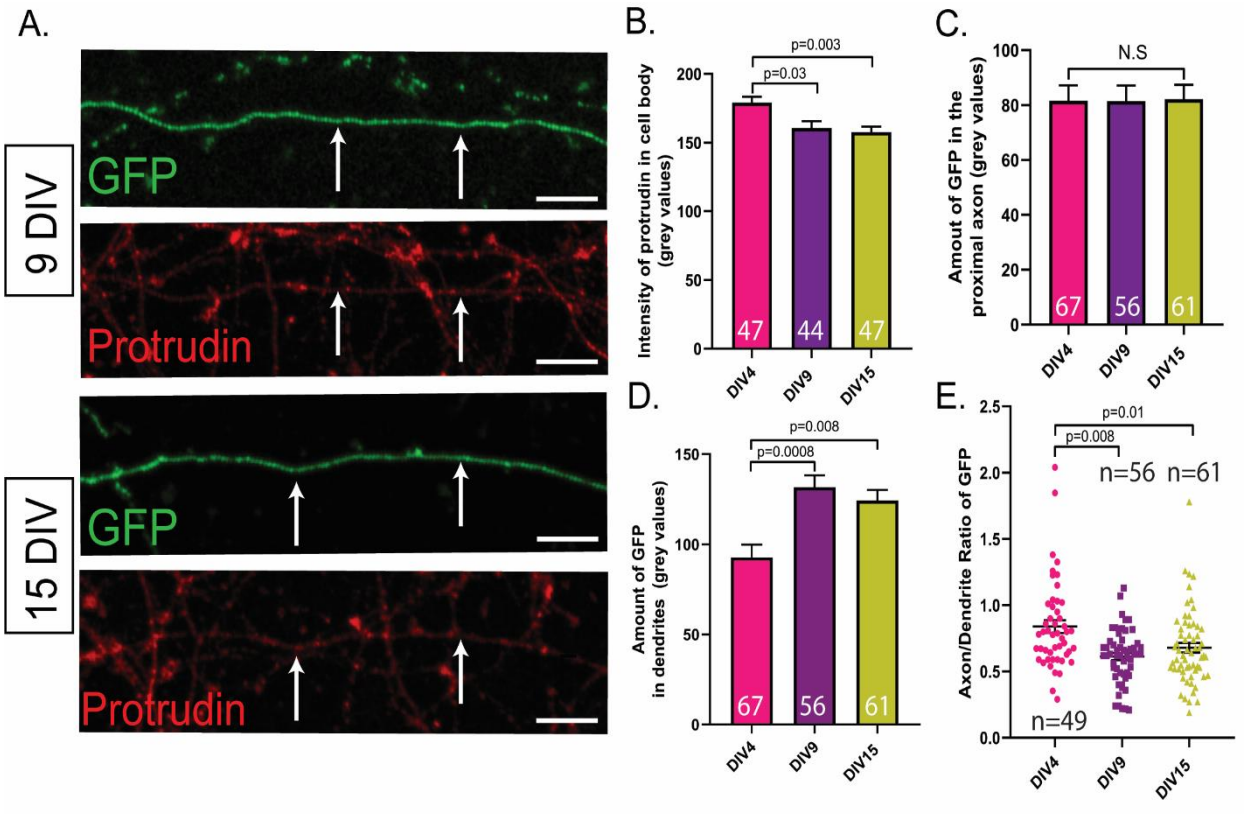

Figure 3.4 Protrudin's distribution in the distal axon of GFP-transfected primary cortical neurons at different stages of development and GFP distribution. A. Distal axon segments immunofluorescence of protrudin. White arrows indicate segments of the axons. Scale bars are 5 µm. B. The intensity of protrudin in the cell body at 4 DIV is higher than that at 9 DIV and 15 DIV (p=0.002, Kruskal-Wallis statistic=12.06, n=4). C. Bar graph to show that GFP amount in the axons of 4 DIV, 9 DIV and 15 DIV neurons does not change with development (p=0.999, one-way ANOVA, n=4). D. Bar graph to show that there is more GFP in the dendrites of 9 DIV and 15 DIV neurons compared to 4 DIV (p=0.0005, Kruskal-Wallis statistic=15.35, n=4). E. Scatter plot showing that the axon-to-dendrite ratio of the GFP protein is higher in 4 DIV compared to 9 DIV and 15 DIV neurons (p=0.0007, Kruskal-Wallis statistic=14.43, n=4). Error bars represent mean ± SEM.

2.2 Protrudin overexpression in PC12 cells

Once protrudin mutants were created and promoters were changed from CMV to synapsin to enable better expression in neuronal cells (see *Methods, Section 3.2.1*), they were first tested in PC12 cells. When overexpressed in PC12s cells, wild-type protrudin was found to co-localise at the end of neurites with Rab11 as previously described (Shirane and Nakayama, 2006) (*Fig. 3.5*). Rab11 is a key molecule involved in the axonal transport of integrin growth receptors as described in *Introduction, Section 3.2.* Protrudin was found to colocalise with the integrin alpha 5 receptor in addition to Rab11 at the end of processes (*Fig. 3.5A).* Furthermore, when either the wild-type or any of the two mutants are overexpressed in PC12s, treated with nerve-growth factor (NGF) for one day, all forms of protrudin were found to localise to the cell body but also to the tip of growing neurites in agreement with previous findings (*Fig. 3.5B*) (Shirane and Nakayama, 2006). The longest neurite and the percentage of neurite-bearing cells were measured in cells overexpressing syn-mCh, syn-mCh-WT, syn-mCh-MUT1 or syn-mCh-MUT2 at 1, 3 and 6 days of NGF treatment. There were no significant differences observed between any of these conditions (*Fig. 3.5C, 3.5D*).

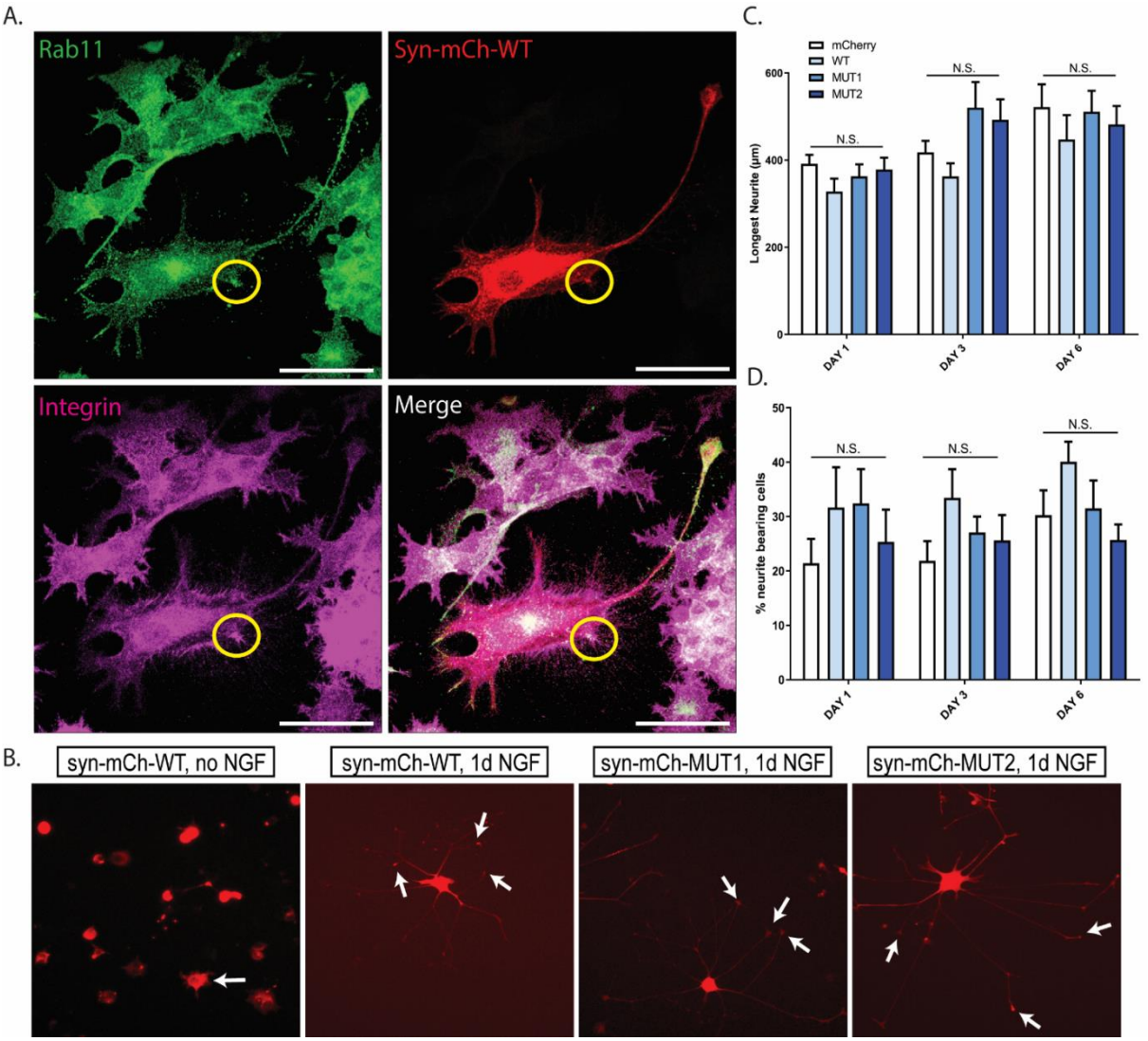

Figure 3.5 Protrudin overexpression in PC12 cells. A. Immunofluorescent images of PC12 cells transfected with syn-mCh-WT protrudin (red) and stained for Rab11 (green) and integrins (magenta). The yellow circle represents areas where protrudin, Rab11 and integrins colocalise. Scale bars are 50µm. B. Immunofluorescent images of PC12 cells overexpressing syn-mCh-WT (with no NGF or treated with NGF for 1 day), syn-mCh-MUT1 and syn-mCh-MUT2 (treated with NGF for 1 day). White arrows represent protrudin at the tip of growing processes. C. Bar graph to show the average longest neurite in cells expressing each construct. There is no significant differences between cells overexpressing syn-mCh, syn-mCh-WT, syn-mCh-MUT1 and syn-mCh-MUT2 treated with NGF for 1 (p=0.3821, Kruskal-Wallis statistic=3.062, n=1), 3 (p=0.162, Kruskal-Wallis statistic=5.134, n=1) or 6 days (p=0.697, Kruskal-Wallis statistic=1.436, n=1). D. Bar graph to show the percentage of neurite bearing cells expressing each construct. There is no significant differences between cells overexpressing syn-mCh, syn-mCh-WT, syn-mCh-MUT1 and syn-mCh-MUT2 treated with NGF for 1 (p=0.345, Kruskal-Wallis statistic=3.317, n=1), 3 (p=0.208, Kruskal-Wallis statistic=4.544, n=1) or 6 days (p=0.093, Kruskal-Wallis statistic=6.410, n=1). Error bars represent mean ± SEM.

2.3 Overexpression of protrudin constructs result in drastically elevated protein levels in primary cortical neurons and PC12 cells

syn-mCh, syn-mCh-WT, syn-mCh-MUT1 and syn-mCh-MUT2 were transfected into 10 DIV neurons which were then fixed at 14 DIV in ice-cold methanol. Neurons were then stained using anti-protrudin antibody (ProteinTech, 1:500) and imaged (*Fig. 3.6A, 3.6B*). The amount of protrudin expression detected by the antibody was measured across the groups in cells expressing the different fluorescent constructs. Cells overexpressing wild-type protrudin (48 times higher) as well as mutant 1 (41 times higher) and mutant 2 (39 times higher) were all found to express higher levels of protrudin compared to cells transfected with empty control mCherry vector (*Fig. 3.6C*).

These results were further validated by overexpressing the same constructs in PC12s cells and lysing them 72 hrs post transfection. The protein lysate was analysed by SDS PAGE and Western blotting, and then by detection with anti-protrudin antibody. The molecular weight of protrudin is 46 kDa and in previous reports the protein has been observed to run between 50-60 kDa on a Western Blot (Shirane and Nakayama, 2006; Matsuzaki *et al.*, 2011). A clear band above the 50 kDa of endogenous protrudin as well as another band at 75 kDa where our wild-type or mutant protrudin constructs were expressed, were detected in all samples (*Fig. 3.*6D). The difference in size could be accounted for as the overexpressed protrudin plasmid contains the protrudin protein which is fused to the mCherry protein (29 kDa). Protrudin has previously been shown to oligomerise so the band at 150 kDa could represent protrudin oligomers (Pantakani *et al.*, 2011).

In summary, all the constructs generated here were expressed reliably in primary rat cortical neurons and PC12 cells and resulted in substantially higher levels of the protrudin protein than normally present in these cells.

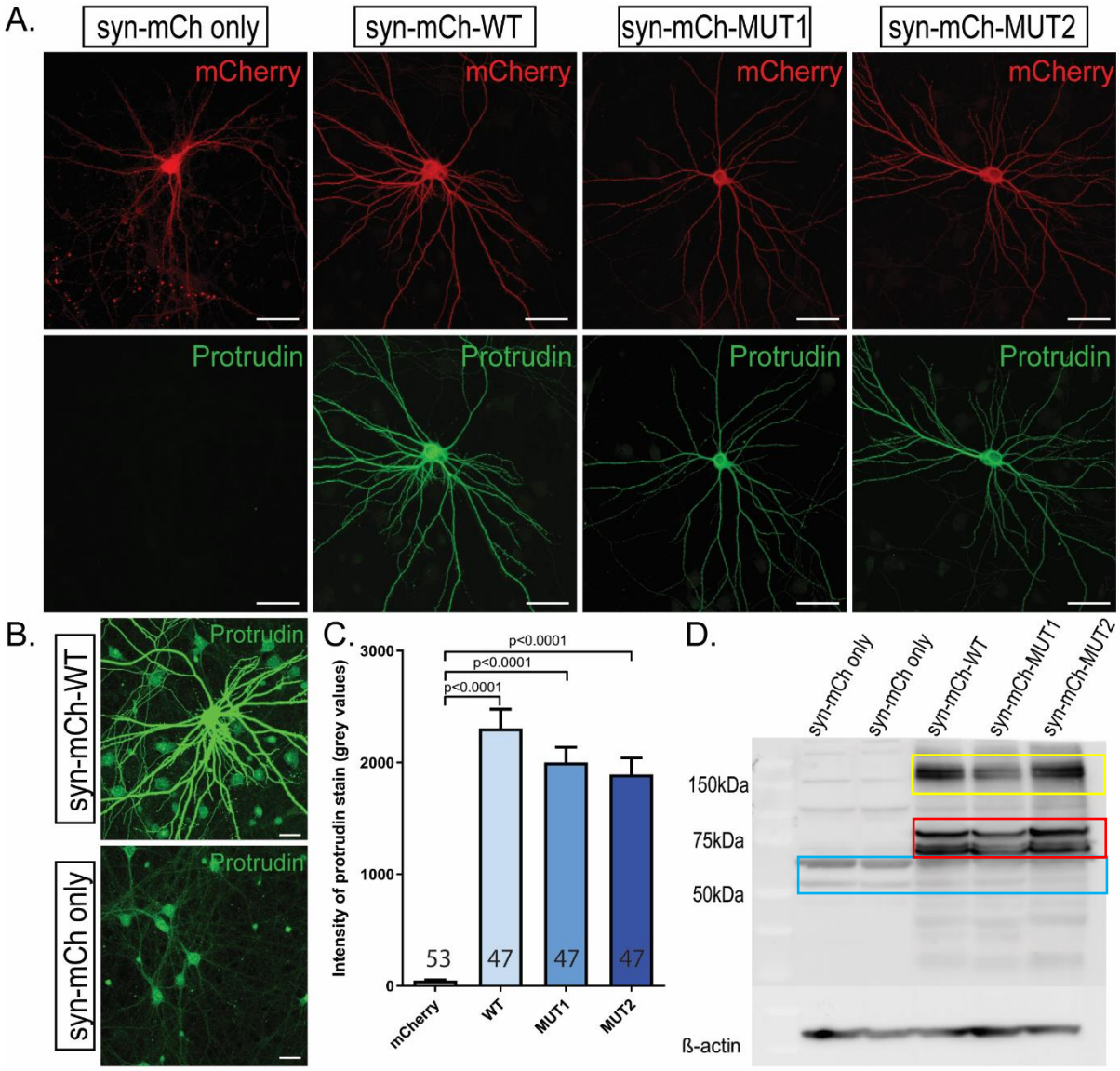

Figure 3.6 Overexpression of synapsin-protrudin plasmid constructs resulted in increased protein levels of protrudin in primary cortical neurons. A. Immunofluorescent images of endogenous mCherry signal from syn-mCh control, syn-mCh-WT, syn-mCh-MUT1 and syn-mCh-MUT2 constructs (red). Protrudin amount is detected by anti-protrudin immunostaining (green). Images were taken at 40x magnification. Scale bars are 20 µm. B. When imaging settings are altered to overexpose neurons expressing protrudin constructs, the endogenous protrudin in cells not overexpressing plasmids could be observed. C. Bar graph to show the average staining intensity of the protrudin in cells expressing the plasmid constructs. Protrudin's staining intensity is significantly higher in cells overexpressing syn-mCh-WT, syn-mCh-MUT1 and syn-mCh-MUT2 protrudin compared to cell expressing control syn-mCh vector (p=0.0001, Kruskal-Wallis statistic=117, n=3). Error bars represent mean ± SEM. D. Western blot image of PC12 cells lysate of cells overexpressing the four different constructs. The blot is stained for protrudin and beta actin to ensure that loading is equal. Blue box indicates the endogenous protrudin, red box indicates overexpressed protrudin-mCherry and yellow box shows overexpressed mCherry-tagged protrudin dimers.

2.4 Overexpression of protrudin causes minimal morphological changes in primary cortical neurons

Once the overexpression efficiency of our constructs was confirmed, their effect on cellular morphology was examined by dendritic tree analysis (Sholl analysis), spine morphology analysis and cell body size.

Dendritic tree analysis and soma size were obtained using semi-automated software – SynD (Schmitz *et al.*, 2011) (see *Methods, Section 5.1.1*). Cortical neurons were transfected at 10 DIV with syn-mCh, syn-mCh-WT, syn-mCh-MUT1 and syn-mCh-MUT2 protrudin constructs and fixed at 14 DIV in PFA (*Fig. 3.7A*). Images were taken at 40x magnification and imported into the software. Cell bodies were first identified and then neurites extending from the cell body out to a radius of 250 µm. The number of processes crossing imaginary concentric circles irradiating from the cell body towards the periphery of the cell (every 10 µm) were automatically counted. There were no significant changes detected in the cell body size of cortical neurons expressing each of the four constructs (*Fig. 3.7B*). The total dendritic length of cells expressing syn-mCh-MUT2 was found to be longer compared to cells expressing syn-mCh only ($p=0.04$) suggesting that mutant 2 protrudin might enhance dendritic length (*Fig. 3.7C*). Interestingly, Sholl analysis revealed that there are no significant differences across the different conditions in dendritic tree complexity (*Fig. 3.7D)* although there is a trend towards cells expressing syn-mCh-MUT2 to have more complex morphologies between 100-200 microns away from the cell body compared to syn-mCh only.

The number and type of dendritic spines was also examined. It was initially observed that overexpressed protrudin is not evident in dendritic spines (data not shown), therefore co-transfection with a GFP-expressing construct was required to analyse spine morphology. Primary cortical neurons were transfected with GFP together with either syn-mCh, syn-mCh-WT, syn-mCh-MUT1 or syn-mCh-MUT2 at 10 DIV and fixed at 14 DIV. The cells were then imaged at 63x. Spine number and morphology in a 20 µm length from the cell body were examined in the Image J Fiji software using the Cell Counter plugin (Schindelin *et al.*, 2012). Each spine was categorised as either stubby, mushroom or thin in accordance to previously defined categories (Hoogenraad and Akhmanova, 2010). Protrudin overexpression (wild-type or mutants) did not have any significant effects on the number or the morphology of dendritic

spines (*Fig. 3.*8). Interestingly, it was observed that syn-mCh-MUT2 protrudin overexpression resulted in protrudin localising more readily to the dendritic spines compared to overexpression of syn-mCh-WT or syn-mCh-MUT1 (*Fig. 3.8A*).

In conclusion, overexpression of wild-type or either of the two constitutively phosphorylated mutant forms of protrudin causes minimal changes in the morphology or function of primary cortical neurons.

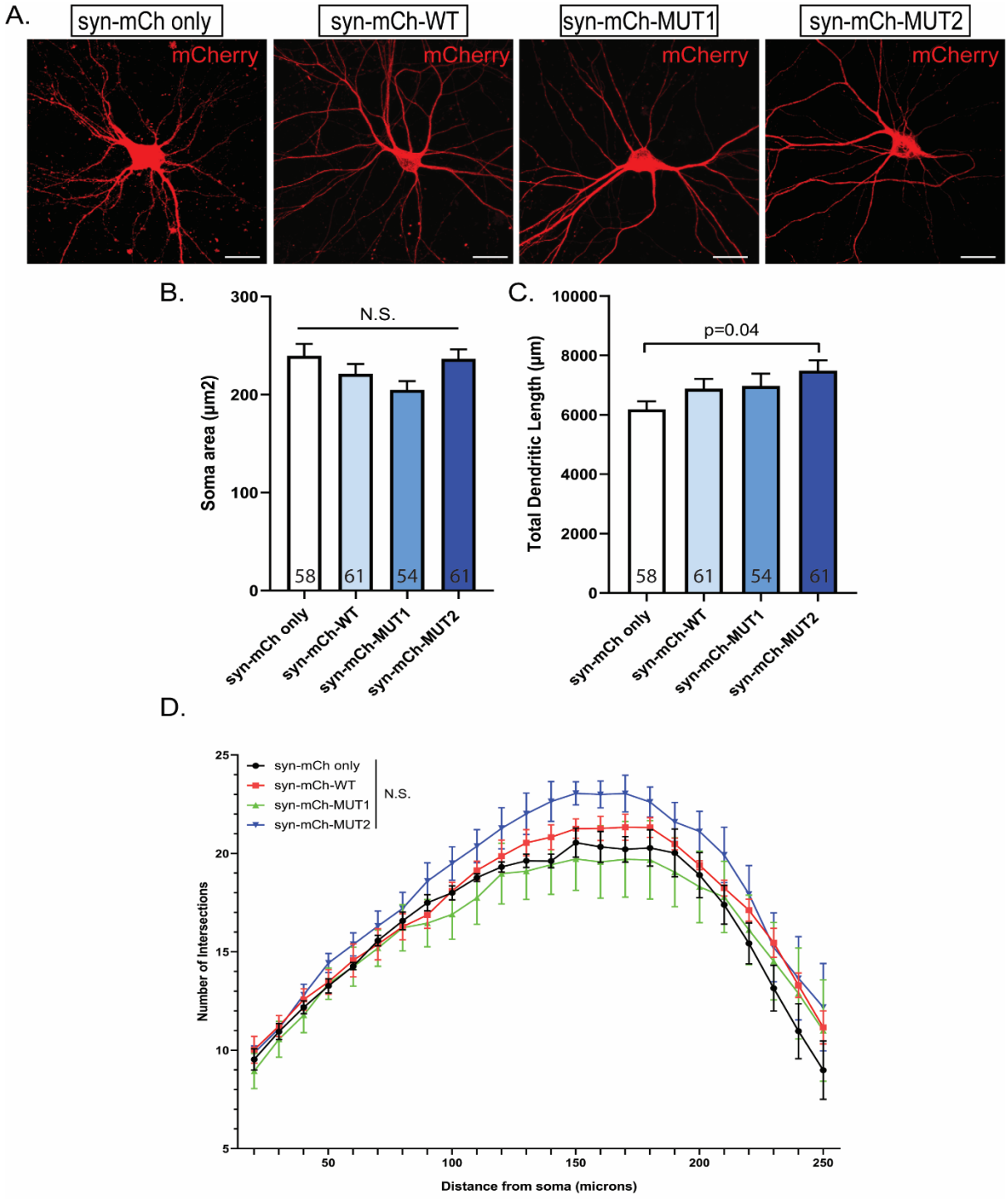

Figure 3.7 Overexpression of synapsin-protrudin plasmid constructs causes minimal morphological changes in primary cortical neurons at 14 DIV in culture. A. Immunofluorescent images of endogenous mCherry signal from syn-mCh control, syn-mCh-WT, syn-mCh-MUT1 and syn-mCh-MUT2 constructs (red). Images were taken at 40x magnification. Scale bars are 20 µm. B. Bar graph to show that there are no significant differences in the average soma area in cells expressing the four different mCherry constructs (p=0.1365, Kruskal-Wallis statistic=5.54, n=4). C. Bar graph to show the dendritic tree total length across the different conditions. Cells overexpressing syn-mCh-MUT2 seem to have a more complex dendritic structure than cells overexpressing syn-mCh control (p=0.04, Kruskal-Wallis statistic=7.391, n=4). D. Line graph to show the dendritic tree complexity of neurons transfected with each construct - the number of intersections at each distance from the cell soma was plotted for each condition. There are no significant differences between the conditions (p=0.150, RM two-way ANOVA, n=4). Error bars represent mean ± SEM.

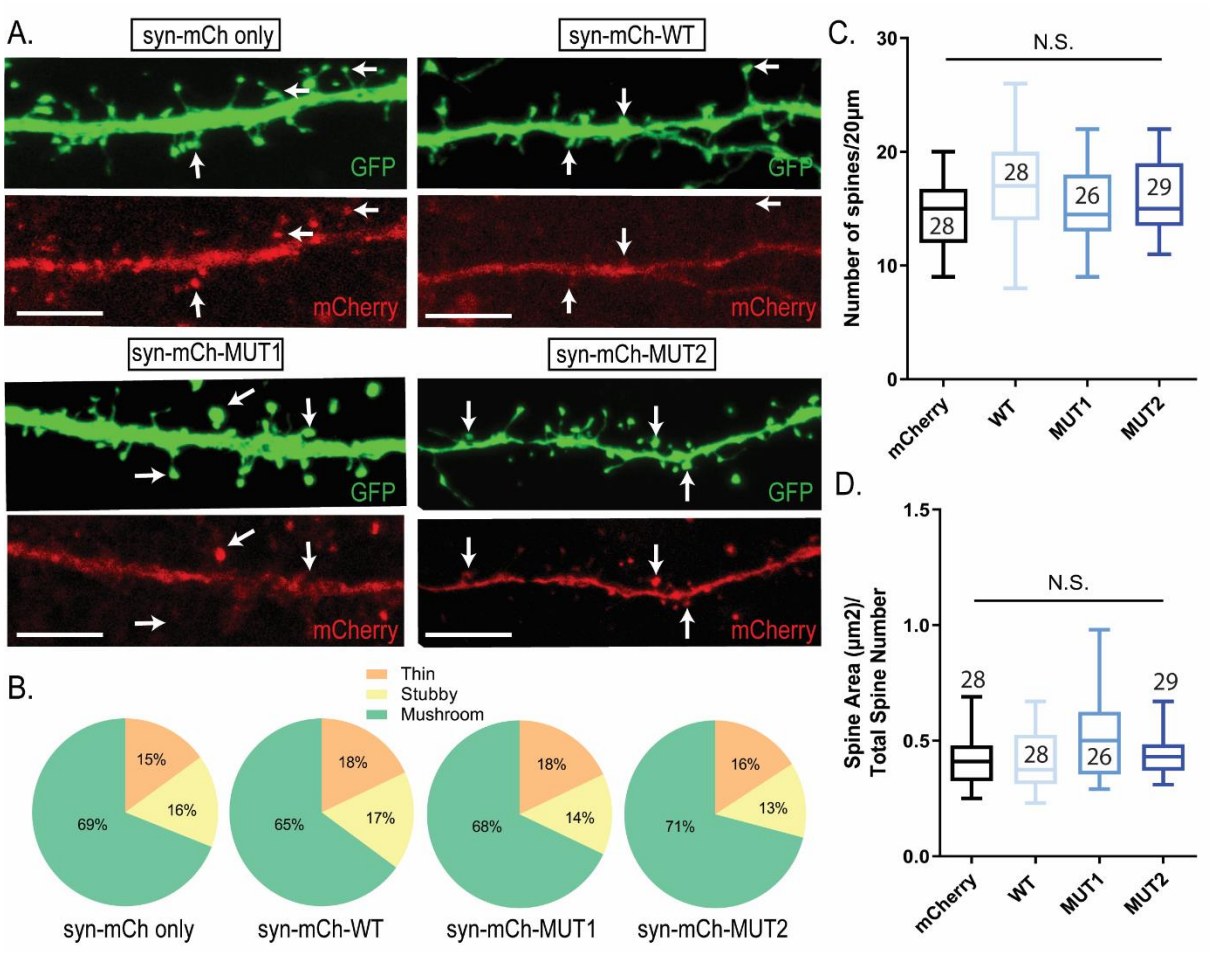

Figure 3.8 Overexpression of synapsin-protrudin plasmid constructs causes no changes to the dendritic spine morphology in 14 DIV primary cortical neurons. A. Representative z-project images of 20 µm z-stack sections examined for dendritic spine number and morphology in cells overexpressing syn-mCh only, syn-mCh-WT, syn-mCh-MUT1 and syn-mCh-MUT2. Images were taken at 63x, 3.5 zoom. White arrows point to individual spines. Scale bars are 5µm. B. Pie charts of the percentages of different spine morphology (thin, stubby, mushroom) in each condition. C. Box plot to show the number of dendritic spines in a 20 µm segment. No significant differences were observed in the number or type of dendritic spines (p=0.075, Kruskal-Wallis statistic=6.89, n=2). D. Box plot to show the spine area (μm^2) per the total number of spines for each condition. There were no significant differences between the four conditions (p=0.127, Kruskal-Wallis statistic=5.699, n=2).

2.5 Overexpression of protrudin enhances axon outgrowth in primary cortical neurons

As described above, overexpression of wild-type or mutant protrudin does not enhance NGF-induced neurite outgrowth in PC12 cells (*Fig. 3.5*). Overexpression of protrudin, however was previously reported to enhance neuronal neurite outgrowth in rat hippocampal neurons at early stages of development (Shirane and Nakayama, 2006). It was therefore not clear whether protrudin would function to promote axon growth in primary cortical neurons developing *in vitro*. Rat primary cortical neurons were, therefore, transfected with syn-mCh, syn-mCh-WT, syn-mCh-MUT1 and syn-mCh-MUT2 protrudin constructs at 2 DIV and fixed in 3% PFA at 4 DIV (*Fig. 3.9A*). The longest process, the number of neurites per cell and the total dendritic length were measured.

The longest neurite (classified as the axon) in cortical neurons overexpressing syn-mCh-MUT1 (921 µm) was significantly longer than syn-mCh only (731 µm) (p=0.005) (*Fig. 3.9C*). Despite not reaching significance, the longest neurites of cells overexpressing syn-mCh-WT (890 µm) or syn-mCh-MUT2 (843 µm) showed a trend towards being longer than syn-mCh only (p=0.152 and 0.239 respectively). The total dendritic length of syn-mCh-MUT1 (265 µm) and syn-mCh-MUT2 (247 µm) was shorter than syn-mCh only (359 µm) (p=0.02 and p=0.002 respectively) but not from syn-mCh-WT (280 µm) (p=0.157) (*Fig. 3.9D*). Lastly, the number of primary neurites (defined as the neurites originating from the cell body) was not found to be significantly different between syn-mCh (7.15 neurites), syn-mCh-WT (6.49 neurites), syn-mCh-MUT1 (6.49 neurites) and syn-mCh-MUT2 (6.28 neurites) (p=0.157) (*Fig. 3.9E*).

This experiment, however had some caveats which are discussed in *Discussion* in detail. One caveat, for example, is that when overexpressing protrudin in primary cortical neurons, the amount reaching the distal axon is smaller than that reaching the proximal axon (*Fig. 3.9B*). During data collection, it was noticed that some axons of neurons expressing protrudin-containing constructs are very long and it becomes hard to trace them as the amount of protrudin declines and the fluorescence is not bright enough at 20x to trace. This immediately introduces a bias towards only measuring length of axons which could be traced, and which are normally shorter. The use of anti-mCherry antibody was also examined as a

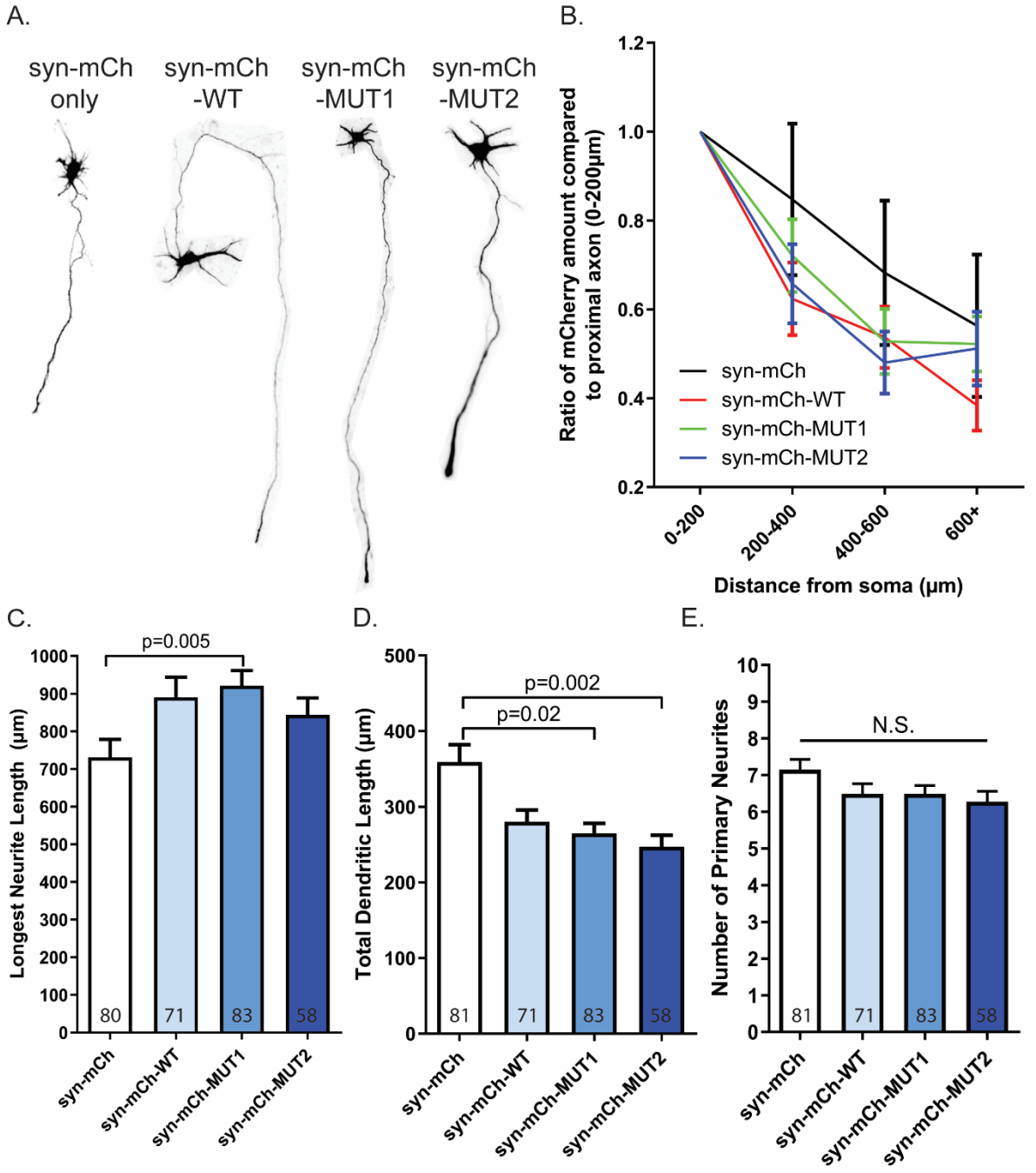

Figure 3.9 Overexpression of synapsin-protrudin constructs enhances axon outgrowth in 4 DIV primary cortical neurons. A. Representative images of 4 DIV neurons overexpressing syn-mCh only, syn-mCh-WT, syn-mCh-MUT1 and syn-mCh-MUT2. Images were taken at 20x. B. A line graph to show reduced amount of protrudin-mCherry signal in distal axon compared to the proximal axon in 14 DIV neurons. C. A bar graph to show that syn-mCh-MUT1 protrudin has longer average longest neurites than syn-mCh only but not than syn-mCh-WT or syn-mCh-MUT2 (p=0.008, Kruskal-Wallis statistic=11.82, n=4). D. A bar graph to show that syn-mCh-MUT1 and syn-mCh-MUT2 protrudin have smaller dendritic length compared to syn-mCh but not to syn-mCh-WT (p=0.002, Kruskal-Wallis statistic=14.62, n=4). E. A bar graph to show that there is no significant difference between the number of primary neurites in 4 DIV cortical neurons overexpressing syn-mCh only, syn-mCh-WT, syn-mCh-MUT1 and syn-mCh-MUT2 (p=0.157, Kruskal-Wallis statistic=5.202, n=4). Error bars represent mean ± SEM.

potential way to improve this experiment. However, similar observations were made even when the antibody was used (data not shown).

In order to address this problem, an additional experiment was carried out where 2 DIV primary cortical neurons were transfected with much brighter constructs – CAG-GFP control, CAG-GFP-WT and CAG-GFP-MUT2 protrudin (*Fig. 3.10A*). These constructs were created as described in *Methods, Section 3.2.3* in order to make viruses for the *in vivo* experiments described in *Chapter 4.* As only protrudin mutant 2 was selected to be included in *in vivo* experiments due to its effects on axon regeneration *in vitro* (see *Chapter 4),* mutant 1 protrudin was not included in these neurite outgrowth experiments.

Our results showed that cells overexpressing CAG-GFP-MUT2 (444 µm) had an axon significantly longer than cells overexpressing CAG-GFP only as a control (342 µm) (p=0.006) (*Fig. 3.10B*). Despite not reaching significance CAG-GFP-WT (387 µm) longest process was longer than CAG-GFP only (p=0.493) (*Fig. 3.10B*). Contrary to our previous experiment, the total dendritic length was not significantly different between cells overexpressing CAG-GFP control (140 µm), CAG-GFP-WT (144 µm) or CAG-GFP-MUT2 (137 µm) protrudin (p=0.668) (*Fig. 3.10C*). Similar to our previous findings, the number of primary neurites was not significantly different between CAG-GFP control (5.75 neurites), CAG-GFP-WT (5.98 neurites) and CAG-GFP-MUT2 (5.57 neurites) protrudin (p=0.656) (*Fig. 3.10D*).

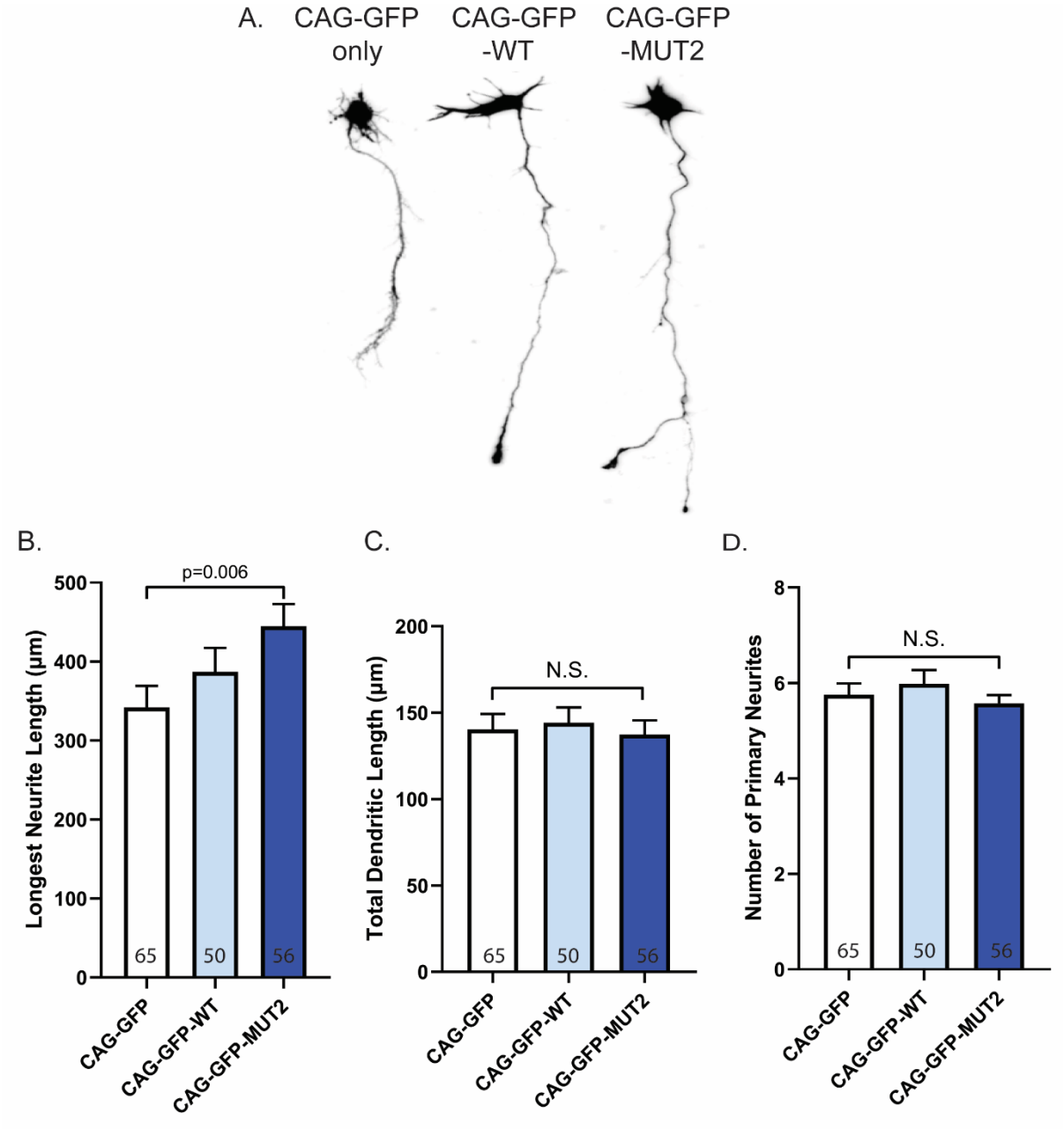

Figure 3.10 Overexpression of CAG-GFP-protrudin plasmid constructs enhances neurite outgrowth in 4 DIV primary cortical neurons. A. Representative images of 4 DIV neurons overexpressing CAG-GFP control, CAG-GFP-WT and CAG-GFP-MUT2 constructs. Images were taken at 20x. B. A bar graph to show that CAG-GFP-MUT2 protrudin-expressing cells have longer average longest neurites than CAG-GFP only but not than CAG-GFP-WT ($p=0.008$, Kruskal-Wallis statistic=9.494, n=4). C. A bar graph to show that there is no significant difference between the total dendritic length in 4 DIV cortical neurons overexpressing CAG-GFP control, CAG-GFP-WT and CAG-GFP-MUT2 ($p=0.668$, Kruskal-Wallis statistic=0.806, n=4). D. A bar graph to show that there is no significant difference between the number of primary neurites in 4 DIV cortical neurons overexpressing CAG-GFP control, CAG-GFP-WT and CAG-GFP-MUT2 ($p=0.665$, Kruskal-Wallis statistic=0.844, n=4). Error bars represent mean ± SEM.

3. Discussion

This chapter focuses on examining the localisation of endogenous protrudin in primary cortical neurons and on studying the effects of wild-type and mutant protrudin overexpression on cell morphology and function. Here, it was demonstrated in two separate paradigms that endogenous protrudin abundance in the axon compared to dendrites declines with maturation. It was also found that overexpression of wild-type and two phosphomimetic forms of protrudin in PC12 cells shows similar distribution to previously published reports where protrudin re-distributes from the pericentrosomal compartment to the end of growing neurites upon NGF treatment. Overexpression did not lead to an effect on neurite outgrowth of PC12 cells upon NGF treatment. Furthermore, overexpression of wild-type and the phosphomimetic mutant forms of protrudin resulted in highly increased amount of the protrudin protein in primary cortical neurons but had minimal effects on cell morphology in terms of soma size, dendritic tree complexity or spine number and type. Lastly, the two phosphomimetic mutants showed promising ability to improve neurite outgrowth in primary cortical neurons.

In previous reports, protrudin has been detected in mouse primary hippocampal neurons at 1 DIV and 3 DIV. At 1 DIV protrudin was found to be localised to the pericentrosomal compartment and to growing neurites. Later on in development (3 DIV), the distribution of protrudin changed and it was abundant in axons, dendrites and especially at the growth cone (Shirane and Nakayama, 2006). Most previous studies examining protrudin distribution were carried out either in cancer cells or in immature neurons. This prompted us to examine the distribution of the protrudin protein in rat primary cortical cultures over development from 2-4 DIV to 14-16 DIV (electrically-active, Koseki *et al.*, 2017) and to explore whether protrudin is distributed differentially in axons and dendrites similar to integrins and Rab11 distribution (Eva *et al.*, 2010; Franssen *et al.*, 2015; Andrews *et al.*, 2016). Upon staining for endogenous protrudin, it was found that the axon-to-dendrite distribution of protrudin is much higher at earlier stages (2-4 DIV) than at later stages of neuronal development and differentiation (7-9 DIV and 14-16 DIV) (*Fig. 3.2*). This phenomenon could be explained by the fact that protrudin seems to be more abundant in the axons at early compared to later stages

of development as there is no change in its amount in the dendrites with maturation. These results suggest that early on in development protrudin is needed in the newly extending axons but then as neurons mature and polarise, the protrudin protein is redistributed towards the cell body and dendrites. This distribution is very similar to other proteins such as Rab11 and integrins which are essential for neurite growth and axon transport (Eva *et al.*, 2010, 2012; Franssen *et al.*, 2015; Andrews *et al.*, 2016).

This experiment, however, had several caveats: firstly, the amount of protrudin in the axon was only measured at the AIS as this is where the neurofascin stain was mostly visible so the amount of protrudin in the distal axons could not be accounted for. Secondly, the neurofascin protein is not expressed at high levels during 2 DIV (Boiko *et al.*, 2007; Yang *et al.*, 2007) so in some of the cases the longest process showing protrudin-positive staining was assumed to be the axon. Furthermore, because no cytosolic protein marker was used to label all neuronal processes, the difference of protrudin's abundance in thick vs. thin processes could not be observed and only processes containing the highest amounts of protrudin which could be visually identified were used in the experiment. Lastly, the amount of protrudin in the cell body seemed to decline with maturation which is contradictory to our RNA sequencing data which points to relatively similar amount of the gene during development. This discrepancy could be attributed to the much higher confluency of the more mature neurons accounting for much higher background staining resulting in artificially lower soma amount levels of protrudin.

In order to improve the above experiment, primary cortical neurons were transfected with a GFP construct. GFP is a cytosolic protein so it readily diffuses in all neuronal processes and it allows for their visualisation. This experiment confirmed the observation that the axon-to-dendrite distribution of protrudin changes with maturation (*Fig. 3.3D*). Again, this reduction was attributed to reduced protrudin levels in the axon rather than a change in the dendrites confirming our previous results. This experiment allowed for the visualisation of the distal axon which revealed that there is very little endogenous protrudin present in the distal axon at later stages of development (*Fig. 3.4A*). This observation led to the hypothesis that overexpressing protrudin in mature neurons, could restore developmental growth state as

one of protrudin's functions in the cell is to aid the anterograde movement of recycling endosomes containing growth-molecules to the tip of axons.

The GFP protein amount was also measured in axons and dendrites to act as a control protein. Interestingly, the axon-to-dendrite ratio of GFP seems to also decline with maturation (*Fig. 3.4B-E*) – this effect was, however a result of increased amount in the dendrites possibly due to their growth with maturation rather than a change in the axon. This suggests that the changes observed with protrudin distribution are axon-specific.

Overall, there were difficulties in validating the anti-protrudin antibody used for the experiments above as no reliable knock-down model of rat endogenous protrudin was achieved (see *Chapter 5*). Therefore, the results obtained should be considered with caution. Currently, other rat cell lines are being tested to create a knockdown system and knock-out mouse tissues is in the processes of being obtained.

Mutagenesis of protrudin was carried out in order to validate whether mimicking phosphorylation of protrudin at ERK phosphorylation sites can potentially have similar effects to those induced by NGF treatment and ERK/MAPK activation without these pathways actually being active. Because separate concurrent experiments in the lab are finding that signalling through pathways downstream of growth factor receptors also declines with development, it was hypothesised that mimicking aspects of their activation such as protrudin phosphorylation might improve neuronal growth potential. This is particularly important in the context of improving growth after injury as discussed in *Chapter 4.*

Mutagenesis site selection was carried out according to the functional mutants which Shirane and Nakayama, 2006 identified. They showed that mutants lacking the same phosphorylation site combinations as in mutant-1 and mutant-2 in this study result in reduced capacity of protrudin for binding to Rab11 upon NGF treatment and ERK/MAPK pathway activation. This suggested that phosphorylation of protrudin at multiple sites in the combinations shown might be necessary for its interaction with Rab11. An interesting observation is that mutant-1 phosphorylation sites are located near the KIF5A-binding site and mutant-2 phosphorylation sites are located near the Rab11-binding site which could

possibly account for different activity of the two mutants. The main purpose for creating a phosphomimetic form of the protrudin protein was to examine its effects on Rab11-dependent transport of endosomes along axons and the effects that any change might have on the regenerative abilities of neurons. To begin with, protrudin constructs contained the cytomegalovirus (CMV) promoter so when attempts were made to transfect primary neuronal cultures, the transfections efficiencies were extremely low. This necessitated changing the promoters of all constructs to a more neuron-specific promoter such as synapsin (SYN) (see *Methods, Section 3.2.1.* Once the synapsin promoter was cloned into all constructs, the transfection efficiency and selectivity were much better, and all further experiments were carried out using these constructs.

The protrudin mutants were first overexpressed in PC12 cells to test their toxicity and effects on PC12 differentiation. Firstly, protrudin was found to co-localise with a known interactor – Rab11 but also with the integrin receptor which is found in Rab11-recycling endosomes (*Fig. 5A*). Interestingly, overexpression of syn-mCh-MUT1 and syn-mCh-MUT2 in PC12 cells was not sufficient to promote neurite extension in PC12 cells (data not shown). This observation suggests that complete activation of the ERK/MAPK pathway by NGF is required for neurite extension in PC12 cells and mimicking a single aspect of its downstream effects does not lead to its full effects. For example, it has been shown before that ERK activation results in ERK translocation to the nucleus where it induces a set of neuron-specific genes needed for neurite outgrowth (Vaudry *et al.*, 2002). Furthermore, the phosphorylation of other downstream targets such as Rap1 aids the sustained activation of the ERK pathway and is required for the ability of PC12 cells to be electrically excitable – another neuron-like feature induced by NGF treatment (York *et al.*, 1998). Although protrudin phosphomimetic mutants do not on their own induce neurite outgrowth in PC12 cells, they show similar redistribution to wild-type protrudin upon NGF treatment – from the pericentrosomal compartment to the end of growing processes (*Fig. 3.5B*). Overexpression of wild-type or mutant protrudin also did not have an effect of the length of newly growing process or on the percentage of neurite-bearing cells after 1, 3 or 6 days of NGF treatment (*Fig 3.5C, 3.5D*).

Before any further experiments were carried out, it was important to examine whether overexpression of wild-type or any of the phosphomimetic mutants cause any

morphological changes in primary cortical neurons. No changes were detected in the cell body area or the complexity of the dendritic tree although syn-mCh-MUT2 protrudin showed a small increase in total dendritic length compared to control (*Fig. 3.*7). Furthermore, there were no significant differences between the number or type of dendritic spines in either of the condition (*Fig. 3.8*). An interesting observation from this experiment is that when wild-type or syn-mCh-MUT1 protrudin is overexpressed, very little protrudin is found in the spines. This could be due to protrudin's association with KIF5 – a microtubule-associated motor protein (Matsuzaki *et al.*, 2011) whereas the structure and the remodelling of dendritic spines is mostly dependent on the actin cytoskeleton (Hotulainen and Hoogenraad, 2010). Neurons overexpressing syn-mCh-MUT2, however, seem to be found more often in spines suggesting that this mutant might be interacting with the actin cytoskeleton and its adaptors too – a hypothesis not yet tested. Overall, overexpression of wild-type or phosphomimetic protrudin in mature neurons did not cause any major morphological changes that could interfere with normal cell function.

Lastly, the effects of protrudin overexpression on neurite outgrowth in immature neurons were also examined. Initially, wild-type and mutant protrudin fused to mCherry were overexpressed in neurons and only Syn-mCh-MUT1 was shown to increase neurite outgrowth although wild-type and mutant 2 protrudin also showed a trend towards increased neurite outgrowth (*Fig. 3.9*). The total dendritic length of neurons overexpressing all forms of protrudin was shorter which could possibly be explained as a compensation for using more cellular building blocks to build a longer axon. Nevertheless, this experiment had a major caveat – during the quantification phase it was observed that some really long axons "dim out" and could not be traced to the axon tip in the culture which automatically introduced a bias that only the shorter, brighter axons were accounted for. The drop in mCherry intensity was measured in older neurons with long axons and indeed, it was shown that the intensity drops dramatically in the distal axon (*Fig. 3.9B*). Interestingly, protrudin abundance in growth cones is very prominent and growth cones could be found easily throughout the culture dish at these early stages of development (data not shown). In order to improve the tracing of protrudin-transfected axons, an alternative approach could be used where neurons are co-transfected with a brighter GFP construct or a mixed culture with GFP-positive neurons from transgenic animals is used (Gomis-Rüth *et al.*, 2014).

In order to improve this experiment, different constructs which were initially created for viral production for *in vivo* experiments where protrudin is fused to GFP instead of mCherry, were used as the fluorescent protein signal was much brighter. Mutant 1 was not included in these experiments as mutant 2 was the only mutant selected for further use *in vivo* due to its effects on axon regeneration *in vitro* (see *Chapter 4*). Overexpression CAG-GFP-MUT2 induced increased neurite outgrowth and CAG-GFP-WT showed a similar trend towards increased neurite outgrowth (*Fig. 3.10B*). There was no effect of protrudin overexpression on total dendritic length or number of primary neurites (*Fig. 3.10C, D*).

These experiments suggest that both protrudin mutants might have some effect on increasing neurite outgrowth in primary cortical neurons. Interestingly, all forms of protrudin accumulated at the tip of the growing axons (*Fig. 3.9A, 3.10A*) suggesting that protrudin might play an important role at the growth cone of newly growing neuronal processes.

CHAPTER IV: PROTRUDIN ENHANCES AXON REGENERATION IN VITRO AND IN VIVO

Summary

This chapter explores the ability of wild-type and mutant protrudin overexpression to aid axon regeneration in primary cortical neurons after laser axotomy and in intact animals after an optic nerve crush. Protrudin is also tested in a neuroprotective paradigm in a rat model of glaucoma, a neurodegenerative disease of the optic nerve.

1. Introduction

In this chapter, three different models of CNS axon regeneration were utilised in order to test the ability of wild-type and constitutively phosphorylated protrudin to enhance axon regeneration.

1.1 In vitro Laser Axotomy

The *in vitro* laser axotomy model of primary cortical neurons is a newly developed method which allows for injury of individual axons and monitoring of their regeneration over 14 hours after the injury. This method has previously been used in our laboratory in two separate studies. In 2017, Koseki et al. showed that E18 primary cortical neurons grown *in vitro* develop electrical properties between 8 and 16 DIV and that they form coordinated

networks. They also showed that this maturational change is accompanied by gene expression changes as observed by RNA sequencing analysis. Maturation of cortical neurons *in vitro* resulted in an increase in the expression of synaptic proteins and a decrease in the levels of proteins involved in neuronal development (Koseki *et al.*, 2017). The regenerative potential of the cortical cultures was also examined: immature neurons (4 DIV) regenerated better after laser axotomy (63%) compared to more mature neurons (24 DIV, 8%). Furthermore, axons cut distally (>800 µm) from the cell body regenerated more poorly than axons cut proximally to the cell body at all developmental stages. Lastly, Koseki and colleagues (2017) showed that axon regeneration of mature cortical neurons could be improved in this model by a genetic manipulation. In this case, overexpression of Rab11 (a small GTPase involved in the axonal transport of growth molecules and which is normally excluded from mature axons) resulted in enhanced axon regeneration (38%) compared to control (11%). This increase in regenerative potential was accompanied by an increase in the trafficking of the growth-associated integrin alpha5 receptor along the axon. This was the first proof of principle experiment in our model that genetic manipulations of axon transport machinery could influence axon regeneration in the CNS *in vitro.*

Another study from our laboratory further strengthened the reproducibility and the validity of our *in vitro* axotomy method and the idea that enhancement of the transport of growth-molecules can boost regeneration. In their study, Eva and colleagues (2017) show that blockade of an ARF6 activator – EFA6, which is enriched at the axon initial segment (AIS) allows for enhanced transport of growth-promoting cargo along the axon and enhances regeneration after laser axotomy (58%) compared to control (27%). Interestingly, EFA6 is not found at the AIS in regenerative DRG neurons and its overexpression in these neurons suppresses their regenerative properties (Eva et al., 2017).

In summary, two genetic manipulations targeting the transport of growth-promoting molecules along mature CNS axons have successfully promoted axon regeneration after laser axotomy in our model. Therefore, *in vitro* laser axotomy in primary cortical neurons was found to be a suitable model to test the ability of wild-type and constitutively phosphorylated protrudin to enhance axon regeneration in a dish.

1.2 Optic Nerve Crush in Mice

In order to test protrudin overexpression as a regenerative intervention of protrudin in the CNS *in vivo*, we used the optic nerve crush model. The optic nerve is a white matter tract connecting the retinal ganglion cells (RGCs) in the retina to their synaptic targets in the contralateral side of the brain. The optic nerve tracts run ipsilaterally from the retina until they reach the optic chiasm – an X-shaped structure where the majority of the axons within each tract cross to the contralateral part of the brain and where they synapse within the superior colliculus (*Fig. 4.1*). The injury in an optic nerve crush model is normally inflicted 1-3mm behind the eyeball and because of the isolation of the optic nerve from any surrounding grey matter, the injury is purely axonal (Templeton and Geisert, 2012). Furthermore, the injury results in a substantial loss of RGC (85-90%) in the retina 2-3 weeks after injury which also allows for testing the effects of different manipulations on RGC survival. This model was used in the current experiments because it is highly reproducible, regeneration could be observed in only 1-2 weeks after injury, and it allows for the testing of both axon regeneration and neuronal survival in the CNS *in vivo.*

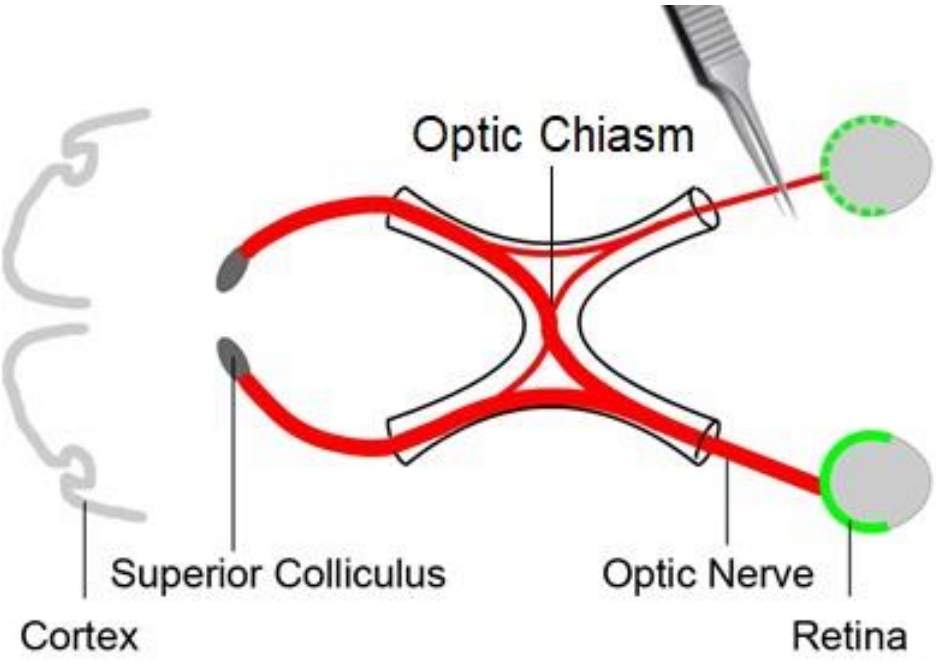

Figure 4.1 A schematic diagram of the anatomy of the optic nerve and the location of the optic nerve crush in a mouse optic nerve crush model (adapted from Tang *et al.*, 2011).

Several studies so far have successfully targeted intracellular pathways to promote axon regeneration after optic nerve crush. For example, deletion of PTEN (phosphatase and tensin homolog), a negative regulator of the mammalian target of rapamycin (mTOR) resulted in improved RGC survival (45%) compared to control (20%) as well improved axon regeneration 2 weeks post crush in transgenic mice with some axons reaching the optic chiasm (but not extending beyond) after 4 weeks post injury (Park *et al.*, 2008). This effect was attributed to maintained activation of the mTOR intracellular pathway which enhances regeneration and survival. In addition, when PTEN deletion is combined with deletion of another intracellular inhibitor - suppressor of cytokine signalling 3 (SOCS3), a negative regulator of Janus kinase/signal transducers and activators of transcription (JAK/STAT) pathway, an additive effect on RGC survival and regeneration was observed (Sun *et al.*, 2011). This study is seminal in showing that activating two separate intracellular pathways that converge to trigger similar molecular effects, can improve CNS axon regeneration. It was also the first study to show regeneration beyond the optic chiasm with some axons entering the brain although no successful connections were formed (Sun *et al.*, 2011).

Recently, co-deletion of PTEN and SOCS3 as well as another treatment targeting several growth factors – a combination of osteopontin (OPN)/insulin-like growth factor 1 (IGF1)/ciliary neurotrophic factor (CNTF), were shown to dramatically enhance regeneration 4 weeks after injury where regenerated axons reach the superior colliculus in the brain and synapse (Bei *et al.*, 2016). The regenerated axons were, however, incapable of electrical conduction and despite robust, long-range regeneration, there was no functional recovery. This deficiency was corrected for by introducing a potassium channel blocker which stimulated the firing activity of newly regenerated neurons, which led to a modest improvement in visual acuity (Bei *et al.*, 2016). Electrical activity is certainly beneficial for repair: in a different study, elevation of mTOR signalling (by injecting an mTOR activator, cRheb1) coupled with visual stimulation or chemogenetic activation of electrical activity, resulted in RGCs regenerating to the correct brain areas, forming functional synapses and improving outcome (Lim *et al.*, 2016). Many other intracellular interventions have been so far used to promote axon regeneration and RGC survival after optic nerve crush such as elevation of cAMP, modulation of multiple transcription factors or expression of CNTF (Leaver *et al.*, 2006; Moore *et al.*, 2009; Kurimoto *et al.*, 2010; de Lima *et al.*, 2012). Advances in technology

have made it possible to track the regenerative pathways of individual cells using clearance techniques and confirmed that long-range axon regeneration is indeed possible, however guidance and targeting to the correct areas in the brain is still a formidable challenge in the field due to the highly dynamic and complex pattern of growth of newly regenerating axons and the lack of appropriate guidance cues (Luo *et al.*, 2013; V Pernet *et al.*, 2013; Bray *et al.*, 2017).

In summary, the optic nerve crush model has proven to be a reliable model to test intracellular interventions for the improvement of axon regeneration, neuronal survival and restoration of function after injury but there remains much to learn about the mechanisms required for successful regeneration. Studying these may help to reveal strategies which allow for guided regeneration. Previous studies in the lab have identified trafficking interventions which might allow for guided growth as a result of the axonal targeting of integrins. Integrins can drive guided regeneration of sensory axons through the spinal cord (Cheah *et al.*, 2016), but it has not been tested whether this might be similarly possible in the optic nerve.

So far, intracellular interventions targeting the trafficking of growth-molecules into CNS axons have been used to promote axon regeneration *in vitro,* but these have not been tested after optic nerve crush. AAV-mediated expression of wild-type and mutant protrudin in the current study is the first of its kind directly targeting axon trafficking pathways to improve axon regeneration and survival. Through this, we aim to achieve an influx of growth-promoting machinery such as integrins in recycling endosomes in order to provide guided growth to the original brain targets of the injured axons.

1.3 Laser Glaucoma Model in Rats

Glaucoma is a condition which features sustained damage to the optic nerve. One of the main associated risks for developing glaucoma is increased intraocular pressure (IOP) due to ineffective drainage of intraocular fluid. In severe cases (approximately 10% of patients), this results in optic nerve axon degeneration, retinal ganglion cell death, and ultimately blindness. IOP lowering treatments are already existent in the clinic, although they are only

effective in some patients whereas others continue deteriorating. Glaucoma is the leading cause of blindness around the world and currently there is no treatment for protecting the cells of the retina or for repairing the damaged nerves (*Glaucoma Facts and Stats | Glaucoma Research Foundation*, 2019).

Several animal models exist which mimic some of the main characteristics of glaucoma. The model used in this study was first described in 2002 (Levkovitch-Verbin *et al.*, 2002) and was later refined in 2010 (Marina, Bull and Martin, 2010). Increased IOP is the main risk for glaucoma, therefore many animal models have focused on elevating IOP and studying the effects downstream of that event. Our model relies on laser photocoagulation (40-60 laser pulses at 532nm wavelength) of the trabecular meshwork surrounding the eye. This normally drains intraocular fluid (aqueous humour), so its disruption results in a build-up of fluid and ocular hypertension (*Fig. 4.2*). This model is simple, relatively fast as many animals could be treated in a single session and IOP elevation is observed in most treated eyes (Marina, Bull and Martin, 2010). The increase in IOP is transient with ocular pressure going back to normal values after 24-48 hours with all eyes returning back to basal level pressure 7 days post injury. For this reason, two insults are required in the space of a week in order to ensure that substantial neuronal damage is triggered. The elevated IOP in turn results in a loss of RGCs in the retina and in some cases up to 50% axonal loss 6 weeks after elevation making this a suitable model for testing neuroprotective therapies.

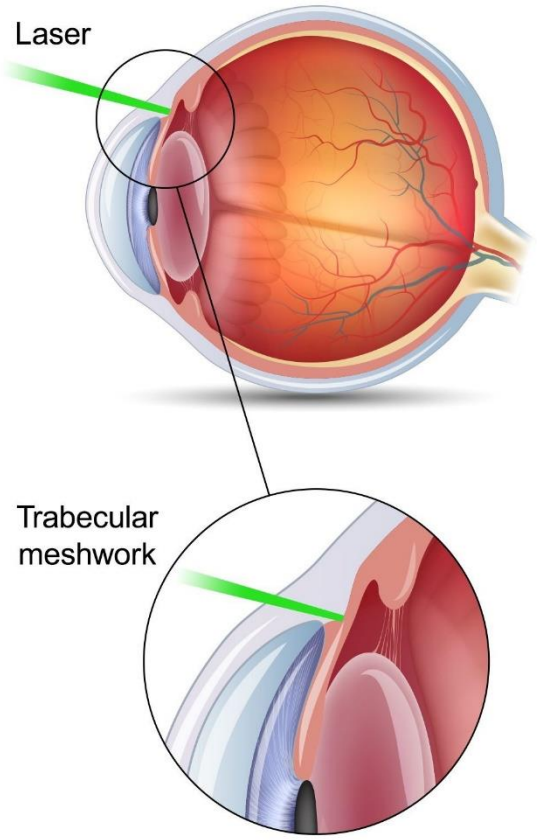

Figure 4.2 A schematic diagram of the anatomy of the eye showing the trabecular meshwork targeted by laser treatment in our model (adapted from Schultz J., 2016).

Several studies have already showed promising neuroprotective results in this model. Neurotrophins such as brain-derived neurotrophic factor (BDNF) and its receptor tyrosine kinase B (TrkB) have previously been shown to be neuroprotective to RGCs. Recently, however, the retrograde transport of BDNF and TrkB along the optic nerve back to the RGC soma was found to be obstructed in experimental glaucoma as well as in patients, which could contribute to the observed cell death (Pease *et al.*, 2000; Quigley *et al.*, 2000). Many studies since have focused on improving the TrkB-BDNF transport and signalling in RGC soma as a neuroprotective strategy. For example, Martin et al. (2003) injected an AAV-virus overexpressing BDNF intravitreally two weeks before inducing high IOP in an experimental rat model of glaucoma. They showed that increasing the levels of BDNF in the eye resulted in improved neuronal survival (32% RGC loss) compared to control (52% RGC loss) (Martin *et al.*, 2003). In a different study, however no positive effect of BDNF or a combined treatment between BDNF and CNTF (ciliary-derived neurotrophic factor) was observed in the same model whereas CNTF alone was found to reduce RGC loss after glaucoma induction by 15 %

(Pease *et al.*, 2009). This effect could have been a result of downregulated expression of the BDNF receptor with high levels of the ligand present or insufficient axonal transport as shown previously. Recently, Osborne and colleagues (2018) refined the previous study and showed that simultaneous expression of BDNF and TrkB from a single virus, resulted in enhanced neuroprotection of RGCs as well as of retinal axons in the optic nerve after elevation of IOP in the same experimental model of glaucoma described here (Osborne *et al.*, 2018).

The TrkB receptor has previously been implicated as a cargo in Rab11-recycling endosomes (Lazo *et al.*, 2013; Song *et al.*, 2015). Therefore, we hypothesised that overexpression of wild-type and specifically constitutively phosphorylated protrudin might additionally result in enhanced transport of this growth-receptor along the axons resulting in neuroprotection similar to the studies described above. Work to test this hypothesis is ongoing in the lab, and so it is not described here. Furthermore, this model was also selected so that the effects of protrudin on another growth-related receptor – integrin alpha 9 could be examined in the optic nerve and in the brain *in vivo.*

2. Results

2.1 Overexpression of protrudin enhances axon regeneration of primary cortical neurons in vitro after laser axotomy

Rat primary cortical neurons were grown in culture for 10 days and were transfected with the constructs described previously – GFP control, syn-mCh-WT, syn-mCh-MUT1 and syn-mCh-MUT2 protrudin (see *Methods, Section 3.1*). Their regenerative abilities were tested at 13-17 DIV in an *in vitro* axotomy model where the injury is inflicted by a laser and injured axons are imaged for 14 hours post injury to look for characteristics of regeneration (*Fig. 4.3, Table 4.1*). All axons were identified based on morphological appearance as the longest neuronal process in the cell. They were traced and cut at least 600 µm away from the cell body as previously described by Koseki *et al.*, 2017.

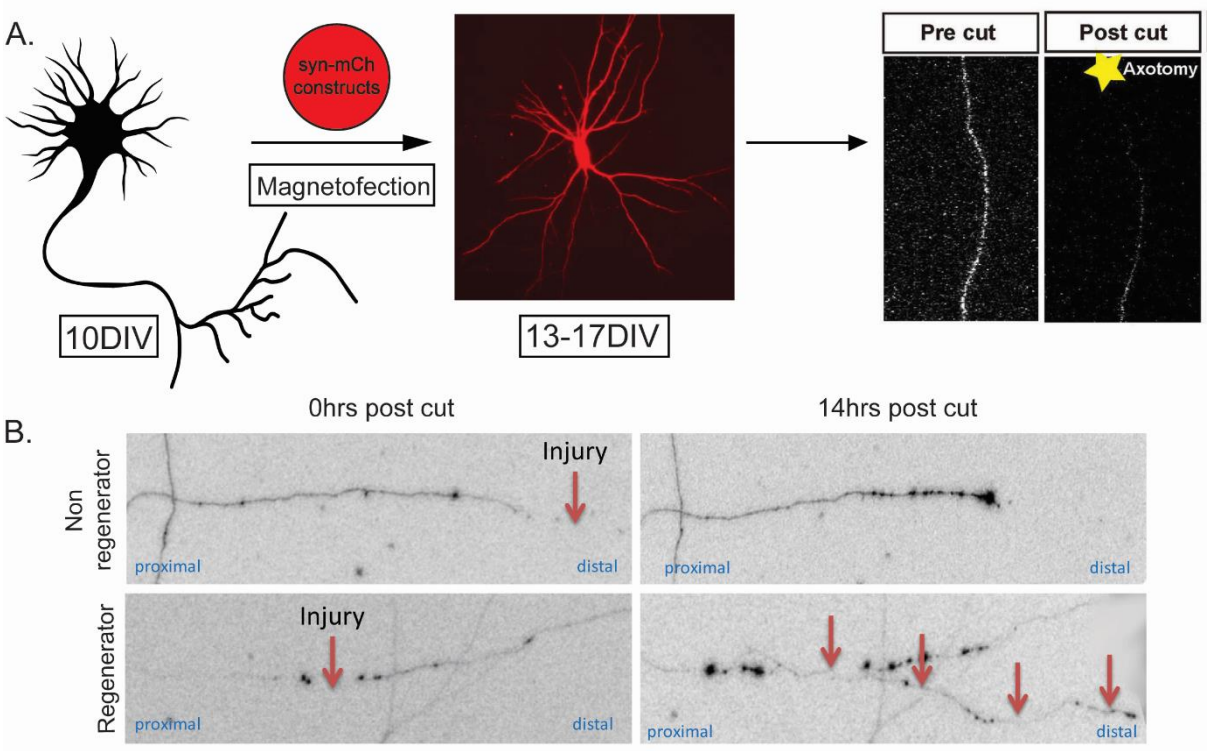

Figure 4.3 Laser axotomy model. A. Experimental set up for carrying out laser axotomy. 10 DIV neurons were transfected with GFP control, syn-mCh-WT, syn-mCh-MUT1 or syn-mCh-MUT2 protrudin using magnetofection. Axons were cut at 13-17 DIV at least 600 µm away from the cell body using a laser beam and were monitored for regeneration for 14 hours after injury. Yellow star indicates the location of the injury (adapted from Koseki *et al.*, 2017). B. An example of non-regenerating and regenerating axons. The red arrows at 0hours post-injury indicate the injury site. The red arrows at 14 hours post-injury indicate a regenerating axon.

Neurons which died and fragmented during the imaging procedure were excluded from the analysis and experiments where more than 50% cell death occurred were excluded. Axons were cut as far as possible from visible branch points and if upon axotomy a branch point became visible within 200 µm of the cut, that particular neuron was excluded from the analysis. Regeneration was classified as the process of re-growth of a cut axon for more than 50 µm after 14 hours of regeneration. Several regenerative parameters were measured in our experiments (*Table 4.1*). At least three independent experiments were carried out per experimental condition and 30-50 neurons were analysed in each group.

Regeneration factor	**Regeneration factors were measured as below when a neuron was categorized as "a regenerator"**
Retraction distance	The length of axon that was lost between the location of axotomy and the initial retraction bulb
Regeneration percentage	The number of neurons that regenerated, over the total neurons which formed a retraction bulb
Regeneration initiation time	The time between the retraction bulb formation and the start of a steady extension lasting more than 1hr and leading to regeneration
Regeneration distance after 2 hours	The length of axon that extended within 2hrs after regeneration initiation
Total Regeneration Distance	The length of axon that extended 14 hours after axotomy
Growth cone area	The maximum growth cone area after regeneration initiation
Branching	The newly growing axon branches into several newly formed individual branches while regenerating
Ectopic Growth	A new branch grows for more than 50µm within 100µm from the retraction bulb

Table 4.1 Table to explain the regeneration factors measured during laser axotomy (adapted from Koseki *et al.*, 2017).

Our initial hypothesis stated that constitutively phosphorylated protrudin (either mutant 1 or mutant 2) will associate more readily with Rab11-GDP than wild-type protrudin, therefore increasing the anterograde transport of growth molecules and ultimately improving regeneration. In this experiment, both constitutively phosphorylated protrudin forms (syn-mCh-MUT1 - 64% and syn-mCh-MUT2 - 70%) but also wild-type protrudin (syn-mCh-WT - 60%) increased the proportion of regenerating axons compared to control (GFP control - 24%) (*Fig. 4.4A)*. Moreover, syn-mCh-MUT1 (6.2hrs) and syn-mCh-MUT2 (5hrs) regenerated faster

than the cells overexpressing GFP control (8.8hrs) (*Fig. 4.4B)*. syn-mCh-WT (6.5hrs) also regenerated faster than control – this difference, however did not reach statistical significance. In addition, syn-mCh-WT (155 μm) and syn-mCh-MUT2 (180 μm) regenerated further distances than the control (95 μm) (*Fig. 4.4C*). Syn-mCh-WT (76 μm) also showed increased regeneration length after 2 hours of initial regeneration compared to GFP only (43 μm) (*Fig. 4.4D)*. No significant differences were observed in the retraction distance between conditions (*Fig. 4.4E*). The maximum growth cone area was reduced when protrudin was overexpressed – syn-mCh-MUT1 protrudin-expressing neurons (10 μm^2) had significantly smaller growth cones than control neurons (18 μm^2) (*Fig. 4.4F*). This result is mostly likely due to the decreased transport of protrudin to the tip of growth cones, rather than growth cones being physically smaller in these conditions (discussed in *Section 2.2*).

Two additional criteria were included when the regeneration data was analysed – the percentage of regenerating neurons which show branching or ectopic growth (*Table 4.1*). Interestingly, when regenerating, neurons expressing all forms of protrudin – syn-mCh-WT (10%), syn-mCh-MUT1 (25%) and syn-mCh-MUT2 (19%) showed increased branching compared to control (0%) (*Fig. 4.4G*). This result might have implications that protrudin could play a role in axon branching. Furthermore, control-expressing cells (64%) showed more ectopic growth, i.e. regenerative growth not from the main branch that was cut but from newly formed or auxiliary branches compared to syn-mCh-WT (10%), syn-mCh-MUT1 (10%) or syn-mCh-MUT2 (15%) (*Fig. 4.4H*).

One caveat of this experiment was, as described in *Chapter 3, Section 2.5*, that the amount or protrudin in the distal axon was lower than that at the proximal axon. This created difficulties when tracing distal axons at large distances compared to our control neurons which were easily traceable. Inducing the injury at further distances away from the cell body, results in decreased axon regeneration (Koseki *et al.*, 2017). In order to account for any discrepancies that might have occurred by having an easily traceable GFP control and dimmer mCherry-fused protrudin protein, we performed an additional experiment in which all control and protrudin-mCherry constructs were co-transfected with GFP to identify distal axons.

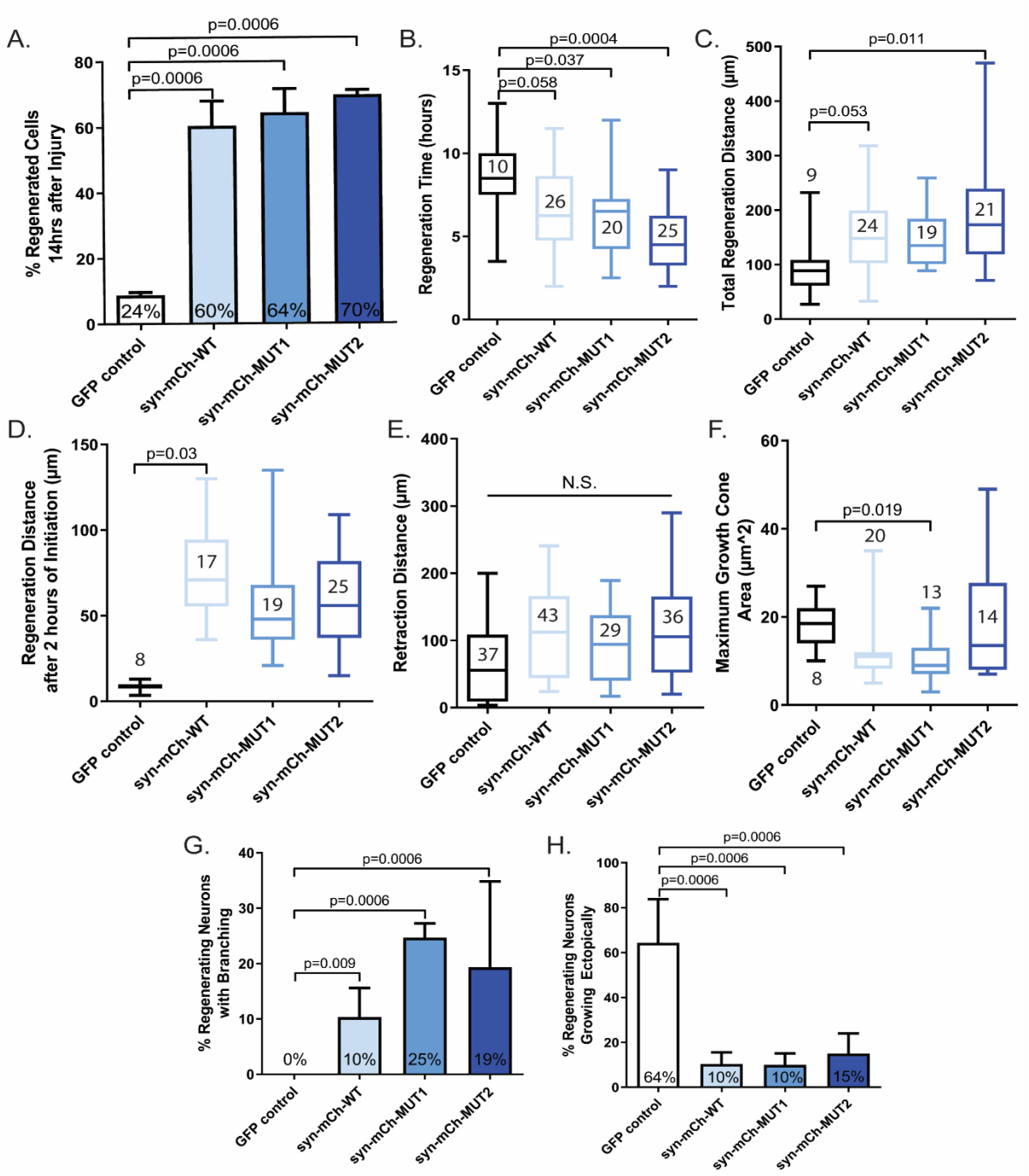

Figure 4.4 Quantification of Axon Regeneration (no GFP). A. Bar graph to show the percentage of regenerating axons (n=3). Syn-mCh-MUT1 and syn-mCh-MUT2 and syn-mCh-WT protrudin increased the proportion of regenerating axons compared to control (p=0.0006) B. Syn-mCh-MUT1 and syn-mCh-MUT2 protrudin initiated the process of regeneration faster compared to control (p=0.0008, one-way ANOVA). C. Box plot to show that syn-mCh-WT and syn-mCh-MUT2 protrudin-expressing cells regenerated further distances than the control (p=0.019, Kruskal-Wallis statistic=9.945). D. Box plot to show that syn-mCh-WT regenerate further distances 2 hours after regeneration initiation compared to control (p=0.0236, Kruskal-Wallis statistic=9.475). E. Box plot to show that there are no changes in the retraction distance between conditions (p=0.264, Kruskal-Wallis statistic=3.976). F. Box plot showing that syn-mCh-MUT1 protrudin-expressing cells have smaller growth cones than control (p=0.0153, Kruskal-Wallis statistic=10.42). G., H. Bar graphs to show the percentage of regenerating neurons which also show branching and ectopic growth. Syn-mCh-WT, syn-mCh-MUT1 and syn-mCh-MUT2 showed more branching (p=0.009, p=0.0006 and p=0.0006 respectively) but less ectopic growth than control (p=0.0006) (n=3). All percentage comparisons were calculated using Fisher's exact test with Bonferroni-Dunn pairwise comparison. Values in box plots represent n numbers. All values show mean ± SEM.

2.2 Overexpression of protrudin together with GFP enhances axon regeneration of primary cortical neurons in vitro after laser axotomy

In order to test whether the regeneration data obtained above is reproducible and valid, primary cortical neurons were transfected at 10 DIV with both GFP control and syn-mCh protrudin constructs (*Fig. 4.5)*. The green channel was used to trace the distal axons. The regenerative ability of the neurons was tested at 13-17 DIV in the same way as described above.

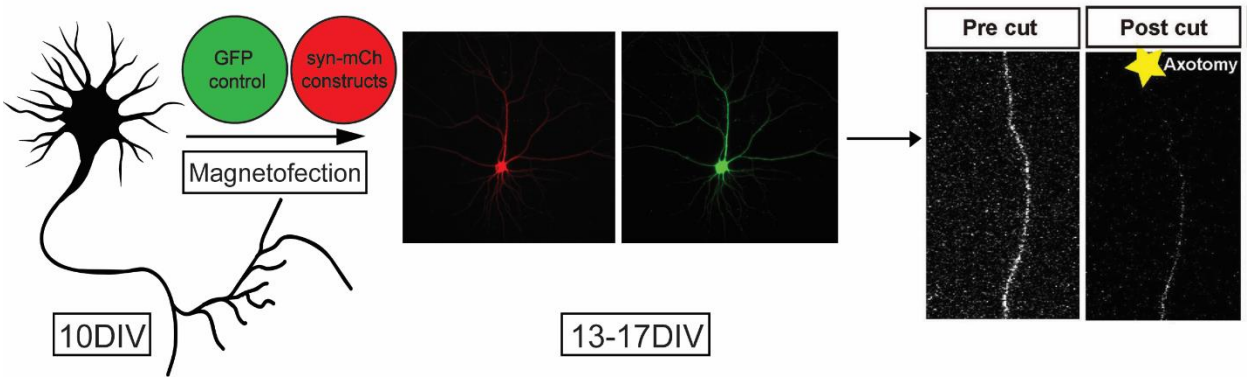

Figure 4.5 Laser axotomy model (with GFP). Experimental set up for laser axotomy. 10 DIV neurons were co-transfected with GFP control and either syn-mCh, syn-mCh-WT, syn-mCh-MUT1 or syn-mCh-MUT2 protrudin using magnetofection. Axons were cut at 13-17 DIV at least 600 µm away from the cell body using a laser beam and were monitored for regeneration for 14 hours after injury. Yellow star indicates the location of the injury.

Similar to our previous findings in neurons expressing protrudin constructs without GFP co-expression, we found that when co-expressed with GFP, both constitutively phosphorylated protrudin forms (syn-mCh-MUT1 - 45% and syn-mCh-MUT2 - 40%) increased the proportion of regenerating axons compared to control (syn-mCh - 22%) (*Fig. 4.6A*). syn-mCh-WT protrudin and GFP (36%) also showed increased regeneration compared to control neurons, however this did not reach significance (p=0.253). In addition, when expressed together with GFP, syn-mCh-WT (167 µm) and syn-mCh-MUT2 (161 µm) again regenerated further distances than the control (87 µm) (*Fig. 4.6C*). Overall, there was less of an increase in regeneration in cells co-expressing protrudin constructs together with GFP than was observed for neurons singly transfected with protrudin constructs alone.

Contrary to our previous findings (*Fig.4.4B*), no significant changes were observed between cells co-expressing syn-mCh, syn-mCh-WT, syn-mCh-MUT1 and syn-mCh-MUT2 together with GFP in the following parameters: regeneration time (8.6, 6.4, 7.5 and 7.3 hours respectively) (*Fig. 4.6B*), distance regenerated after 2 hours of regeneration initiation (42, 51, 55 and 54 µm respectively) (*Fig. 4D*), or the maximum growth cone area (12, 16, 13 and 15 μm^2 respectively) (*Fig. 4.6F*). Similar to our previous observations, no significant differences were observed in the retraction distance between conditions (85, 97, 101 and 84 µm respectively) (*Fig. 4.6E*).

Interestingly, when regenerating, neurons expressing both constitutively phosphorylated protrudin together with GFP control – syn-mCh-MUT1 (15%) and syn-mCh-MUT2 (12%) but not syn-mCh-WT (7%) showed increased branching compared to control (0%) (*Fig. 4.6G*). Unlike in the experiment described above (*Fig. 4.4H*), here there were no significant differences between the percentage of neurons showing ectopic regenerative growth between the conditions – GFP co-expressed with either syn-mCh (38%), syn-mCh-WT (35%), syn-mCh-MUT1 (42%) and syn-mCh-MUT2 (37%) (*Fig. 4.6H*).

This experiment showed that when co-expressed with GFP, overexpression of all forms of protrudin failed to initiate a regenerative response as robust as when expressed on their own (*Fig. 4.4*). It was hypothesised that this discrepancy could be due to reduced protrudin expression, as the translational machinery of the cells is also occupied with producing the GFP protein. This hypothesis was addressed by measuring the levels of protrudin in neurons which express protrudin constructs either on their own or together with GFP (*Fig. 4.7A, B*). By measuring the intensity of mCherry-fused protrudin in the cell body of cells expressing syn-mCh-WT (10 392 grey values), syn-mCh-MUT1 (8367 grey values) or syn-mCh-MUT2 (8068 grey values), we found a significantly higher fluorescent signal than was detected in cells expressing the same constructs together with GFP control plasmid (2869, 2366 and 3086 grey values respectively ($p<0.0001$) (*Fig. 4.7C*).

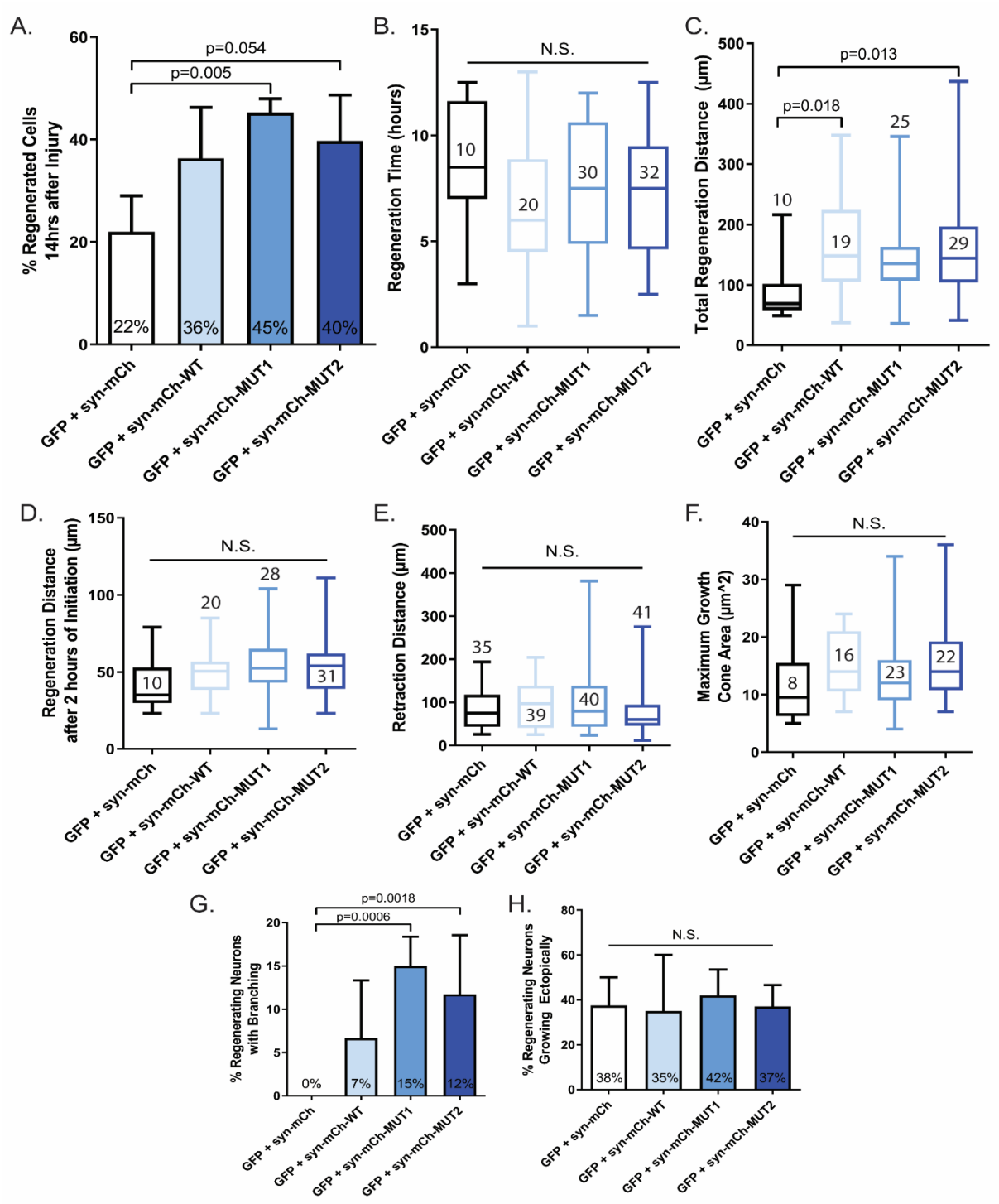

Figure 4.6 Quantification of Axon Regeneration (with GFP). A. Bar graph to show the percentage of regenerating axons (n=3). Syn-mCh-MUT1 protrudin increased the proportion of regenerating axons compared to control (p=0.005) B. No differences were observed in the regeneration time between conditions (p=0.2644). C. Box plot to show that syn-mCh-WT and syn-mCh-MUT2 protrudin-expressing cells regenerated further distances than the control (p=0.0130, Kruskal-Wallis statistic=10.78). D., E., F. Box plots that there are no significant differences between conditions in the regeneration distance after 2 hours of regeneration (p=0.2811, one-way ANOVA), in the retraction distance (p=0.7416, Kruskal-Wallis statistic=1.247) or the maximum growth cone area (p=0.1878, Kruskal-Wallis statistic=4.791). G., H. Bar graphs to show the percentage of regenerating neurons which also show branching and ectopic growth. Syn-mCh-MUT1 and syn-mCh-MUT2 showed more branching (p=0.0006 and p=0.0018 respectively) compared to control. No differences were observed in the percentage of neurons growing ectopically (p=0.7762). All percentage comparisons were calculated using Fisher's exact test with Bonferroni-Dunn pairwise comparison. Values in box plots represent n numbers. All values show mean ± SEM.

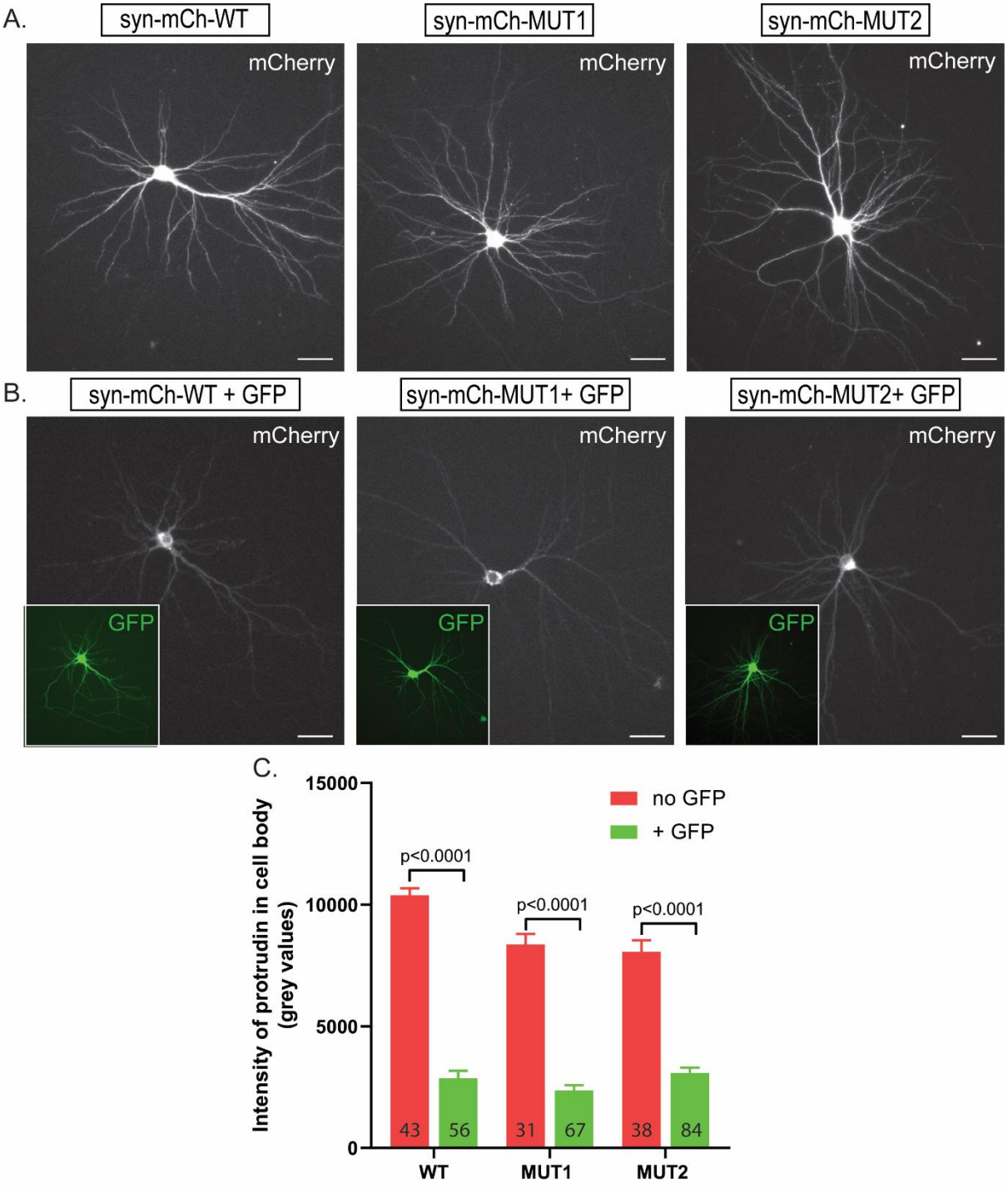

Figure 4.7 Protrudin Intensity in the Soma. A., B. Immunofluorescence images of cells expressing either syn-mCh-WT, syn-mCh-MUT1 and syn-mCh-MUT2 protrudin expressed on its own or in combination with GFP control plasmid. Images are taken at 40x. Scale bars are 20 µm. C. Bar graph to show the difference in mCherry-fused protrudin intensity in the soma. Cells overexpressing the three protrudin constructs on their own showed significantly higher intensity in the soma compared to cells expressing the protrudin constructs in combination with GFP ($p<0.0001$, two-tailed student t test).

During the *in vitro* axotomy experiments expressing mCherry-fused protrudin constructs without GFP co-expression (*Fig. 4.3 and 4.4*), protrudin was observed to localise to the tip of regenerating axons (*Fig. 4.8A*). All three forms of protrudin (WT, MUT1 and MUT2) accumulated in the area proximal to the injury soon after axotomy (1-2 hours) (*Fig. 4.8A*). All forms of protrudin were also observed to accumulate in the retraction bulb that forms after injury as well as in the growth cone of regenerating axons and at branch points in axons (*Fig. 4.8A*). Protrudin, however appeared to be at the base of the growth cone rather than in the dynamic edge. This observation was later confirmed by co-expression of a GFP control plasmid together with the protrudin constructs (*Fig. 4.8B*). GFP readily fills up the whole growth cone so it allows for visualisation of the full size of the growth cone. In control neurons, co-expressing syn-mCh together with GFP, both proteins are observed filling the whole growth cone in uninjured as well as in regenerating axons (*Fig. 4.8B)*. In uninjured neurons expressing syn-mCh-protrudin (this was observed for all forms of protrudin) together with GFP, unlike the GFP protein which readily fills the growth cone, protrudin was mostly found at the base of growth cone in small amounts (*Fig. 4.8B)*. In newly formed growth cones after injury, protrudin seems to invade most of the base of the growth cone but it is still not observed at the dynamic edge. These findings are not surprising as protrudin associates with kinesin 1 (Matsuzaki *et al.*, 2011) which is a motor protein engaging with the microtubule (MT) cytoskeleton. The shaft of the growth cone contains bundles of stable MTs along which axon transport of protrudin is possible, whereas the dynamic edge contains unstable and dynamic MT and actin polymers (Blanquie and Bradke, 2018). These observations hint at a localised role for protrudin at the site of growth cone redevelopment, and is in keeping with the known function of protrudin in the distal part of cellular protrusions (Shirane and Nakayama, 2006).

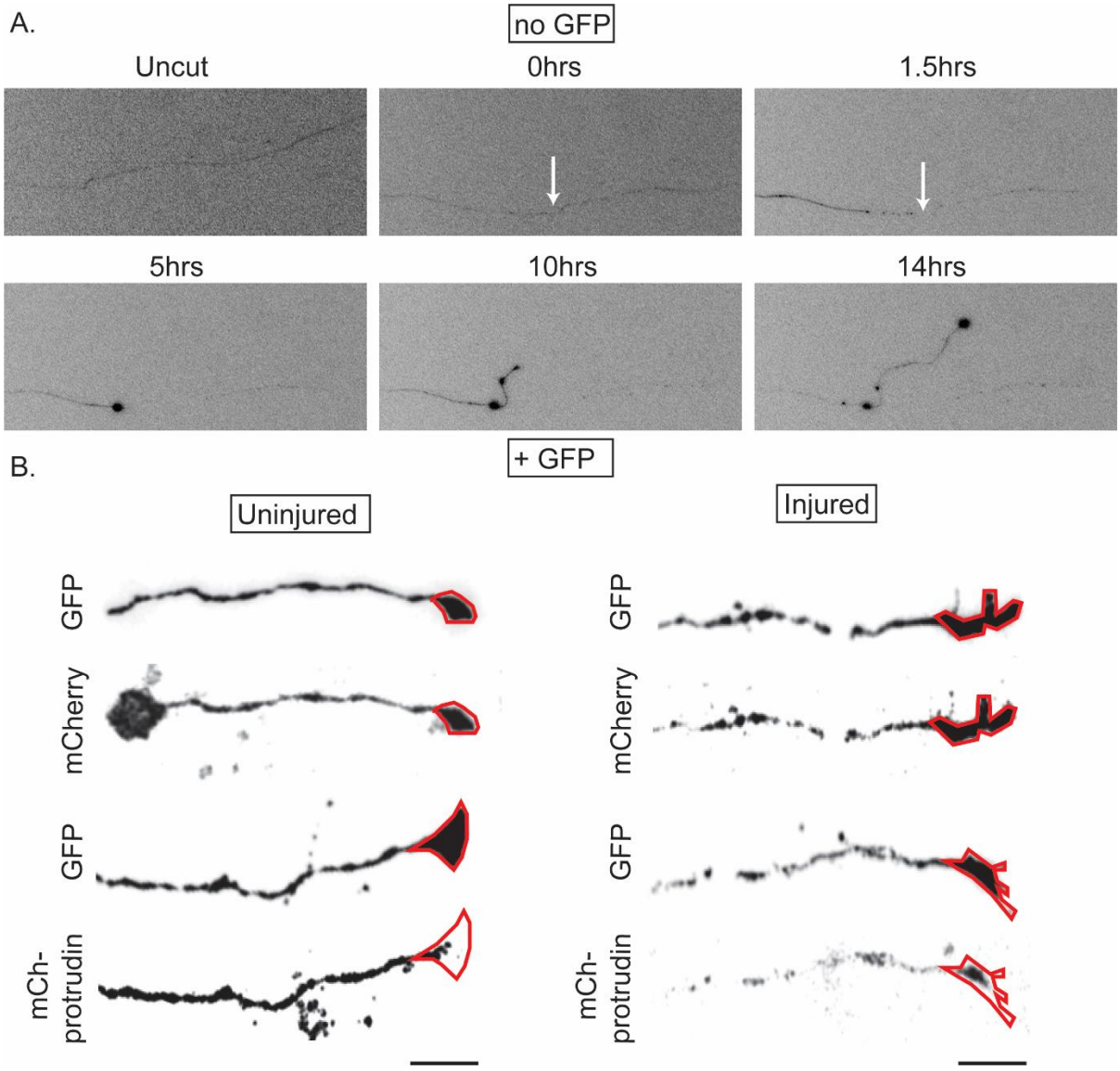

Figure 4.8 Protrudin Localisation in Regenerating axons. A. A series of images showing a regenerating axon of a cell overexpressing syn-mCh-MUT2 protrudin without GFP co-expression at different time points in the regenerative process. White arrows indicate the location of the laser injury. B. Series of images showing GFP and mCh-fused protrudin at the growth cone in neurons co-expressing both constructs. Growth cones from uninjured axons or from laser injured axons which have formed a new growth cone and initiated the regenerative process are shown here. Red outlines represent the full area of the growth cone as measured by the GFP signal. Scale bars are 10µm.

2.3 Overexpression of protrudin enhances axon regeneration of retinal ganglion cell axons in vivo after optic nerve crush

Based on the regeneration data obtained above *(Fig. 4.4*) wild-type and mutant 2 protrudin (as the mutant which had the highest effect on regeneration) were inserted into AAV2-CAG vectors for viral production as described in *Methods, Section 3.2.3* with the aim to test regeneration of CNS neurons *in vivo*. The newly designed viral DNA plasmids were first transfected into 10 DIV cortical neurons in order to assess the extent of protrudin overexpression from these vectors in cultured cortical neurons at 14 DIV. Neurons overexpressing either CAG-GFP-WT (3087 grey values) or CAG-GFP-MUT2 (3071 grey values) protrudin, showed dramatically increased staining intensity for the protrudin protein compared to control neurons only expressing CAG-GFP (204 grey values) or negative control where primary antibody is not used (10 grey values) (*Fig. 4.9*).

After validating that the DNA viral plasmid resulted in high expression of the protrudin protein *in vitro*, AAV2 viruses were produced by Raymond Fields at the NINDS Viral Production Core at the National Institutes of Health. Viruses containing CAG-GFP, CAG-GFP-WT protrudin and CAG-GFP-MUT2 protrudin were named AAV2-CAG-GFP, AAV2-CAG-WT and AAV2-CAG-MUT2 respectively. These viruses were injected in mouse retinas and their transduction efficiency of retinal ganglion cells (RGCs) was examined. All three viruses were widely expressed throughout the retina (*Fig. 4.10A*). As there were axons observed in the retinal wholemounts, it was assumed that most transduced cells are of neuronal phenotype. To validate this, RGCs were immunostained for RGC marker – RBPMS (Rodriguez, de Sevilla Müller and Brecha, 2014) and the % of RBPMS-positive and GFP-positive neurons upon viral expression was calculated – 27% of control AAV-CAG-GFP, 20% of AAV2-CAG-WT and 14% AAV2-CAG-MUT2 expressing cells were also RGCs (*Fig. 4.10B, C*). Some of the cells were, however expressing at relative low levels so a refined experiment with higher n number and improved microscopy settings is currently carried out in order to obtain more reliable results. Lastly, GFP signal from the GFP only virus or from GFP-fused protrudin, was reliably detected in axons in the optic nerve at different distances (*Fig. 4.10D*).

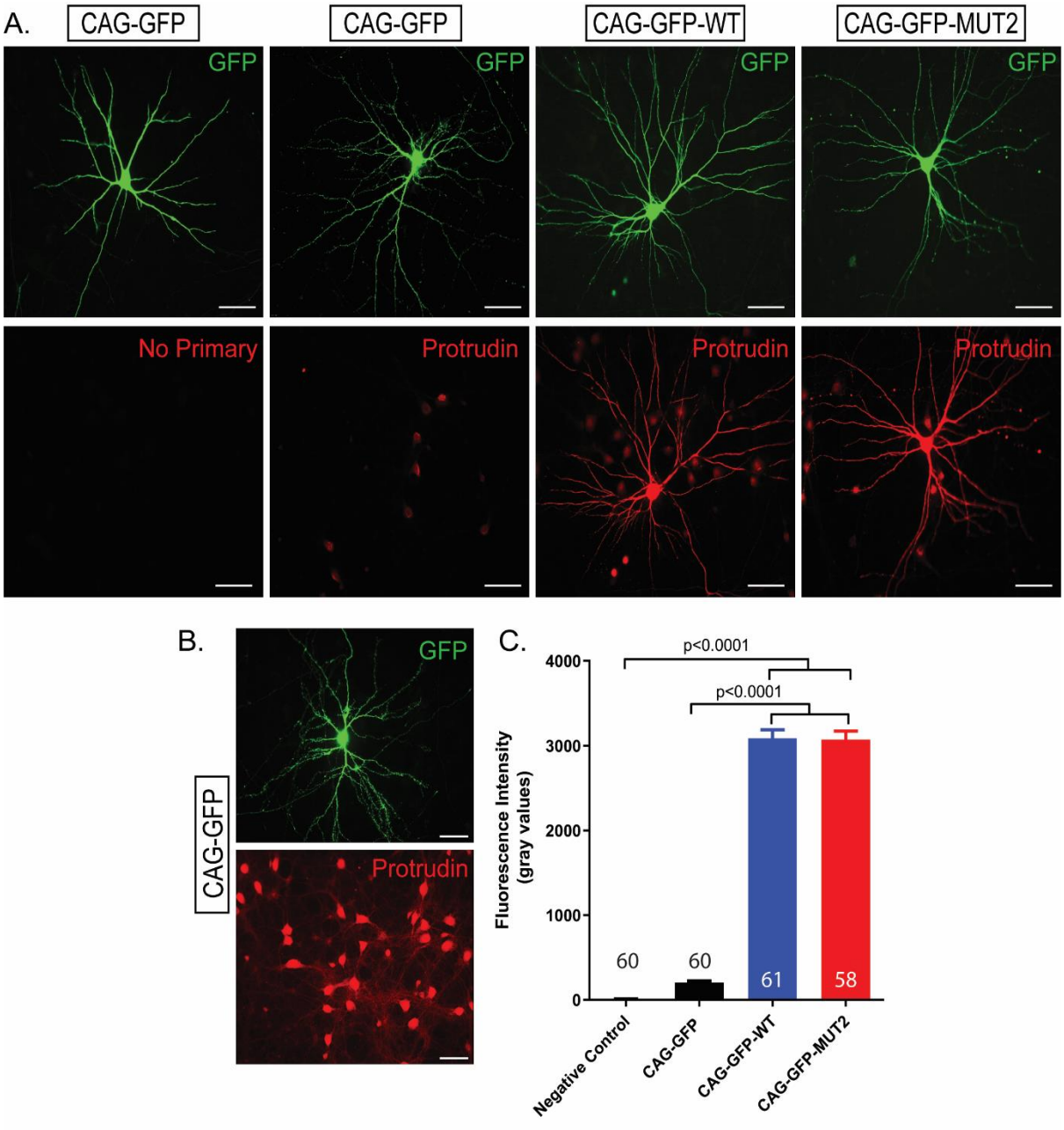

Figure 4.9 Overexpression of CAG-protrudin plasmid constructs resulted in increased protein levels of protrudin in primary cortical neurons. A. Immunofluorescent images of endogenous GFP signal from CAG-GFP only, CAG-GFP-WT and CAG-GFP-MUT2 protrudin (green). Protrudin amount is detected by anti-protrudin immunostaining (red). Images were taken at 40x magnification. Scale bars are 20 µm. B. When imaging settings are altered to overexpose neurons expressing protrudin, the endogenous protrudin in cells not overexpressing plasmids could be observed. C. Bar graph to show the average staining intensity of the protrudin in cells expressing the plasmid constructs. Protrudin's staining intensity is significantly higher in cells overexpressing CAG-GFP-WT and CAG-GFP-MUT2 protrudin compared to cell expressing control CAG-GFP only vector ($p=0.0001$, Kruskal-Wallis statistic=142.7, n=3). Error bars represent mean ± SEM.

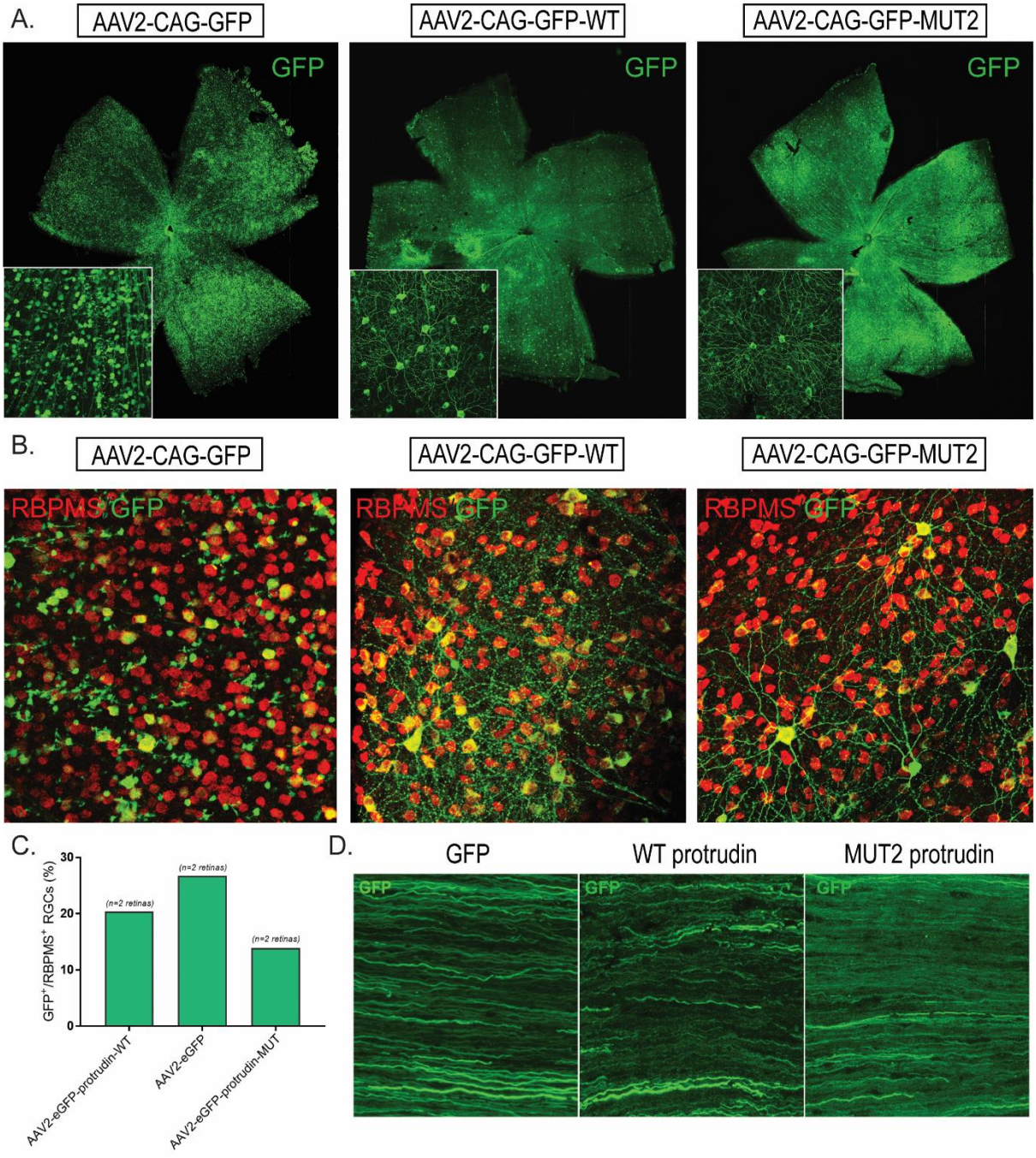

Figure 4.10 Protrudin viral constructs are expressed in RGCs throughout the retina and the optic nerve. A. Retinal wholemounts showing GFP-positive cells which have been transduced with one of three viruses: AAV2-CAG-GFP, AAV2-CAG-GFP-WT or AAV2-CAG-GFP-MUT2 protrudin. B. Immunostained images with RBPMS retinal ganglion cell marker (red) showing co-localisation between the virally infected cells (GFP) and RGCs. C. A bar graph showing robust viral expression in RGC-positive cells. For all three viruses, between 14-27% of all RGCs are also GFP-positive. (n=2 per condition). D. Immunofluorescent images showing robust GFP expression in axons of the optic nerve in all three conditions.

After expression of the viral constructs was tested in the retina, all three viruses - AAV2-CAG-GFP (n=8), AAV2-CAG-GFP-WT protrudin (n=8) and AAV2-CAG-GFP-MUT2 protrudin (n=9) were injected intravitreally in three groups of adult mice to specifically target the RGCs (see *Methods, Section 7.2*) (*Fig. 4.11A*). Two weeks following injection, optic nerve crush was performed as described in *Methods, Section 7.3* to injure the RGC axons, and after an additional two weeks, the anterograde axon tracer – cholera toxin ß (CTB) was injected to visualise regenerating axons as described in previous studies (Park *et al.*, 2008; de Lima *et al.*, 2012; Bray *et al.*, 2017; Yao *et al.*, 2018).

A significant increase was observed in the number of axons that regenerated beyond the crush lesion in mice whose RGCs expressed either the mutant or wild-type protrudin when compared with mice transduced with the GFP control – at 0.25 mm distal to the lesion there were 629±213, 379±101 and 44±18 axons respectively ($p<0.0001$), at 0.50 mm distal to the lesion site there were 433±180, 234±73 and 8±4 axons respectively ($p<0.0001$, $p=0.01$) (*Fig. 4.11B, 4.11C*). There were also more regenerating axons expressing mutant protrudin (221±120 axons) compared to those expressing GFP control (6±3 axons) at 0.75mm distal to the injury site ($p=0.01$) (*Fig. 4.11C*). In addition, mice injected with mutant protrudin showed increased RGC regeneration after injury compared to those injected with wild-type protrudin at 0.25 mm ($p=0.0027$) and at 0.50 mm ($p=0.022$) from the crush site (*Fig. 4.11C*). Regenerating axons were found at the furthest distance of 0.75 mm for control CAG-GFP transduced animals, of 2.75 mm for CAG-GFP-WT protrudin transduced animals and of 3.5 mm for CAG-GFP-MUT2 protrudin transduced animals. These results suggest that mutant protrudin induced the most robust regeneration, to a substantial distance past the injury site after only 2 weeks post crush.

In order to confirm that the axons observed are indeed regenerating rather than spared axons, a CTB anterograde tracer was injected one day before the tissue was collected. In addition, the optic nerves were also stained for GAP43 – a developmentally downregulated protein which is re-expressed upon injury in regenerating neurons (Tetzlaff *et al.*, 1989, 1991; Meyer, Miotke and Benowitz, 1994). A reliable co-localisation between CTB and GAP43 was found throughout the nerve in all conditions (*Fig. 4.12*). Interestingly, AAV2 control GFP-expressing axons were much brighter than those expressing AAV wild-type or mutant protrudin. Additionally, the GFP detection pattern for protrudin was irregular. These

observations could suggest that there are still debris from degenerating axons around or that protrudin is less readily transported into the distal axon after crush as the GFP signal is visible on the proximal side of the crush. Further analysis is needed in order to characterise protrudin transport in the optic nerve, and these are being undertaken by other members of our group as part of on-going projects.

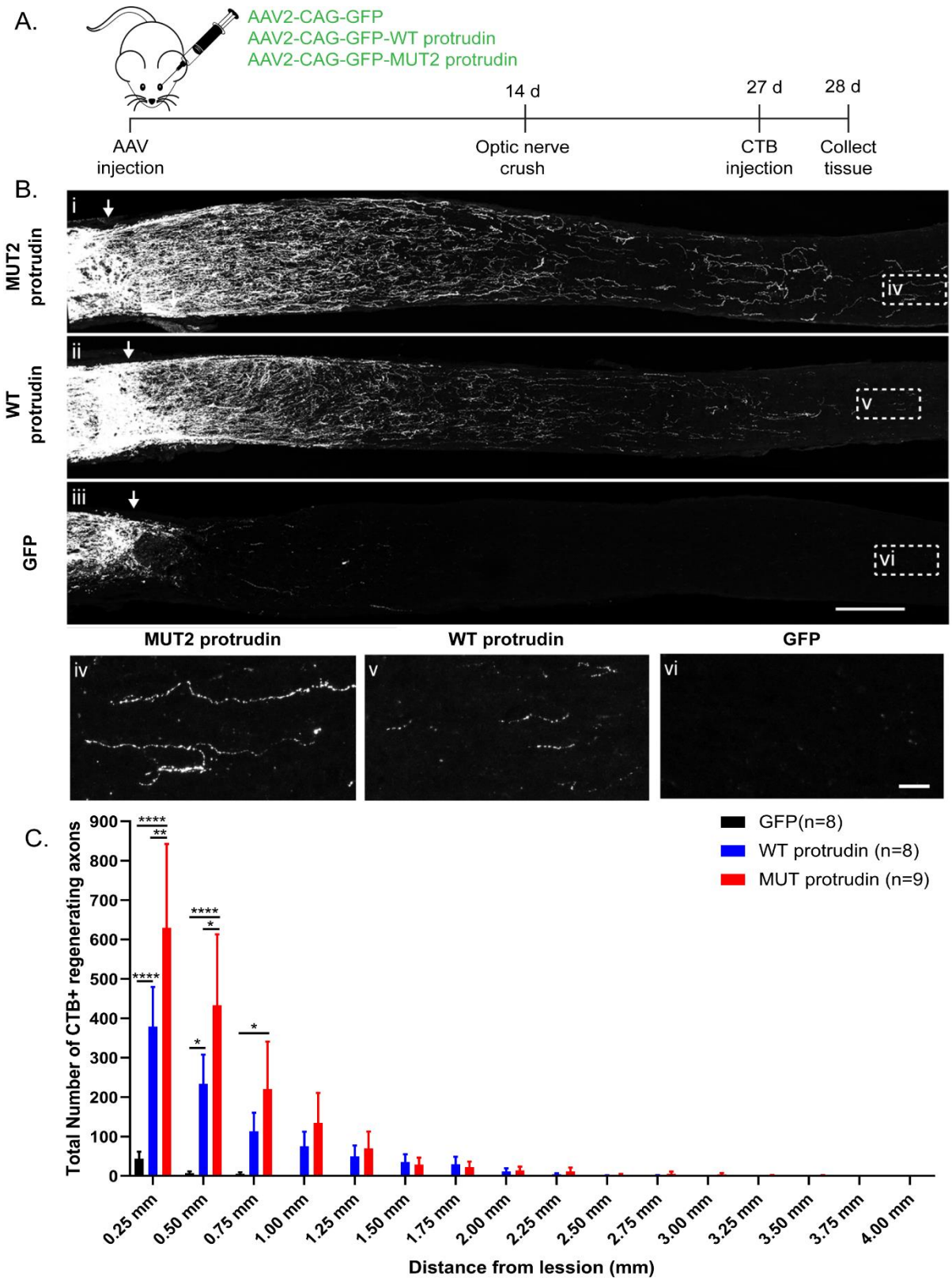

Figure 4.11 Protrudin enhances regeneration of RGC axons. A. Experiment timeline. B. Micrographs showing CTB-labelled axons in the optic nerves of mice treated with viruses carrying the mutant (MUT2) or wildtype (WT) protrudin or the GFP control. Arrows indicate lesion site. Insets (iv-vi) show regenerating axons in the distal optic nerve. Scale bar = 200 µm, insets = 20 µm (n=8-9 animals/group). C. Graph showing the number of regenerating axons at distances distal to the lesion site, displayed as mean ± SEM. Statistical significance was determined by two-way ANOVA with Bonferroni post-hoc test for multiple comparisons. ** $p < 0.005$, *** $p < 0.001$, **** $p < 0.0001$

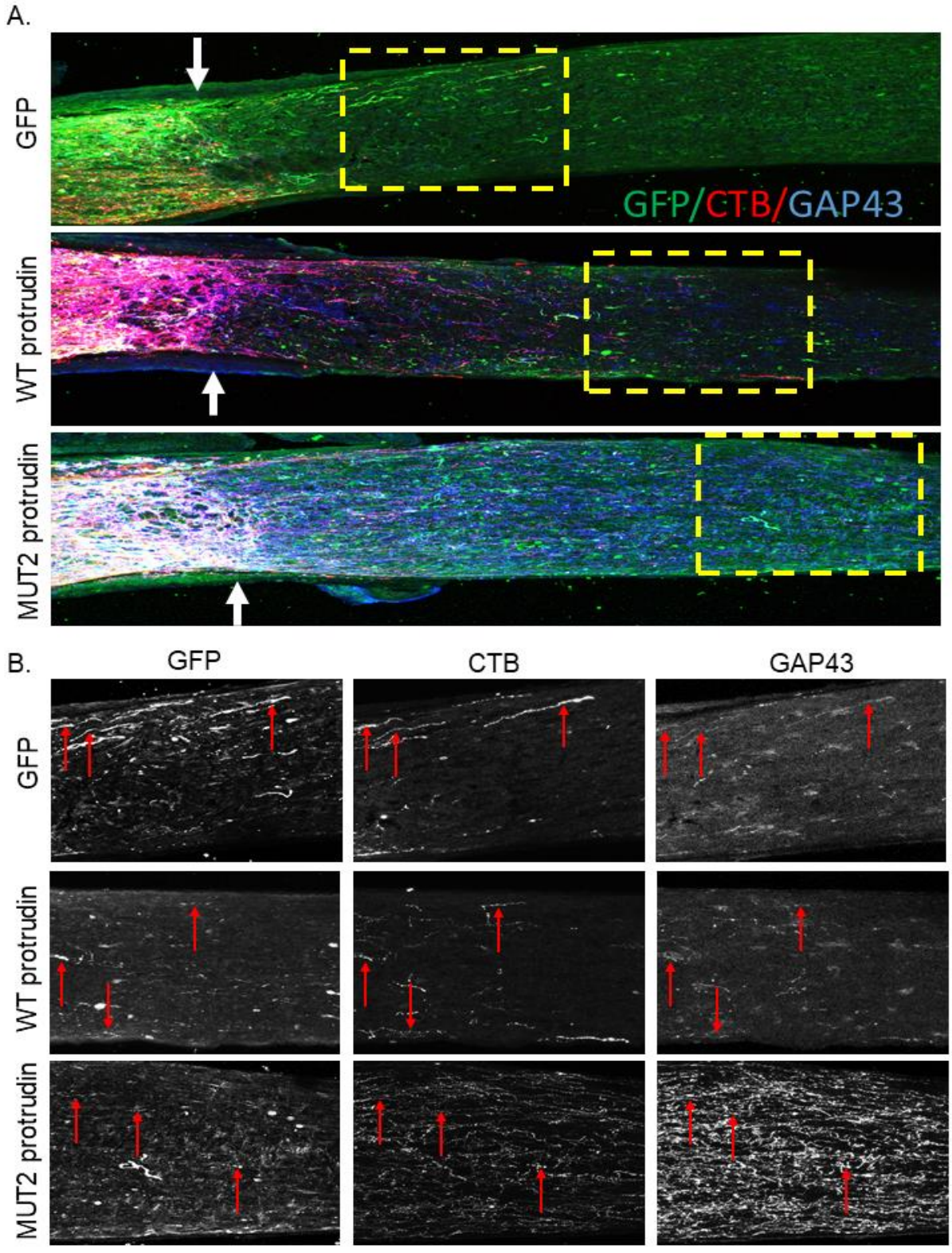

Figure 4.12 Regenerating axons are GAP43-positive and CTB positive. A. Immunolabelled optic nerve sections for GAP-43, CTB and GFP. Dotted yellow rectangles indicate insets shown in panel B. B. Zoomed in insets from optic nerves expressing either AAV2-CAG-GFP control, AAV2-CAG-GFP-WT and AAV2-CAG-GFP-MUT2 protrudin. Red arrows show regenerating axons where GFP, CTB and GAP43 all colocalise.

2.4 Constitutively phosphorylated protrudin has a modest effect on retinal ganglion cell neuroprotection in a model of glaucoma

In the experiments above, it was observed that in optic nerves transduced with wild-type or mutant protrudin virus, there appeared to be some remnants of degenerating axons 2 weeks post injury to the nerve. These did not label for CTB or GAP43 and were not evident in control nerves expressing GFP alone. Additionally, some mutant forms of protrudin (see *Chapter 5*) seemed to have an effect on cell survival so it was hypothesised that in addition to protrudin's effect on neuroregeneration, the protein might play a role in neuroprotection too.

To test this hypothesis, a laser model of glaucoma was used to examine the effect of protrudin overexpression on RGC survival in the retina but also on integrin transport *in vivo* in both healthy and injured RGC axons. Glaucoma is a condition associated with increased intraocular pressure (IOP) that in severe cases leads to optic nerve axon degeneration, RGC loss and ultimately blindness. In rats, a rise in intraocular pressure is observed after laser treatment which disrupts the trabecular meshwork (the drainage system of the eye). Sprague Dawley rats were injected with AAV2-CAG-GFP (n=8), AAV2-CAG-GFP-WT-protrudin (n=9) or AAV2-CAG-GFP-MUT-protrudin (n=9) together in combination with AAV2-CAG-IntegrinA9-V5 (*Fig. 4.13A*). 2 weeks post-injection a laser was applied to the left eye to cause a rise in IOP. 24 hours later, elevation of IOP was confirmed (as described in *Methods, Section 7.4*) (*Fig. 4.13C)*. Because IOP returns back to normal levels after several days (around 20 mmHg), the same procedure was repeated a week later where a second laser insult was applied to the same eye in order to maintain elevated IOP. IOP elevation was again confirmed 24 hours later (*Fig. 4.13C*). All animals were sacrificed 4 weeks after the second laser injury.

In previous experiments from our lab (data not shown), the increase in IOP resulted in a significant decrease in the number of surviving RGC cells in the retina of the injured eye. In this experiment, the number of RGC in the retina (quantified as described in *Methods, Section 5.3.2)* significantly decreased after injury in animals injected with AAV2-CAG-GFP-WT protrudin (2031 RGCs/mm2) but not in those injected with AAV2-CAG-GFP-MUT2 protrudin (2305 RGCs/mm^2) or AAV2-CAG-GFP control (2351 RGCs/mm2) compared to uninjured animals (2803 RGCs/mm^2) (*Fig.4.13D*).

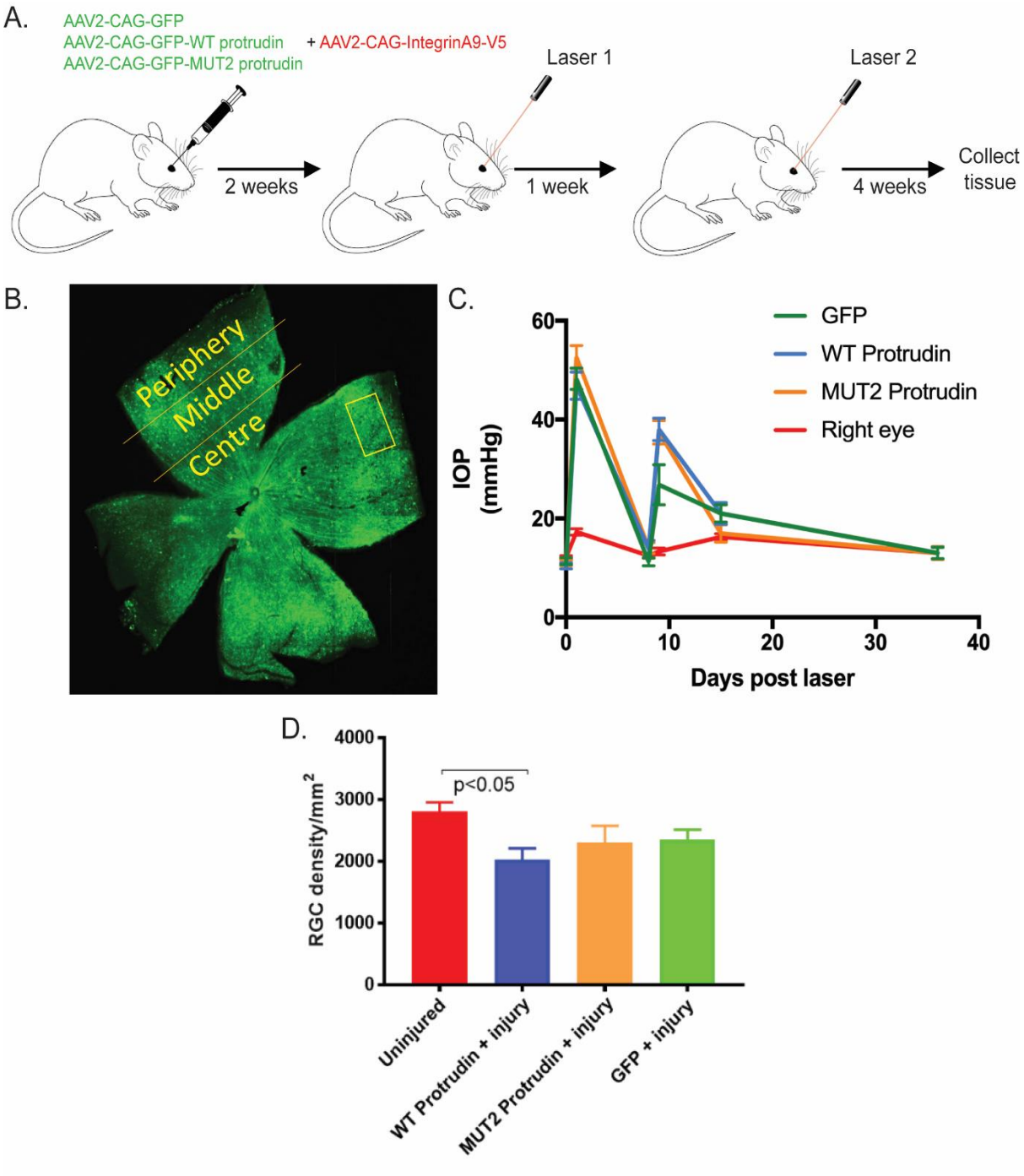

Figure 4.13 Constitutively phosphorylated protrudin enhances RGC survival after glaucoma injury. A. Experiment timeline. B. Wholemount retinas were prepared from injured and uninjured eyes and stained for Brn3a (RGC marker). 24 representative images were taken per retina – 6 per retinal quadrant (2 from the centre, 2 from the middle and 2 from the periphery) and RGC density was calculated. C. Intraocular pressure profiles of the three treatment groups during the experiment. D. The density of RGC in the WT protrudin injected animals which received injury was lower than uninjured eyes, displayed as mean ± SEM (p=0.0138). Statistical significance was determined by two-way ANOVA with Bonferroni post-hoc test for multiple comparison.

Interestingly, rats injected with GFP control virus together with integrin alpha 9 did not show the reduced number of RGCs that was predicted from previous studies (around 50% RGC loss). This could have been a result of inadequate raise in IOP after the second laser treatment in the control group (10 mmHg lower) compared to the other two groups (*Fig. 4.13C*). Furthermore, the Brn3a staining which was used as a marker of RGCs seemed to be of variable quality across the different retinas. Optic nerve resin embedding and axon counts by ultrathin sectioning are currently being performed as described previously (Marina, Bull and Martin, 2010) in order to confirm these results by examining axonal neuroprotection too. Nonetheless, the current findings show that MUT2 protrudin has a modest neuroprotective effect compared to WT protrudin on RGC survival in the retina after glaucoma. However, our overall interpretation of these results is inconclusive due to the data from the control group.

In addition to RGC survival, the transport of anterograde axon tracer CTB from the injured eye to the contralateral side of the brain (particularly, in the superior colliculus area) was measured (*Fig. 4.14A*). In previous studies in our lab (data not shown), this transport was shown to be compromised in glaucoma-induced eyes possibly due to the high amount of cell death but also through some effects on axon transport itself. It was, therefore, hypothesised that the fluorescent intensity, area and volume of CTB-positive signal in the right superior colliculus (where the left, injured eye axons project) will be smaller than that of the left superior colliculus. The area and intensity of the CTB tracer in the superior colliculus as well as volumetric analysis were carried out as described in *Methods, Section 5.3.1.* In this experiment, no significant differences were observed in the CTB-positive area multiplied by the average intensity between the different conditions ($p=0.3411$). Although the CTB area x intensity showed a trend towards being lower in the right (injured) superior colliculus compared to the left (uninjured) superior colliculus within each condition, the trend did not reach significance (*Fig. 4.14B*). Furthermore, volumetric analysis was performed as described in Chiasseu and colleagues (2017). No significant differences were observed in the volume of CTB-positive signal across the brains of animals of each condition ($p=0.5961$) (*Fig. 4.14C)*. Again, despite there being a trend towards decreased CTB volume in injured animals compared to uninjured, the trend did not reach significance.

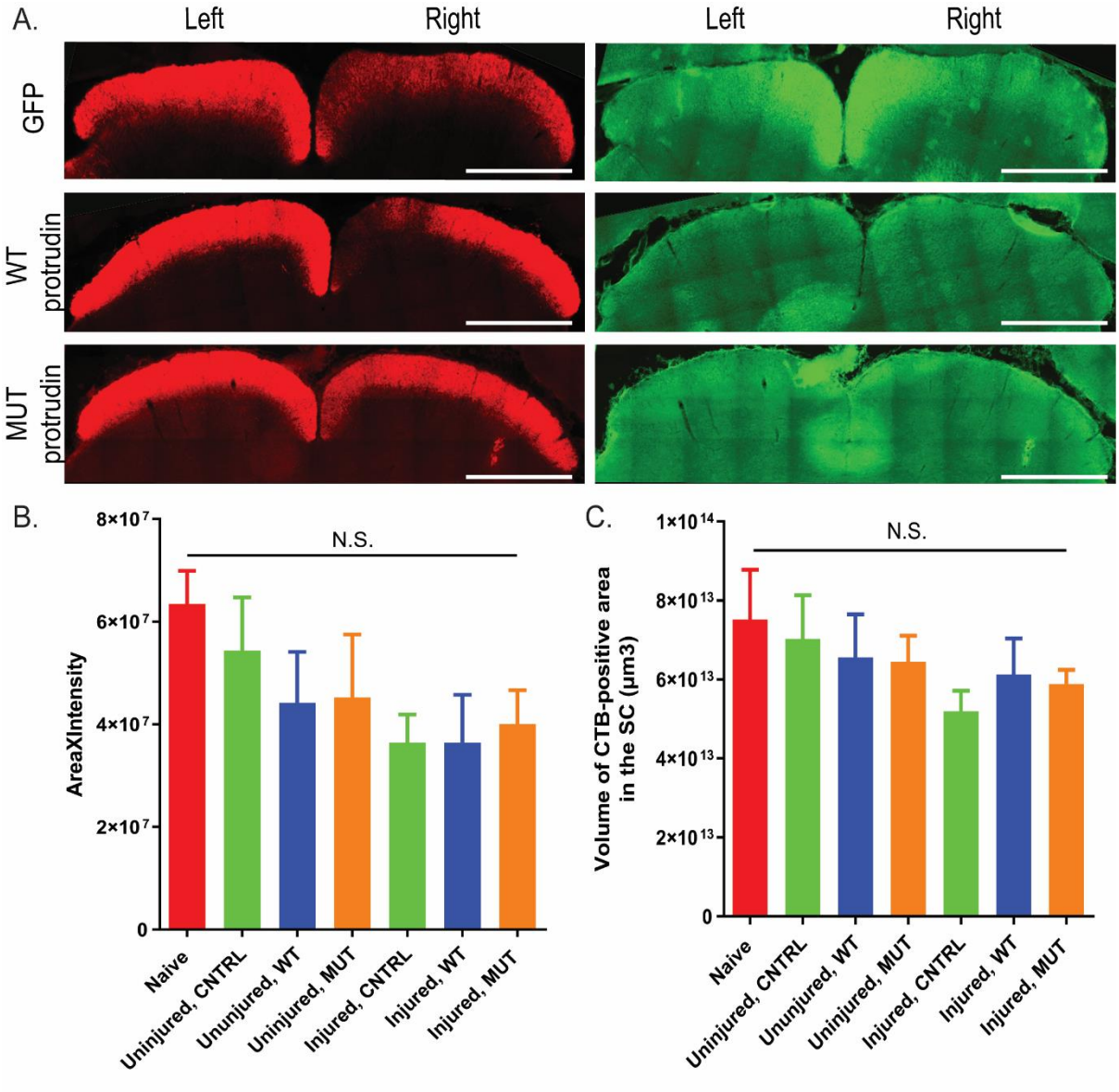

Figure 4.14 CTB-positive area in the superior colliculus. A. Immunofluorescent images of CTB-positive area and GFP detected by anti-GFP antibody in the left (uninjured) and the right (injured) superior colliculus. Images are taken at 20x. Scale bars are 1mm. B. No significant changes are observed in the area of CTB signal multiplied by its intensity across the different conditions (p=0.3411, one-way ANOVA, n=8 in each condition). C. No significant changes were observed in the volume of CTB-positive area across the superior colliculus (p=0.5961, one-way ANOVA, n=8 in each condition). Error bars represent mean ± SEM.

Initially, the GFP signal in the superior colliculus was going to be measured in order to calculate the transport of the GFP-tagged protrudin to the brain along RGC axons. The detected GFP pattern, however appeared irregular across different animals so the experiment needs to be repeated in order to carry out those analyses.

In this experiment, integrin-alpha9 virus was injected in conjunction with the protrudin viruses in order to assess the effect of overexpressing protrudin on integrin transport *in vivo.* The integrin virus contained V5 tag which was detected *in vivo* using anti-V5 tag antibody. Several antibodies were utilised in order to visualise the V5-tagged integrin. In the retina, anti-V5 antibody (Bioss Inc, 1:250) showed reliable staining and cells stained for V5-tagged integrin co-localised with GFP-tagged protrudin and CTB-positive cells (*Fig. 4.15A*). In optic nerve sections and in the superior colliculus, however, reliable staining with anti-V5 antibody could not be achieved (*Fig. 4.15B, C*). Even though there seems to be positive staining in the optic nerve compared to negative control, the staining appears irregular and not the correct pattern for integrin receptor vesicles moving along axons. A similar problem was observed with the anti-V5 tag staining in the superior colliculus. Furthermore, as the brain sections were much thicker (50 µm) than the retinal and optic nerve sections (14 µm), the antibody penetration might have been compromised.

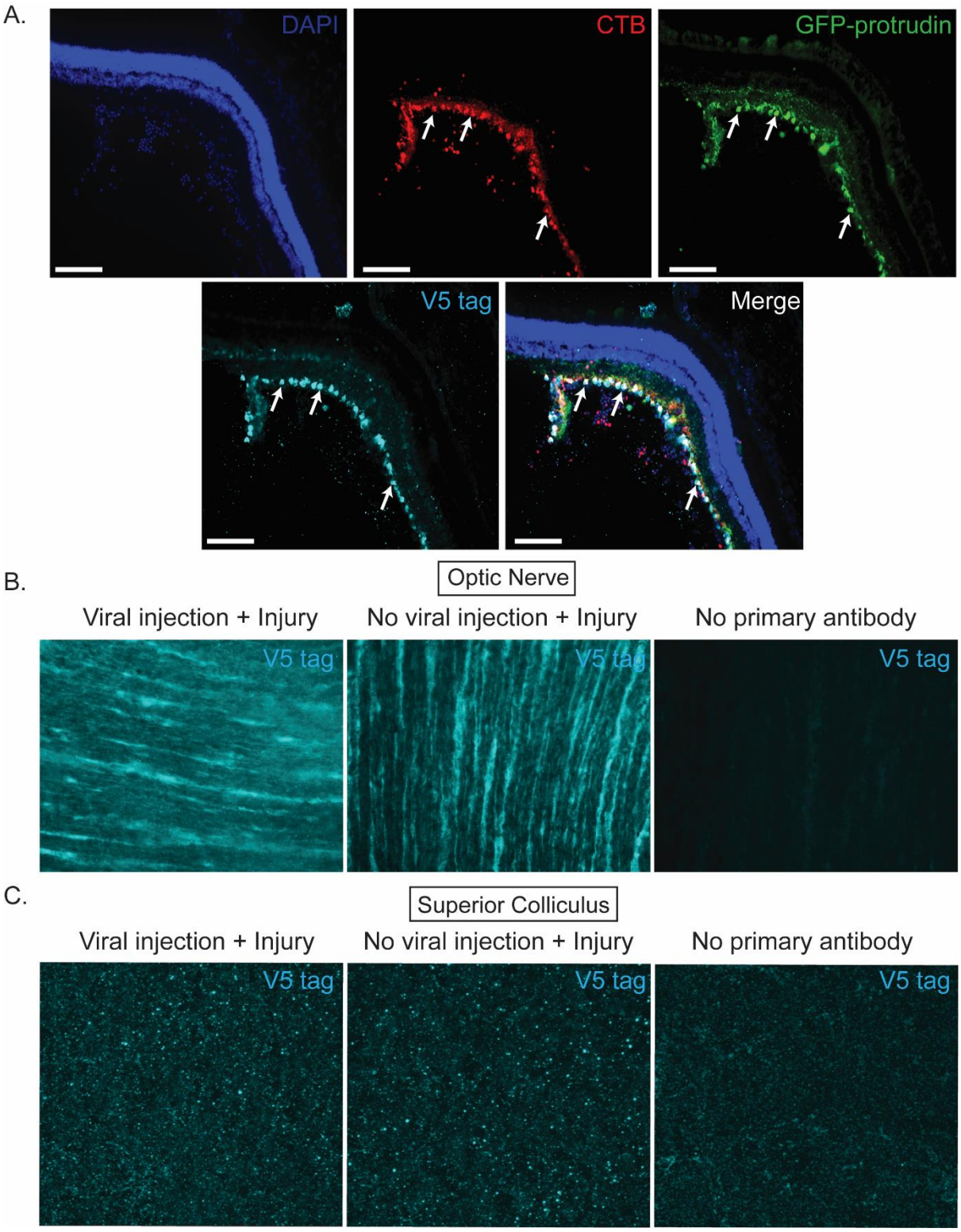

Figure 4.15 Integrin detection in the retina, the optic nerve and the brain A. Immunofluorescent images of retinal sections transduced with AAV2-CAG-GFP-MUT2 protrudin and AAV2-CAG-IntegrinA9-V5. Sections were stained for DAPI (dark blue), CTB (red), GFP (green) and V5 (turquoise). Images were taken at 20x magnification. Scale bars are 100 µm. White arrows represent cells co-expressing all three CTB, GFP and V5 simultaneously. B. Optic nerve sections from different conditions – viral injection and injury, no viral injection and injury and no primary antibody with an anti-V5 antibody. C. Superior colliculus sections from different conditions – viral injection and injury, no viral injection and injury and no primary antibody with an anti-V5 antibody.

3. Discussion

In this chapter, protrudin's ability to promote axon regeneration and neuroprotection was examined in several cellular and animal models. Overexpression of wild-type and two forms of constitutively phosphorylated protrudin were firstly found to promote axon regeneration in primary cortical neurons after laser axotomy *in vitro.* Additionally, viral expression of wild-type and constitutively phosphorylated protrudin enhanced axon regeneration in the optic nerve after an optic nerve crush injury in mice. Lastly, constitutively phosphorylated protrudin showed mild neuroprotective properties in improving retinal ganglion cell survival in a rat laser model of glaucoma.

The initial hypothesis of this thesis stated that constitutive phosphorylation of protrudin could result in enhanced axon transport of growth-promoting molecules which could result in enhanced axon regeneration of CNS neurons which seem to have low levels of growth machinery in their axons. *In vitro* regeneration data showed that both phosphomimetic forms of protrudin but also wild-type protrudin enhanced axon regeneration after injury (*Fig. 4.4*). The percentage of regenerating axons especially in the mutant 2 condition (70%) was found to be higher than some of the best treatments utilised in our lab in this model system such as depletion of EFA6 – an ARF6 activator in the axon (59%) (Eva *et al.*, 2017), dominant negative Rab11 (38%) (Koseki *et al.*, 2017) and hyperactive PI3K alpha (69%) (Barber, Evans, Nieuwenhuis and Eva, unpublished data). Furthermore, this experiment showed that this system provides a reliable platform to test the extent of axon regeneration after different genetic manipulations. The percentage of regenerating control neurons is reasonably consistent (20-30%) when axotomy was performed by different researchers who cultured their own primary cortical neurons and used various control plasmids (CAG-mCherry, CMV-mCherry, Syn-mCherry, CAG-GFP, dual promoter GFP, turbo RFP and scrambled shRNA control). One limitation of our *in vitro* laser axotomy system might be that there is a cap of the percentage of regenerating neurons as more than 86% successful regeneration in a single experiment, has not so far been achieved.

Interestingly, it was observed that overexpression of wild-type protrudin was on its own capable of enhancing axon regeneration despite to a lesser extent than the phosphomimetic mutants (*Fig. 4.4, 4.6).* This result was not predicted by the hypothesis. This observation could be due to the fact that protrudin on its own is scarce in the axon and when overexpressed, it allows for axonal functions that are normally supressed in mature CNS neurons. Our RNA sequencing data in the same primary cortical neurons shows that indeed protrudin is not expressed at very high levels in neurons throughout development and into adulthood (Koseki *et al.*, 2017, see *Chapter 3*). Another explanation could be that the wild-type protrudin protein becomes phosphorylated by endogenous kinases when overexpressed, therefore producing effects similar to mutants 1 and 2. More experiments on the function of the two different mutants need to be carried out in order to elucidate this mechanism. For example, various kinase inhibitors could be added to our neuronal cultures once transfected with wild-type or phosphomimetic mutants before axotomy, in order to test whether the wild-type protein is indeed being phosphorylated inside the cell. It may also be that we chose to do axotomy at an intermediate time point when some regenerative capacity remains. At this time there may be more active signalling through the pathways that phosphorylate protrudin than say at 21 DIV. In the past we have found negligible regenerative capacity at this time point.

Several other interesting observations were made during the laser axotomy experiments. For example, overexpressed protrudin was mostly observed in the shaft but not at the dynamic tips of the growth cones of regenerating axons (*Fig. 4.8*). This effect could be due to the fact that protrudin associated with KIF5 for long-range transport along microtubules and once it reaches the actin-filled periphery of the growth cone (Dent, Gupton and Gertler, 2011), it stops being transported into the tip of the growth cone. This is further supported by the observation that protrudin also does not fill dendritic spines which are also rich in F-actin (Penzes and Rafalovich, 2012) (see *Chapter 3, Section 2.3*). Future work is needed in order to study protrudin's interaction with the actin cytoskeleton, if any. Another interesting observation was that a small percentage (10-25%) of the regenerating axons overexpressing wild-type, mutant 1 or mutant 2 protrudin seem to divert from the classic axon regeneration where the axon grows from the retraction bulb of the severed process, but instead result in the formation of multiple branches (*Fig. 4.4G, 4.6G*). Interestingly, protrudin was visualised at branch points in the axon in healthy and injured axons. This might suggest that protrudin

could promote reorganisation of the cytoskeleton in order to induce branching and therefore, growth in multiple different directions (Kalil and Dent, 2014). Furthermore, a recent paper points towards the endoplasmic reticulum (ER) serving as a microtubule-organising platform (Farías *et al.*, 2019) and protrudin as a ER-resident protein interacting with MT cytoskeleton could allow for MT branching at the ER.

We also performed the same *in vitro* laser axotomy but co-expressing GFP with the different protrudin constructs (*Fig. 4.6*). The GFP construct that was used as a control expresses GFP under SFFV promoter and emerald green under the ubiquitin promoter. This dual promoter construct results in really high expression pattern which possibly engages a large amount of intracellular transcription and translation machinery for the production of the GFP protein. This could be one reason why reduced amount of protrudin expression was observed than when protrudin is expressed on its own (*Fig. 4.7*). Nevertheless, neurons co-expressing protrudin and GFP follow the same pattern of percentage of regenerating axons, with the two phosphomimetic mutants performing better than wild-type protrudin but all exceeding the regeneration seen in control (*Fig. 4.6*). Despite that, the extent of regeneration was much reduced (40-45% with GFP compared to 60-70% without GFP) which suggests that protrudin's action on axon regeneration might be dose-dependent. In summary, the *in vitro* laser axotomy experiments when protrudin is expressed on its own or in combination with GFP, show three overriding characteristics of overexpressing the protrudin protein – enhancement of the percentage of regenerating cells, increased total distance of re-growth in regenerating neurons and increased axon branching.

In order to validate the *in vitro* regeneration results, the optic nerve crush model was chosen as an *in vivo* model of axon regeneration. Some of the most effective treatments in promoting regeneration in this model target intracellular signalling pathways and are performed in transgenic animals carrying mutations in these genes since birth. For example, one of the most potent interventions up to date is a conditional deletion of the PTEN in adult RGCs resulting in improved regeneration and neuronal survival after optic nerve crush which was attributed to upregulation of the mTOR signalling pathway (Park *et al.*, 2008). Since this discovery many studies focused on blocking the effects of PTEN using short-hairpin RNAs, CRISPR and pharmacological agents or on using combinational therapies with other

molecules, and have achieved various degrees of success in promoting axon growth after injury in the CNS (Ohtake, Hayat and Li, 2015). PTEN however, acts as a tumour suppressor gene and knocking it down has shown to cause tumour formation in several animal models so its wide use as an axon regeneration promoter is very limited. Many interventions that promote regeneration in the optic nerve have subsequently been demonstrated to have relevance in the spinal cord but have not yet been able to stimulate robust regeneration of the CST. Ultimately, our aim is to restore CNS regeneration both in the optic nerve and in the spinal cord. Better and more translatable therapies are needed, and our experiments with protrudin in the optic nerve are a starting point to testing protrudin as a pro-regenerative molecule, but also as a means for enabling integrin transport. Currently, the ability of wild-type and mutant protrudin to enhance axon regeneration in the spinal cord after a dorsal transection is being tested in our laboratory.

In the current study, adult mice were treated by delivering a virus directly to the eye only for 2 weeks before an optic nerve crush. It was shown that expressing wild-type and also phosphorylated mutant protrudin results in dramatically increased axon regeneration in the optic nerve, only 2 weeks after optic nerve crush (*Fig. 4.11*). One of the previous studies showing most potent regenerative effect in the optic nerve and which highly resembles the current experimental setup and timeline, used viral delivery of super-agonist to the CNTF receptor (ciliary neurotrophic factor) to Muller glial cells (Pernet *et al.*, 2013). In their study, Pernet and colleagues achieved the regeneration of 500-600 neuronal fibres 0.5 mm past the injury site. This study, however focused on manipulating the glial cells to enhance RGC regeneration. In one of the most successful studies targeting RGCs to improve regeneration with a similar experimental design to ours, an activator of the mTOR pathway was injected intravitreally and 2 weeks later an optic nerve crush was performed (Lim *et al.,* 2016). Three weeks post-injury, less than 100 axons were observed at 0.5 mm and when combined with visual stimulation, the number of regenerating axons dramatically increased to 250-300 at 0.5 mm away from the injury (Lim *et al.*, 2016). These axons showed target-specific regeneration to the correct brain areas and formed functional synapses to improve visual acuity (Lim *et al.*, 2016). Expression of mutant protrudin allowed for 400-500 neuronal fibres to reach the 0.5 mm mark by 2 weeks after injury suggesting that this intervention is comparable to some of the most potent interventions reported to date. Perhaps more importantly, the other work

presented in this thesis also demonstrates a number of mechanisms that are involved in mediating protrudin's regenerative effects. These will be further examined by other members of the group and may even lead to the identification of other regenerative interventions which could be translated to clinical treatments.

Unfortunately, the retinal wholemounts from the optic nerve crush experiments were unsuccessfully stained for RGC markers and subsequently mounted, so the effects of protrudin overexpression on neuronal survival after optic nerve crush could not be analysed in this experiment but will be the subject of future experiments. Another interesting suggestion for future experiments is to explore the identity of the cells transduced with the protrudin virus. So far most regenerative RGCs have been shown to be alpha-type (Duan *et al.*, 2015; Daniel, Clark and McDowell, 2018) but it is not improbable that the protrudin virus is enabling regeneration from other RGC cell types, not implicated as regenerative before or that have not previously been induced to regenerate by genetic manipulations. It will also be important to include a longer time point after the optic nerve crush (4 or 8 weeks) in order to observe whether the regenerating axons cross the optic chiasm and reach the brain to form the correct connections to allow for functional repair. This is an important question as stimulation of axon growth after injury is often disorganised and very few treatments result in long-range, targeted regrowth. Another future possibility is to use combinatorial approaches to further stimulate and direct axon growth. One such possibility is combining the protrudin treatment with extracellular matrix modifications such as the use of chondroitinase ABC (ChABC) (which removes inhibitory CSPGs) – an approach which has been shown to be beneficial for axon regeneration after optic nerve crush (Pearson *et al.*, 2018).

Lastly, the role of protrudin on neuroprotection and axonal transport in a rat model of glaucoma, was also examined. Overexpression of constitutively phosphorylated protrudin was mildly neuroprotective by increasing the number of surviving RGCs after the elevation in IOP (*Fig. 4.13*). A major caveat to this experiment was that the IOP in control rats injected with GFP virus only did not increase as high as in the other two groups after the second laser injury. This could have been the reason why no significant RGC loss in the retina in the control group was observed. Alternatively, maybe overexpression of integrin alpha 9 together with the control virus could be sufficient to induce neuroprotection. The effects of the integrin alpha 9 receptor on neuroprotection have not been examined yet in this model. If this is the

case, however, that could suggest that wild-type protrudin and integrin alpha 9 interaction is not beneficial for neuroprotection as there is still a reduction in the number of surviving RGCs in that condition (*Fig. 4.13*). Further experiments where the increase in IOP in control rats is sufficient enough to cause neuronal cell death and to examine the effects of integrin alpha 9 on neuroprotection of RGCs are still needed. As the model utilised is extremely variable between animals even of the same group, increasing the n number for each group could also prove to be an improvement in order to detect any small differences.

The transport of CTB tracer along RGC axons to the superior colliculus in the brain was previously used as an indicator of the health and functionally of RGCs after an injury (Chiasseu *et al.*, 2017). In this experiment, there was no significant difference in the area, intensity or the volume of the CTB-positive signal in the superior colliculus between the different groups *(Fig. 4.14*). The transport of CTB to the right side of the superior colliculus where injured axons from the left eye synapse, does indeed seem to be more compromised to that of the left superior colliculus – none of the differences observed are, however, significant.

Finally, the main reason for injecting the integrin alpha 9 virus together with the other conditions, was to examine the normal transport of integrins in the optic nerve and whether this transport is affected by protrudin overexpression. Previously, the same integrin virus was shown to be transported into a small number of axons in the optic nerve (Andrews *et al.*, 2016), but this transport was not extensively studied. In the current study, although the integrin virus expression was reliably detected in the retina by using anti-V5 tag antibody, its detection in the optic nerve or in the superior colliculus in the brain was not optimal (*Fig. 4.15)*. Further experiments are needed in order to identify antibodies to reliably detect the integrin virus in the optic nerve and the brain, so its long-range transport could be reliably studied. To this end we have recently had useful suggestions from Melissa Andrews, who previously performed the *in vivo* integrin transport studies (Andrews *et al.*, 2016). It will also be interesting to study the transport of endogenous or overexpressed TrkB receptor and to examine whether enhanced TrkB receptor trafficking along the axon could explain phosphorylated protrudin's neuroprotective effects. There are currently projects in the lab to examine in detail the transport of integrin alpha 9, TrkB and Rab11 into RGC axons in the optic nerve. It will be important to determine what percentage of axons allow for their transport normally, and whether this can be altered through protrudin manipulation.

CHAPTER V: MECHANISMS OF PROTRUDIN ACTION ON AXON REGENERATION

Summary

In this chapter, the mechanisms by which protrudin functions to promote axon regeneration are examined. Firstly, we aimed at suppressing the expression of endogenous rat protrudin in primary cortical neurons with the use of shRNA or CRISPR-Cas9 constructs in order to study its involvement in axon regeneration. The original selection of protrudin for regeneration studies was due to its potential as a facilitator of Rab11 axonal transport. Here, the transport of Rab11 and integrins in the axons of mature cortical neurons was studied upon protrudin overexpression using immunocytochemistry and live-cell imaging. In addition to its ability to bind Rab11, protrudin has several other significant molecular properties. Protrudin's regenerative mechanism of action was therefore further tested by mutagenesis of its key domains and examination of the resulting effects after *in vitro* laser axotomy.

1. Introduction

Wild-type and phosphomimetic protrudin promote axon regeneration *in vitro* after laser axotomy and *in vivo* after optic nerve crush as described in *Chapter 4.* This chapter explores whether this increase in regenerative potential is due to an increased interaction with Rab11 resulting in enhanced transport of integrins into the axon. It also sets out to investigate

whether further properties of protrudin are also involved in mediating its regenerative effects, by dissecting protrudin's various molecular domains.

1.1 Protrudin's role in axonal transport of integrins and Rab11

Integrins are essential growth-associated receptors which during development are involved in axon growth and guidance and in adulthood support synaptic function (Nieuwenhuis *et al.*, 2018). Integrins have previously been shown to be excluded from mature axons (Bi *et al.*, 2001; Mortillo *et al.*, 2012; Franssen *et al.*, 2015; Andrews *et al.*, 2016). This developmental redistribution contributes to the regenerative failure of mature CNS neurons (Franssen *et al.*, 2015; Eva *et al.*, 2017). Interestingly, overexpressing integrin and/or its activator kindlin can enhance sensory, PNS axon regeneration in CNS environment *in vitro* and *in vivo* (Andrews *et al.*, 2009; Tan *et al.*, 2012; Cheah *et al.*, 2016). Our group is currently working towards using this integrin strategy to enhance axon regeneration of corticospinal tract axons descending from the brain into the spinal cord, however overexpressed integrins are not readily transported into CNS axons (Andrews *et al.*, 2016). Therefore, other methods to improve the transport of integrins into the axon need to be considered.

One such strategy of enhancing the amount of integrins in CNS axons has been to modify the expression or the activation state of two small GTPases involved in axonal integrin transport – Rab11 and ARF6 (Eva *et al.*, 2010). For example, overexpression of Rab11 into primary cortical neurons *in vitro* resulted in enhanced integrin amount in axons and improved axon regeneration after laser axotomy (Koseki *et al.*, 2017). Furthermore, inactivation of ARF6 by suppressing EFA6 (an ARF6 activator, located within the AIS) allows transport of integrins into the axon and improves axon regeneration after laser axotomy (Eva *et al.*, 2017). These studies were the first two reports to suggest that manipulations of the internal axonal transport machinery of CNS axons can improve their regenerative potential. As protrudin is an adaptor protein involved in axonal transport which links Rab11-bound endosomes and the motor protein kinesin, its overexpression might have similar effects to Rab11 overexpression or ARF6 inactivation.

This chapter aims to establish a reliable knockdown system of endogenous protrudin by using shRNA and CRISPR constructs *in vitro* in order to study the contribution of the endogenous rat protein to axon regeneration. Furthermore, co-immunoprecipitation experiments are carried out to examine whether constitutively phosphorylated protrudin associates more readily with Rab11 as hypothesised. Finally, two different methods (immunocytochemistry and live-cell imaging) are used to assess whether Rab11 and integrin vesicles are more readily transported into CNS axons overexpressing protrudin or phosphomimetic protrudin.

1.2 Protrudin protein domains

Overexpression of both wild-type and phosphomimetic protrudin were shown to enhance axon regeneration both *in vitro* and *in vivo,* with constitutively phosphorylated protrudin exerting the most robust regenerative effect (see *Chapter 4*). This prompted us to examine the mechanisms by which protrudin facilitates axon regeneration. As protrudin contains multiple protein interaction domains that mediate diverse molecular functions, examining the contribution of each of these domains to aiding axon regeneration might shed light on novel mechanisms that are required for successful CNS regeneration. Protrudin contains a Rab11-binding domain (RBD), 3 hydrophobic domains which principally target to the ER membrane (TM-1, TM-2 and TM-3), an FFAT motif which mediates interaction with the ER contact site protein – VAP-A, a coiled-coiled domain (CC) and a FYVE domain (a phosphoinositide-binding domain). In addition, the protein interacts with a microtubule-severing protein – spastin at its N-terminus and motor proteins from the kinesin-1 family such as kinesin 5 (KIF5). In order to examine which of these interactions of the protrudin protein are important for its role on axon regeneration – six domain mutants (ΔFYVE, ΔFFAT, ΔKIF5, ΔSpastin, ΔRBD (Rab11-binding domain), ΔER were created as described in *Methods, Section 3* (*Fig. 5.1*). These mutants were transfected into cortical neurons and their ability to enhance axon regeneration was compared to a positive control – constitutively phosphorylated mutant 2 protrudin, which robustly enhances axon regeneration (*Chapter 4*).

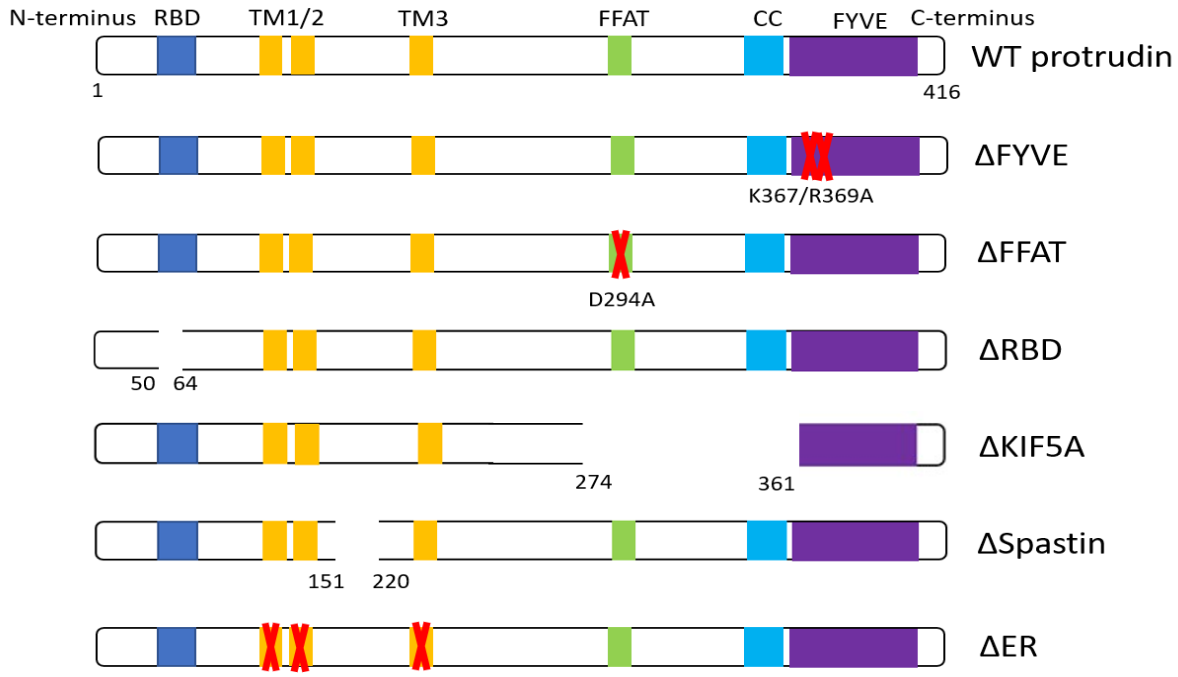

Figure 5.1 Schematic diagram of protrudin domain mutants. ΔFYVE and ΔFFAT domain mutants were created by substitution of lysine (367) and arginine (369) for alanine and aspartic acid (294) for alanine respectively (Saita *et al.*, 2009; Gil *et al.*, 2012). Rab11-binding domain mutant (ΔRBD) was created by deleting amino acids 50-64 (Shirane and Nakayama, 2006). KIF5-binding mutant (ΔKIF5) lacked amino acids 274-361 (Matsuzaki *et al.*, 2011), spastin mutant protrudin (ΔSpastin) had amino acids 151 to 220 removed (Zhang *et al.*, 2012) and ER mutant protrudin where the three transmembrane domains (TM1 (67–87a), TM2 (89–109aa) and TM3 (180–214aa) are removed so protrudin cannot associate with membranes (Chang, Lee and Blackstone, 2013).

Most of these mutants have been examined in different paradigms before. For example, ΔER protrudin mutant (missing the three hydrophobic regions) results in translocation of the protrudin protein from the ER structures to the cytoplasm and is unable to rescue changes in ER morphology induced by siRNA treatment against protrudin (Chang, Lee and Blackstone, 2013). The ΔFFAT domain mutant was shown to be essential for protrudin's interaction with ER-resident protein – VAP-A (Saita *et al.*, 2009). The FFAT motif is also found in other proteins which play a role in the transfer of lipids between the ER and other organelles such as the Golgi apparatus (Kawano *et al.*, 2006). When the ΔFFAT mutant protrudin is overexpressed in HeLa cells, the percentage of cells extending neurites is significantly reduced compared to those overexpressing the wild-type (Saita *et al.*, 2009). In addition, ΔFYVE protrudin results in decreased affinity for lipids, which subsequently prevents the enhancement of neurite outgrowth normally seen with wild-type protrudin in primary hippocampal neurons (Gil *et al.*, 2012). The effects of these mutants are described in detail in *Introduction, Section 4.*

2. Results

2.1 No sufficient endogenous protrudin knockdown was achieved using shRNAs constructs in primary cortical neurons

In order to understand whether endogenous protrudin plays a role in the regenerative enhancement observed in *in vitro* axotomy (*Chapter 4)* after human protrudin overexpression in rat primary cortical neurons, rat-specific shRNAs and CRISPR constructs were designed to silence the endogenous rat protrudin (see *Methods).*

Firstly, PC12 cells and rat primary cortical neurons were transfected with 4 shRNA constructs (shRNA_A, shRNA_B, shRNA_C and shRNA_D from OriGene, *see Methods*). Cells were fixed either 4 or 7 days post transfection and stained with anti-protrudin antibody and the amount of protrudin fluorescence in the cell body was measured (*Fig. 5.2A).* In PC12s, overexpression of shRNAs for 4 days does not result in a reduced protrudin staining intensity in any of the conditions compared to cells overexpressing scrambled shRNA control (*Fig. 5.2B).* On the contrary, in one of the conditions – in PC12s overexpressing shRNA_B (61 grey values), the intensity of protrudin in the cell body increased rather than decreased compared to scrambled control (49 grey values) ($p<0.0001$). In order to validate these results, cells overexpressing each shRNA construct were lysed 4 days post transfection and ran on a Western Blot to examine the amount of protrudin in lysate (*Fig. 5.2C)* When the amount of protrudin was calculated as a ratio of loading control – beta-actin, there were no significant differences across the conditions and control ($p=0.776$) (*Fig. 5.2D)* which confirms the immunocytochemistry results from above. One caveat of these experiments was that the transfection efficiency varied considerably between conditions. In order to bypass this problem, the two shRNAs which showed the highest decrease in protrudin intensity after immunocytochemistry – shRNA_A and shRNA_D were transfected in PC12s. Cells were then treated with puromycin antibiotic in order to select for the cells expressing the constructs and grown until they formed colonies. Individual colonies were selected and expanded to create cell lines stably expressing either scrambled RNA, shRNA_A or shRNA_D. In these cells, no significant changes were observed in the protrudin protein amount after Western blot or in the protrudin mRNA amount after RNA analysis (data not shown).

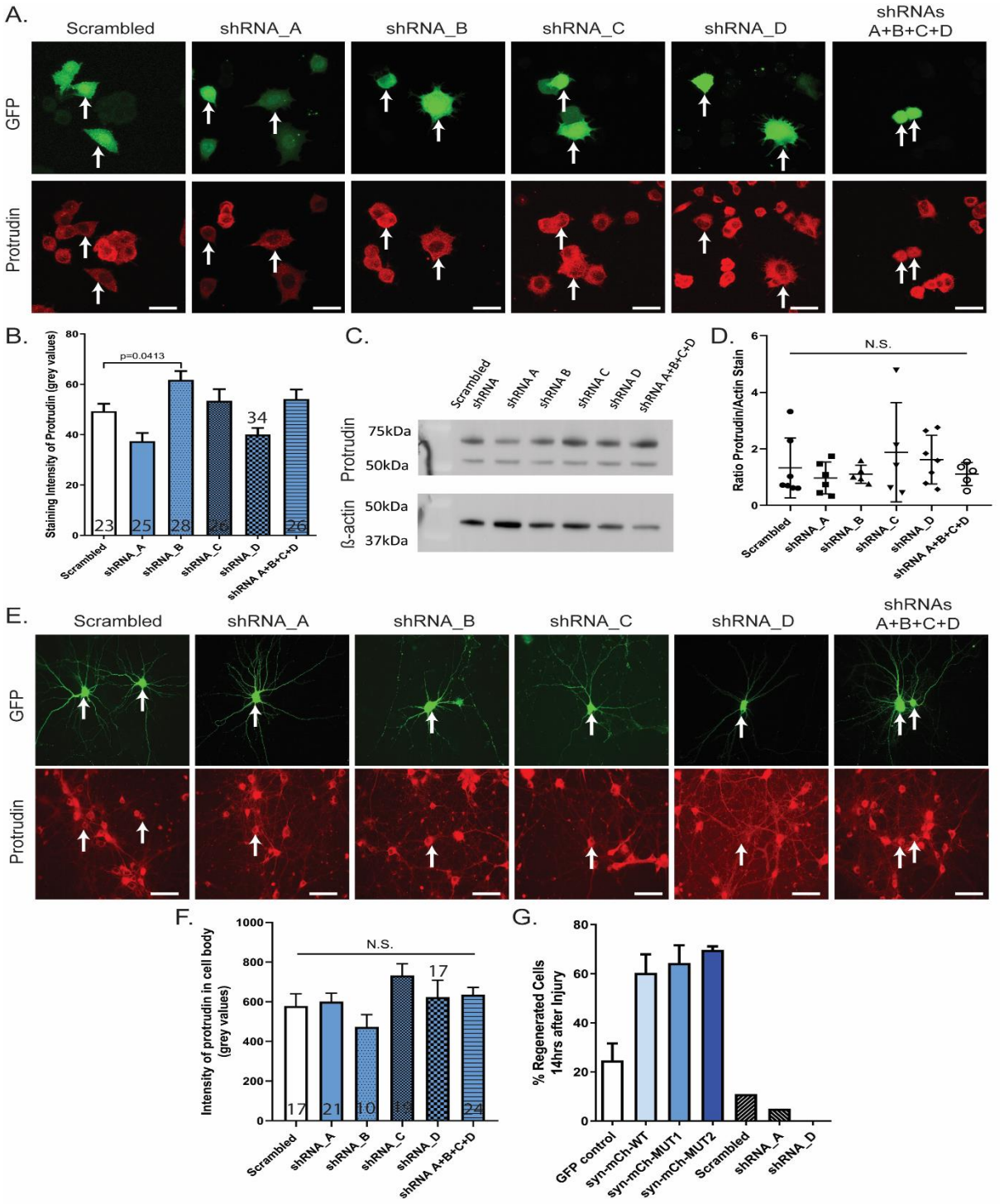

Figure 5.2 shRNAs against rat protrudin do not result in sufficient protrudin knockdown. A. Immunofluorescence images of PC12s expressing shRNA_A, shRNA_B, shRNA_C, shRNA_D or a combination of all four (green) and stained for protrudin (red). Images are taken at 63x. Scale bars are 20 µm. B. Overexpressing each shRNA does not result in significant decrease of protrudin staining compared to scrambled control. On the contrary shRNA_B causes increased amount of protrudin staining ($p<0.0001$, Kruskal-Wallis=34.12, n=2) C. Example Western blots of PC12 cells lysates. D. Quantification of the amount of protrudin staining on Western blots as a ratio of beta-actin staining as a loading control. There are no significant differences between any of the conditions ($p=0.7762$, Kruskal-Wallis statistic=2.568, n=5). E. Immunofluorescence images of primary cortical neurons expressing each construct. Images are taken at 40x. Scale bars are 20 µm. F. Bar graph to show that there are no significant changes were observed in protrudin staining intensity when overexpressing each construct ($p=0.101$, Kruskal-Wallis statistic=9.182, n=2). G. Bar graph to show the percentage of regenerating axons after laser axotomy of neurons overexpression scrambled control and 2 shRNAs - shRNA_A and shRNA_D.

The shRNA constructs were also validated in rat primary cortical neurons. 10 DIV neurons were transfected with each shRNA construct - shRNA_A, shRNA_B, shRNA_C or shRNA_D or a combination of all four and fixed at 14 DIV. They were then immunostained for the protrudin protein (*Fig. 5.2E).* Again, no significant changes were observed in the expression of the protrudin protein with either shRNA construct compared to scrambled control after 4 days of expression (p=0.101) (*Fig. 5.2F).* There were generally three types of protrudin staining observed in cells expressing shRNA constructs – either the protrudin staining did not differ majorly from non-transfected surrounding cells (highest proportion of cells), or the protrudin staining was very bright in the nucleus suggesting that the antibody has some non-specific staining or the intensity of protrudin staining was highly reduced indicating that the knockdown is working (lowest proportion of cells). Another approach was used where neurons were transfected for a total of 7-10 days in case the turnover of the protrudin protein was longer. Expressing the shRNA constructs in neurons for more than 4 days, however, resulted in substantial cell death and toxicity (data not shown). Due to these variable observations, shRNAs were not taken forward for regeneration experiments. While the validation experiments were taking place, however, small number of laser axotomies were carried out in neurons expressing either scrambled, shRNA_A or shRNA_D and very low regeneration rates were observed (11%, 5% and 0% respectively) (*Fig. 5.2G).* These results suggested that the neurons transfected with the shRNA constructs had poor overall health and that the shRNA construct might be toxic to some extent.

2.2 Partial protrudin knockdown was achieved using CRISPR-Cas9 constructs in primary cortical neurons

As the shRNA constructs were shown to be toxic in neurons, another approach was used to knockdown endogenous rat protrudin. Three different rat-specific sgRNA sequences, targeting different regions of the protrudin gene, were designed and cloned into CRISPR-Cas9 constructs (see *Methods*). A control non-targeting RNA (nsgCRISPR) was used as a control. These constructs were then transfected into primary cortical neurons either at 3 DIV or at 10 DIV and neurons were fixed at 15 DIV and stained for HA-tag to detect the CRISPR-Cas9 construct and the protrudin antibody (*Fig. 5.3A).*

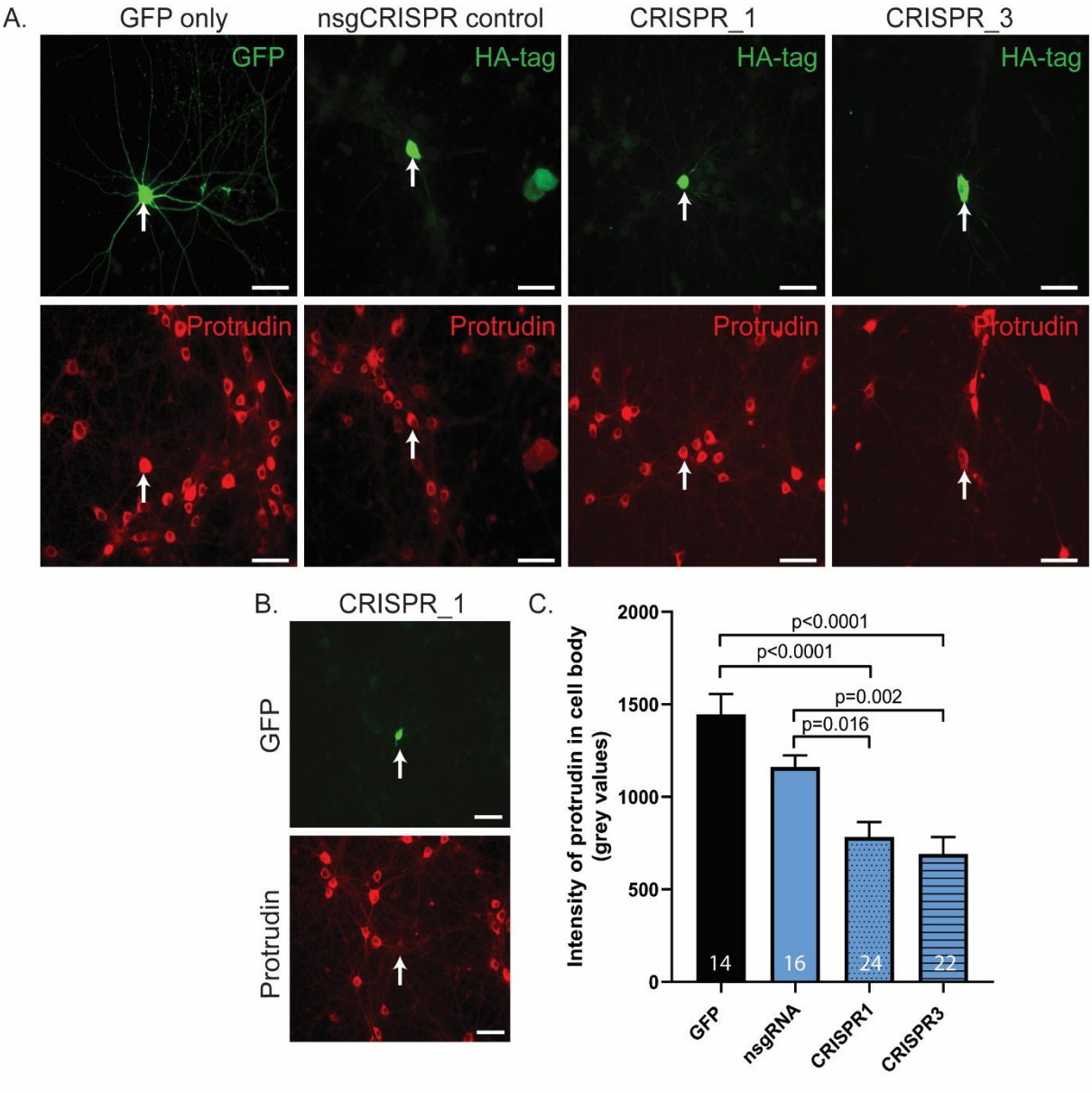

Figure 5.3 CRISPR constructs against rat protrudin result in partial protrudin knockdown. A. Immunofluorescence images of primary cortical neurons expressing GFP alone, nsgCRISPR control, CRISPR_1 or CRISPR_3 (green) and stained for protrudin (red). Images are taken at 40x. Scale bars are 20 µm. B. Example images of a cell transfected with CRISPR_1 which shows complete knockdown as there is no protrudin staining. Images were taken at 40x. Scale bars are 20 µm. C. Bar graph to show that rat primary cortical neurons overexpressing CRISPR_1 and CRISPR_3 constructs show reduced amount of protrudin staining intensity in the cell body compared to nsgCRISPR control or GFP only control ($p<0.0001$, one-way ANOVA, n=2). Error bars represent ± SEM.

By four days after transfection there were no significant changes in protrudin intensity in cells expressing CRISPR_1 or CRISPR_3 compared to CRISPR control (data not shown). By twelve days after transfection, however there was a decrease in protrudin intensity in cells expressing CRISPR_1 (783 grey values) or CRISPR_3 (691 grey values) compared to nsgCRISPR control (1161 grey values) or GFP only control (1447 grey values) ($p<0.0001$) (*Fig. 5.3C).* This difference was, however, mostly attributed to a small proportion of cells expressing CRISPR_1 and CRISPR3 constructs which had no or very little protrudin staining (*Fig. 5.3B)*. The rest of the cells had similar amount of protrudin compared to the two controls. It was difficult to study whether the cells showing vigorous knockdown of protrudin, are healthy and protrudin is reliably knocked down or if they have simply undergone apoptosis as the CRISPR constructs only localised to the cell body. In order to test the viability of these cells, a further stain for cell death markers should be added to the staining procedure. Also, due to the variability observed in each condition, more rigorous analysis of what proportion of all transfected cells show a knockdown and whether the percentage is high enough to use these cells in *in vitro* regeneration experiments, is needed.

In summary, the CRISPR method of protrudin knockdown seems to be more effective in knocking down the protein in primary cortical neurons while keeping the neurons alive. However, further analyses are needed in order to validate its value in studying axon regeneration in rat primary cortical neurons.

The original intention of the protrudin silencing approach was three-fold. Firstly, to be able to determine an endogenous role for protrudin in the regulation of axon growth or regeneration. Secondly, to be able to express protrudin deletion mutants on a background of depleted protrudin (all protrudin mutants are human and would not be targeted by the shRNA or CRISPR constructs, thereby acting as resistant constructs). Thirdly, our hypothesis was that phosphomimetic protrudin would mimic phosphorylation by enzymes functioning downstream from growth factors (Shirane and Nakayama, 2006). We reasoned that this would be necessary due to diminished signalling in more mature neurons. Our finding that wild-type protrudin stimulated regeneration to a similar degree as the phosphomutants suggested that the endogenous protein was perhaps also phosphorylated at the stage when axotomy was performed. Depleting endogenous protrudin may have allowed for a detectable

difference between expression of wild-type protrudin compared to the phosphomimetics. The problems encountered in trying to deplete endogenous protrudin led to the focus on the experiments described below.

2.3 Wild-type and constitutively phosphorylated protrudin bind to all forms of the Rab11 protein

In this section, we address the interaction between protrudin constructs and Rab11. In previous reports, wild-type protrudin was shown to bind to small GTPase Rab11 (Shirane and Nakayama, 2006). In their experiments, Shirane and colleagues showed that wild-type protrudin binds to Rab11 and that this interaction is strengthened by addition of NGF which activates the ERK-MAPK pathways and increases protrudin phosphorylation. Protrudin was also shown to bind preferentially to a GTP-deficient form of Rab11 (S25N) but not to a GTP-bound form lacking GTPase activity (Q70L) (Shirane and Nakayama, 2006). Furthermore, this interaction between Rab11-GDP and protrudin was shown to be required for neurite outgrowth in PC12 cells upon NGF treatment.

In this thesis, phosphomimetic mutants were created in order to enhance the interaction between protrudin and Rab11-GDP without having to activate intracellular pathways such as the ERK/MAPK pathway. In order to examine whether the phosphomimetic mutants have an enhanced affinity for Rab11, co-immunoprecipitation studies were carried out in HeLa cells where GFP only, GFP-WT protrudin or GFP-MUT2 protrudin were co-transfected with either mCherry-Rab11-WT, a dominant negative form of Rab11 – RFP-Rab11-DN (GDP-bound, S25N) and a constitutively active form of Rab11 – RFP-Rab11-CA (GTP-bound, Q70L). Cells were lysed 48 hours post transfection and co-immunoprecipitation was carried out on an anti-GFP magnetic bead column as described in *Methods* (*Fig. 5.4A).* Once the proteins that were bound to the column were eluted, they were next analysed by SDS-PAGE (*Fig. 5.4B).*

The experiment showed that both forms of protrudin – GFP-WT protrudin and GFP-MUT2 protrudin bound to all three forms of Rab11 including the constitutively active form of Rab11 (GTP-bound) in contradiction with previous studies (*Fig. 5.4B)* (Shirane and Nakayama, 2006). From the initial hypothesis that constitutively active protrudin will bind more Rab11-GDP

(S25N), a thicker band was expected when RFP-Rab11-DN is co-precipitated with GFP-MUT2 protrudin compared to when co-precipitated with GFP-WT protrudin. Wild-type and phosphomimetic protrudin appeared, however to be binding to similar extent to all forms of Rab11 after multiple experiments (*Fig. 5.4B).* There were no significant differences between wild-type and constitutively phosphorylated protrudin in their binding to wild-type Rab11 ($p=0.7179$, $n=4$), to GDP-bound Rab11 ($p>0.999$, $n=3$) or to GTP-bound Rab11 ($p>0.999$, $n=3$) (*Fig. 5.4C)*.

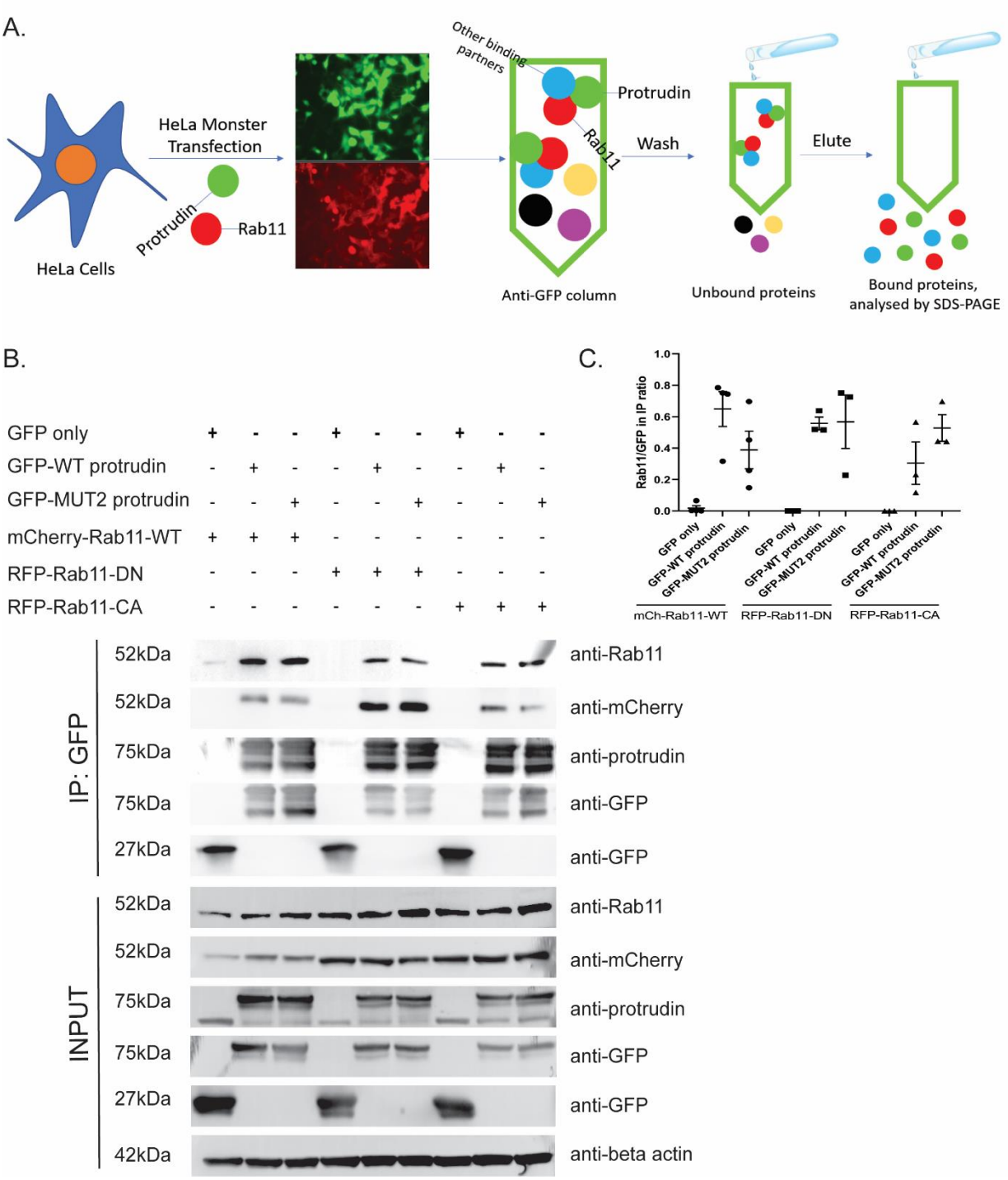

Figure 5.4 Co-Immunoprecipitation of protrudin and Rab11. A. A schematic diagram to describe the co-immunoprecipitation methodology. B. Immunoblots from IP and input to show that wild-type and also constitutively phosphorylated protrudin bind to all forms of Rab11. GFP only does not bind to any forms of Rab11. C. Quantification of the band density of Rab11 in IP after immunoblotting with anti-Rab11 antibody from several different experiments (n=3-4). There were no differences observed between the binding of wild-type and mutant protrudin to any one form of Rab11.

2.4 The axon-to-dendrite ratio of Rab11 or integrin does not change majorly after protrudin overexpression using immunohistochemistry

After observing such robust effects of protrudin overexpression on axon regeneration both *in vitro* and *in vivo* (see *Chapter 4*), the next question was whether this effect is a result of increased transport of growth-promoting molecules into the axon. Immunocytochemistry for Rab11 and integrin was carried out on cortical neurons overexpressing control or protrudin constructs (*Fig. 5.5A)*. The amount of endogenous Rab11 and integrins in the proximal and distal part of the axon was measured as described in *Methods.*

The average axon/dendrite ratio of Rab11 was higher in neurons expressing syn-mCh-MUT2 (ratio=1.1) compared to that in neurons expressing syn-mCh control (ratio=0.67) (p=0.006) (*Fig. 5.5B).* This change in the axon/dendrite ratio seems to be caused by a trend towards less Rab11 in dendrites (17 grey values) and a trend towards more Rab11 in the axons (14 grey values) of neurons expressing syn-mCh-MUT2 despite that no significant changes were observed in these parameters compared to control (25 grey values in dendrites and 11 grey values) (*Fig. 5.5C, 5.5D).* Neurons expressing syn-mCh-MUT1 showed a decreased amount of Rab11 in dendrites (15 grey values) compared to syn-mCh control (25 grey values) (p=0.019) and a decreased amount in the axon (9.7 grey values) compared to neurons expressing syn-mCh-MUT2 (14 grey values) (p=0.011) (*Fig. 5.5C, 5.5D).* No significant changes were observed in the axon/dendrite ratio of Rab11 in neurons expressing syn-mCh-WT (p>0.999) or syn-mCh-MUT1 (p=0.7835) compared to neurons expressing control (*Fig. 5.5B).*

Cortical neurons were further stained for 2 different integrins – integrin beta-1 and integrin alpha-5. The α5β1 integrin receptor has previously been detected extensively in the CNS and has been proposed to play a role after injury in the fibronectin-rich scar (Nieuwenhuis *et al.*, 2018). Endogenous integrin alpha 5 is also one of the few integrins which has previously been detected axonally in rat tissue using immunohistochemical analysis (King, McBride and Priestley, 2001). In this study, the integrin beta-1 staining was unreliable and unquantifiable, so no further experiments were carried out with this antibody (data not shown). When neurons were stained for integrin alpha-5, there were no significant changes in the axon-to dendrite ratio or of the amount of integrin in dendrites of cells expressing syn-mCh control,

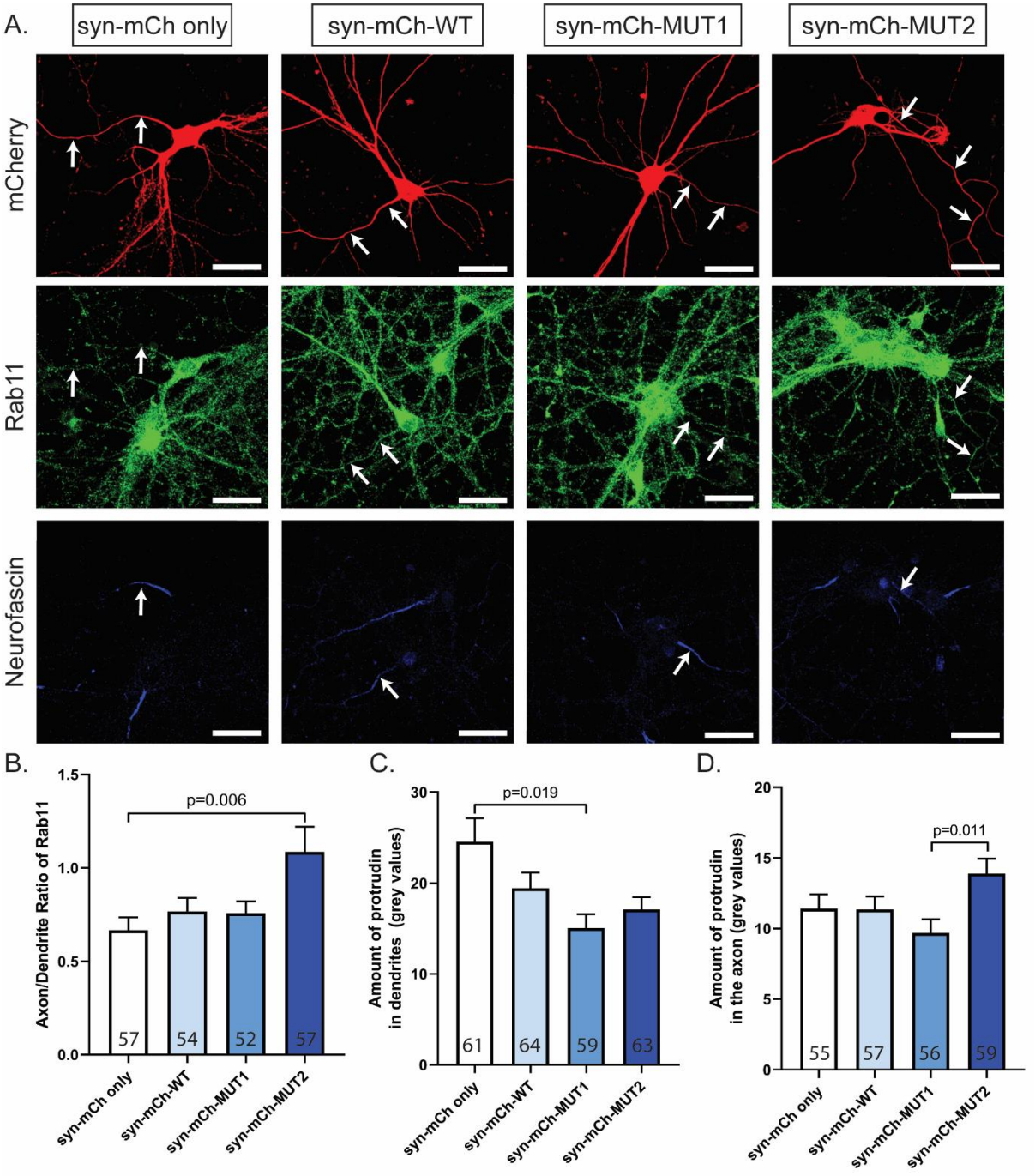

Figure 5.5 Immunocytochemical analysis of Rab11 in primary cortical neurons. A. Immunofluorescent images of endogenous mCherry signal from syn-mCh control, syn-mCh-WT, syn-mCh-MUT1 and syn-mCh-MUT2 constructs (red), Rab11 detected by immune staining (green) and neurofascin as an axon initial segment marker (blue). Images were taken at 40x magnification. Scale bars are 20 µm. B. Bar graph to show that the axon-to-dendrite ratio of Rab11 in cells expressing syn-mCh-MUT2 is higher than that in cells expressing syn-mCh control (p=0.0113, Kruskal-Wallis statistic=11.09, n=5). C. Bar graph to show that cells expressing syn-mCh-MUT1 show decreased intensity of Rab11 in their dendrites compared to control (p=0.0273, Kruskal-Wallis statistic=9.157, n=5). D. Bar graph to show that the Rab11 intensity in the axons of cells expressing syn-mCh-MUT2 is higher than that of cells expressing syn-mCh-MUT1 (p=0.0208, Kruskal-Wallis statistic=9.755, n=5). Error bars represent ± SEM.

syn-mCh-WT, syn-mCh-MUT1 or syn-mCh-MUT2 protrudin (p=0.259 and p=0.0919 respectively, n=3) (*Fig. 5.6A, B, D).* There were some small changes observed in the amount of integrin alpha 5 in the axons – neurons expressing syn-mCh-WT (22 grey values) had higher intensity of integrin staining compared to syn-mCh control (11 grey values, p=0.016) or syn-mCh-MUT1 (10 grey values) (p=0.011) (*Fig. 5.6C)*.

Both antibodies (against Rab11 and against integrin alpha 5), however, produced high background staining which was difficult to analyse, especially in the case of integrin. Furthermore, both integrins and Rab11 were previously shown to be excluded from mature axons of primary neurons (Franssen *et al.*, 2015; Koseki *et al.*, 2017) so subtle differences in their expression level and transport along the axons, are very unlikely to be detected by immunocytochemistry which presents a single time-point to detect highly dynamic vesicles along the axon. Therefore, further testing was needed in order to validate these results - live-cell imaging experiments were carried out as a more reliable source to measure integrin and Rab11 amount in axons in real time and allows for visualisation of the distal axon which was difficult to trace in the immunocytochemical analysis.

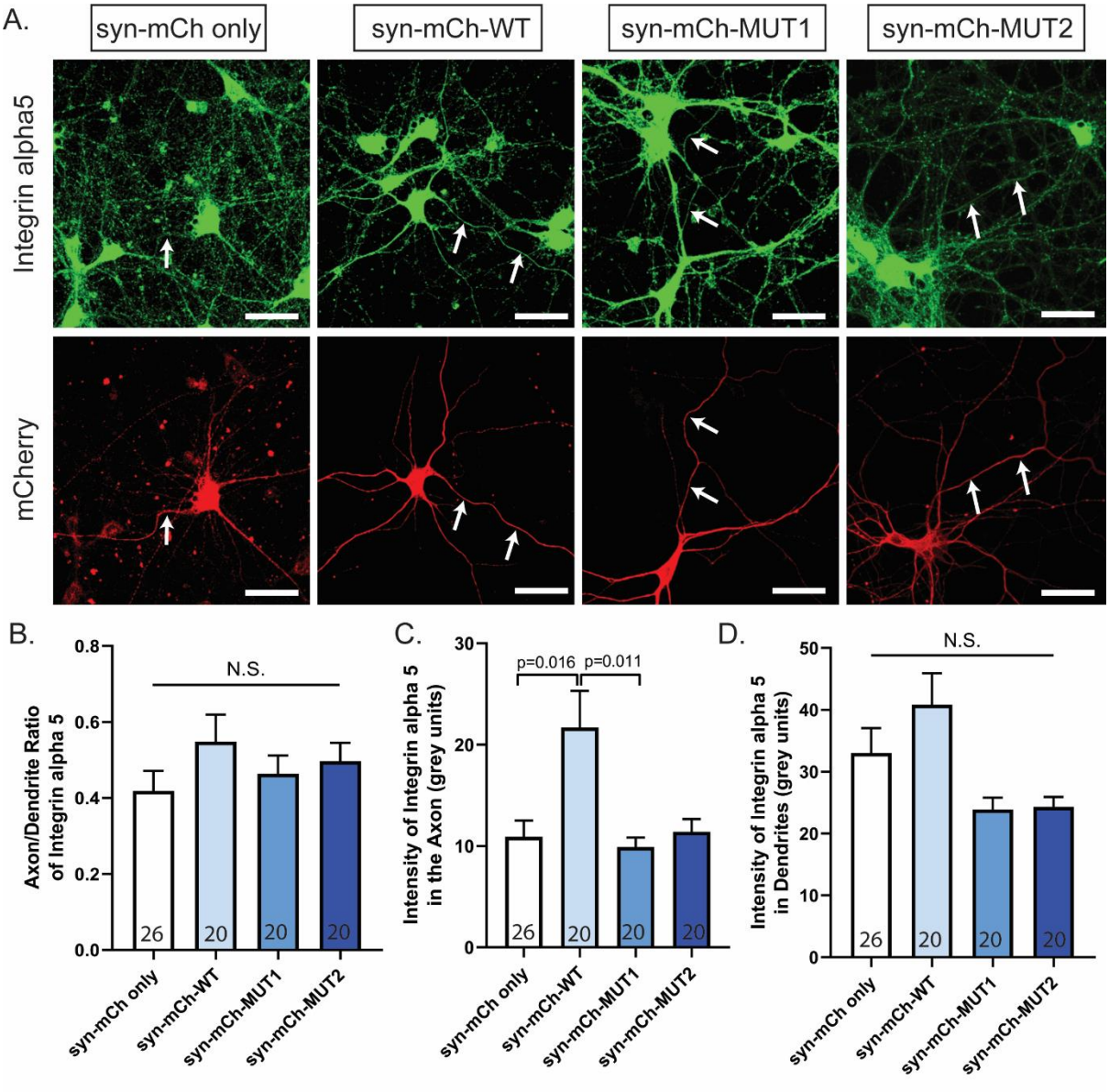

Figure 5.6 Immunocytochemical analysis of integrin alpha 5 in primary cortical neurons. A. Immunofluorescent images of endogenous mCherry signal from syn-mCh control, syn-mCh-WT, syn-mCh-MUT1 and syn-mCh-MUT2 constructs (red) and integrin alpha 5 detected by immune staining (green). Images were taken at 40x magnification. Scale bars are 20 µm. B. Bar graph to show that there are no significant changes in the axon-to-dendrite ratio of integrin alpha 5 across the different conditions (p=0.259, Kruskal-Wallis statistic=4.017, n=3). C. Bar graph to show that cells expressing syn-mCh-WT show increased intensity of integrin alpha 5 in the axon compared to control or syn-mCh-MUT1-expressing neurons (p=0.0048, Kruskal-Wallis statistic=12.95, n=3). D. Bar graph to show that there are no differences in the intensity of integrin alpha 5 in dendrites of neurons expressing each construct (p=0.0919, Kruskal-Wallis=6.445, n=3). Error bars represent ± SEM.

2.5 Axonal transport of Rab11 and integrin vesicles increases in the distal axon upon protrudin overexpression as observed by live-cell imaging

In order to study whether overexpression of protrudin resulted in an increased amount of Rab11- or integrin alpha9-positive endosomes in the axon, live-cell imaging experiments were performed as described in *Methods, Section 5.2.* Syn-GFP-integrinα9 and syn-GFP-Rab11 constructs were co-expressed with syn-mCh control, syn-mCh-WT or syn-mCh-MUT2 protrudin constructs in 10 DIV primary cortical neurons. Axonal transport of Rab11 and integrin vesicles was imaged live using a spinning-disc confocal microscope at 13-17 DIV. The number of vesicles and their direction of transport was measured in the proximal part of the axon (within 100-200 µm of the cell body), in the distal part of the axon (beyond 600 µm) and at the growth cone where possible. Four types of transport were observed and measured in these axons – anterograde (towards the tip of the axon), retrograde (towards the cell body), bidirectional (vesicles moving in both directions but with net movement of less than 2 µm) and static (vesicles with a total movement of less than 2 µm during their visible lifetime) (described in detail in Eva *et al.*, 2010, 2012). At least 40 different axons were analysed in each condition.

When examining Rab11 transport (*Fig. 5.7A)* in the proximal and distal axon, the length of axonal segment in which transport was measured did not differ significantly across the conditions (*Fig. 5.7B).* Our results showed that there were more Rab11-positive vesicles in neurons overexpressing syn-mCh-WT protrudin (26 vesicles) compared to control in the proximal axon (21 vesicles, $p=0.008$). In addition, neurons overexpressing syn-mCh-WT protrudin (21 vesicles) or syn-mCh-MUT2 protrudin (19 vesicles) also showed increased number of Rab11-positive vesicles in the distal axon compared to control (14 vesicles, $p<0.0001$ and $p=0.0008$ respectively) (*Fig. 5.7C).* These findings suggest that overexpression of either form of protrudin results in increased number of Rab11 endosomes in distal axons. When examining the different types of transport, there were no significant changes observed in anterograde ($p=0.293$, one-way ANOVA), retrograde ($p=0.844$, one-way ANOVA) or bidirectional ($p=0.169$, one-way ANOVA) transport, proximally (*Fig. 5.7D).* There was an increased number of static vesicles in neurons overexpressing WT protrudin compared to control in the proximal axon ($p=0.006$, Kruskal-Wallis statistic=10.10) (*Fig. 5.7D).* Distally,

there were more particles moving retrogradely in axons expressing WT protrudin compared to control (p=0.016, Kruskal-Wallis statistic=8.197) and more particles moving bidirectionally in axons expressing WT and MUT2 protrudin compared to control (p=0.0002, Kruskal-Wallis statistic=16.60) (*Fig. 5.7D).* There were no significant changes observed in the anterograde (p=0.136, one-way ANOVA) or static vesicle transport (p=0.105, Kruskal-Wallis Statistic=4.499) in the distal axon across conditions (*Fig. 5.7D).*

Although there is a small increase in the number of Rab11 vesicles in the growth cones of neurons expressing MUT2 protrudin compared to control, no significant changes were observed across the different conditions (*Fig. 5.7C*). There were also no significant changes in the number of vesicles moving anterogradely (p=0.108, Kruskal-Wallis statistic=4.441), retrogradely (p=0.113, Krukal-Wallis statistic=4.368), bidirectionally (p=0.747, Kruskal-Wallis statistic=0.584) or being static (p=0.197, Kruskal-Wallis statistic=3.243) in the growth cones of different conditions (*Fig. 5.7D).* As the length of the axon segment analysed in the growth cone was significantly longer in MUT2-expressing neurons compared to control (p=0.032) (*Fig. 5.7B)*, all measurements for transport in growth cones were calculated as number of vesicles per a specific distance (in this case, 50 μm).

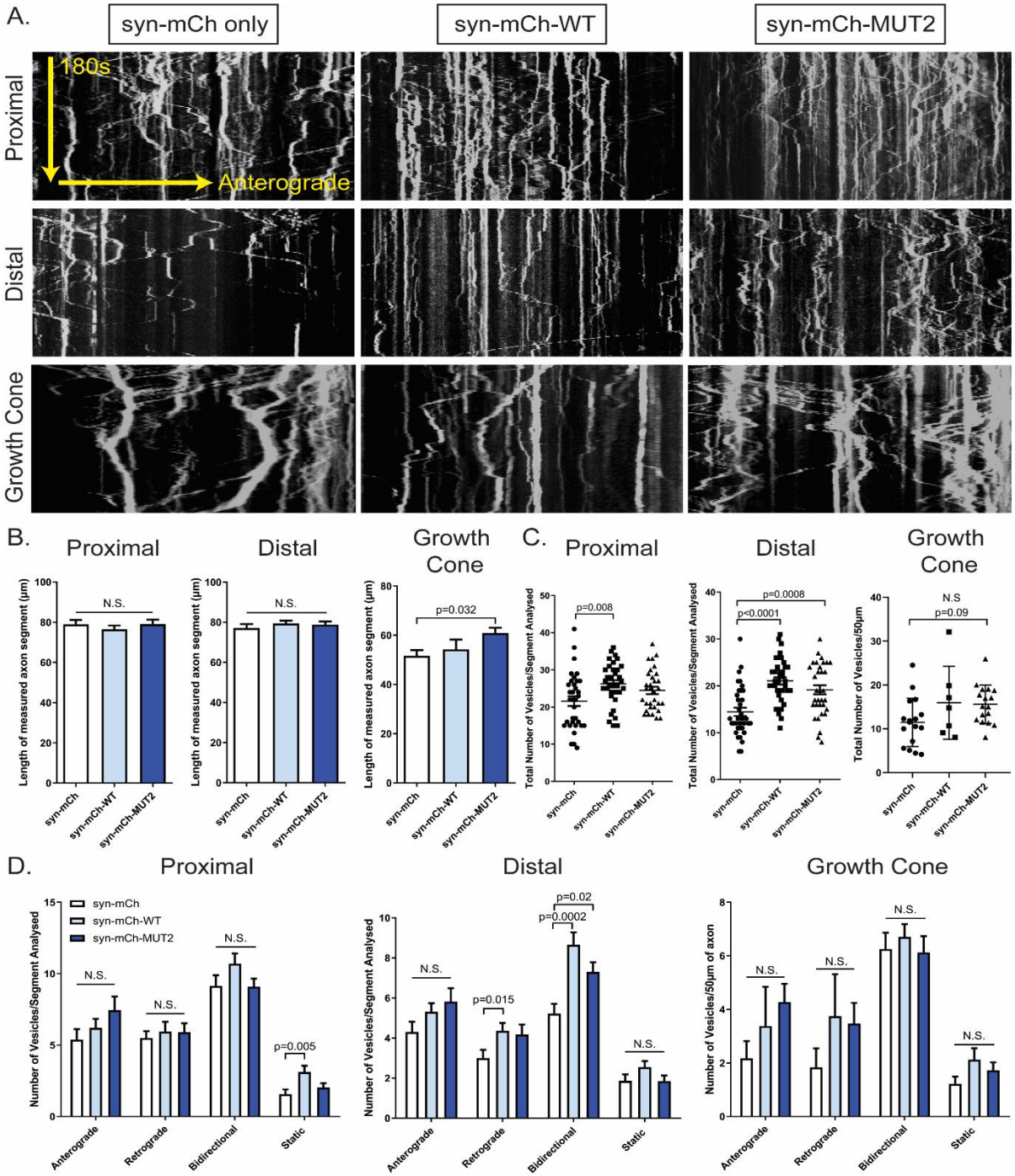

Figure 5.7 Transport of Rab11 endosomes along axons of mature cortical neurons. A. Kymographs showing the dynamics of syn-GFP-Rab11 in the proximal and distal axon as well as in growth cones of neurons expressing syn-mCh control, syn-mCh-WT or syn-mCh-MUT2 protrudin. B. The length of the segments measured for the analysis was not significantly different between the conditions in the proximal (p=0.634, one-way ANOVA) or distal (p=0.617, one-way ANOVA) axon but differed in growth cones (p=0.0383, Kruskal-Wallis statistic=6.527). C. Quantification of the number of Rab11 vesicles (n=4). There were more Rab11 vesicles in axons expressing WT protrudin compared to control in the proximal (p=0.008, one-way ANOVA) and in the distal axon (p=0.0001, one-way ANOVA) as well as in axons expressing MUT2 compared to control in the distal axon (p=0.0008, one-way ANOVA). There were no differences in growth cones (p=0.07, one-way ANOVA). D. Bar graphs representing the number of vesicles being transported anterogradely, retrogradely, bidirectionally or being static across conditions. Proximally, neurons expressing WT protrudin had more static vesicles than control neurons (p=0.005). Distally, there was more retrograde transport in cells expressing WT protrudin (p=0.015) as well as more bidirectional transport in cells expressing WT (p=0.0002) and MUT2 (p=0.02) protrudin compared to control. There were no changes in the different transports in growth cones. Error bars represent mean ± SEM.

Similar results were obtained when observing the transport of integrin alpha 9-containing vesicles in axons overexpressing either syn-mCh control, syn-mCh-WT or syn-mCh-MUT2 protrudin (*Fig. 5.8A)*. As hypothesised, there were more integrin-positive vesicles in neurons overexpressing syn-mCh-WT protrudin (14 vesicles) or syn-mCh-MUT2 (13 vesicles) compared to control neurons (9 vesicles) in the distal axon ($p<0.0001$ and $p=0.0005$ respectively) (*Fig. 5.8C).* No significant changes were observed in the number of integrin vesicles in the proximal axons or in the grown cones of neurons expressing a control plasmid (21 and 5 vesicles respectively), WT (24 and 8 vesicles respectively) or MUT2 protrudin (23 vesicles and 10 vesicles respectively) (*Fig. 5.8C).*

When examining the different types of transport, proximally there were no significant changes observed in anterograde ($p=0.578$, one-way ANOVA), retrograde ($p=0.641$, one-way ANOVA), bidirectional ($p=0.559$, one-way ANOVA) or static ($p=0.111$, one-way ANOVA) transport (*Fig. 5.8D).* Distally, there were more particles moving anterogradely in axons expressing WT protrudin ($p=0.006$) or MUT2 protrudin ($p=0.007$) compared to control and more particles moving retrogradely in axons expressing MUT2 protrudin compared to control ($p=0.0002$) (*Fig. 5.8D).* There were no significant changes observed in the bidirectional ($p=0.136$, one-way ANOVA) or static vesicle transport ($p=0.051$, Kruskal-Wallis Statistic=5.951) in the distal axon across conditions (*Fig. 5.8D).*

There were also no significant changes in the number of vesicles moving anterogradely ($p=0.644$, Kruskal-Wallis statistic=0.875), retrogradely ($p=0.202$, Kruskal-Wallis statistic=3.191), bidirectionally ($p=0.535$, Kruskal-Wallis statistic=1.251) or being static ($p=0.811$, Kruskal-Wallis statistic=0.4191) in the growth cones of different conditions (*Fig. 5.8D).* As the average length of the axon segments analysed was significantly longer in WT and MUT2-expressing neurons compared to control ($p=0.02$) (*Fig. 5.8B)*, all measurements for transport in growth cones were calculated as number of vesicles per a specific distance (in this case, 50 µm). Even though no significant changes were observed in growth cones, the number of growth cones (approximately 10-15 growth cones per condition) in which transport was examined was significantly lower than the number of proximal or distal axons (approximately 40-50 axonal sections per condition). There are several reasons for this discrepancy – firstly, some distal axons were difficult to trace beyond 800 microns from the

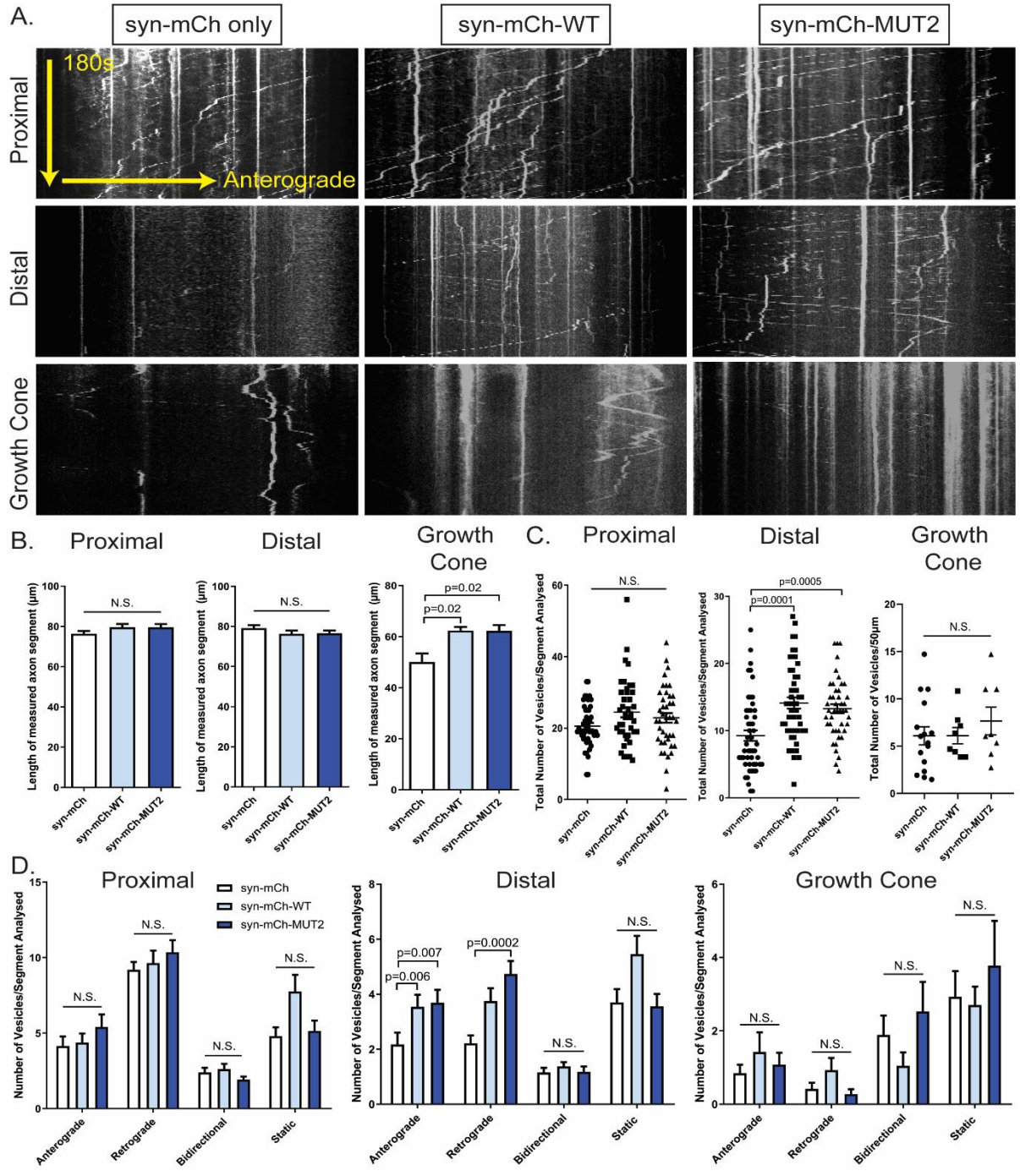

Figure 5.8 Transport of integrin alpha 9 vesicles along axons of mature cortical neurons. A. Kymographs showing the dynamics of syn-GFP-integrinα9 in the proximal and distal axon as well as in growth cones of neurons expressing syn-mCh control, syn-mCh-WT or syn-mCh-MUT2 protrudin. B. The length of the segments measured for the analysis was not significantly different between the conditions in the proximal (p=0.218, one-way ANOVA) or distal (p=0.271, Kruskal-Wallis statistic=2.609) axon but differed in growth cones (p=0.0076, one-way ANOVA) C. Quantification of the number of integrin vesicles (n=5). There were more integrin vesicles in axons expressing WT or MUT2 protrudin compared to control in distal axons (p<0.0001, Kruskal-Wallis statistic=21.81). There were no differences in the proximal axon (p=0.149, Kruskal-Wallis statistic=3.797) or in growth cones (p=0.559, one-way ANOVA). D. Bar graphs representing the number of vesicles being transported anterogradely, retrogradely, bidirectionally or being static across conditions. There were no significant differences in transport in the proximal axon or growth cones. In the distal axon, there were more vesicles moving anterogradely in neurons expressing WT and MUT2 protrudin compared to control (p=0.0019, Kruskal-Wallis statistic=12.57) and there were more vesicles moving retrogradely in neurons expressing MUT2 protrudin compared to control (p=0.0003, Kruskal-Wallis statistic=16.46). Error bars represent mean ± SEM.

cell body (as described in *Chapter 3*); and secondly, protrudin does not fill growth cones completely as it is only visible at the base, so growth cones are difficult to find in the dish (as described in *Chapter 4*). Further analysis of the transport in growth cones is needed in order to confirm these results.

Co-localisation between Rab11 and integrin vesicles with control plasmid, WT or MUT2 protrudin (*Fig. 5.9A*) was also measured during live image acquisition and was expressed as a percentage of total vesicles observed (*Fig. 5.9B)*. Rab11 vesicles co-localised more readily with WT (29%) and MUT2 (29%) protrudin vesicles compared to control (18%) ($p<0.0001$, one-way ANOVA) (*Fig. 5.9C)*. Similarly, integrin vesicles showed increased co-localisation with WT (17%) and MUT2 (21%) protrudin compared to control (13%) ($p<0.0001$, Kruskal-Wallis statistic=24.15) (*Fig. 5.9D)*. Although there was no statistical difference between WT and MUT2 co-localisation with Rab11 or integrin alpha9, in both conditions MUT2 protrudin showed higher co-localisation than WT protrudin as predicted by our hypothesis that constitutive phosphorylation will result in increased association.

In summary, overexpression of either wild-type or mutant protrudin results in increased number of Rab11 and integrin alpha9-containing vesicles in the distal axon. In addition, there is an increased amount of active (anterograde and retrograde) transport of these vesicles in the distal axons of neurons expressing WT or MUT2 protrudin. These observations are important as the distal axon is the most usual site of axonal injury and this is where the most pronounced absence of Rab11 and integrins is evident. Therefore, being able to improve Rab11 and integrin transport in this part of the axon might explain the increased regenerative ability of neurons overexpressing protrudin. Lastly, both WT and MUT2 protrudin vesicles co-localised more with Rab11 and integrin confirming previous results that protrudin associates with Rab11-positive endosomes. Furthermore, this is the first evidence to show that a proportion of integrin-containing vesicles in the axon is transported in a protrudin-dependent manner.

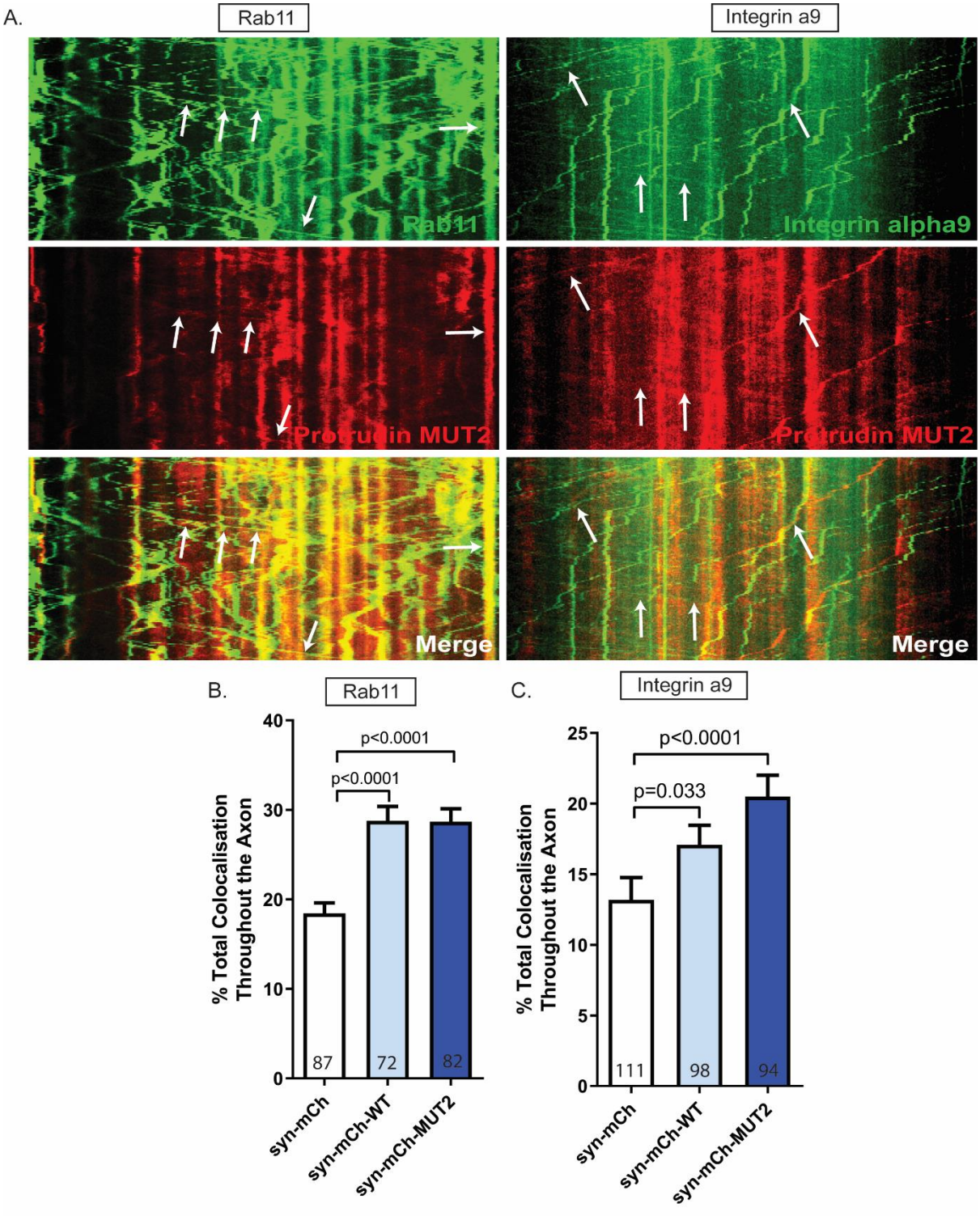

Figure 5.9 Rab11 and integrin alpha9 colocalise with wild-type and MUT2 protrudin in the axon. A. Representative kymographs for MUT2 protrudin (red) and Rab11 (green) or Integrin alpha 9 (green) and a merged image from which the number of vesicles containing both proteins (yellow) was measured. B. Quantification of the total percentage of co-localisation between Rab11 vesicles and control or protrudin plasmids as a function of the total number of Rab11 vesicles observed per axon segment. There were more Rab11 vesicles which also contained WT or MUT2 protrudin compared to control (One-way ANOVA, $p<0.0001$). C. Bar graph to show that there are more integrin vesicles containing WT (17%) or MUT2 (21%) protrudin compared to control protein (13%) ($p<0.0001$, Kruskal-Wallis statistic=24.15). Error bars represent mean ± SEM.

2.6 Protrudin aids axon regeneration via multiple molecular pathways

The results obtained during the regeneration experiments described in *Chapter 4,* showed that overexpressing wild-type protrudin on its own, promotes regeneration after laser injury in cultured cells and after optic nerve crush. The transport data above suggest that this is associated with an increase in both Rab11 and integrin transport into the distal axon. Protrudin is, however, a complex protein with numerous cellular functions as described in *Introduction,* therefore we hypothesised that there might be other molecular pathways through which protrudin is promoting axon regeneration, beyond the transport of growth-promoting molecules.

To test this, five more mutant forms of the protrudin protein were created – each disrupting a specific region of the protein important for its involvement in various molecular pathways (endoplasmic reticulum shaping, axonal transport, phospholipid interactions, microtubule severing, etc.) *(Fig. 5.1).* Rat primary cortical neurons were then grown in culture for 10 days and were transfected with each of the constructs described (control, ΔFYVE, ΔFFAT, ΔKIF5, ΔSpastin, ΔRBD, ΔER and MUT2 protrudin as positive control). Their regenerative abilities were tested in the *in vitro* axotomy model described in *Chapter 4* for their effects on axon regeneration.

Strikingly, expression of either ΔSpastin or ΔRBD protrudin mutants in primary cortical neurons at 10 DIV, resulted in cell death (*Fig. 5.10A)* in the majority of the transfected cells. This effect seemed to be cortical-neuron-specific and dose-dependent because the two constructs had no adverse effects when transfected in PC12 cells or when co-expressed with a GFP control vector where some neurons in which the expression of the mutant was dampened down, survived (data not shown). Due to the adverse effects these two mutants had on primary cortical neurons, their effect on regenerative ability could not be examined. These results suggested that the overexpression of ΔSpastin and ΔRBD protrudin interfered with endogenous protrudin function and that the interactions of protrudin with spastin and Rab11 might be essential for neuronal health and survival.

The rest of the mutants did not result in any immediately obvious morphological or functional changes so their effect on regenerative ability could be tested. Overexpression of

all four mutants of protrudin - ΔFYVE (43%, n=4), ΔFFAT (48%, n=4), ΔKIF5 (46%, n=4) and ΔER (35%, n=2) resulted in decreased percentage of regenerating axons compared to neurons overexpressing positive control – syn-mCh-MUT2 protrudin (86%, n=1) which was previously described to promote axon regeneration (see *Chapter 4*) (*Fig. 5.10C*). Furthermore, the percentage of regenerating axons in all four mutant conditions, did not significantly differ from syn-mCh control only (33%, n=6). More axotomies are currently being carried out with ΔER and syn-mCh-MUT2 positive control in order to increase the n number of experiments. These results suggest that mutating any of the domains described above results in reduced ability of protrudin to promote axon regeneration. There were no significant differences in other parameters measured during axotomy such as the time of regeneration (*Fig. 5.10E)*, the total regenerative distance (*Fig. 5.10D)*, the regeneration distance after 2 hours (*Fig. 5.10H)*, the retraction distance (*Fig. 5.10F)* or the maximum growth cone area (*Fig. 5.10G)*.

From these experiments we concluded that protrudin promotes regeneration through multiple mechanisms, some of which, such as endoplasmic reticulum (ER) involvement have not previously been well-studied with regards to the process of axon regeneration. These findings prompted us to hypothesise that protrudin acts as a scaffold molecule bringing multiple molecules, organelles and cellular components together at the tip of growing axons and that its reduced levels in mature axons might contribute to regenerative failure.

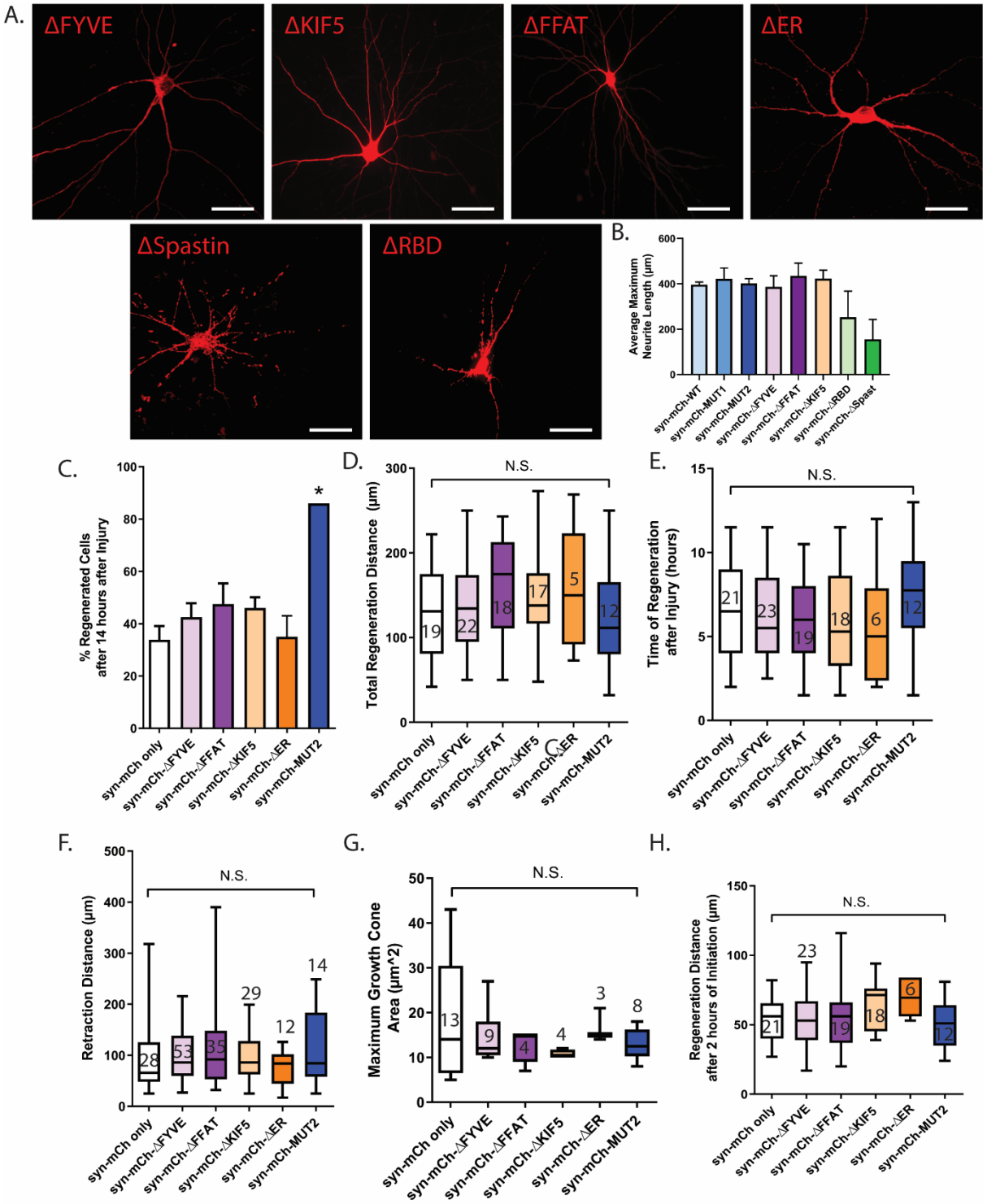

Figure 5.10 Overexpression of protrudin mutants suppresses protrudin's effect on axon regeneration. A. Immunofluorescent images of endogenous mCherry signal from different protrudin mutants. The ΔSpastin and ΔRBD mutants resulted in cell death when overexpressed in neurons at 10 DIV and suppressed neurite outgrowth at 3 DIV (B.) Images are taken at 40x magnification. Scale bars are 20 µm. C. The percentage of regenerating axons in neurons overexpressing syn-mCh-MUT2 protrudin is significantly higher than neurons overexpressing syn-mCh control or any of the functional domain mutants (p=0.0015, Fisher's exact test with Bonferroni-Dunn pairwise comparison). D., E., F., G., H. There were no significant differences between the time of regeneration after injury (p=0.6107, Kruskal-Wallis statistic=3.584), the total distance regenerated (p=0.3454, Kruskal-Wallis statistic=5.616), the regeneration distance 2 hours after regeneration initiation (p=0.1778, Kruskal-Wallis statistic=7.630), the maximum growth cone area (p=0.6619, Kruskal-Wallis statistic=3.248) or the retraction distance (p=0.5887, Kruskal-Wallis statistic=3.732) between any of the conditions.

2.7 Constitutively phosphorylated protrudin colocalises better with Rab7 in the cell body and REEP5 in growth cones compared to wild-type protrudin

Recently, protrudin's co-localisation with another Rab protein – Rab7 (a marker of late endosomes) was also examined, initially in the cell body. Syn-mCh-WT and syn-mCh-MUT2 protrudin was overexpressed in 10 DIV primary cortical neurons which were fixed at 14 DIV and stained for endogenous Rab7 (*Fig. 5.11A).* Mutant protrudin showed more co-localisation with Rab7 in the cell body of mature neurons (41%) compared to wild-type protrudin (22%) (p=0.002, Man-Whitney test) (*Fig. 5.11B)*. Furthermore, protrudin's co-localisation with a resident smooth endoplasmic reticulum protein – REEP5 was also tested. It was observed that mutant protrudin co-localised more with REEP5 in the distal axon and in growth cones (*Fig. 5.11C).* The Rab7 co-localisation experiment was carried out twice and the REEP5 experiment once so further repetitions are needed in order to confirm these results and observations. Rab7 is difficult to trace in the axon so in order to perform these experiments, we are currently co-transfecting wild-type or mutant protrudin with Rab7-GFP construct in order to observe the effects in the axon. Furthermore, the specificity of REEP5 and another smooth ER marker – reticulon-4 antibodies (Farías *et al.*, 2019) is currently being tested against ER lumen markers such as KDEL in order to find the best marker for endogenous ER in primary cortical neurons

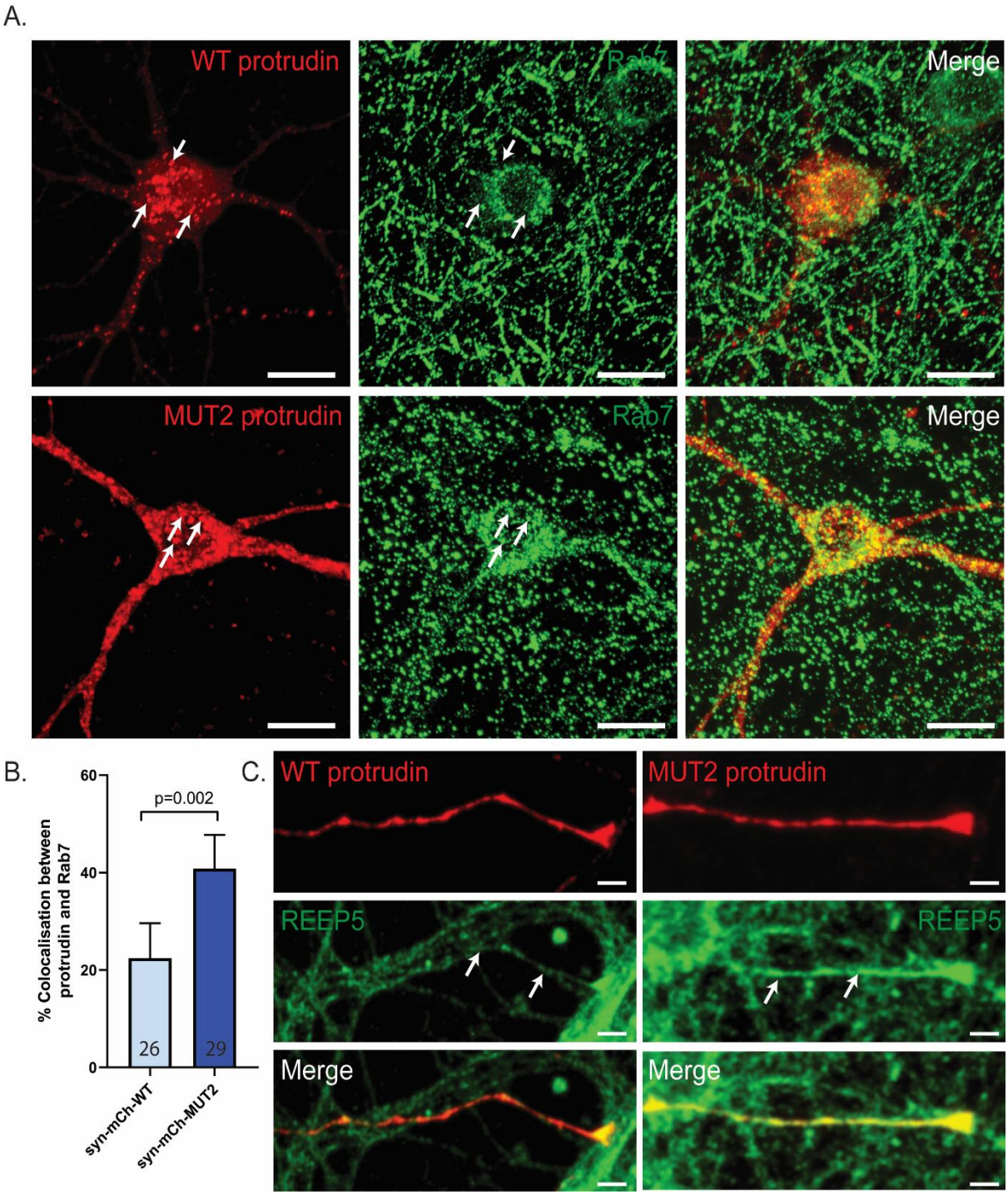

Figure 5.11 Protrudin co-localises with Rab7 in the cell body and REEP5 in the growth cone. A. Immunofluorescent images of endogenous mCherry signal from wild-type and mutant 2 protrudin (red) in cells stained for Rab7 (green). Images are taken at 63x magnification. Scale bars are 10 µm. White arrows point at protrudin-filled vesicular structures in the cell body. B. Bar graph to show that syn-mCh-MUT2 protrudin co-localises better with Rab7 in the cell body compared to syn-mCh-WT protrudin (p=0.002, Man-Whitney test). Error bars represent mean ± SEM. C. Immunofluorescent images representing endogenous mCherry signal from WT and MUT2 protrudin constructs (red) and stained ER marker REEP5 (green). Images are taken at 40x. Scale bars are 5 µm. White arrows follow the axon to the growth cone in the protrudin channel.

3. Discussion

In this chapter, the mechanisms behind protrudin's action on axon regeneration are explored. Overexpression of wild-type and mutant protrudin resulted in increased axonal transport of Rab11 and integrins into the distal part of the axon. This increase could in part explain the regenerative properties of protrudin, given the mounting evidence that increased transport of these molecules can facilitate CNS regeneration (Eva *et al.*, 2017; Koseki *et al.*, 2017). Protrudin's involvement in ER shaping and function, lipid transfer, lysosomal transport and axonal transport were all implicated in the process of axon regeneration by studying protrudin's functional mutants.

Overexpression of wild-type and constitutively active protrudin resulted in enhanced axon regeneration *in vitro* as described in *Chapter 4.* In this system, however the human protrudin was overexpressed on top of the endogenous rat protein and the interaction between the two proteins or their individual involvement in boosting axon regeneration was difficult to study. A system where the endogenous protein is knocked down could be valuable for studying whether protrudin is required and necessary for basal levels of axon regeneration in mature neurons. Previously, successful knockdown of protrudin was performed using siRNA constructs in RPE-1 cells (human retinal pigmented epithelial cells) and in HEK293 (from human embryonic kidney) after 48 hours (Hong *et al.*, 2017) as well as in HeLa cells (Connell et al., unpublished data). Protrudin has also been previously knocked down in zebrafish using morpholinos and this resulted in developmental impairments (Zhang *et al.*, 2012) as well as in human monocytes using siRNA where it resulted in compromised phagocytosis and toll-like receptor expression (Lindholm et al., unpublished data). These studies, however, showed a reliable knockdown in human protrudin protein. Knockdown of endogenous rat protrudin in PC12s or rat primary neurons has not been documented so far.

In order to distinguish between the effects of endogenous rat protrudin and the overexpressed human protrudin, endogenous protrudin knockdown was attempted by two methods. Firstly, rat-specific protrudin shRNA constructs (OriGene) were transfected transiently in PC12 cells for 4 days with the aim to reduce the protrudin protein expression.

There were, however, no significant changes in the intensity of protrudin staining in the cell body analysed by immunocytochemistry or in the amount of protrudin protein in the lysate analysed by SDS-PAGE compared to scrambled shRNA control (*Fig. 5.2A-D).* Furthermore, PC12 cells expressing two of the four shRNAs in stable lines, showed no differences in the amount of the protrudin protein as analysed by SDS-PAGE (data not shown). There were also no differences when shRNAs were expressed in primary cortical neurons for 4 days in the amount of the protrudin protein in the soma as analysed by immunofluorescence (*Fig. 5.2E-G).* It was observed that when transfected for longer periods of times – 7 or 10 days, primary cortical neurons started to show some changes in the amount of protrudin, but this also resulted in increased toxicity and in compromised cell survival.

There are several reasons why no robust knockdown is observed using the shRNAs. Firstly, as discussed in *Chapter 3,* there is very little protrudin during the development of rat primary cortical neurons *in vitro* to begin with - knocking down the already sparse protein and reliably detecting it could be a challenge. Furthermore, the protrudin protein turnover has not been previously documented in neurons so a substantial knockdown might require longer expression of shRNAs which in our case resulted in toxicity. Lastly, protrudin antibody used in all experiments produced high amount of background especially in more mature cultures, so detecting a small difference in protrudin expression might prove a challenging task.

These could explain why robust expression was not detected in primary cortical neurons, but in PC12s, the protein is expressed at high levels and the antibody works reliably. One reason for the failure to detect differences in protrudin levels in PC12 cells, could be that low and variable transfection rates were achieved for Western blot analysis (data not shown). In order to bypass these obstacles, lines of PC12 cells stably expressing two shRNAs which showed promising results after immunocytochemistry – shRNA_A and shRNA_D, were generated. These, however also did not show significant changes in protrudin levels after SDS-PAGE analysis which could be attributed to the long period of time needed to create and expand the stable lines (approximately 2-3 weeks) during which time the cells may have compensated by protrudin upregulation. In summary, no reliable knockdown was achieved in PC12s or in primary cortical neurons using rat-specific shRNAs against protrudin.

Another approach was using the CRISPR-Cas9 system to knockdown endogenous rat protrudin. In this experiment, shorter version of the Cas9 protein from *Staphylococcus aureus* (saCas9) was used in order to fit all components into a single plasmid (Friedland et al., 2015). Three different sgRNA sequences against rat protrudin were designed to target different regions of the protrudin gene (see *Methods*). There were difficulties in sequencing and obtaining a pure sample of the plasmid containing the CRISPR_2 sequence, so this plasmid was not used for initial experiments. CRISPR constructs 1 and 3 showed promising results in knocking down protrudin when overexpressed in primary cortical neurons for more than 10 days. They appeared less toxic and a percentage of cells showed substantial knockdown of protrudin as analysed by immunocytochemistry (*Fig. 5.3).* As described in *Results above*, however, the viability of these cells needs to be tested in further experiments in order to validate these constructs and their use for future experiments. Unfortunately, as neuronal transfection only results in 1% of neurons being transfected in primary cortical cultures, no reliable SDS-PAGE analysis could be carried in neurons to validate the reduced amount of protrudin protein.

In summary, the CRISPR-saCas9 constructs showed more promising results in knocking down endogenous rat protrudin than using shRNAs in terms of efficiency and viability. However, due to the variability in the knockdown achieved and the fact that there is very little detectable protrudin in these cells in the first place, the rest of the experiments were carried out as initially described by overexpressing human protrudin in addition to the rat endogenous protein.

Our initial hypothesis was that creating constitutively phosphorylated protrudin will increase the interaction between protrudin and Rab11-GDP. Firstly, immunoprecipitation (IP) was carried out by overexpressing wild-type and mutant protrudin and blotting for endogenous Rab11. In these experiments, however, no band was detected for endogenous Rab11 in the IP immunoblotting (data not shown). Therefore, a new experiment was designed where wild-type or mutant protrudin (fused to GFP) was co-expressed together with either one of three forms of Rab11 (WT, GTP-bound form and GDP-bound form, fused to RFP or mCherry) in HeLa cells which were then lysed. The lysate was then passed through a magnetic anti-GFP column where protrudin-GFP and its binding partners attached and after several

washes to remove unbound proteins, the final eluate was analysed by SDS-PAGE and blotted for Rab11 (*Fig. 5.4A*). It was anticipated that increased interaction between mutant protrudin and the GDP-bound form of Rab11 (RFP-Rab11-DN) will produce visibly thicker band on the IP blot. The overexpression of both protrudin and Rab11 was reliably detected in the input blots with staining for protrudin, GFP, Rab11 and mCherry (*Fig. 5.4).* Protrudin was also successfully pulled down in the GFP column as the overexpressed protein was reliably detected in the IP blot (*Fig. 5.4)* The overexpressed protrudin in the pull down showed monomeric (at 75 kDa) and oligomeric forms (at 150 kDa, data not shown) as previously described suggesting that the protein has retained its normal binding properties (Pantakani *et al.*, 2011). There were, however no obvious differences in the amount of wild-type or mutant protrudin binding any more to a particular form of Rab11. Although our experiment was designed in a similar fashion to the experiments performed by Shirane and Nakayama (2006), we found that both forms of protrudin associated with all forms of Rab11 which is contradictory to their findings that protrudin preferentially binds Rab11-GDP (Shirane and Nakayama, 2006). One caveat of this study might be that the two proteins were overexpressed, and this might result in some unusual interactions which are not characteristic of the physiological situation. Furthermore, co-immunoprecipitation is a semi-quantitative method to detect protein-protein interactions and could be highly dependent on the transfection rate of the cell lines, the levels of protein expression in each condition, the capacity of the column and so on. This makes the method better suited for qualitative rather than quantitative analysis. In order to improve this experiment in the future, achieving detection of endogenous Rab11 is desired as well as the use of a quantitative method such as GST pull down, for example.

It was then anticipated that if mutant protrudin does indeed interact more readily with Rab11-GDP and the whole complex moves anterogradely, then more Rab11 as well as some of its cargo – integrins, will be detected in the axons of neurons overexpressing mutant protrudin. This hypothesis was first tested utilising immunocytochemistry in primary cortical neurons. There were minimal changes in the amount of Rab11 and no changes detected in integrin staining in the axons of cells expressing wild-type or mutant protrudin (*Fig. 5.5, 5.6).* These results could be due to the fact that Rab11-recycling endosomes carrying integrins and other growth receptors could be stationary or highly dynamic structures moving up and down

the axons at speeds ranging between 0.2-0.5 µm/s (Prekeris, Foletti and Scheller, 1999). Using immunocytochemistry which relies on a single time point might not be reliable. Furthermore, the antibodies against Rab11 and integrin alpha 5 produced inconsistent results and high background staining, which could make the detection of subtle changes very challenging. Therefore, live-cell imaging of Rab11 and integrin endosomes in the proximal and distal axon as well as in the growth cone was carried out using spinning-disc confocal microscopy.

Similar to previous studies, our live-cell imaging experiments confirmed that the majority of Rab11-positive vesicles traffic bidirectionally (Eva *et al.*, 2010) whereas the bulk of integrin-containing endosomes undergoes retrograde movement (Franssen *et al.*, 2015). In this study, overexpression of wild-type and constitutively phosphorylated mutant protrudin resulted in increased retrograde and bidirectional transport of Rab11 and in enhanced anterograde and retrograde transport of integrins in the distal axon (*Fig. 5.7, 5.8).* There were also more Rab11 and integrin-positive vesicles present in the distal axon and these vesicles colocalised more readily with protrudin (especially mutant protrudin) compared to control (*Fig. 5.7, 5.8, 5.9).* Even though no statistical differences were observed, constitutively phosphorylated protrudin seem to have increased co-localisation with integrin vesicles than wild-type protrudin and to have a larger effect on their active transport in the distal axon. In this study, only one integrin (alpha 9) was examined. After injury, one of the most highly upregulated components of the extracellular matrix is tenascin-C, which is a substrate for integrin alpha 9 (Fawcett and Asher, 1999). We chose to focus on integrin alpha 9 receptor as this subunit is absent in adult neurons which prevents them from regenerating or growing through tenascin-rich areas such as the glial scar after injury. Integrin alpha 9 upregulation in adult DRGs has been shown to improve axon growth and regeneration *in vivo* and *in vitro* on the otherwise inhibitory tenascin-C (Andrews *et al.*, 2009). In addition, different forms of the integrin receptor have previously been shown to co-localise with Rab11-positive vesicles (Eva *et al.*, 2010). Rab11 has also been shown to transport many other growth molecules along the axon such as the transferrin receptor, insulin growth-factor receptor (Romanelli *et al.*, 2007) and tyrosine-kinase B receptor (Hollis *et al.*, 2009b). Therefore, we cannot conclude that the regenerative effect we observe with protrudin overexpression is solely due to increased amount of integrin in the axons. It will be interesting to examine other forms of integrin

receptor as well as other growth-associated receptors and their trafficking in mature axons upon protrudin overexpression.

The fact that wild-type protrudin enhanced axon regeneration *in vitro* after laser axotomy and *in vivo* after optic nerve crush, suggest that additional cellular processes other than axon transport of growth-molecules could also be involved in mediating protrudin's action on axon growth. Therefore, a battery of mutants was created in order to test which interactions of protrudin are necessary for its growth-promoting effect. Each mutant was overexpressed in 10 DIV primary cortical neurons and laser axotomy was carried out between 13-17 DIV. It was hypothesised all mutants will act to suppress neurite outgrowth in culture and that some mutants will have a predominant effect on suppressing axon regeneration compared to others. Interestingly, overexpression of mutants which attenuate protrudin's interaction with spastin (microtubule-severing protein) or with Rab11, resulted in cortical neuron but not PC12 cell death (*Fig. 5.10A)*. This finding suggests that protrudin's interaction with these molecules is necessary for basic neuron function, and therefore neuronal survival. Due to the toxic effects of these two mutant forms, their effects on axon regeneration could not be tested.

The effects of all mutants on neurite outgrowth were tested in 2 DIV neurons which were fixed and imaged using Cellomics (as described in *Methods*). Only ΔSpastin and ΔRBD mutants showed to have significant effect in reducing neurite outgrowth from this assay *(Fig. 5.10B).* Some of the other mutants have also been previously shown to reduced neurite outgrowth in different cell types (*see Introduction*) – this effect, however was not replicated here. There were many caveats with this experiment. The main one was that the cortical neurons were imaged at 10x in order to obtained images for the whole wells of a 24-well plate. However, as the mCherry constructs express at quite low levels, in some cases the software could not distinguish between an axon and the background resulting in underestimating the length of some exceptionally long axons. Further experiments conducted at higher magnification or with a brighter marker are desired in order to validate these results. Interestingly, in younger cells overexpression of ΔSpastin and ΔRBD showed a larger proportion of surviving cells compared to when overexpressed in mature neurons (data not shown).

When testing the protrudin mutants in our paradigm of laser axotomy, all four mutants (ΔFYVE, ΔFFAT, ΔKIF5, ΔER) resulted in decreased proportion of regenerating axons down to control levels compared to positive control neurons expressing a phosphomimetic form of protrudin (*Fig. 5.10C).* The mutants had no effect on any of the other parameters measured during axotomy such as the time of regeneration, the distance regenerated, the size of the growth cone or the retraction distance (*Fig. 5.10D-H)*. Interestingly, neurons overexpressing syn-mCh-MUT2 previously showed decreased time of regeneration and increased total regeneration distance compared to control *(see Chapter 4).* This result was not replicated in the current study – the discrepancy seems to be due to the fact that in this study a different control plasmid was used (syn-mCh only) which seems to regenerate faster and further than our previous GFP dual control plasmid. These findings suggest that overexpression of dual GFP control plasmid could have some toxic effects on the cell and decrease regenerative potential (also discussed in *Chapter 4)*. The percentage of regenerating axons, however did not differ between the two controls suggesting that these cells still have decreased regenerative potential to begin with and that overexpression of constitutively active protrudin results in dramatic enhancement of regeneration. Furthermore, only one positive control experiment and two ΔER mutant experiments were carried out to date so further testing is performed at the moment in order to complete the data set.

The data presented here indicate that the association between protrudin and the ER is essential for its ability to enable axon regeneration. Importantly, the ΔER protrudin mutant has the most prominent effect of all mutants tested, with its expression completely failing to stimulate axon regeneration *(Fig. 5.10C).* This mutant has previously been shown to result in dissociation of protrudin from membranous structures and its accumulation in cytoplasm (Chang, Lee and Blackstone, 2013). An important part of the regenerative mechanism acting within the ER is indicated by the effect of deleting the FFAT domain. This domain is required for protrudin's interaction with the ER-resident protein VAP-A and its removal also sharply reduces protrudin's ability to stimulate growth. These combined data indicate that the ER and ER contact sites are key players in protrudin-mediated regeneration and suggest an important new role for the ER in CNS axon regeneration.

The involvement of the ER in axon regeneration has not been tested in mammalian CNS neurons before. One previous study has presented correlative evidence implicating not only the ER but also the protrudin-binding protein-spastin in axon but not dendrite regeneration due to their accumulation at the tips of regenerating axons after axonal injury in *Drosophila* (Rao *et al.*, 2016). In some preliminary experiments, we found that there is more ER (shown by REEP5 marker) in the growth-cones of neurons expressing mutant 2 protrudin but not wild-type or control plasmids (*Fig. 5.11)*. Speculatively, protrudin's interaction with the ER, endosomal organelles and kinesin could be important for trafficking ER into the axon towards the site of growth/injury because the ER itself is reported to hitchhike on motile organelles (Guo *et al.*, 2018). An increased ER presence here could, provide the necessary lipids and membrane components required for axon elongation. Smooth ER was previously found to form a continuous network throughout the whole axon – a network referred to as a "neuron within a neuron" (Berridge, 1998) which is held in place by ER-resident proteins such as reticulons and REEPs (Yalçın *et al.*, 2017). Mutations in these proteins have previously been shown to cause hereditary spastic paraplegia (HSP). In animal models, defective reticulons and REEP proteins lead to disruption of the continuous ER network where fewer but larger tubules as well as breaks in the ER are observed, specifically in the distal axon (O'Sullivan *et al.*, 2012; Yalçın *et al.*, 2017). As axonal ER normally plays important functions such as calcium buffering, lipid biosynthesis and membrane trafficking, these mutations resulted in an increased ER stress, changes in the microtubule cytoskeleton and mitochondria (O'Sullivan *et al.*, 2012). These changes support a model where disruption of ER structure and function within the distal axon could be the basis for the distal neurodegeneration observed in HSP. In this sense, enrichment of smooth ER at the growth cone as seen when constitutively phosphorylated protrudin is overexpressed can aid axonal functions of other organelles and components and therefore, improve axon regeneration. Currently, high-resolution structured illumination microscopy (SIM) is being performed in our laboratory in collaboration with Dr Evan Reid's laboratory in order to examine the precise structure and amount of ER in the distal axon and in the growth cone upon protrudin overexpression.

One possible mechanism through which ER, enriched at growing processes could support axon regeneration is by rapid plasma membrane (PM) expansion and lipid synthesis and transfer. The interface between the ER and PM has previously been shown to play a key

role in calcium buffering, lipid shuttling and cell signalling (Gallo, Vannier and Galli, 2016). During developmental growth, secretory vesicles fuse with the plasma membrane – a process mediated by SNARE proteins (Martinez-Arca *et al.*, 2000; Alberts *et al.*, 2003). Interestingly, blockade of vesicular trafficking have little effect on the transport of lipids, which suggests that other non-vesicular processes of lipid transfer might play a role in membrane expansion during growth (Voelker, 2009). For example, lipid transport proteins were shown to be able to directly influence the trafficking of lipids from the ER to the PM (Lalanne and Ponsin, 2000; Levine, 2004). In a recent study, a vesicle-independent lipid transfer from the ER to the PM was demonstrated where Sec22b – an ER-resident SNARE interacted directly with syntaxin 1 on the PM to create pockets through which a large amount of lipids could be transported without a requirement for membrane fusion (Petkovic *et al.*, 2014). This process allows for bulk transfer of lipids form the ER to the membrane and is essential for developmental axon growth. In our study, similar mechanisms could be working whereby protrudin drags more ER into the tip of injured processes and positions it in close apposition to the PM which in turn could facilitate more efficient transfer of already synthetised lipids from ER to PM and allow for rapid expansion of the plasma membrane at the growth cone – a requirement for successful axon regeneration.

Interestingly, the ΔKIF5 protrudin mutant was expected to reduce the amount of protrudin in the axon due to decreased anterograde movement. However, protrudin was still visible in the axon allowing for laser axotomy to be performed. This could be due to the large overexpression of the protein which allows it to freely diffuse in the axon or there is a possibility that protrudin interacts with other families of KIF proteins, not just kinesin 1. Nonetheless, the mutant still resulted in decreased regenerative potential suggesting that anterograde axonal transport of protrudin is indeed required for its effects on axon regeneration.

Lastly, a mutation in the FYVE domain of protrudin which is important for its binding to phosphoinositides is also required for axon regeneration. Recently, novel techniques requiring the introduction of unnatural amino acids to the protrudin protein were used to covalently trap transient interactors of the protein *in vivo.* These identified numerous protrudin interactors, including molecules involved in DNA repair, ubiquitination, translation

and vesicle-related proteins (Zhang *et al.*, 2017). One particularly interesting interactor of protrudin was fatty acid synthase (FASN) (Zhang *et al.*, 2017). Fatty acid synthase is an enzyme involved in the synthesis of lipids which is transported in Rab18-endosomes. Interestingly, adding a FASN inhibitor to HeLa cells overexpressing protrudin, results not only in decreased protrudin levels, lower amounts of free fatty acids but also to impaired process formation suggesting that FASN interaction with protrudin is a likely source of lipid material for membrane expansion during neurite outgrowth (Zhang *et al.*, 2017). A model was proposed where protrudin recruits FASN for lipid biosynthesis within the tubular ER which in turn facilitates membrane expansion and increases membrane fluidity during the process of neurite outgrowth. The role of lipid biosynthesis and transfer upon protrudin overexpression and the enhancement of regenerative potential was not studied in detail in this thesis but would be an interesting avenue to explore in future studies.

Another interesting observation was that overexpressed phosphorylated protrudin resulted in an increased number of Rab7-positive endosomes in the cell bodies of mature cortical neurons (*Fig. 5.11*). As the phosphorylation mutation of protrudin was introduced in the Rab11-binding domain, it is not unlikely, that this mutation could also influence the binding of other Rab proteins (such as Rab7). In a recent study, the role of the protrudin-Rab7 interaction was studied in the light of forming membrane contact sites between the ER and recycling endosomes (Raiborg *et al.*, 2015). ER-endosome contact sites are quite unique – these sites cover 3-5% of the endosomal surface and 99% of endosomes remain in contact with the ER while trafficking (Raiborg *et al.*, 2015). Protrudin was shown to colocalise with LAMP1-positive late endosomes and lysosomes in HeLa cells upon overexpression (Raiborg *et al.*, 2015). Interestingly, ER-resident protrudin was shown to be recruited to late endosomes by binding to Rab7-GTP (a late endosomal marker but also a protein involved in long-range retrograde signalling) and this interaction resulted in the formation of multiple ER-endosome contact sites (Raiborg *et al.*, 2015). This process was shown to be facilitated by protrudin loading kinesin 1 motors onto FYCO1 – a protein found on late endosomes which results in their displacement along microtubules towards the tip of growing processes. Accumulation of late endosomes at the growing tip then results in fusion with the plasma membrane and release of contents. This process seems to be imperative for the aiding of neurite outgrowth as when FYCO1 or Rab7 are depleted in HeLa cells, protrudin-mediated process formation is

compromised. The significance of these results lies in the fact that this could be a potential mechanism for providing lipids and proteins to the protrusion tip membrane that are favourable for protrusion extension. However, an important caveat is that our RNA sequencing data of cortical neurons developing *in vitro* (Koseki *et al.*, 2017) indicate that FYCO1 is expressed at very low levels throughout cortical neuron development and into adulthood. Further analysis of the levels of protein expression are therefore required in these neurons. Interestingly, in a recent study, protrudin-FYCO1-Kinesin-Rab7-dependent displacement of late endosomes to the plasma membrane has been shown to result in activation of the mTOR pathway and suppression of autophagy (Hong *et al.*, 2017), both of which have previously been identified in the process of axon regeneration (Park *et al.*, 2008; Ban *et al.*, 2013). Here, we showed that protrudin has an effect on the amount and distribution of Rab7-positive late endosomes and therefore could influence the autophagosome-lysosomal pathways in the cell. Several other organelles (e.g. mitochondria, proteasomes and autophagosomes) and their distribution have been associated with reduced regenerative ability in adult CNS axons (*see Introduction*), therefore studying the transport of those along axons overexpressing protrudin is an interesting suggestion for future experiments.

Lastly, one further possible mechanism of protrudin enhancing axon regeneration could be through its interaction with the microtubule-severing protein - spastin. Microtubule (MT) dynamics play a critical role an important player in successful growth cone formation and axon regeneration (Blanquie and Bradke, 2018). For example, disorganised MTs in retraction bulbs were shown to be indicative of regenerative failure (Erturk *et al.*, 2007) whereas the addition of low doses of MT-stabilising drug – taxol, resulted in organised MT bundles, enhanced axon growth and improved outcome after injury (Erturk *et al.*, 2007; Witte, Neukirchen and Bradke, 2008). Recent studies showed that spastin, similarly to protrudin, localises to ER-endosome contact sites and is involved in receptor trafficking and ER shaping (Allison *et al.*, 2013, 2017). Our collaborators in Dr Evan Reid's laboratory showed that spastin regulated protrudin-dependent neurite outgrowth. When an HSP-associated mutant form of spastin which lacks its MT-severing properties was introduced, enhanced neurite outgrowth was observed in cultured neurons (Connell *et al.,* unpublished data). Spastin might act as an inhibitor of protrudin-induced neurite outgrowth either by introducing physical breakage of the MT tracks which prevents long-range protrudin transport to the tip of growing neurites or

by preferential loading of dyneins at new MT ends resulting in enhanced minus-end directed transport. These results are further supported by a recent study where knockdown of fidgetin – another spastin-like MT-severing protein resulted in enhanced regeneration by increasing the mass of the liable microtubules in the axon – recapitulating the situation during development (Matamoros *et al.*, 2019). In our study, the interaction between spastin and protrudin was difficult to study due to the reduced viability of mature cortical neurons expressing ΔSpastin protrudin. Further experiments involving spastin knockdown in our system could provide valuable insight into this interaction's involvement in axon regeneration. Furthermore, studying the MT dynamics in protrudin-expressing neurons is another future avenue. In the current experiments, live-cell imaging of EB3 – a MT-plus end binding protein was attempted (data not shown); however, no reliable results were obtained.

In summary, we propose a model where protrudin acts from within the ER as a scaffolding molecule bringing together multiple molecules, organelles and cellular components (*Fig. 5.12)* at the tip of growing axons/site of injury and that its reduced levels in mature axons might contribute to their regenerative failure.

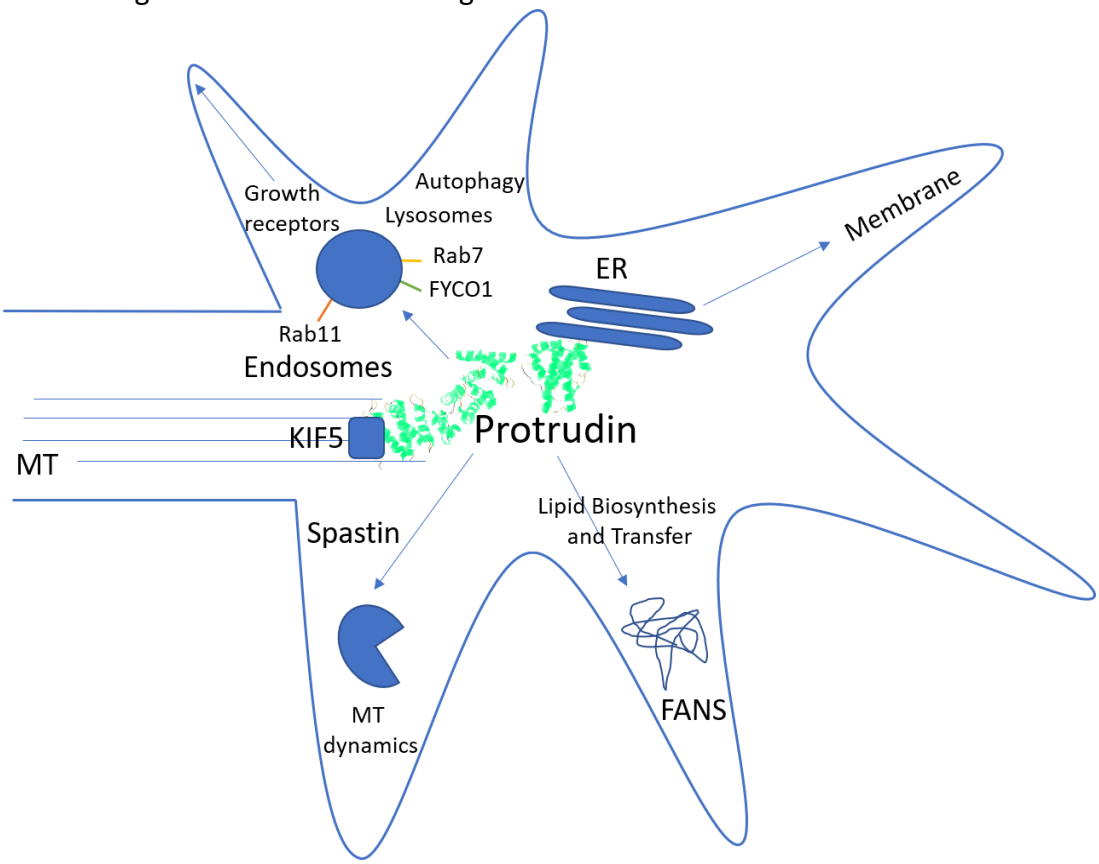

Figure 5.12 Schematic of protrudin's action at the growth cone. A model where protrudin is transported along MTs, acts from within the ER and interacts with spastin and FASN in order to deliver membrane and the correct components and receptors for axon growth.

CHAPTER VI: TRANSCRIPTION FACTORS AS A TOOL TO REVERSE MATURATION AND REGENERATIVE ABILITY OF ADULT CORTICAL NEURONS

1. Introduction

1.1 Developmental Transcriptional Programs

During development neurons extend long processes to reach their final target cells. More than 100 billion axons extend their way through the brain using guidance cues to create a complex network of 100 trillion synapses (O'Donnell, Chance and Bashaw, 2009). This process is tightly regulated by turning on specific transcription factor programmes as a result of signals from the growth cone to the nucleus which in turn activate genes important for growth (da Silva and Wang, 2011). In addition to these internal changes, the extracellular environment around the growing axons also changes in order to guide them to the correct targets and to prevent the formation of faulty synapses (Sheppard, Hamilton and Pearlman, 1991).

Once CNS neurons have formed synapses, their genetic expression milieu dramatically changes driving the post-mitotic neuron to switch from a growth-competent to a growth-incompetent state. Some of the changes that occur are decreased expression in many growth components such as cytoskeletal elements (e.g. actin and growth-associated tubulin elements), in transcription factors driving growth associated-gene expression and in signalling molecules (Smith and Skene, 1997; Hoffman, 2010; Tedeschi and Bradke, 2017). In addition,

redistribution of some growth-associated receptors such as TrkB and integrins from the axon to the somatodendritic compartment, also occurs (Hollis *et al.*, 2009b; Franssen *et al.*, 2015; Andrews *et al.*, 2016). Furthermore, some synaptic proteins which start being expressed at the time, have the ability to instruct the expression of growth inhibiting molecules (Tedeschi *et al.*, 2016). This decline in neuronal growth capacity likely occur as an evolutionary control mechanism to prevent aberrant growth and excessive synapse formation and acts as a critical period during which the expression of growth-promoting genes is restricted. These changes have been postulated to be responsible for the decline in the regenerative ability of adult CNS neurons (Smith and Skene, 1997). It is well characterised that mature CNS axon regenerate poorly compared to immature CNS axons (Bregman *et al.*, 1989; Nicholls and Saunders, 1996).

The decline in regenerative ability of CNS neurons with maturation as well as the intrinsic and extrinsic processes accompanying this change are reviewed in detail in *Introduction.*

1.2 Regeneration-associated Transcriptional Programs

Interestingly, not all neurons lose their regenerative ability with maturation. Some regenerative types of neurons such as PNS neurons continue to express growth-related proteins even during maturation suggesting that there are gene expression and transcriptional changes affecting the regenerative state of a neuron (Smith and Skene, 1997; Plunet, Kwon and Tetzlaff, 2002). For example, after an injury to the PNS, a robust regenerative response is generated by increasing the growth ability but also by decreasing the inhibitory effects of the extracellular environment of the PNS axons. This response is referred to as regeneration-associated growth (RAG) response (Abe and Cavalli, 2008; van Kesteren *et al.*, 2011) and is mediated through transcriptional changes affecting gene expression and axon transport (Smith and Skene, 1997; Mason *et al.*, 2002; Starkey *et al.*, 2009; Geeven *et al.*, 2011; Petrova and Eva, 2018).

In addition, some CNS axons also regenerate when provided with a growth-permissive environment of a peripheral graft (Aguayo, David and Bray, 1981). These regeneration-capable CNS axons have also been shown to upregulate the RAG programme (Mason *et al.*, 2002; Murray *et al.*, 2011). In fact, the rapid induction of a RAG response in the PNS has been

shown to be necessary and sufficient for successful regeneration because when RNA polymerase inhibitors are applied, the regenerative response is blocked (Smith and Skene, 1997; Cai *et al.*, 2002).

What does a RAG transcriptional program include? The RAG transcriptional program involves the activation or suppression of numerous transcription factors and transcriptional elements which in turn either upregulate or downregulate specific genes involved in axon growth (Ma and Willis, 2015). Some of the genes with altered expression during the induction of the RAG program include cytoskeletal and growth cone elements (e.g. GAP43), transcription factors (e.g. ATF3), cell adhesion molecules (e.g. integrins) and neuropeptides (e.g. NPY and CGRP). At first glance, many of these regenerative genes which are upregulated during PNS or CNS regeneration through peripheral nerve grafts resemble genes involved in early axon growth and development but whose expression dramatically declines with age (Doster *et al.*, 1991; Tetzlaff *et al.*, 1994; Mason *et al.*, 2002; Hoffman, 2010) In fact, it has been proposed that successful regeneration require the re-expression of genetic profiles normally important in developmental growth (Bendotti, Servadio and Samanin, 1991; Mearow *et al.*, 1994)

In the non-regenerating CNS, however, many of these developmental and RAG programs fail to be elicited which could be one of the main reasons for the regenerative failure of these neurons (Tetzlaff *et al.*, 1994).

Interestingly, many of the studies mentioned above show that many aspects of neuroregeneration recapitulate development and that both processes share similar molecular players (reviewed in Harel and Strittmatter, 2006 and Hilton and Bradke, 2017). In this sense, understanding the transition from early to late neuronal development might be essential to identifying factors contributing to the regenerative failure of mature neurons. Recapitulation of these transcriptional programs in mature CNS axons could offer a reliable new method to boost CNS neurons' otherwise poor regenerative potential by stimulating developmental-like axon growth even after the process of maturation has ceased.

1.3 Boosting CNS Regeneration by Manipulating Regeneration-associated Genes

Many studies so far focused on studying effector genes which seem to change their expression during development when CNS neurons transit from regenerative to non-regenerative state. For example, manipulating signalling pathways downregulated with development such as the ERK-MAPK (Hollis *et al.*, 2009b) and mTOR (Park *et al.*, 2008; Liu *et al.*, 2010) pathway have been shown to improve CNS regeneration in the optic nerve and to some extent in the corticospinal tract. Another approach was to restore axonal integrins which are preferentially re-distributed to the somatodenritic compartment with maturation – an approach which also yielded relative success in promoting axon regeneration of the central branch of DRG neurons (Franssen *et al.*, 2015; Andrews *et al.*, 2016; Cheah *et al.*, 2016).

Recently, studying the regenerative response after injury in regenerating neurons allowed for the identification of numerous regeneration-associated genes (RAGs) such as ATF3, Jun and GAP43. These genes have been shown to be upregulated after injury in the PNS but fail to be expressed after a CNS lesion (Jenkins and Hunt, 1991; Tetzlaff *et al.*, 1991; Schwaiger *et al.*, 2000; Tsujino *et al.*, 2000). As a result, several studies examined whether overexpression of these molecules in the CNS could increase the intrinsic capacity of mature CNS axons to grow. For example, overexpression of cytoskeletal protein GAP-43 could, in fact, boost spontaneous axon sprouting in DRG axons or CNS axons (Aigner *et al.*, 1995) but does not promote long-range axon regeneration after spinal cord injury (Neumann and Woolf, 1999; Bomze *et al.*, 2001). Furthermore, overexpression of GAP-43 in cerebellar Purkinje cells increased the level of sprouting after axotomy but did not result in enhanced axon growth in a growth-permitting embryonic grafts (Buffo *et al.*, 1997).

Another example of a RAG upregulation is via overexpression of cyclic adenosine monophosphate (cAMP) which results in multiple molecular cascades resulting in altered gene expression and modest increase in axon regeneration in vivo after CNS injury (Neumann *et al.*, 2002; Qiu *et al.*, 2002). Developmentally “younger” neurons have been shown to have higher levels of cAMP and therefore regenerate better (Cai *et al.*, 2001). The overexpression of cAMP itself, however, is not sufficient to produce sustained long-range regeneration as conditioning lesion in the PNS still initiates more robust regenerative response (Blesch *et al.*, 2012).

These studies suggested that expressing individual components of regenerative response which are important for growth, could improve the regenerative response to some extent but it is not sufficient to promote long-range axon regeneration in the CNS. This observation makes sense when the scope of the regenerative response is considered – thousands of genes were shown to be differentially expressed after injury in numerous studies (summarised in Ma and Willis, 2015). It is only predictable, that manipulating a single gene, or a combination of effector genes will not be sufficient to initiate and sustain long-range regeneration.

Recently more efforts have been concentrated on identifying networks of transcription factors which regulate large sets of pro-regenerative genes. For example, deletion of the target effector RAG - integrin a7 (normally elevated in PNS but not CNS injury), results in a small decrease or delay in reinnervation and functional recovery after peripheral nerve injury (Werner *et al.*, 2000). However, if a transcription factor upstream of this RAG effector such as c-Jun is manipulated, the effects are much more profound. Deletion of c-Jun caused a 4-fold decrease in reinnervation after facial motoneuron axotomy (Raivich *et al.*, 2004). This example highlights the need to identify transcription factors involved in developmental growth and in the regenerative response in order to design manipulations targeting a large set of genes important for axon growth rather than individual genes and pathways.

1.4 Boosting CNS regeneration with Transcription Factors

1.4.1 Identifying Networks of Transcription Factors

As described above, the regenerative abilities of PNS and CNS neurons as well immature and mature neurons are very different with PNS and young neurons being able to sustain a robust regenerative response whereas mature CNS neurons fail to self-repair and re-grow after injury (Ramon y Cajal, 1928). Numerous studies have utilised these differences in order to create differential genome-wide expression and transcriptional profiles of regenerating vs. non-regenerating and immature vs. mature neurons in order to identify molecules and pathways which are active during developmental growth and regeneration.

Some studies, for example, examined differentially active transcription factors (TFs) in mature PNS (dorsal root ganglion) vs CNS (cerebellar granule) neurons (Smith *et al.*, 2011). They found 32 TFs enriched in the DRG in comparison to the CNS. Overexpression of one of the identified transcription factors – STAT3, in CNS cerebellar granule cells resulted in increased neurite outgrowth (Smith *et al.*, 2011). The most comprehensive study up to date examines the genome-wide transcriptional changes in regenerating PNS neurons after injury by exploring multiple time points after injury, comparing five injury models from different laboratories and cross-referencing to existing literature (Chandran *et al.*, 2016). They identified 16 RAG transcription factors which provide cross-talk between multiple pathways involved in axon growth and are differentially expressed in regenerating peripheral neurons after injury. Of these RAG TFs, 10 promoted neurite outgrowth in an *in vitro* DRG culture assay. Remarkably, this study identified networks of gene expression changes which could be targeted pharmacologically with an FDA-approved drug – ambroxol. Treatment with ambroxol increased the expression of several components of the PNS transcriptional network, promotes neurite outgrowth *in vitro* and had a modest effect on CNS regeneration *in vivo* after optic nerve crush (Chandran *et al.*, 2016). These results confirm that identifying key transcription factors in development and regeneration could bring new light to the regenerative processes and with that, new treatable drug targets to boost regeneration.

1.4.2 Manipulating Single Transcription Factors for Regeneration

Large sequencing and microarray studies like the ones described above have identified numerous transcription factors which are not only developmentally regulated but also play a role in axon growth after injury. As a result, a myriad of studies where genetic manipulation of single transcription factors was used as a strategy to boost CNS axon growth and regeneration, followed.

Several members of the KLF family of transcription factors are developmentally regulated. For example, growth-incompetent mature retinal ganglion cells (RGCs) express lower levels of growth-promoting factors (KLF6 and KLF7) and higher levels of growth-restricting factors (KLF4 and KLF9) (Moore *et al.*, 2009). Indeed, transgenic knockdown of KLF4 resulted in improved axon growth *in vitro* and *in vivo* after optic nerve crush without affecting

survival suggesting that this improvement is due to increased regenerative capacity (Moore *et al.*, 2009). Interestingly, KLF7 is upregulated in the PNS but not in the CNS after injury (Zou *et al.*, 2009). When overexpressed in postnatal cortical neurons or cortical slices, KLF7 promoted axon growth (Blackmore *et al.*, 2010, 2012a) as well as it significantly enhanced axon regeneration in the adult CST, albeit with no functional improvement (Blackmore *et al.*, 2012a).

Another transcription factor commonly used as a single TF manipulation to promote axon growth after injury is ATF3. ATF3 is upregulated in regenerating PNS neurons and also in regenerating thalamic neurons in the presence of peripheral nerve grafts but not in the CNS (Tsujino *et al.*, 2000; Campbell *et al.*, 2005). ATF3 promotes neurite outgrowth when introduced into various different cell types (Nakagomi *et al.*, 2003; Pearson *et al.*, 2003; Seijffers, Allchorne and Woolf, 2006). Furthermore, ATF3-mutant mice show reduced ability for axon regeneration after peripheral nerve injury and suppressed neurite outgrowth in cultured DRG neurons again supporting the role of ATF3 in axon growth and elongation after injury (Gey *et al.*, 2016). Interestingly, overexpression of ATF3 improved the regeneration capacity of the DRG peripheral branch axons similar to a conditioning lesion (Seijffers, Mills and Woolf, 2007). This treatment, however, could not overcome the myelin inhibition when DRG neurons are cultures on myelin substrate or after dorsal column injury. ATF3 overexpression elevated some but not all regeneration-associated genes needed for successful regeneration in the PNS - an increase in c-Jun, Hsp27, and SPRR1A but not of GAP-43, CAP-23, integrin a7, or STAT3 was observed (Seijffers, Mills and Woolf, 2007). Despite the promising results, however ATF3 overexpression could not recapitulated the effects of a conditioning lesion where injury to the peripheral axon enables its central branch to regenerate faster beyond the lesion site (Richardson and Issa, no date; Neumann and Woolf, 1999). These findings do not mean, however, that ATF3 is not involved in CNS growth and regeneration. On the contrary, they point out that ATF3 might act in a coordinated network with other transcription factors as it activates a specific branch of the regenerative response.

Sox11 and STAT3 are two other transcription factors which are downregulated with development but upregulated after PNS (not after CNS) injury. Overexpression of Sox11 in adult RGCs changed their genetic profile to more “immature-like” one and improved axon regeneration after optic nerve crush (Norsworthy *et al.*, 2017). Surprisingly, Sox11 was toxic

to alpha-RGCs (the most common cell type to regenerate after optic nerve crush manipulations) but promoted outgrowth from other RGC cell types, highlighting the importance of targeting the right manipulations to the right cell types and brain areas. Moreover, overexpression of Sox11 in the CST improved sprouting and axon growth but resulted in worsening of the functional outcome (Wang *et al.*, 2015) suggesting that promoting directed, functionally relevant axon growth should be the major goal in the field of axon regeneration. Lastly, a constitutively active form of STAT3 (STAT3-CA) resulted in axon regeneration of RGCs 2 weeks post optic nerve crush (Mehta *et al.*, 2016). In addition, STAT3A that was overexpressed in DRGs, allowed for sprouting and axon outgrowth of the central branch of the DRG but did not aid elongation (Bareyre *et al.*, 2011). This study highlighted the importance of making sure that transcription factors which are overexpressed become active and that different TFs might play different roles at different stages in the regenerative process.

Not only transcriptional activators but transcriptional repressors suppressing the expression of RAGs in maturation could play an important role in the regenerative decline with age. For example, repressor element-1 silencing transcription factor (REST) is widely expressed during embryogenesis but its downregulation in later stages of neuronal differentiation is essential for the acquisition of the neuronal phenotype (Noh *et al.*, 2012). In mature neurons, REST is found at basal levels and acts to repress the expression of RAGs. In a recent paper, Oh and colleagues (2018) show that REST is epigenetically repressed upon injury in order to allow for axon regeneration (Oh *et al.*, 2018). In a follow-up study, REST was deleted in DRGs and CST which increased activation of pro-regenerative intracellular pathways and promoted growth after T10 spinal cord injury with more axons growing towards the injury site but not past it (Cheng et al., unpublished data, personal communication).

All the studies described in this section target individual transcription factors implicated in neuronal developmental axon growth or axon regeneration, or both. They mostly show enhanced neurite outgrowth in vitro, attenuated PNS response after injury and modest effects on axon regeneration in the CNS. None of them, however, result in complete initiation and maintenance of the RAG program and axon regeneration. The functional improvement in many of them is negligent if not non-existent and they all point towards the

need for using combinational therapies of multiple transcription factors or identifying pharmacological agents which alter effector genes broadly.

1.4.3 Manipulating Multiple Transcription Factors for Regeneration

Only recently, several laboratories have attempted combinational transcription factors approach to improve axon growth and regeneration. In the study described above, Chandran and others (2016) identified several TFs involved in the PNS regenerative response after injury. They show that a combination between ATF3 and c-Jun acts in synergy to improve neurite outgrowth more than each transcription factor individually. In a different study, however, where four transcription factors (ATF3, c-Jun, Smad1 and STAT3) were virally delivered to DRGs, the combinatorial effect on axon regeneration after injury was comparable to the effect of ATF3 overexpression alone (Fagoe *et al.*, 2015). One reason why there is a discrepancy in the two studies described above could be that each TF is expressed to a different extent such that in one of the studies optimal levels are achieved to affect transcription but not in the other. These studies underline the need to achieve more subtle control of expression levels and stress the importance of temporal expression of each transcription factor. Timing is another factor to be considered when using multiple transcription factors. For example, Sox3 and Sox11 have both been shown to be important for axon growth and regeneration. However, in order for them to exhibit these effects Sox3 expression has to precede that of Sox11 transiently (Bergsland *et al.*, 2011). Therefore, prolonged overexpression which is typical of many treatments will be insufficient in this case (Venkatesh and Blackmore, 2017).

There are more than 1000 TF in the genome with several already identified by multiple studies to be involved in axon regeneration in vivo, giving rise to countless possibilities of combinatorial treatments (Venkatesh and Blackmore, 2017). When designing improved strategies for multiple transcription factors expression, it is important to consider how their activity is regulated and whether their expression levels depend on one another. For example, STAT3 drives SOCS3 expression which in turn acts as a negative regulator to suppress STAT3

activity. In that case, SOC3 deletion is the most effective way to enhance STAT3 activity as overexpression of STAT3 will only exacerbate the negative feedback loop (Venkatesh and Blackmore, 2017). Lastly, the effects of TFs on chromatin remodelling should also be considered. Some TFs, for example, have the ability to access closed chromatin and to open it up to allow other TFs to bind. Furthermore, developmental changes in the chromatin structure have recently been shown to contribute to restricted axon growth (Venkatesh *et al.*, 2018). It is, therefore important that mechanisms for opening chromatin are employed, as overexpression of TFs that cannot access the DNA will likely not yield positive results.

1.5 Epigenetic modifications in development and regeneration

In order to design effective strategies to boost CNS axon regeneration via the application of combinations of transcription factors, additional epigenetic modifications should also be considered in order to allow the TFs to access the DNA and induce a large repertoire of developmentally silenced regeneration-associated genes.

One epigenetic mechanism is DNA methylation. DNA methylation patterns and epigenetic changes in general are established during early development in order to suppress the expression of genes involved in axon outgrowth once neurons have matured (Ma *et al.*, 2010; Venkatesh *et al.*, 2016). Interestingly the DNA methylation pattern changes upon PNS but not CNS injury to allow for rapid outgrowth and functional recovery (Lindner *et al.*, 2014). In a recent study, Weng *et al.* (2017) showed that demethylation of RAGs by Tet3 was elevated after sciatic nerve injury and was required for the re-expression of regeneration-associated genes to drive the PNS regenerative response. This upregulation of demethylation have also previously been described in another study (Loh *et al.*, 2017) where differential demethylation was observed after peripheral and central injury which might confer the differential regenerative response in those two systems. These studies challenged the standing dogma that the methylation pattern of the genome is fixed after development is complete which allowed for the identification of new targets to improve regeneration by targeting DNA methylation.

Another mechanism of epigenetic regulation is histone acetylation. Histones are acetylated by enzymes called histone acetyltransferases (HATs). PCAF, for example, is

HAT which associates with the promoters of known pro-regenerative genes and drives their expression after peripheral injury (Puttagunta *et al.*, 2014). The importance of acetylation was first highlighted in a study where PCAF upregulation is shown to improve axonal outgrowth not only through the acetylation of RAGs but also by acetylation of regeneration-associated transcription factors such as p53. P53 is in turn more active and can affect a wider array of effector molecules (Gaub *et al.*, 2010). These findings were further supported by observations that PCAF overexpression in the optic nerve and spinal cord enhances the regenerative response of these CNS components (Tedeschi *et al.*, 2009; Puttagunta *et al.*, 2014). On the other hand, inhibition of the deacetylase – HDAC1 also results in increased acetylation of regeneration-associated SMAD1, which in turn drives the regeneration response and allows for sensory axon regeneration (Finelli *et al.*, 2013; Finelli, Wong and Zou, 2013) although without some classical RAG upregulation.

All of these studies highlight the importance of epigenetic changes but much like the use of single transcription factors underline the need to combining multiple treatments as single manipulations do increase growth and regeneration but fail to induce the full regenerative response which leads to functional recovery after injury.

1.6 Rejuvenation of mature neurons – approach

One of the most remarkable studies of the last few centuries showed that cell fate can actually be altered by the addition of a combination of transcription factors (Oct3/4, Sox2, Klf4, and c-Myc) to fibroblasts resulting in their de-differentiation into pluripotent stem cells (Takahashi and Yamanaka, 2006), confirming the possibility of altering cell fate and function by delivering a cocktail of TFs. For regeneration, this has implications that multiple TFs need to be delivered to convert a neuron from a mature, growth-incapable cell to more immature like growth state. Interestingly, fully differentiated post-mitotic cortical neurons have recently been reprogrammed from one neuronal subtype to another by the forced expression of transcription factor Fezf2 *in vivo* (Rouaux and Arlotta, 2013). These studies reveal the enormous potential that delivery of the correct combination of activated transcription factors can regulate and influence not only the molecular milieu but also the fate of post-mitotic CNS neurons not only in development but also after injury resulting in functional recovery.

2. Aims and Hypothesis

Most studies described above either consider developmental or regeneration-associated changes of transcription factors in order to design genetic manipulations to boost CNS regenerative ability. Our study here is the first of its kind where bioinformatic analysis was performed on several sets of data from injury models as well as from developmental changes in mature cortical neurons *in vitro*. The data was compared across 12 species and a comprehensive list of TFs involved in neuronal development and regeneration was established. What differentiates our study from others in the field is the establishment of an *in vitro* injury system where multiple different combinations of transcription factors could be tested for reversing maturational state and therefore improving growth and regeneration before animal models are utilised. Furthermore, as a comprehensive RNA sequencing analysis was performed in our system, maturity markers at different developmental stages could be identified and used as a quick screening mechanism to identify transcription factors combinations that alter developmental state and improve regeneration.

2.1 Hypothesis

Our hypothesis is that the application of a combination of transcription factors involved in axon growth during development and after regeneration to mature primary cortical neurons will result in altering their developmental stage to an earlier time point which will in turn aid regeneration after laser axotomy.

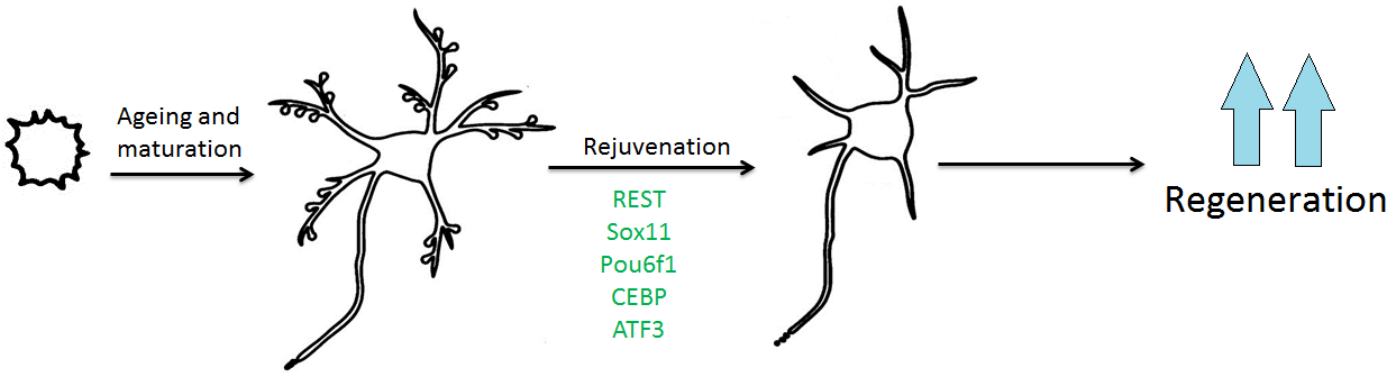

2.2 Aims

Aim 1: To identify maturity markers at different stages of neuronal maturation in primary cortical cultures

Aim 2: To test the ability of several candidate transcription factors to bring cortical neurons to an earlier developmental stage with the aid of the maturity markers

Aim 3: To test whether a change in developmental status can serve to improve axon regeneration after laser axotomy in primary cortical neurons

3. Methods

3.1 Plasmid Constructs and Antibodies

3.1.1 Plasmid Constructs

Transcription factor constructs were kindly provided by Prof. Joost Verhaagen, The Netherlands Institute for Neuroscience (ATF3, CEBP, Sox11, Egr constructs), Dr Lawrence Moon, King's College London (pCMV-SPORT6-sox4 construct) and Prof. Vance Lemmon and Prof. John Bixby, University of Miami (STAT3ACA constructs). REST transcription factor construct (pHR'-NRSF-CITE-GFP construct) was obtained from AddGene (plasmid #21310). Pou6f1 construct was obtained (Myc-DDK-tagged) was purchased from OriGene.

3.1.2 Primary Antibodies

Rabbit polyclonal anti-tropomyosin-1 (Abcam, ab55915, 1:100); chicken polyclonal anti-68kDa-neurofilament (Abcam; ab134460, 1:1000); rabbit polyclonal anti-MAP1A (Abcam, ab89648, 5 mg/µL), rabbit polyclonal anti-doublecortin (Abcam, ab18723, 5 mg/µL); rabbit monoclonal anti-TUBA4A (Abcam, ab177479, 1:100); rabbit polyclonal anti-tropomyosin 4 (EMD Millipore, AB5449, 1:500); mouse monoclonal anti-CGRP (Abcam, ab81887, 1:100); rabbit polyclonal anti-OMgP (Abcam, ab101567, 1:1000); rabbit polyclonal anti-Vangl2 (Merck, ABN373, 1:500); rabbit polyclonal anti-ATF3 (SantaCruz, Sc-188, 1:500).

3.2 Candidate Maturity Markers and Transcription Factor Selection

A collaborative study between the following laboratories - Lemmon/Bixby, Bradke, Verhaagen, Moon and Fawcett, was set up in order to create a list of candidate transcription factors whose expression might be important for neuronal growth during development and in regeneration (*Table 6.1*).Initial molecular targets were obtained after RNA sequencing studies and molecular profiling in PNS neurons after successful regeneration carried out by Prof. Joost Verhaagen and Valleria Cavalli. Further RNA sequencing experiments on primary cortical cultures during different developmental stages (at 1, 4, 8, 16, 24 DIV) were carried out by Hiroaki Koseki to identify molecules which might be relevant to axon growth in development. The molecules which showed the greatest change in mRNA transcript expression in development and in regeneration were identified. Promoter analysis of the

selected genes was then applied by Matt Mason to map common transcription factors. The list of candidate transcription factors was refined by comparing the promoter for the same gene in 12 different species in order to ensure that the candidate transcription factors have the potential to regulate growth and regeneration genes across multiple species via common pathways. The list was finally narrowed down by literature studies. Several candidate markers of maturity *in vitro* were also identified using the same strategy (*Table 6.1*). An additional criterion of selecting maturity markers was that a reliable antibody exists in the marker and that the maturity marker of interest has a well-described expression pattern in the cell.

Candidate Maturity Markers	DIV1	DIV4	DIV8	DIV16	DIV24	Fold Difference
Doublecortin (DCX)	265.5	282.9	211.7	76.7	13.3	↓ 20x
Tropomyosin 4 (TPM4)	308.5	196.4	119.9	51.1	75.7	↓ 4x
Planar Cell Polarity Protein 2 (Vangl2)	34.6	19.5	12.5	6.0	2.2	↓ 17x
Microtubule-associated protein 1A (MAP1A)	11.3	21.5	49.0	80.0	78.3	↑ 7x
Tubulin 4A (TUBA4A)	1.2	7.2	22.9	140.7	210.3	↑ 175x
68kDa Neurofilament (NEFL)	4.4	24.6	81.9	258.1	522.9	↑ 130x
Tropomyosin 1 (TPM1)	38.6	72	112.4	167.3	232.4	↑ 6x
Calcitonin gene-related peptide (CGRP)	0.2	1.1	5.6	116.5	326.4	↑ 1630x
Oligodendrocyte Myelin Glycoprotein (OMgP)	2.5	4.4	20.5	47.0	82.9	↑ 32x
Candidate Transcription Factors	**DIV1**	**DIV4**	**DIV8**	**DIV16**	**DIV24**	**Fold Difference**
REST	13.7	6.5	2.4	1.9	1.4	↓10x
Sox11	214.5	126.9	35.7	13.5	7.9	↓27x
CEBP	24.8	16.2	8.7	9.7	8.0	↓3x
Pou6f1	23.6	16.7	12.2	9.4	10.9	↓2x
ATF3	5.0	0.6	0.3	0.6	1.2	↓4x

Figure 6.1 Table with the final list of candidate maturity markers and transcription factors which was obtained after the results of several RNA sequencing studies were analysed using bioinformatics. Their mRNA expression levels and fold difference in primary cortical cultures at 1, 4, 8, 16, 24 DIV in primary cortical cultures are also shown. The values in each box represent average values from at least 4 independent experiments.

3.3 Cell Culture and Transfections

Cortical neurons were dissected from E18 Sprague Dawley rat embryos and plated on acid washed coverslips in a 24-well plate at density of $8x10^4$cells/coverslip. All surfaces were coated with poly-D-lysine. The cells were grown in serum-free MACS Neurobasal Media supplemented with 2% GS21 and 1% GlutaMAX supplements at 37°C in 7% CO_2 incubator. Cortical neurons (1 DIV) on coverslips were transfected using lipofectamine 2000 reagent (ThermoFisher Scientific) as follows: 3.6µg of DNA plasmid were mixed with 400µL NB media and 6.6µL lipofectamine 2000. The reaction was kept for 30 minutes at room temperature and then added to a 1 mL of freshly warmed-up NB media supplemented with GlutaMAX for 1 hour at 37°C. The transfection media was then removed, and the original media was transferred back to the imaging dishes. Plasmid reporter gene expression was observed 48 hours post-transfection.

3.4 Immunocytochemistry

Cortical neurons were fixed in 3% PFA for 15 minutes and then thoroughly washed and kept in PBS at 4°C. Cells were permeabilised in 3% BSA in PBS and 0.1% Triton for 5 minutes and then blocking solution was added (3% BSA in PBS) for 1 hour at room temperature. Primary antibodies (listed in 2.1.2) were added at the correct concentration and kept overnight at 4°C. On the next day antibodies were washed 3 times in PBS for 5 minutes. Secondary antibodies (listed in Methods, 1.2.2) were applied at the correct concentration for 1 hour at room temperature in a dark chamber. The cells were then washed twice in 1xPBS and twice in 1xTNS (5-minute washes) and the coverslips were removed from the 24-well plate and mounted using Diamond anti-fade mounting agent with DAPI (Molecular Probes) or FluorSave mounting reagent (Calbiochem) onto glass slides.

3.5 Microscopy

Images of immunostained cells were taken with a confocal microscope (Leica DMI 4000 B) using LAS-AF software (Leica Systems). For maturity marker identification, staining intensity for each developmental stage for a particular marker were initially tested. The settings to visualise the brightest maturational state were used as standard settings to examine all maturational states for the particular maturity marker for a particular staining

experiment. A z-stack of images was obtained through each cell by taking an image at every 0.5µm thickness and an average intensity z-projection was created. On average 15-20 cells were examined per condition per staining experiment, so in cases were n=3 45-60 cells were examined per condition. Immunofluorescent intensity was measured in the LAS-AF software by outlining the cell body using the polygon tool (*Fig. 6.2A)* The exact same shape which measured a single cell body was placed immediately next to the cell body where no obvious staining or other cells were present in order to measure background (*Fig. 6.2B)*. The final measurements were obtained by subtracting the background for each cell from its measurement in the cell body.

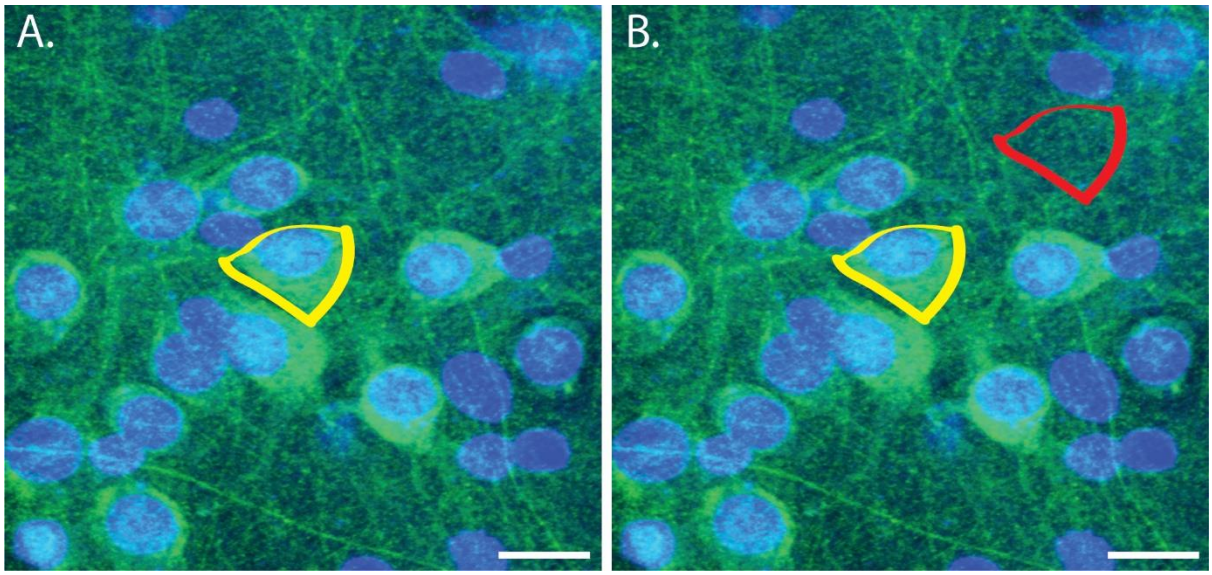

Figure 6.2 Figure to represent measuring strategy for maturity markers protein expression. A. Using the polygon tool an area around a single cell was outlined (yellow) and the intensity was measured. B. Using the exact same region of interest, the intensity of an area which is in proximity of the measured cell but does not contain any recognisable cell bodies or process, was also measured as a background (red). Scale bars are 10 µm.

3.6 Statistics

Statistical analysis was performed using GraphPad Prism 7.0 (GraphPad Software, La Jolla, CA). Each data set was individually tested for normal distribution using the D'Agostino-Pearson normality test. When data was normally distributed one-way ANOVA with multiple comparisons was used to test statistical significance between the experimental groups with Tukey's post hoc test. Data from different staining experiments for a particular experimental group were tested for statistical difference using Kruskal-Wallis test in order to determine

whether values could be combined together. When the sets were not significantly different from each other, the means from each procedure were used when making comparisons between the groups. In cases where the sets were significantly different from each other, the data was normalised to 2-3 DIV intensity and the means of the normalised values were compared. All statistics were carried out at 95% confidence intervals, therefore a significant threshold of $p<0.05$ was used in all analyses.

4. Results

4.1 Doublecortin, 68 kDa Neurofilament, Calcitonin Gene-related Peptide and Tubulin 4a Were Identified as Reliable Maturity Markers

Using the data and the analysis available from our collaborative project and from the RNA sequencing studies carried out in our primary cortical cultures during different ages, several candidate markers of maturity *in vitro* were identified as described in *Methods*. Maturity marker selection was essential at this stage in order to ensure that the effects on the maturational state of the neurons, which any future transcription factors manipulations might have, could be reliably detected. Immunocytochemistry for all the candidate maturity markers was carried out in order to validate whether the changes in mRNA transcript could be recapitulated by the protein levels at each different stage.

After at least three independent stainings, four maturity markers were selected for future studies – 68 kDa Neurofilament (NEFL) and calcitonin gene-related peptide (CGRP) were selected as potential late maturity markers, doublecortin (DCX) as a potential early maturity marker and tubulin 4a (TUBA4A) as a good 7 DIV marker (*Fig. 6.3A*). All of these molecules showed significant changes in fluorescent intensity levels across the different ages which are consistent with our RNA sequencing results.

NEFL staining intensity was significantly higher at 13-14 DIV (101 grey values) compared to 2-3 DIV (55 grey values) ($p=0.0263$, $n=4$). CGRP staining showed higher intensity levels at 13-14 DIV (72 grey values) compared to 2-3 DIV (29 grey values, $p=0.0052$) and to 6-7 DIV (43 grey values) ($p=0.0341$, $n=3$). DCX intensity was significantly lower at 13-14 DIV (102 grey values) compared to 2-3 DIV (203 grey values, $p=0.0001$) and to 6-7 DIV (205 grey values, $p=0.0001$, $n=4$). TUBA4A staining intensity was significantly higher at 6-7 DIV (1945 grey values, $p=0.0005$) and at 13-14 DIV (1327 grey values, $p=0.018$) compared to 2-3 DIV (507 grey values, $n=4$) (*Fig. 6.3B)*.

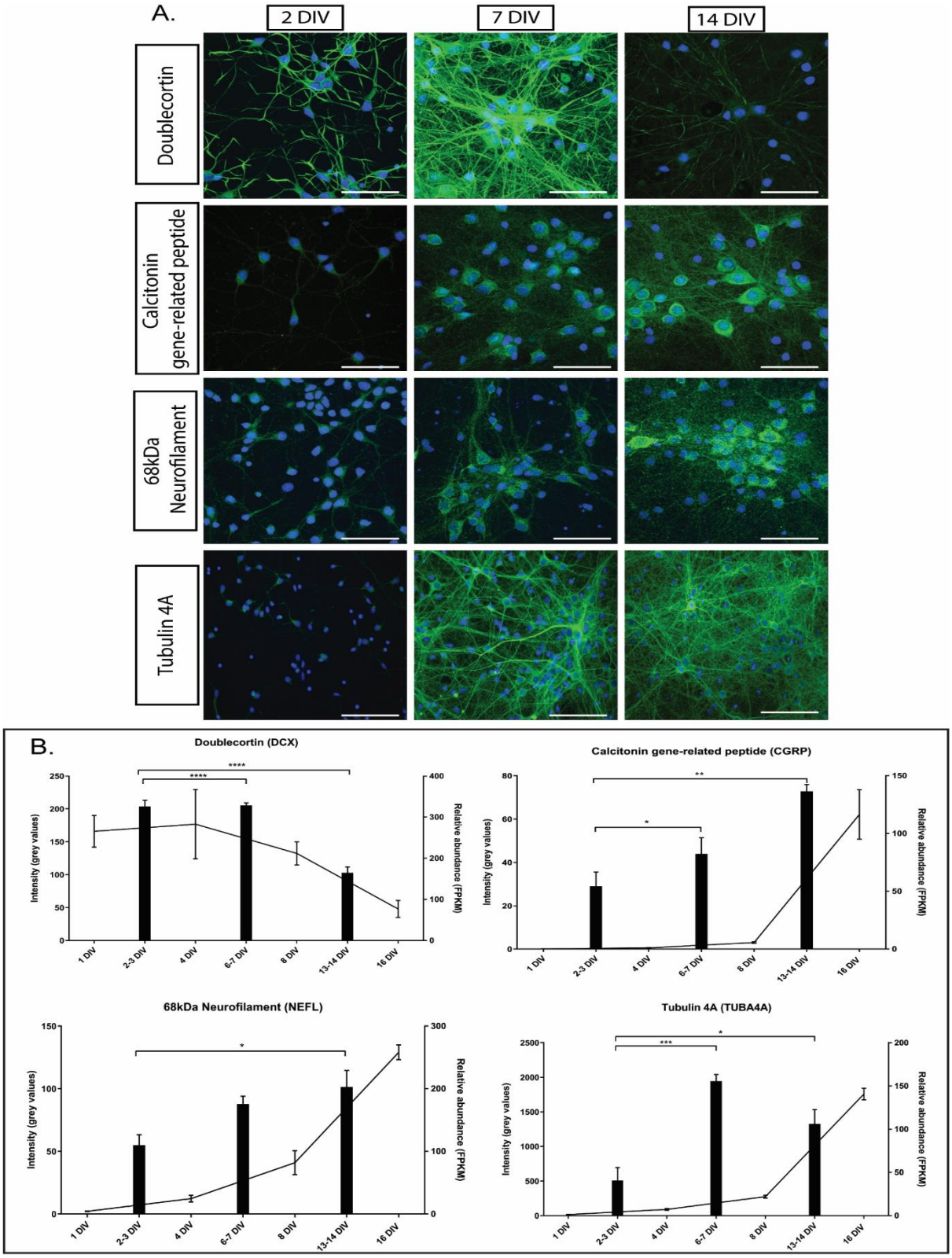

<u>Figure 6.3</u> DCX, CGRP, NEFL and TUBA4A are reliable maturity markers in primary cortical neurons. A. Immunofluorescent images of 68 kDa neurofilament, calcitonin gene-related peptide, doublecortin and tubulin 4a in primary cortical neurons during different stages of development. Scale bar is 50 µm. Images were taken at 40x. B Graphs showing the RNA expression levels on the right axis (line) and the staining intensity (bars) on the left axis for each molecule examined. Error bars represent mean ± SEM. One-way ANOVA was performed in all experiments.

4.2 Tropomyosin 1 and Oligodendrocyte-myelin Glycoprotein (OMgP) were Identified as Potential Late Maturity Markers

Two other molecules – tropomyosin 1 and oligodendrocyte-myelin glycoprotein (OMgP) were examined as potential late maturity markers. Tropomyosin 1 staining intensity varied between different experiments, so the values were normalised to 2-3 DIV values in each individual experiment. Tropomyosin 1 showed a trend towards high protein levels at 13-14 DIV (2.6 normalised intensity ratio) compared to 2-3 DIV (1 normalised intensity ratio, p=0.08, n=3). OMgP staining also showed a trend towards higher amount of protein at 13-14 DIV (2072 grey values) compared to 6-7 DIV (2108 grey values, p=0.1) and 2-3 DIV (1259 grey values, p=0.1, n=2). Despite that, these results did not reach statistical significance of <0.05 (*Fig. 6.4*).

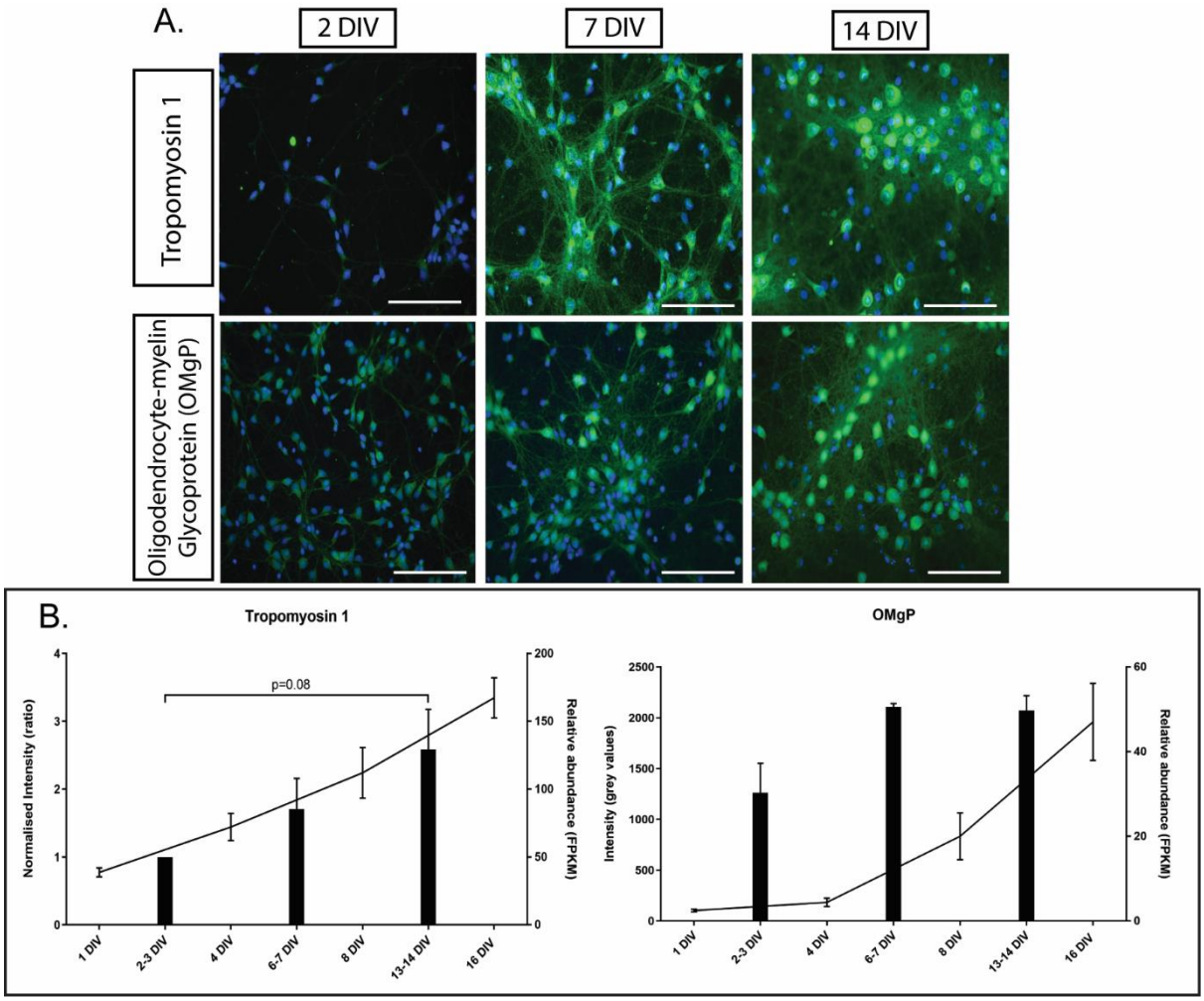

Figure 6.4 Tropomyosin 1 and OMgP might act as late maturity markers. A. Immunofluorescent images of tropomyosin 1 and oligodendrocyte-myelin glycoprotein (OMgP) in primary cortical neurons during different stages of development. Scale bar is 50 µm. Images were taken at 40x. B Graphs showing the RNA expression levels on the right axis and the staining intensity on the left axis for both molecules. Error bars represent mean ± SEM. One-way ANOVA was performed in all experiments.

4.3 Tropomyosin 4, Microtubule-associated protein 1A (MAP1A) and VANGL Planar Cell Polarity Protein 2 (VANGL2) did not Prove to be Reliable Maturity Markers

Some tested markers did not follow the predicted RNA sequencing pattern of immunostaining. For example, microtubule-associated protein 1A (MAP1A) had increased RNA levels with maturation. However, the staining intensity of the protein did not change significantly between the three different timepoints of maturation – 2-3 DIV (1 normalised intensity ratio), 6-7 DIV (1.1 normalised intensity ratio) and 13-14 DIV (0.99 normalised intensity ratio) (p=0.96, n=2) (*Fig. 6.5)*. Unlike the RNA sequencing data which shows a decrease in tropomyosin 4 RNA levels with maturation, the immunostaining showed the opposite trend towards an increase in the protein level from 2-3 DIV (1 normalised intensity ratio) to 6-7 DIV (1.5 normalised intensity ratio) and 13-14 DIV (2.4 normalised intensity ratio) (p=0.16, n=3) (*Fig. 6.5)*. Again, contrary to the change in RNA levels with maturation, Vangl2 shows an increase in immunostaining intensity with maturation from 2-3 DIV (1 normalised intensity ratio) to 6-7 DIV (1.9 normalised intensity ratio) and 13-14 DIV (1.7 normalised intensity ratio) (p=0.39, n=2) (*Fig. 6.5)*. In all three cases, there was a significant variation between the staining intensity measured in individual experiments, so the data was presented as normalised values to 2-3 DIV.

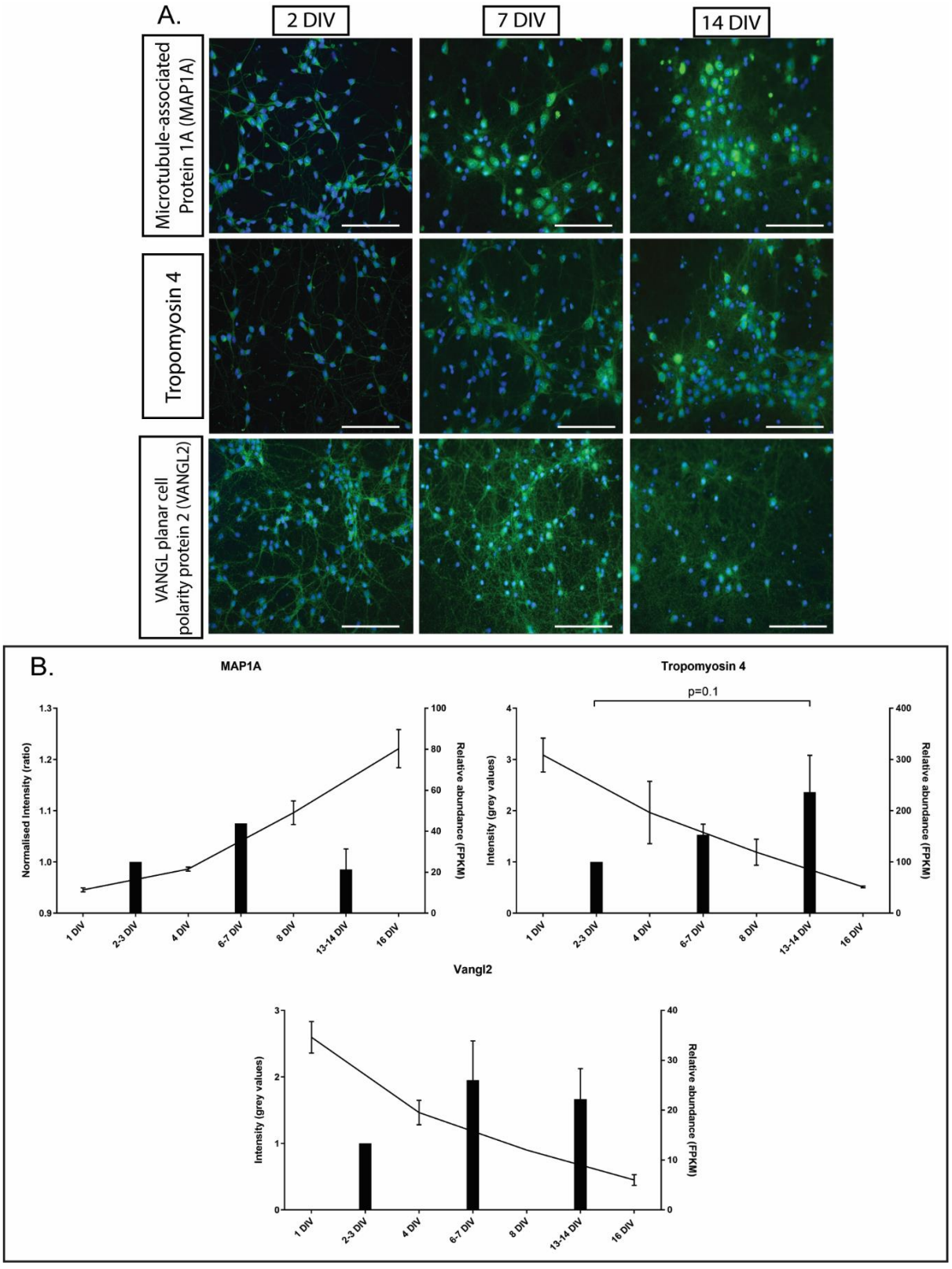

Figure 6.5 MAP1A, tropomyosin 4 and VANGL2 showed staining intensity results different to RNA sequencing data. A. Immunofluorescent images of microtubule-associated protein 1A (MAP1A), tropomyosin 4 and Vangl2 in primary cortical neurons during different stages of development. Scale bar is 50 µm. Images were taken at 40x. B Graphs showing the RNA expression levels on the right axis and the staining intensity on the left axis for both molecules. Error bars represent mean ± SEM. One-way ANOVA was performed in all experiments.

4.4 ATF3 Could Potentially Act as a Positive Control of Rejuvenation

ATF3 is a transcription factor involved in multiple developmental and regenerative processes. ATF3 was transfected into primary cortical neurons at 1 DIV and cells were fixed at 3 DIV, 6 DIV and 14 DIV in development (*Fig. 6.6A)*. The cells were then stained with two late maturity markers – CGRP and 68 kDa neurofilament which both show increased immunostaining intensity with maturation. We hypothesised that overexpressing ATF3 could reverse the maturational state of the neurons and therefore, influence the expression of the maturity markers. Contrary to our hypothesis, CGRP intensity was still higher with maturation at 14 DIV (996 grey values) compared to 3 DIV (349 grey values) ($p=0.001$) and 6 DIV (470 grey values) ($p=0.04$) (*Fig. 6.6B)*. The intensity did not increase from 3 DIV to 6 DIV, however which differs from our findings above. 68 kDa neurofilament, on the other hand, had altered expression levels of expression with maturation upon ATF3 expression with it being equal at all stages of development – 3 DIV (1154 grey values), 6 DIV (1241 grey values) and 14 DIV (1179 grey values) ($p=0.733$) (*Fig. 6.6C)*. These results suggest that ATF3 overexpression alters the expression of some known maturity markers and might affect the maturational state of mature neurons.

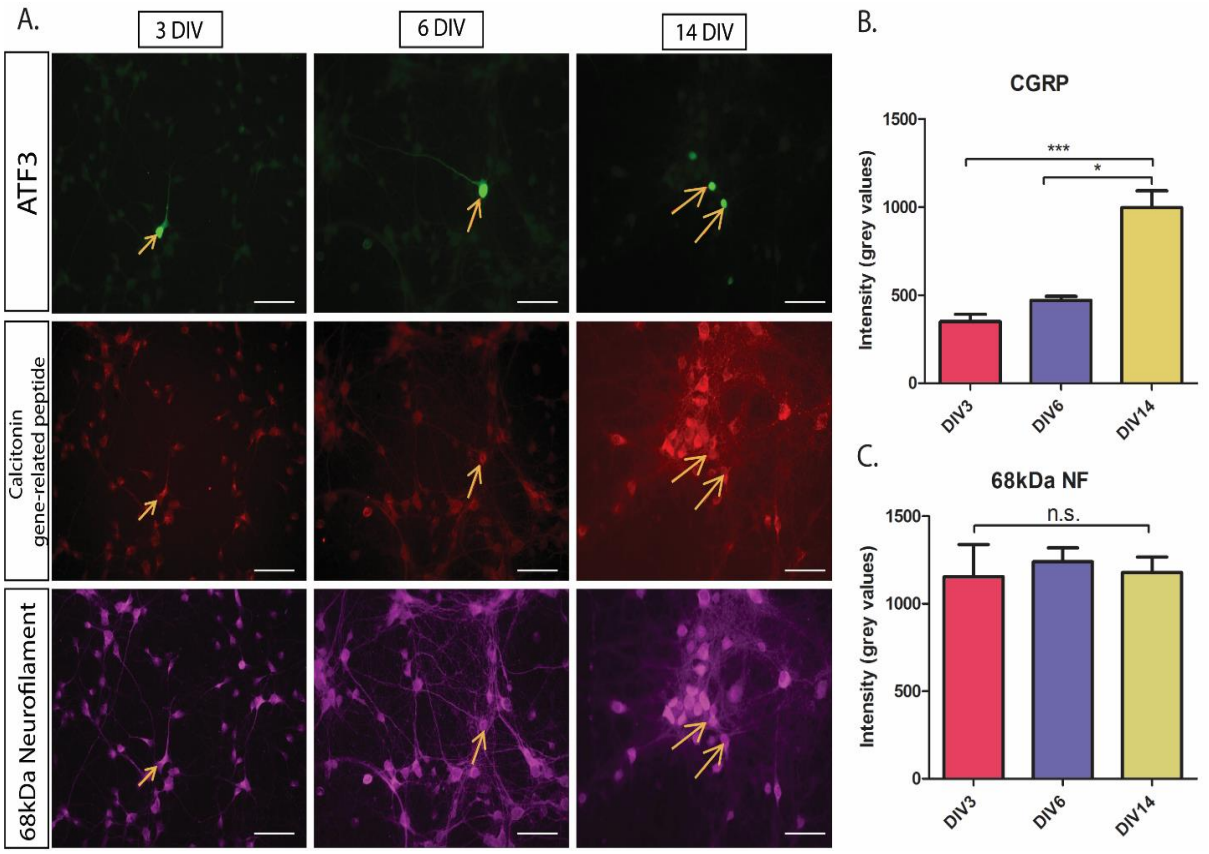

Figure 6.6 ATF3 overexpression results in altered maturity marker expression. A. Immunofluorescent images of primary cortical neurons transfected with ATF3 at 1 DIV and stained for two different maturity markers at 3 DIV, 6 DIV and 14 DIV. Scale bars are 50 µm. Images are taken at 40x. B. A graph to quantify the immunostaining intensity of CGRP during different developmental stages. C. A graph to quantify the immunostaining intensity of 68 kDa neurofilament during different developmental stages. Error bars represent mean ± SEM. One-way ANOVA was performed in all experiments.

4.5 Combinations of Transcription Factors Could Potentially Bring Neurons to an Earlier Maturational State

The main hypothesis of our study was to identify combinations of transcription factors involved in neuronal development and regeneration which could reverse the maturational state of adult primary cortical neurons *in vitro.* Preliminary testing showed that several combinations might have an effect (*Fig. 6.7A)*. For example, co-expression of CEBP and ATF3 at 1 DIV resulted in still elevated intensity of the CGRP protein at 8 DIV (17 grey values) compared to 2 DIV (11 grey values) (p=0.01) (*Fig. 6.7B)*. Contrary to our previous findings that CGRP is expressed to a higher extent at 16 DIV neurons, there was no change in the staining intensity between 2 DIV (11 grey values) and 16 DIV (14 grey values) upon CEBP and ATF3 co-transfection (*Fig. 6.7B)*. These results suggest that an overexpression of a combination of two transcription factors whose expression goes down during development, could decrease the abundance of a late maturity marker - CGRP in mature cortical neurons.

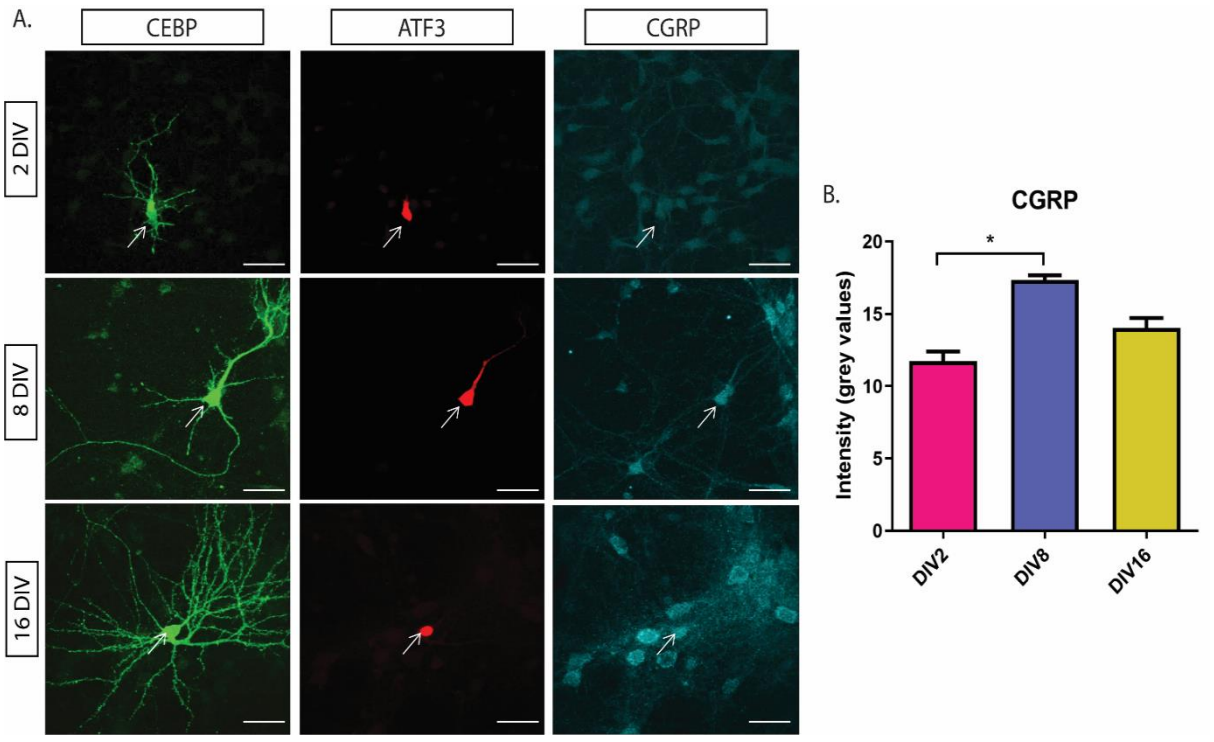

Figure 6.7 CEBP and ATF3 co-expression results in altered maturity marker expression. A. Immunofluorescent images of primary cortical neurons transfected with CEBP and ATF3 at 1 DIV and stained for late maturity marker CGRP at 2 DIV, 8 DIV and 16 DIV. Scale bars are 50 µm. Images are taken at 40x. B. A graph to quantify the immunostaining intensity of CGRP during different developmental stages. Error bars represent mean ± SEM. One-way ANOVA was performed in all experiments.

5. Discussion

The current study is first of its kind to identify markers of maturation in an *in vitro* system which could be used to test the ability of combinations of transcription factors to rejuvenate adult neurons. This study will advance the knowledge in the field as it will show whether reversing the intrinsic maturational state of adult neurons is necessary and sufficient to improve regenerative ability.

The current study aimed at testing candidate transcription factors identified in a large collaborative study on their ability to bring mature neurons back to an earlier developmental stage, and the potential effects this could have on regeneration. Our hypothesis relied on the premises that the candidate transcription factors show high expression levels early in development which gradually decline with maturation, so a forceful expression should mimic early developmental programmes. In order to do this, an essential step had to be taken where molecules at different stages of maturation had to be identified in our primary cortical cultures. All candidate markers of maturity were chosen not only on the basis of highest change in RNA transcript expression with age in our primary cortical cultures but also due to their relevance in development and regeneration in the literature. Out of all nine (*Fig. 6.3-6.5*) candidate maturity markers, four were taken forward based on the observation that staining for the protein showed pattern of intensity similar to the patterns observed in RNA transcript levels and were easy to detect – DCX, NEFL, CGRP and TUBA4A (*Fig. 6.3)*. All four candidate maturity markers and their relevance in neuronal development and axon regeneration is discussed below.

Doublecortin (DCX), for example, is a cytoskeletal protein which has been shown to serve as a new-born neuronal marker in young migrating neuroblasts in chicks due to its high expression levels early in development. Doublecortin-labelled cells are also present in regenerating chick spinal cord which is less mature and more plastic (Whalley *et al.*, 2009). DCX is also expressed by newly born neurons and is then quickly downregulated in mature neurons (Gleeson *et al.*, 1999). Mutations in doublecortin have been linked to several conditions where there is abnormal migration of neurons through the cortex early in development (des Portes *et al.*, 1998). This effect was for many years thought to be caused merely by changes in the cytoskeleton. Recent study, however, points towards a new

mechanism - a knockdown of doublecortin resulted in impaired KIF1-mediated transport of Vamp2, a cargo molecule of KIF1 suggesting that doublecortin might actually influence the transport of cargo along microtubule tracts (Liu *et al.*, 2012). The authors proposed that doublecortin might regulate trafficking of signalling molecules to specific neuronal domains, and that cargo reaching these domains could be essential for proper function and migration (Liu *et al.*, 2012). Recently, doublecortin-like kinase, a member of the DCX family has been shown to act through distinct mechanism in aiding neuronal survival and in promoting axon elongation and regeneration both in PNS and CNS axons after axotomy (Nawabi *et al.*, 2015).

Another selected marker is calcitonin gene-related peptide (CGRP). CGRP is highly expressed in various brain areas (in particular in the cortex and the spinal cord) during early development in the rat embryo (starting at E16) (Terrado *et al.*, 1999). CGRP has been shown to be located at the tip of growing neurites upon sciatic nerve injury as well as upon peripheral axotomy (Li *et al.*, 2004). CGRP levels increase with maturation in our primary cortical neurons (*Fig. 6.1, Fig 6.3B)*. What is intriguing is that ATF3-labelled neurons with high expression of ATF3 after injury show low CGRP expression levels (Li *et al.*, 2004). ATF3 is one of our candidate transcription factors and it is possible that the high levels of ATF3 observed after axotomy are due to recapitulation of early developmental transcriptional programmes. This activation in turn results in reverting neurons to an earlier maturation state, hence the reduced amount of CGRP.

68 kDa neurofilament – a major intermediate filament of mature neurons was also chosen as a potential maturity marker. The expression levels of 68 kDa neurofilament have previously been reported to be low during development as well as during regeneration in rat sensory neurons (Hoffman and Cleveland, 1988). The authors proposed that the developmental program for cytoskeleton gene expression is recapitulated during axonal regeneration as 68 kDa neurofilament becomes downregulated upon an insult to the adult neuron which normally expresses high levels of the protein. 68 kDa neurofilament mRNA levels are particularly strongly expressed in regions which develop postnatally in the brain such as the cerebellum and cerebrum (Wang *et al.*, 2012). It has also been proposed that this developmental expression pattern could be explained by retrograde transport of signal molecules so that once a neuron has reached its target cell and matured, retrograde signals are initiated to increase and maintain 68 kDa neurofilament expression. Interestingly another

cytoskeletal molecule – tubulin 4A (TUBA4A) showed promising results in our staining experiments as a 7 DIV marker (*Fig. 6.3B)*. TUBA4A levels have been shown previously to dramatically increase with age (up to 50-fold) and to play an important part in human motor cortex development such that mutations in it result in familial amyotrophic lateral sclerosis, a rapidly progressing neurodegenerative disease (Smith *et al.*, 2014).

Once markers of maturation which could be used to predict the stage of maturity in the primary cortical cultures were identified, several experiments were carried out where different transcription factors were transfected in 1 DIV cultured neurons. The cells were then grown to 14 DIV, fixed and stained for doublecortin, 68 kDa neurofilament or CGRP to assess maturational state.

Transcription factor ATF3 has previously been identified in numerous studies as essential for early neuronal development and regeneration after injury as summarised above. ATF3 levels decrease four-fold during the development of primary cortical neurons *in vitro* from 1 DIV to 24 DIV (*Fig. 6.1*). For these reasons, ATF3 was used as a positive control to test whether its forced overexpression in mature neurons can cause maturity marker expression to follow a different expression pattern resembling early neuronal states. In this study, ATF3 showed promising results as a reliable positive control transcription factor as it induced slight changes in the expression of late marker CGRP at 7 DIV and more dramatic changes in 68 kDA neurofilament at 7 DIV and 14 DIV indicating a change in maturational state of these adult neurons (*Fig. 6.6)*. However, only 2 independent experiments were performed using ATF3, so these results are not conclusive and further testing is needed. Testing other maturity markers which reliably showed a maturational change such as DCX and TUBA4A might also strengthen the current results. Furthermore, other transcription factors such as Klf7 and STAT3A-CA could also be reliable positive controls due to their well-studied effects on axon regeneration (Qiu *et al.*, 2005; Blackmore *et al.*, 2012b; He and Jin, 2016). These, however, have not been tested in our paradigm yet.

Most of the DNA constructs that we obtained from different collaborators contained the GFP expression tag, so the first combination of TFs tested that might have relevance to one another was the combination – ATF3 (no tag) and CEBP (GFP-tagged). The role of ATF3 in development and regeneration is extensively reviewed the *Introduction of this Chapter*. CEBP

has previously been shown to be upregulated after axonal injury and to be involved in the regenerative response in C. elegans (Li, Hisamoto and Matsumoto, 2015). Knockdown of CEBP in the normally regenerating fresh water snail – *L. stagnalis,* delays axon regeneration and functional recovery (Aleksic and Feng, 2012). In the adult mouse, CEBP is upregulated after facial motoneuron injury and acts to aid regeneration by increasing the expression of RAGs such as tubulin a1 and GAP43 and its silencing disrupts the regenerative process (Nadeau *et al.*, 2005; Lopez de Heredia and Magoulas, 2013). ATF3 and CEBP are transcription factors from the same bZIP (basic region/leucine zipper) transcription factor family. ATF3 and CEBP interact in a way that they form a heterodimer which binds to the ATF3 promoter and further regulates its expression upon various stresses such as nutrient depletion (Pan *et al.*, 2007).

Combination of these two transcription factors showed some changes in the expression of one of the selected maturity markers – CGRP (*Fig. 6.7*). This experiment, however was only performed once so further studies are needed. Other maturity markers should also be tested with this combination of transcription factors.

The current study has several limitations. For example, our microscopy system permitted only the imaging of 4 fluorescent channels, one of which was always the DAPI channel. Therefore, should experiments are carried with a combination of two or three transcription factor, only one 1 maturity marker could be observed. Therefore, new constructs which do not have a fluorescent tag will be ideal for use. This approach might also be more biologically relevant as the tag might interfere with the activity of the transcription factor. Furthermore, extensive characterisation of the co-transfection rates and expression amounts between two, three or more transcription factors should be carried out.

In addition, many of our transcription factor constructs contained the CMV promoter which as discussed in *Methods, Section 3.2.1* was not very efficient in primary cortical neurons. Therefore, in order to obtain higher transfection rates and neuron-specific expression of the transcription factors, the CMV promoter should be exchanged with the synapsin promoter for future experiments.

The role of vp16 and vp64 sequences in transcription factor activation has recently been extensively studied. vp16, for example is a DNA motif from *Herpes Simplex* virus which is widely used and clinically approved (Rajagopalan *et al.*, 2007) to promote better expression

rates and strong transcriptional activation. It acts by recruiting co-factors and acetyl transferases to affect chromatin remodelling (Mehta *et al.*, 2016). Fusion of vp16 to various transcription factors such as CREB and STAT3 enhances their activity majorly and results in improved regeneration compared to the transcription factor alone (Gao *et al.*, 2004; Hirai, Tani and Kikyo, 2010; Blackmore *et al.*, 2012b). The efficacy of adding the vp64 sequence is still being investigated in the process of axon regeneration. For future experiments, cloning these sequences into our candidate transcription factors could ensure that the transcription factors that are being overexpressed are actually activated and that a level of epigenetic control exists.

This experiment highlighted the complexity of combining multiple transcription factors and the numerous consideration that have to be taken – in an ideal situation all TFs from our list will have no tags but will possess the activational motif vp16 and the synapsin promoter, the co-transfection efficiency will be above 90% and we will have reliable antibodies to detect each one as well as the maturity markers. The ultimate aim of this study is to test multiple combinations of transcription factors which are relevant for regeneration in mature cortical neurons for their ability to reverse maturational state of the neurons using maturity markers. For future studies, combinations which successfully alter the developmental stage of mature CNS neurons to a more developmentally immature one, will be tested for their ability to improved axon growth and regeneration in an in vitro laser axotomy system. For further functional effects, AIS markers will be used in order to study Rab11 and integrin distribution and trafficking in adult neurons upon transcription factor application.

CONCLUSION AND FUTURE DIRECTIONS

In this thesis, two independent strategies to improve axon regeneration in the CNS by targeting intracellular mechanisms, were explored. One strategy involved expressing combinations of developmentally downregulated transcriptions factors which were identified from several large RNA sequencing databases (see *Chapter 6*). This approach relied on upregulating genes which are normally important for developmental growth in order to boost axon regeneration in the adult. Nine candidate maturity markers to help us predict the maturational state of our primary neuronal cultures were identified from previous RNA sequencing studies and tested in our model. Four markers – calcitonin gene-related peptide, 68 kDa neurofilament, doublecortin and tubulin 4a showed reliable staining at different stages of development (Koseki *et al.*, 2017). Some preliminary data suggested that overexpression of ATF3 on its own or in combination with another transcription factor – CEBP in primary cortical neurons, resulted in altered expression of some of our maturity markers. These findings highlighted the potential of our *in vitro* system as a valuable tool to identify combinations of transcription factors which could induce a change in the regenerative state of mature CNS neurons. This system could also help us inform future animal studies without having to test each combination *in vivo*. Much work, however is still needed in order to optimise this tool and to advance our knowledge of what transcription factor combinations could be beneficial for axon regeneration.

Many studies to date, have focused on targeting individual molecular players in large intracellular pathways which normally produce an array of downstream effects. Some of these studies have been successful in improving sprouting and/or axon regeneration as well as achieving modest functional recovery (Park *et al.*, 2008; Liu *et al.*, 2010; Blackmore *et al.*, 2012b; de Lima *et al.*, 2012). Despite that, the exact cellular and molecular mechanisms triggering this axon growth are still largely unknown. Recently, another approach emerged which not only boosted PNS axon regeneration through the non-permissive CNS environment but also provided some indication of the mechanisms required for targeted axon growth – this approach involved overexpression of integrins together with their activator - kindlin which allowed for their axonal transport into the axon (Cheah *et al.*, 2016). It is well

documented now, that a developmental change occurs in CNS neurons where growth-promoting receptors become removed from the fully developed axon and instead are concentrated in the somatodendritic compartment of the cell (Hollis *et al.*, 2009; Franssen *et al.*, 2015; Andrews *et al.*, 2016). This re-distribution has also been named as one of the key factors that contribute to adult CNS decline in regenerative ability. Overexpressing activated integrins in the CNS, however, might not be a viable approach to improve axon regeneration as overexpressed integrins are actively removed from mature CNS axons.

For these reasons, the second strategy used in this thesis to enhance axon regeneration after injury involved targeting one component of the transport machinery that traffics integrins into the axon – the adaptor protein protrudin (see *Chapter 3-5*). Protrudin is a membrane-bound protein which acts as a linker protein between Rab11-positive recycling endosomes containing integrins and kinesin 1 – a motor protein involved in anterograde axon transport (Shirane and Nakayama, 2006; Matsuzaki *et al.*, 2011). Phosphorylated protrudin was, in particular shown to be essential for the anterograde movement of the whole complex to the tip of growing processes in PC12 cells. Our hypothesis, therefore stated that overexpressing a constitutively phosphorylated form of protrudin in adult CNS neurons could improve the anterograde transport of several growth receptors which are contained within Rab11-tagged endosomes and therefore, might be beneficial for axon growth after injury.

We discovered that endogenous protrudin is found at low levels in mature CNS neurons and it is not upregulated after injury. Furthermore, there is less protrudin in axons compared to dendrites as primary cortical neurons mature *in vitro,* similar to other growth machinery and cargo. Overexpression of either wild-type or constitutively phosphorylated protrudin resulted in improved axon regeneration of rat primary cortical neurons after *in vitro* laser axotomy and in adult retinal ganglion cells after an optic nerve crush *in vivo*. This increase in regenerative potential was attributed to the increased amount of integrins and Rab11-positive vesicles in the distal axons of neurons overexpressing either form of protrudin. Interestingly, overexpression of wild-type protrudin improves regeneration both *in vitro* and *in vivo,* despite at a lesser extent compared to the phosphomimetic mutant. By creating several molecular domain mutants of protrudin, we were able to dissect the mechanisms that mediate protrudin-driven axon regeneration. For example, protrudin's association with the ER, with KIF5 and ER-resident protein – VAP-A as well as its involvement in lipid transfer were

all shown to be essential for its effects on axon regeneration. In addition, protrudin binding to spastin and Rab11 seem to be important for overall neuronal health as mutations in these binding sites resulted in neuronal cell death. From these results, we created a working model where protrudin acts as a scaffolding molecule bringing together multiple other molecules (growth factor receptors, motor proteins, late-endosomal proteins), organelles (ER, endosomes, lysosomes) and cellular components (lipids, membrane components) together at the tip of growing axons and that its reduced levels in mature axons could be contributing to the regenerative failure in mature neurons. In this model, we also hypothesised that protrudin functions from within the ER to target not only regenerative machinery but also ER itself into the distal part of the axon. After injury, the re-construction of new plasma membrane is key for axon growth. Therefore, the establishment of functional ER could play a crucial role in this process in order to supply the materials required for axon regeneration.

Recently there have been tremendous advances in gene therapy targeting the eye with the first successful clinical trials in humans being reported over the past few years (Walsh, 2019; Xue *et al.*, 2018). Our studies revealed that phosphomimetic protrudin has the potential to treat diseases in the eye that lead to loss of optic nerve axons, such as advanced glaucoma. Phosphorylated protrudin is currently being tested in our laboratory for its ability to improve regeneration in a spinal cord injury model and to grant neuroprotection in the eye following the induction of glaucoma. In addition to its potential suitability for gene therapy, protrudin's properties of interaction with multiple proteins and its involvement in various cellular pathways, will also prove to be a valuable tool for identifying mechanisms required for successful axon regeneration. Investigating these may lead to the identification of new targets for either gene therapy or pharmacological intervention which could ultimately improve recovery after axonal injury in the brain, eye or spinal cord.

REFERENCES

Abe, N. and Cavalli, V. (2008) 'Nerve injury signaling', *Current Opinion in Neurobiology*, 18(3), pp. 276–283. doi: 10.1016/j.conb.2008.06.005.

Aguayo, A. J., David, S. and Bray, G. M. (1981) 'Influences of the glial environment on the elongation of axons after injury: transplantation studies in adult rodents.', *The Journal of experimental biology*, 95, pp. 231–40. Available at: http://www.ncbi.nlm.nih.gov/pubmed/7334319 (Accessed: 1 March 2019).

Aigner, L. *et al.* (1995) 'Overexpression of the neural growth-associated protein GAP-43 induces nerve sprouting in the adult nervous system of transgenic mice.', *Cell*, 83(2), pp. 269–78. Available at: http://www.ncbi.nlm.nih.gov/pubmed/7585944 (Accessed: 19 March 2019).

Alberts, P. *et al.* (2003) 'Cross Talk between Tetanus Neurotoxin-insensitive Vesicle-associated Membrane Protein-mediated Transport and L1-mediated Adhesion', *Molecular Biology of the Cell*, 14(10), pp. 4207–4220. doi: 10.1091/mbc.e03-03-0147.

Aleksic, M. and Feng, Z.-P. (2012) 'Identification of the role of C/EBP in neurite regeneration following microarray analysis of a L. stagnalisCNS injury model', *BMC Neuroscience*, 13(1), p. 2. doi: 10.1186/1471-2202-13-2.

Allison, R. *et al.* (2013) 'An ESCRT–spastin interaction promotes fission of recycling tubules from the endosome', *J Cell Biol*. Rockefeller University Press, 202(3), pp. 527–543. doi: 10.1083/JCB.201211045.

Allison, R. *et al.* (2017) 'Defects in ER–endosome contacts impact lysosome function in hereditary spastic paraplegia', *J Cell Biol*. Rockefeller University Press, 216(5), pp. 1337–1355. doi: 10.1083/JCB.201609033.

Andrews, M. R. *et al.* (2009) '9 Integrin Promotes Neurite Outgrowth on Tenascin-C and Enhances Sensory Axon Regeneration', *Journal of Neuroscience*, 29(17), pp. 5546–5557. doi: 10.1523/JNEUROSCI.0759-09.2009.

Andrews, M. R. *et al.* (2016) 'Axonal Localization of Integrins in the CNS Is Neuronal Type and Age Dependent.', *eNeuro*. Society for Neuroscience, 3(4). doi: 10.1523/ENEURO.0029-16.2016.

Ascano, M. *et al.* (2009) 'Axonal Targeting of Trk Receptors via Transcytosis Regulates Sensitivity to Neurotrophin Responses', *Journal of Neuroscience*, 29(37), pp. 11674–11685. doi: 10.1523/JNEUROSCI.1542-09.2009.

Ban, B.-K. *et al.* (2013) 'Autophagy negatively regulates early axon growth in cortical neurons.', *Molecular and cellular biology*. American Society for Microbiology Journals, 33(19), pp. 3907–19. doi: 10.1128/MCB.00627-13.

Bareyre, F. M. *et al.* (2011) 'In vivo imaging reveals a phase-specific role of STAT3 during central and peripheral nervous system axon regeneration.', *Proceedings of the National Academy of Sciences of the United States of America*. National Academy of Sciences, 108(15), pp. 6282–7. doi: 10.1073/pnas.1015239108.

Barritt, A. W. *et al.* (2006) 'Chondroitinase ABC promotes sprouting of intact and injured spinal systems after spinal cord injury.', *The Journal of neuroscience : the official journal of the Society for Neuroscience*. Europe PMC Funders, 26(42), pp. 10856–67. doi: 10.1523/JNEUROSCI.2980-06.2006.

Bartsch, U. *et al.* (1995) 'Lack of evidence that myelin-associated glycoprotein is a major inhibitor of axonal regeneration in the CNS.', *Neuron*, 15(6), pp. 1375–81. Available at: http://www.ncbi.nlm.nih.gov/pubmed/8845160 (Accessed: 1 March 2019).

Bei, F. *et al.* (2016) 'Restoration of Visual Function by Enhancing Conduction in Regenerated Axons', *Cell*. Elsevier Inc., 164(1–2), pp. 219–232. doi: 10.1016/j.cell.2015.11.036.

Belin, S., Norsworthy, M. and He, Z. (2014) 'Independent control of aging and axon regeneration.', *Cell metabolism*. NIH Public Access, 19(3), pp. 354–6. doi: 10.1016/j.cmet.2014.02.014.

Bendotti, C., Servadio, A. and Samanin, R. (1991) 'Distribution of GAP-43 mRNA in the brain stem of adult rats as evidenced by in situ hybridization: localization within monoaminergic neurons.', *The Journal of neuroscience : the official journal of the Society for Neuroscience*, 11(3), pp. 600–7. Available at: http://www.ncbi.nlm.nih.gov/pubmed/1672151 (Accessed: 19 March 2019).

Benfey, M. and Aguayo, A. J. (1982) 'Extensive elongation of axons from rat brain into peripheral nerve grafts', *Nature*. Nature Publishing Group, 296(5853), pp. 150–152. doi: 10.1038/296150a0.

Bergsland, M. *et al.* (2011) 'Sequentially acting Sox transcription factors in neural lineage development', *Genes & Development*, 25(23), pp. 2453–2464. doi: 10.1101/gad.176008.111.

Berridge, M. J. (1998) 'Neuronal calcium signaling.', *Neuron*. Elsevier, 21(1), pp. 13–26. doi: 10.1016/S0896-6273(00)80510-3.

Bhattacharyya, A. *et al.* (1997) 'Trk Receptors Function As Rapid Retrograde Signal Carriers in the Adult Nervous System', *Journal of Neuroscience*. Society for Neuroscience, 17(18), pp. 7007–7016. doi: 10.1523/JNEUROSCI.17-18-07007.1997.

Bi, X. *et al.* (2001) 'Polarized distribution of alpha5 integrin in dendrites of hippocampal and cortical neurons.', *The Journal of comparative neurology*, 435(2), pp. 184–93. Available at: http://www.ncbi.nlm.nih.gov/pubmed/11391640 (Accessed: 20 March 2019).

Bisicchia, E. *et al.* (2017) 'Autophagy Inhibition Favors Survival of Rubrospinal Neurons After Spinal Cord Hemisection', *Molecular Neurobiology*, 54(7), pp. 4896–4907. doi: 10.1007/s12035-016-0031-z.

Blackmore, M. G. *et al.* (2010) 'High content screening of cortical neurons identifies novel regulators of axon growth', *Molecular and Cellular Neuroscience*, 44(1), pp. 43–54. doi: 10.1016/j.mcn.2010.02.002.

Blackmore, M. G. *et al.* (2012a) 'Kruppel-like Factor 7 engineered for transcriptional activation promotes axon regeneration in the adult corticospinal tract', *Proceedings of the National Academy of Sciences*, 109(19), pp. 7517–7522. doi: 10.1073/pnas.1120684109.

Blackmore, M. G. *et al.* (2012b) 'Kruppel-like Factor 7 engineered for transcriptional activation promotes axon regeneration in the adult corticospinal tract', *Proceedings of the National Academy of Sciences*, 109(19), pp. 7517–7522. doi: 10.1073/pnas.1120684109.

Blackmore, M. and Letourneau, P. C. (2006) 'Changes within maturing neurons limit axonal regeneration in the developing spinal cord', *Journal of Neurobiology*, 66(4), pp. 348–360. doi: 10.1002/neu.20224.

Blanquie, O. and Bradke, F. (2018) 'Cytoskeleton dynamics in axon regeneration', *Current Opinion in Neurobiology*, 51, pp. 60–69. doi: 10.1016/j.conb.2018.02.024.

Bleher, R. and Martin, R. (2001) 'Ribosomes in the squid giant axon.', *Neuroscience*, 107(3), pp. 527–34. Available at: http://www.ncbi.nlm.nih.gov/pubmed/11719007 (Accessed: 7 March 2019).

Blesch, A. *et al.* (2004) 'Axonal responses to cellularly delivered NT-4/5 after spinal cord injury', *Molecular and Cellular Neuroscience*, 27(2), pp. 190–201. doi: 10.1016/j.mcn.2004.06.007.

Blesch, A. *et al.* (2012) 'Conditioning lesions before or after spinal cord injury recruit broad genetic mechanisms that sustain axonal regeneration: superiority to camp-mediated effects.', *Experimental neurology*. NIH Public Access, 235(1), pp. 162–73. doi: 10.1016/j.expneurol.2011.12.037.

Blesch, A. and Tuszynski, M. H. (2003) 'Cellular GDNF delivery promotes growth of motor and dorsal column sensory axons after partial and complete spinal cord transections and induces remyelination', *The Journal of*

Comparative Neurology, 467(3), pp. 403–417. doi: 10.1002/cne.10934.

Boiko, T. *et al.* (2007) 'Ankyrin-Dependent and -Independent Mechanisms Orchestrate Axonal Compartmentalization of L1 Family Members Neurofascin and L1/Neuron-Glia Cell Adhesion Molecule', *Journal of Neuroscience*, 27(3), pp. 590–603. doi: 10.1523/JNEUROSCI.4302-06.2007.

Bomze, H. M. *et al.* (2001) 'Spinal axon regeneration evoked by replacing two growth cone proteins in adult neurons', *Nature Neuroscience*, 4(1), pp. 38–43. doi: 10.1038/82881.

Bonanomi, D. *et al.* (2008) 'Identification of a developmentally regulated pathway of membrane retrieval in neuronal growth cones', *Journal of Cell Science*, 121(22), pp. 3757–3769. doi: 10.1242/jcs.033803.

Bos, J. L., Rehmann, H. and Wittinghofer, A. (2007) 'GEFs and GAPs: Critical Elements in the Control of Small G Proteins', *Cell*. Cell Press, 129(5), pp. 865–877. doi: 10.1016/J.CELL.2007.05.018.

Bradbury, E. J. *et al.* (2002) 'Chondroitinase ABC promotes functional recovery after spinal cord injury', *Nature*, 416(6881), pp. 636–640. doi: 10.1038/416636a.

Bradke, F., Fawcett, J. W. and Spira, M. E. (2012) 'Assembly of a new growth cone after axotomy: the precursor to axon regeneration', *Nature Reviews Neuroscience*, 13(3), pp. 183–193. doi: 10.1038/nrn3176.

Bradke, F. and Marín, O. (2014) 'Editorial overview: Development and regeneration: Nervous system development and regeneration', *Current Opinion in Neurobiology*, 27, pp. iv–vi. doi: 10.1016/j.conb.2014.05.007.

Bray, E. R. *et al.* (2017) '3D Visualization of Individual Regenerating Retinal Ganglion Cell Axons Reveals Surprisingly Complex Growth Paths', *eneuro*, 4(4), p. ENEURO.0093-17.2017. doi: 10.1523/ENEURO.0093-17.2017.

Bregman, B. S. *et al.* (1989) 'Extension of the critical period for developmental plasticity of the corticospinal pathway', *The Journal of Comparative Neurology*, 282(3), pp. 355–370. doi: 10.1002/cne.902820304.

Buffo, A. *et al.* (1997) 'Targeted overexpression of the neurite growth-associated protein B-50/GAP-43 in cerebellar Purkinje cells induces sprouting after axotomy but not axon regeneration into growth-permissive transplants.', *The Journal of neuroscience : the official journal of the Society for Neuroscience*, 17(22), pp. 8778–91. Available at: http://www.ncbi.nlm.nih.gov/pubmed/9348347 (Accessed: 19 March 2019).

Byrne, A. B. *et al.* (2014) 'Insulin/IGF1 signaling inhibits age-dependent axon regeneration.', *Neuron*. NIH Public Access, 81(3), pp. 561–73. doi: 10.1016/j.neuron.2013.11.019.

Cai, D. *et al.* (2001) 'Neuronal cyclic AMP controls the developmental loss in ability of axons to regenerate.', *The Journal of neuroscience : the official journal of the Society for Neuroscience*, 21(13), pp. 4731–9. Available at: http://www.ncbi.nlm.nih.gov/pubmed/11425900 (Accessed: 19 March 2019).

Cai, D. *et al.* (2002) 'Arginase I and polyamines act downstream from cyclic AMP in overcoming inhibition of axonal growth MAG and myelin in vitro.', *Neuron*, 35(4), pp. 711–9. Available at: http://www.ncbi.nlm.nih.gov/pubmed/12194870 (Accessed: 19 March 2019).

Cai, Q. *et al.* (2010) 'Snapin-Regulated Late Endosomal Transport Is Critical for Efficient Autophagy-Lysosomal Function in Neurons', *Neuron*, 68(1), pp. 73–86. doi: 10.1016/j.neuron.2010.09.022.

Campbell, G. *et al.* (2005) 'Upregulation of activating transcription factor 3 (ATF3) by intrinsic CNS neurons regenerating axons into peripheral nerve grafts', *Experimental Neurology*, 192(2), pp. 340–347. doi: 10.1016/j.expneurol.2004.11.026.

Cartoni, R. *et al.* (2016) 'The Mammalian-Specific Protein Armcx1 Regulates Mitochondrial Transport during Axon Regeneration.', *Neuron*. NIH Public Access, 92(6), pp. 1294–1307. doi: 10.1016/j.neuron.2016.10.060.

Caswell, P. T. *et al.* (2008) 'Rab-coupling protein coordinates recycling of alpha5beta1 integrin and EGFR1 to promote cell migration in 3D microenvironments.', *The Journal of cell biology*. The Rockefeller University Press, 183(1), pp. 143–55. doi: 10.1083/jcb.200804140.

Chandran, V. *et al.* (2016) 'A Systems-Level Analysis of the Peripheral Nerve Intrinsic Axonal Growth Program', *Neuron*, 89(5), pp. 956–970. doi: 10.1016/j.neuron.2016.01.034.

Chang, D. T. W. and Reynolds, I. J. (2006) 'Differences in mitochondrial movement and morphology in young and mature primary cortical neurons in culture', *Neuroscience*, 141(2), pp. 727–736. doi: 10.1016/j.neuroscience.2006.01.034.

Chang, J., Lee, S. and Blackstone, C. (2013) 'Protrudin binds atlastins and endoplasmic reticulum-shaping proteins and regulates network formation', *Proceedings of the National Academy of Sciences*, 110(37), pp. 14954–14959. doi: 10.1073/pnas.1307391110.

Cheah, M. *et al.* (2016) 'Expression of an Activated Integrin Promotes Long-Distance Sensory Axon Regeneration in the Spinal Cord', *Journal of Neuroscience*, 36(27), pp. 7283–7297. doi: 10.1523/JNEUROSCI.0901-16.2016.

Chen, D. F., Jhaveri, S. and Schneider, G. E. (1995) *Intrinsic changes in developing retinal neurons result in regenerative failure of their axons (organotypic coculture/superior colliculus/axon regeneration/target innervation/Syrian hamster)*, *Neurobiology*. Available at: https://www.pnas.org/content/pnas/92/16/7287.full.pdf (Accessed: 21 March 2019).

Chen, K. *et al.* (2013) 'RNA-Seq Characterization of Spinal Cord Injury Transcriptome in Acute/Subacute Phases: A Resource for Understanding the Pathology at the Systems Level', *PLoS ONE*. Edited by M. Hetman. Public Library of Science, 8(8), p. e72567. doi: 10.1371/journal.pone.0072567.

Cheng, P.-L. *et al.* (2011) 'Self-amplifying autocrine actions of BDNF in axon development', *Proceedings of the National Academy of Sciences*, 108(45), pp. 18430–18435. doi: 10.1073/pnas.1115907108.

Cheng, X.-T. *et al.* (2015) 'Axonal autophagosomes recruit dynein for retrograde transport through fusion with late endosomes', *The Journal of Cell Biology*, 209(3), pp. 377–386. doi: 10.1083/jcb.201412046.

Chiasseu, M. *et al.* (2017) 'Tau accumulation in the retina promotes early neuronal dysfunction and precedes brain pathology in a mouse model of Alzheimer's disease', *Molecular Neurodegeneration*. BioMed Central, 12(1), p. 58. doi: 10.1186/s13024-017-0199-3.

Cioni, J.-M. *et al.* (2019) 'Late Endosomes Act as mRNA Translation Platforms and Sustain Mitochondria in Axons', *Cell*. Cell Press, 176(1–2), p. 56–72.e15. doi: 10.1016/J.CELL.2018.11.030.

Correia, S. S. *et al.* (2008) 'Motor protein–dependent transport of AMPA receptors into spines during long-term potentiation', *Nature Neuroscience*, 11(4), pp. 457–466. doi: 10.1038/nn2063.

Cosker, K. E., Courchesne, S. L. and Segal, R. A. (2008) 'Action in the axon: generation and transport of signaling endosomes.', *Current opinion in neurobiology*. NIH Public Access, 18(3), pp. 270–5. doi: 10.1016/j.conb.2008.08.005.

Covello, G. *et al.* (2014) 'An electroporation protocol for efficient DNA transfection in PC12 cells.', *Cytotechnology*. Springer, 66(4), pp. 543–53. doi: 10.1007/s10616-013-9608-9.

Cox, L. J. *et al.* (2008) 'Intra-axonal translation and retrograde trafficking of CREB promotes neuronal survival', *Nature Cell Biology*, 10(2), pp. 149–159. doi: 10.1038/ncb1677.

D'Souza-Schorey, C. and Chavrier, P. (2006) 'ARF proteins: roles in membrane traffic and beyond', *Nature Reviews Molecular Cell Biology*. Nature Publishing Group, 7(5), pp. 347–358. doi: 10.1038/nrm1910.

Daniel, S., Clark, A. and McDowell, C. (2018) 'Subtype-specific response of retinal ganglion cells to optic nerve

crush', *Cell Death Discovery*. Nature Publishing Group, 4(1), p. 67. doi: 10.1038/s41420-018-0069-y.

David, S. and Aguayo, A. J. (1981) 'Axonal elongation into peripheral nervous system "bridges" after central nervous system injury in adult rats.', *Science (New York, N.Y.)*. American Association for the Advancement of Science, 214(4523), pp. 931–3. doi: 10.1126/SCIENCE.6171034.

Dent, E. W., Gupton, S. L. and Gertler, F. B. (2011) 'The growth cone cytoskeleton in axon outgrowth and guidance.', *Cold Spring Harbor perspectives in biology*. Cold Spring Harbor Laboratory Press, 3(3). doi: 10.1101/cshperspect.a001800.

Dergham, P. *et al.* (2002) 'Rho signaling pathway targeted to promote spinal cord repair.', *The Journal of neuroscience : the official journal of the Society for Neuroscience*, 22(15), pp. 6570–7. doi: 20026637.

Dervishi, I. *et al.* (2018) 'Protein-protein interactions reveal key canonical pathways, upstream regulators, interactome domains, and novel targets in ALS', *Scientific Reports*. Nature Publishing Group, 8(1), p. 14732. doi: 10.1038/s41598-018-32902-4.

Doster, S. K. *et al.* (1991) 'Expression of the growth-associated protein GAP-43 in adult rat retinal ganglion cells following axon injury.', *Neuron*, 6(4), pp. 635–47. Available at: http://www.ncbi.nlm.nih.gov/pubmed/1826603 (Accessed: 19 March 2019).

Duan, X. *et al.* (2015) 'Subtype-Specific Regeneration of Retinal Ganglion Cells following Axotomy: Effects of Osteopontin and mTOR Signaling', *Neuron*, 85(6), pp. 1244–1256. doi: 10.1016/j.neuron.2015.02.017.

Dupraz, S. *et al.* (2009) 'The TC10-Exo70 Complex Is Essential for Membrane Expansion and Axonal Specification in Developing Neurons', *Journal of Neuroscience*, 29(42), pp. 13292–13301. doi: 10.1523/JNEUROSCI.3907-09.2009.

Dupraz, S. *et al.* (2013) 'The Insulin-Like Growth Factor 1 Receptor Is Essential for Axonal Regeneration in Adult Central Nervous System Neurons', *PLoS ONE*. Edited by A. H. Kihara, 8(1), p. e54462. doi: 10.1371/journal.pone.0054462.

English, A. W. *et al.* (2013) 'Small-molecule trkB agonists promote axon regeneration in cut peripheral nerves.', *Proceedings of the National Academy of Sciences of the United States of America*. National Academy of Sciences, 110(40), pp. 16217–22. doi: 10.1073/pnas.1303646110.

Erturk, A. *et al.* (2007) 'Disorganized Microtubules Underlie the Formation of Retraction Bulbs and the Failure of Axonal Regeneration', *Journal of Neuroscience*, 27(34), pp. 9169–9180. doi: 10.1523/JNEUROSCI.0612-07.2007.

Esteves da Silva, M. *et al.* (2015) 'Positioning of AMPA Receptor-Containing Endosomes Regulates Synapse Architecture', *Cell Reports*, 13(5), pp. 933–943. doi: 10.1016/j.celrep.2015.09.062.

Eva, R. *et al.* (2010) 'Rab11 and Its Effector Rab Coupling Protein Contribute to the Trafficking of 1 Integrins during Axon Growth in Adult Dorsal Root Ganglion Neurons and PC12 Cells', *Journal of Neuroscience*, 30(35), pp. 11654–11669. doi: 10.1523/JNEUROSCI.2425-10.2010.

Eva, R. *et al.* (2012) 'ARF6 Directs Axon Transport and Traffic of Integrins and Regulates Axon Growth in Adult DRG Neurons', *Journal of Neuroscience*, 32(30), pp. 10352–10364. doi: 10.1523/JNEUROSCI.1409-12.2012.

Eva, R. *et al.* (2017) 'EFA6 regulates selective polarised transport and axon regeneration from the axon initial segment.', *Journal of cell science*. The Company of Biologists Ltd, 130(21), pp. 3663–3675. doi: 10.1242/jcs.207423.

Fagoe, N. D. *et al.* (2015) 'Overexpression of ATF3 or the combination of ATF3, c-Jun, STAT3 and Smad1 promotes regeneration of the central axon branch of sensory neurons but without synergistic effects', *Human Molecular Genetics*, 24(23), pp. 6788–6800. doi: 10.1093/hmg/ddv383.

Farías, G. G. *et al.* (2017) 'BORC/kinesin-1 ensemble drives polarized transport of lysosomes into the axon', *Proceedings of the National Academy of Sciences*, 114(14), pp. E2955–E2964. doi: 10.1073/pnas.1616363114.

Farías, G. G. *et al.* (2019) 'Feedback-Driven Mechanisms between Microtubules and the Endoplasmic Reticulum Instruct Neuronal Polarity', *Neuron*. doi: 10.1016/j.neuron.2019.01.030.

Fawcett, J. W. and Asher, R. A. (1999) 'The glial scar and central nervous system repair.', *Brain research bulletin*, 49(6), pp. 377–91. Available at: http://www.ncbi.nlm.nih.gov/pubmed/10483914 (Accessed: 1 March 2019).

Finelli, M. J. *et al.* (2013) 'Differential Phosphorylation of Smad1 Integrates BMP and Neurotrophin Pathways through Erk/Dusp in Axon Development', *Cell Reports*, 3(5), pp. 1592–1606. doi: 10.1016/j.celrep.2013.04.011.

Finelli, M. J., Wong, J. K. and Zou, H. (2013) 'Epigenetic regulation of sensory axon regeneration after spinal cord injury.', *The Journal of neuroscience : the official journal of the Society for Neuroscience*. Society for Neuroscience, 33(50), pp. 19664–76. doi: 10.1523/JNEUROSCI.0589-13.2013.

Fisher, D. *et al.* (2011) 'Leukocyte common antigen-related phosphatase is a functional receptor for chondroitin sulfate proteoglycan axon growth inhibitors.', *The Journal of neuroscience : the official journal of the Society for Neuroscience*. NIH Public Access, 31(40), pp. 14051–66. doi: 10.1523/JNEUROSCI.1737-11.2011.

Franssen, E. H. P. *et al.* (2015) 'Exclusion of Integrins from CNS Axons Is Regulated by Arf6 Activation and the AIS', *Journal of Neuroscience*, 35(21), pp. 8359–8375. doi: 10.1523/JNEUROSCI.2850-14.2015.

Freund, P. *et al.* (2006) 'Nogo-A–specific antibody treatment enhances sprouting and functional recovery after cervical lesion in adult primates', *Nature Medicine*. Nature Publishing Group, 12(7), pp. 790–792. doi: 10.1038/nm1436.

Fu, M., Nirschl, J. J. and Holzbaur, E. L. F. (2014) 'LC3 Binding to the Scaffolding Protein JIP1 Regulates Processive Dynein-Driven Transport of Autophagosomes', *Developmental Cell*, 29(5), pp. 577–590. doi: 10.1016/j.devcel.2014.04.015.

Gabriela Otero, M. *et al.* (2018) *Proteasome stress leads to APP axonal transport defects by promoting its amyloidogenic processing in lysosomes*. Available at: http://jcs.biologists.org/content/joces/early/2018/05/02/jcs.214536.full.pdf (Accessed: 6 March 2019).

Gallo, A., Vannier, C. and Galli, T. (2016) 'Endoplasmic Reticulum–Plasma Membrane Associations:Structures and Functions', *Annual Review of Cell and Developmental Biology*. Annual Reviews , 32(1), pp. 279–301. doi: 10.1146/annurev-cellbio-111315-125024.

Gao, Y. *et al.* (2004) 'Activated CREB Is Sufficient to Overcome Inhibitors in Myelin and Promote Spinal Axon Regeneration In Vivo', *Neuron*, 44(4), pp. 609–621. doi: 10.1016/j.neuron.2004.10.030.

Gates, M. A., Tai, C. C. and Macklis, J. D. (2000) 'Neocortical neurons lacking the protein-tyrosine kinase B receptor display abnormal differentiation and process elongation in vitro and in vivo.', *Neuroscience*, 98(3), pp. 437–47. Available at: http://www.ncbi.nlm.nih.gov/pubmed/10869838 (Accessed: 5 March 2019).

Gaub, P. *et al.* (2010) 'HDAC inhibition promotes neuronal outgrowth and counteracts growth cone collapse through CBP/p300 and P/CAF-dependent p53 acetylation', *Cell Death & Differentiation*, 17(9), pp. 1392–1408. doi: 10.1038/cdd.2009.216.

Geeven, G. *et al.* (2011) 'LLM3D: a log-linear modeling-based method to predict functional gene regulatory interactions from genome-wide expression data', *Nucleic Acids Research*, 39(13), pp. 5313–5327. doi: 10.1093/nar/gkr139.

Geoffroy, C. G. *et al.* (2016) 'Evidence for an Age-Dependent Decline in Axon Regeneration in the Adult Mammalian Central Nervous System.', *Cell reports*. Elsevier, 15(2), pp. 238–46. doi: 10.1016/j.celrep.2016.03.028.

Gey, M. *et al.* (2016) 'Atf3 mutant mice show reduced axon regeneration and impaired regeneration-associated gene induction after peripheral nerve injury.', *Open biology*. The Royal Society, 6(8). doi: 10.1098/rsob.160091.

Gibson, D. G. *et al.* (2009) 'Enzymatic assembly of DNA molecules up to several hundred kilobases', *Nature Methods*, 6(5), pp. 343–345. doi: 10.1038/nmeth.1318.

Gibson, D. G. (2011) 'Enzymatic Assembly of Overlapping DNA Fragments', in *Methods in enzymology*, pp. 349–361. doi: 10.1016/B978-0-12-385120-8.00015-2.

Gil, J.-E. *et al.* (2012) 'Phosphoinositides Differentially Regulate Protrudin Localization through the FYVE Domain', *Journal of Biological Chemistry*, 287(49), pp. 41268–41276. doi: 10.1074/jbc.M112.419127.

Gilley, J. *et al.* (2012) 'Age-dependent axonal transport and locomotor changes and tau hypophosphorylation in a "P301L" tau knockin mouse', *Neurobiology of Aging*. Elsevier, 33(3), p. 621.e1-621.e15. doi: 10.1016/J.NEUROBIOLAGING.2011.02.014.

Glaucoma Facts and Stats | Glaucoma Research Foundation (no date). Available at: https://www.glaucoma.org/glaucoma/glaucoma-facts-and-stats.php (Accessed: 28 February 2019).

Gleeson, J. G. *et al.* (1999) 'Doublecortin is a microtubule-associated protein and is expressed widely by migrating neurons.', *Neuron*, 23(2), pp. 257–71. Available at: http://www.ncbi.nlm.nih.gov/pubmed/10399933 (Accessed: 20 March 2019).

Goldberg, J. L. *et al.* (2002) 'Retinal Ganglion Cells Do Not Extend Axons by Default: Promotion by Neurotrophic Signaling and Electrical Activity', *Neuron*. Cell Press, 33(5), pp. 689–702. doi: 10.1016/S0896-6273(02)00602-5.

Gomis-Rüth, S. *et al.* (2014) 'Single-cell axotomy of cultured hippocampal neurons integrated in neuronal circuits', *Nature Protocols*, 9(5), pp. 1028–1037. doi: 10.1038/nprot.2014.069.

Gong, B. *et al.* (2016) 'The Ubiquitin-Proteasome System: Potential Therapeutic Targets for Alzheimer's Disease and Spinal Cord Injury', *Frontiers in Molecular Neuroscience*, 9, p. 4. doi: 10.3389/fnmol.2016.00004.

GrandPré, T., Li, S. and Strittmatter, S. M. (2002) 'Nogo-66 receptor antagonist peptide promotes axonal regeneration', *Nature*. Nature Publishing Group, 417(6888), pp. 547–551. doi: 10.1038/417547a.

Gumy, L. F. *et al.* (2011) 'Transcriptome analysis of embryonic and adult sensory axons reveals changes in mRNA repertoire localization', *RNA*, 17(1), pp. 85–98. doi: 10.1261/rna.2386111.

Gumy, L. F. *et al.* (2013) 'The Kinesin-2 Family Member KIF3C Regulates Microtubule Dynamics and Is Required for Axon Growth and Regeneration', *Journal of Neuroscience*, 33(28), pp. 11329–11345. doi: 10.1523/JNEUROSCI.5221-12.2013.

Gumy, L. F. *et al.* (2017) 'MAP2 Defines a Pre-axonal Filtering Zone to Regulate KIF1- versus KIF5-Dependent Cargo Transport in Sensory Neurons', *Neuron*, 94(2), p. 347–362.e7. doi: 10.1016/j.neuron.2017.03.046.

Gumy, L. F., Tan, C. L. and Fawcett, J. W. (2010) 'The role of local protein synthesis and degradation in axon regeneration.', *Experimental neurology*. Elsevier, 223(1), pp. 28–37. doi: 10.1016/j.expneurol.2009.06.004.

Guo, Y. *et al.* (2018) 'Visualizing Intracellular Organelle and Cytoskeletal Interactions at Nanoscale Resolution on Millisecond Timescales', *Cell*. Cell Press, 175(5), p. 1430–1442.e17. doi: 10.1016/J.CELL.2018.09.057.

Hafidi, A., Lanjun, G. and Sanes, D. H. (1999) 'Age-dependent failure of axon regeneration in organotypic culture of gerbil auditory midbrain.', *Journal of neurobiology*, 41(2), pp. 267–80. Available at: http://www.ncbi.nlm.nih.gov/pubmed/10512983 (Accessed: 2 March 2019).

Harel, N. Y. and Strittmatter, S. M. (2006) 'Can regenerating axons recapitulate developmental guidance during recovery from spinal cord injury?', *Nature Reviews Neuroscience*, 7(8), pp. 603–616. doi: 10.1038/nrn1957.

Haugsten, E. M. *et al.* (2014) 'Photoactivation Approaches Reveal a Role for Rab11 in FGFR4 Recycling and Signalling', *Traffic*. John Wiley & Sons, Ltd (10.1111), 15(6), pp. 665–683. doi: 10.1111/tra.12168.

He, Z. and Jin, Y. (2016) 'Intrinsic Control of Axon Regeneration', *Neuron*, 90(3), pp. 437–451. doi: 10.1016/j.neuron.2016.04.022.

Hellal, F. *et al.* (2011) 'Microtubule Stabilization Reduces Scarring and Causes Axon Regeneration After Spinal Cord Injury', *Science*, 331(6019), pp. 928–931. doi: 10.1126/science.1201148.

Hilton, B. J. and Bradke, F. (2017) 'Can injured adult CNS axons regenerate by recapitulating development?', *Development*, 144(19), pp. 3417–3429. doi: 10.1242/dev.148312.

Hirai, H., Tani, T. and Kikyo, N. (2010) 'Structure and functions of powerful transactivators: VP16, MyoD and FoxA', *The International Journal of Developmental Biology*, 54(11–12), pp. 1589–1596. doi: 10.1387/ijdb.103194hh.

Hoffman, P. N. *et al.* (1983) 'Slowing of the axonal transport of neurofilament proteins during development.', *The Journal of neuroscience : the official journal of the Society for Neuroscience*, 3(8), pp. 1694–700. Available at: http://www.ncbi.nlm.nih.gov/pubmed/6192231 (Accessed: 4 March 2019).

Hoffman, P. N. (1989) 'Expression of GAP-43, a rapidly transported growth-associated protein, and class II beta tubulin, a slowly transported cytoskeletal protein, are coordinated in regenerating neurons.', *The Journal of neuroscience : the official journal of the Society for Neuroscience*, 9(3), pp. 893–7. Available at: http://www.ncbi.nlm.nih.gov/pubmed/2494308 (Accessed: 4 March 2019).

Hoffman, P. N. (2010) 'A conditioning lesion induces changes in gene expression and axonal transport that enhance regeneration by increasing the intrinsic growth state of axons', *Experimental Neurology*, 223(1), pp. 11–18. doi: 10.1016/j.expneurol.2009.09.006.

Hoffman, P. N. and Cleveland, D. W. (1988) 'Neurofilament and tubulin expression recapitulates the developmental program during axonal regeneration: induction of a specific beta-tubulin isotype.', *Proceedings of the National Academy of Sciences of the United States of America*. National Academy of Sciences, 85(12), pp. 4530–3. doi: 10.1073/PNAS.85.12.4530.

Hollenbeck, P. J. (1993) 'Products of endocytosis and autophagy are retrieved from axons by regulated retrograde organelle transport.', *The Journal of cell biology*. The Rockefeller University Press, 121(2), pp. 305–15. Available at: http://www.ncbi.nlm.nih.gov/pubmed/7682217 (Accessed: 4 March 2019).

Hollenbeck, P. J. and Bray, D. (1987) 'Rapidly transported organelles containing membrane and cytoskeletal components: their relation to axonal growth.', *The Journal of cell biology*. The Rockefeller University Press, 105(6 Pt 1), pp. 2827–35. Available at: http://www.ncbi.nlm.nih.gov/pubmed/3693400 (Accessed: 4 March 2019).

Hollis, E. R. *et al.* (2009) 'IGF-I gene delivery promotes corticospinal neuronal survival but not regeneration after adult CNS injury.', *Experimental neurology*. NIH Public Access, 215(1), pp. 53–9. doi: 10.1016/j.expneurol.2008.09.014.

Hollis, E. R. *et al.* (2009) 'Induction of corticospinal regeneration by lentiviral trkB-induced Erk activation', *Proceedings of the National Academy of Sciences*, 106(17), pp. 7215–7220. doi: 10.1073/pnas.0810624106.

Holt, C. E. and Schuman, E. M. (2013) 'The Central Dogma Decentralized: New Perspectives on RNA Function and Local Translation in Neurons', *Neuron*, 80(3), pp. 648–657. doi: 10.1016/j.neuron.2013.10.036.

Hong, Z. *et al.* (2017) 'PtdIns3P controls mTORC1 signaling through lysosomal positioning', *J Cell Biol*. Rockefeller University Press, 216(12), pp. 4217–4233. doi: 10.1083/JCB.201611073.

Hoogenraad, C. C. and Akhmanova, A. (2010) 'Dendritic Spine Plasticity: New Regulatory Roles of Dynamic Microtubules', *The Neuroscientist*, 16(6), pp. 650–661. doi: 10.1177/1073858410386357.

Hotulainen, P. and Hoogenraad, C. C. (2010) 'Actin in dendritic spines: connecting dynamics to function.', *The Journal of cell biology*. Rockefeller University Press, 189(4), pp. 619–29. doi: 10.1083/jcb.201003008.

Hou, H. *et al.* (2013) 'Acute spinal cord injury could cause activation of autophagy in dorsal root ganglia', *Spinal Cord*. Nature Publishing Group, 51(9), pp. 679–682. doi: 10.1038/sc.2013.52.

Hsu, M.-T. *et al.* (2015) 'Stage-Dependent Axon Transport of Proteasomes Contributes to Axon Development', *Developmental Cell*, 35(4), pp. 418–431. doi: 10.1016/j.devcel.2015.10.018.

Hu, J. and Selzer, M. (2017) 'RhoA as a target to promote neuronal survival and axon regeneration', *Neural Regeneration Research*. Medknow Publications and Media Pvt. Ltd., 12(4), p. 525. doi: 10.4103/1673-5374.205080.

Huang, S.-H. *et al.* (2013) 'BDNF-Dependent Recycling Facilitates TrkB Translocation to Postsynaptic Density during LTP via a Rab11-Dependent Pathway', *Journal of Neuroscience*, 33(21), pp. 9214–9230. doi: 10.1523/JNEUROSCI.3256-12.2013.

Huang, Z. *et al.* (2017) 'OUP accepted manuscript', *Acta Biochimica et Biophysica Sinica*, 49(8), pp. 689–695. doi: 10.1093/abbs/gmx068.

Huebner, E. A. and Strittmatter, S. M. (2009) 'Axon regeneration in the peripheral and central nervous systems.', *Results and problems in cell differentiation*. NIH Public Access, 48, pp. 339–51. doi: 10.1007/400_2009_19.

Husebye, H. *et al.* (2010) 'The Rab11a GTPase Controls Toll-like Receptor 4-Induced Activation of Interferon Regulatory Factor-3 on Phagosomes'. doi: 10.1016/j.immuni.2010.09.010.

Illis, L. S. (2011) 'Central nervous system regeneration does not occur LS Illis', 50. doi: 10.1038/sc.2011.132.

Jenkins, R. and Hunt, S. P. (1991) 'Long-term increase in the levels of c-jun mRNA and jun protein-like immunoreactivity in motor and sensory neurons following axon damage.', *Neuroscience letters*, 129(1), pp. 107–10. Available at: http://www.ncbi.nlm.nih.gov/pubmed/1922958 (Accessed: 19 March 2019).

Jones, L. L. *et al.* (2001) 'Neurotrophic factors, cellular bridges and gene therapy for spinal cord injury.', *The Journal of physiology*, 533(Pt 1), pp. 83–9. Available at: http://www.ncbi.nlm.nih.gov/pubmed/11351016 (Accessed: 1 March 2019).

Jung, H., Yoon, B. C. and Holt, C. E. (2012) 'Axonal mRNA localization and local protein synthesis in nervous system assembly, maintenance and repair', *Nature Reviews Neuroscience*, 13(5), pp. 308–324. doi: 10.1038/nrn3210.

Kalil, K. and Dent, E. W. (2014) 'Branch management: mechanisms of axon branching in the developing vertebrate CNS', *Nature Reviews Neuroscience*, 15(1), pp. 7–18. doi: 10.1038/nrn3650.

Kalil T., R. T. (1979) *Regrowth of Severed Axons in the Neonatal Central Nervous System: Establishment of Normal Connections*. Available at: http://science.sciencemag.org/ (Accessed: 2 March 2019).

Kang, J.-S. *et al.* (2008) 'Docking of Axonal Mitochondria by Syntaphilin Controls Their Mobility and Affects Short-Term Facilitation', *Cell*, 132(1), pp. 137–148. doi: 10.1016/j.cell.2007.11.024.

Kaplan, A. *et al.* (2017) 'Small-Molecule Stabilization of 14-3-3 Protein-Protein Interactions Stimulates Axon Regeneration', *Neuron*, 93(5), p. 1082–1093.e5. doi: 10.1016/j.neuron.2017.02.018.

Kawano, M. *et al.* (2006) 'Efficient Trafficking of Ceramide from the Endoplasmic Reticulum to the Golgi Apparatus Requires a VAMP-associated Protein-interacting FFAT Motif of CERT', *Journal of Biological Chemistry*, 281(40), pp. 30279–30288. doi: 10.1074/jbc.M605032200.

Keifer, J. and Kalil, K. (1991) 'Effects of infant versus adult pyramidal tract lesions on locomotor behavior in

hamsters', *Experimental Neurology*. Academic Press, 111(1), pp. 98–105. doi: 10.1016/0014-4886(91)90055-H.

Keller, J. N., Huang, F. F. and Markesbery, W. R. (2000) 'Decreased levels of proteasome activity and proteasome expression in aging spinal cord.', *Neuroscience*, 98(1), pp. 149–56. Available at: http://www.ncbi.nlm.nih.gov/pubmed/10858621 (Accessed: 7 March 2019).

van Kesteren, R. E. *et al.* (2011) 'A Gene Network Perspective on Axonal Regeneration', *Frontiers in Molecular Neuroscience*, 4, p. 46. doi: 10.3389/fnmol.2011.00046.

Kim, J.-E. *et al.* (2003) 'Axon Regeneration in Young Adult Mice Lacking Nogo-A/B', *Neuron*. Cell Press, 38(2), pp. 187–199. doi: 10.1016/S0896-6273(03)00147-8.

Kim, J.-E. *et al.* (2004) 'Nogo-66 Receptor Prevents Raphespinal and Rubrospinal Axon Regeneration and Limits Functional Recovery from Spinal Cord Injury', *Neuron*, 44(3), pp. 439–451. doi: 10.1016/j.neuron.2004.10.015.

King, V. R., McBride, A. and Priestley, J. V (2001) 'Immunohistochemical expression of the alpha5 integrin subunit in the normal adult rat central nervous system.', *Journal of neurocytology*, 30(3), pp. 243–52. Available at: http://www.ncbi.nlm.nih.gov/pubmed/11709630 (Accessed: 27 March 2019).

Koch, J. C. *et al.* (2014) 'Viral vector-mediated downregulation of RhoA increases survival and axonal regeneration of retinal ganglion cells', *Frontiers in Cellular Neuroscience*. Frontiers, 8, p. 273. doi: 10.3389/fncel.2014.00273.

Kononenko, N. L. *et al.* (2017) 'Retrograde transport of TrkB-containing autophagosomes via the adaptor AP-2 mediates neuronal complexity and prevents neurodegeneration', *Nature Communications*, 8, p. 14819. doi: 10.1038/ncomms14819.

Koseki, H. *et al.* (2017) 'Selective rab11 transport and the intrinsic regenerative ability of CNS axons', *eLife*, 6. doi: 10.7554/eLife.26956.

Kulkarni, A., Chen, J. and Maday, S. (2018) 'Neuronal autophagy and intercellular regulation of homeostasis in the brain', *Current Opinion in Neurobiology*. Elsevier Current Trends, 51, pp. 29–36. doi: 10.1016/J.CONB.2018.02.008.

Kurimoto, T. *et al.* (2010) 'Development/Plasticity/Repair Long-Distance Axon Regeneration in the Mature Optic Nerve: Contributions of Oncomodulin, cAMP, and pten Gene Deletion'. doi: 10.1523/JNEUROSCI.4340-10.2010.

Kwon, B. K. *et al.* (2004) 'Rubrospinal neurons fail to respond to brain-derived neurotrophic factor applied to the spinal cord injury site 2 months after cervical axotomy', *Experimental Neurology*, 189(1), pp. 45–57. doi: 10.1016/j.expneurol.2004.05.034.

Lalanne, F. and Ponsin, G. (2000) 'Mechanism of the phospholipid transfer protein-mediated transfer of phospholipids from model lipid vesicles to high density lipoproteins.', *Biochimica et biophysica acta*, 1487(1), pp. 82–91. Available at: http://www.ncbi.nlm.nih.gov/pubmed/10962290 (Accessed: 6 June 2019).

Lazo, O. M. *et al.* (2013) 'BDNF regulates Rab11-mediated recycling endosome dynamics to induce dendritic branching.', *The Journal of neuroscience : the official journal of the Society for Neuroscience*. Society for Neuroscience, 33(14), pp. 6112–22. doi: 10.1523/JNEUROSCI.4630-12.2013.

Leaver, S. G. *et al.* (2006) 'AAV-mediated expression of CNTF promotes long-term survival and regeneration of adult rat retinal ganglion cells', *Gene Therapy*. Nature Publishing Group, 13(18), pp. 1328–1341. doi: 10.1038/sj.gt.3302791.

Lee, J. K. *et al.* (2010) 'Assessing Spinal Axon Regeneration and Sprouting in Nogo-, MAG-, and OMgp-Deficient Mice', *Neuron*, 66(5), pp. 663–670. doi: 10.1016/j.neuron.2010.05.002.

Lehmann, M. *et al.* (1999) 'Inactivation of Rho signaling pathway promotes CNS axon regeneration.', *The Journal*

of neuroscience : the official journal of the Society for Neuroscience, 19(17), pp. 7537–47. Available at: http://www.ncbi.nlm.nih.gov/pubmed/10460260 (Accessed: 2 March 2019).

Leibinger, M. *et al.* (2017) 'Boosting CNS axon regeneration by harnessing antagonistic effects of GSK3 activity', *Proceedings of the National Academy of Sciences*, 114(27), pp. E5454–E5463. doi: 10.1073/pnas.1621225114.

Leon, S. *et al.* (2000) 'Lens injury stimulates axon regeneration in the mature rat optic nerve.', *The Journal of neuroscience : the official journal of the Society for Neuroscience*, 20(12), pp. 4615–4626. doi: 20/12/4615 [pii].

Levine, T. (2004) 'Short-range intracellular trafficking of small molecules across endoplasmic reticulum junctions', *Trends in Cell Biology*, 14(9), pp. 483–490. doi: 10.1016/j.tcb.2004.07.017.

Levkovitch-Verbin, H. *et al.* (2002) 'Translimbal laser photocoagulation to the trabecular meshwork as a model of glaucoma in rats.', *Investigative ophthalmology & visual science*, 43(2), pp. 402–10. Available at: http://www.ncbi.nlm.nih.gov/pubmed/11818384 (Accessed: 15 March 2019).

Lewis, T. L. *et al.* (2016) 'Progressive Decrease of Mitochondrial Motility during Maturation of Cortical Axons In Vitro and In Vivo', *Current Biology*, 26(19), pp. 2602–2608. doi: 10.1016/j.cub.2016.07.064.

Li, C., Hisamoto, N. and Matsumoto, K. (2015) 'Axon Regeneration Is Regulated by Ets–C/EBP Transcription Complexes Generated by Activation of the cAMP/Ca2+ Signaling Pathways', *PLOS Genetics*. Edited by K. Ashrafi. Public Library of Science, 11(10), p. e1005603. doi: 10.1371/journal.pgen.1005603.

Li, D., Field, P. M. and Raisman, G. (1995) 'Failure of Axon Regeneration in Postnatal Rat Entorhino-hippocampal Slice Coculture is Due to Maturation of the Axon, not that of the Pathway or Target', *European Journal of Neuroscience*. John Wiley & Sons, Ltd (10.1111), 7(6), pp. 1164–1171. doi: 10.1111/j.1460-9568.1995.tb01106.x.

Li, X.-Q. *et al.* (2004) 'CGRP peptide and regenerating sensory axons.', *Journal of neuropathology and experimental neurology*, 63(10), pp. 1092–103. Available at: http://www.ncbi.nlm.nih.gov/pubmed/15535136 (Accessed: 20 March 2019).

Liebscher, T. *et al.* (2005) 'Nogo-A antibody improves regeneration and locomotion of spinal cord-injured rats', *Annals of Neurology*. John Wiley & Sons, Ltd, 58(5), pp. 706–719. doi: 10.1002/ana.20627.

Lim, J.-H. A., Stafford, B. K., Nguyen, P. L., Lien, B. V, Wang, C., Zukor, K., He, Z. and Huberman, A. D. (2016) 'Neural activity promotes long-distance, target-specific regeneration of adult retinal axons', *Nature Neuroscience*. Nature Publishing Group, (July), pp. 1–14. doi: 10.1038/nn.4340.

Lim, J.-H. A., Stafford, B. K., Nguyen, P. L., Lien, B. V, Wang, C., Zukor, K., He, Z. and Huberman, A. D. (2016) 'Neural activity promotes long-distance, target-specific regeneration of adult retinal axons', *Nature Neuroscience*, 19(8), pp. 1073–1084. doi: 10.1038/nn.4340.

de Lima, S. *et al.* (2012) 'Full-length axon regeneration in the adult mouse optic nerve and partial recovery of simple visual behaviors', *Proceedings of the National Academy of Sciences*, 109(23), pp. 9149–9154. doi: 10.1073/pnas.1119449109.

Lindner, R. *et al.* (2014) 'DNA methylation temporal profiling following peripheral versus central nervous system axotomy', *Scientific Data*. Nature Publishing Group, 1, p. 140038. doi: 10.1038/sdata.2014.38.

Liu, J. S. *et al.* (2012) 'Molecular Basis for Specific Regulation of Neuronal Kinesin-3 Motors by Doublecortin Family Proteins', *Molecular Cell*, 47(5), pp. 707–721. doi: 10.1016/j.molcel.2012.06.025.

Liu, K. *et al.* (2010) 'PTEN deletion enhances the regenerative ability of adult corticospinal neurons', *Nature Neuroscience*. Nature Publishing Group, 13(9), pp. 1075–1081. doi: 10.1038/nn.2603.

Liu, S. *et al.* (2015) 'Disrupted autophagy after spinal cord injury is associated with ER stress and neuronal cell death.', *Cell death & disease*. Nature Publishing Group, 6(1), p. e1582. doi: 10.1038/cddis.2014.527.

Liu, Y. *et al.* (2017) 'A Sensitized IGF1 Treatment Restores Corticospinal Axon-Dependent Functions', *Neuron*, 95(4), p. 817–833.e4. doi: 10.1016/j.neuron.2017.07.037.

Loh, Y.-H. E. *et al.* (2017) 'Comprehensive mapping of 5-hydroxymethylcytosine epigenetic dynamics in axon regeneration', *Epigenetics*, 12(2), pp. 77–92. doi: 10.1080/15592294.2016.1264560.

Lopez de Heredia, L. and Magoulas, C. (2013) 'Lack of the transcription factor C/EBPδ impairs the intrinsic capacity of peripheral neurons for regeneration.', *Experimental neurology*, 239, pp. 148–57. doi: 10.1016/j.expneurol.2012.10.012.

Lu, P., Blesch, A. and Tuszynski, M. H. (2001) 'Neurotrophism without neurotropism: BDNF promotes survival but not growth of lesioned corticospinal neurons.', *The Journal of comparative neurology*, 436(4), pp. 456–70. Available at: http://www.ncbi.nlm.nih.gov/pubmed/11447589 (Accessed: 5 March 2019).

Lu, P. and Tuszynski, M. H. (2008) 'Growth factors and combinatorial therapies for CNS regeneration', *Experimental Neurology*, 209(2), pp. 313–320. doi: 10.1016/j.expneurol.2007.08.004.

Luo, X. *et al.* (2013) 'Three-dimensional evaluation of retinal ganglion cell axon regeneration and pathfinding in whole mouse tissue after injury', *Experimental Neurology*, 247, pp. 653–662. doi: 10.1016/j.expneurol.2013.03.001.

Ma, D. K. *et al.* (2010) 'Epigenetic choreographers of neurogenesis in the adult mammalian brain', *Nature Neuroscience*, 13(11), pp. 1338–1344. doi: 10.1038/nn.2672.

Ma, T. C. and Willis, D. E. (2015) 'What makes a RAG regeneration associated?', *Frontiers in Molecular Neuroscience*, 8, p. 43. doi: 10.3389/fnmol.2015.00043.

Maday, S. and Holzbaur, E. L. F. (2014) 'Article Autophagosome Biogenesis in Primary Neurons Follows an Ordered and Spatially Regulated Pathway', *Developmental Cell*, 30, pp. 71–85. doi: 10.1016/j.devcel.2014.06.001.

Maday, S. and Holzbaur, E. L. F. (2016) 'Compartment-Specific Regulation of Autophagy in Primary Neurons', *The Journal of Neuroscience*, 36(22), pp. 5933–5945. doi: 10.1523/JNEUROSCI.4401-15.2016.

Maday, S., Wallace, K. E. and Holzbaur, E. L. F. (2012) 'Autophagosomes initiate distally and mature during transport toward the cell soma in primary neurons', *The Journal of Cell Biology*, 196(4), pp. 407–417. doi: 10.1083/jcb.201106120.

Mannan, A. U. *et al.* (2006) 'ZFYVE27 (SPG33), a Novel Spastin-Binding Protein, Is Mutated in Hereditary Spastic Paraplegia', *The American Journal of Human Genetics*, 79(2), pp. 351–357. doi: 10.1086/504927.

Mar, F. M. *et al.* (2014) 'CNS Axons Globally Increase Axonal Transport after Peripheral Conditioning', *Journal of Neuroscience*, 34(17), pp. 5965–5970. doi: 10.1523/JNEUROSCI.4680-13.2014.

Marina, N., Bull, N. D. and Martin, K. R. (2010) 'A semiautomated targeted sampling method to assess optic nerve axonal loss in a rat model of glaucoma', *Nature Protocols*, 5(10), pp. 1642–1651. doi: 10.1038/nprot.2010.128.

Martignoni, M., Riano, E. and Rugarli, E. I. (2008) 'The role of ZFYVE27/protrudin in hereditary spastic paraplegia.', *American journal of human genetics*. Elsevier, 83(1), pp. 127-8; author reply 128-30. doi: 10.1016/j.ajhg.2008.05.014.

Martin, K. R. G. *et al.* (2003) 'Gene Therapy with Brain-Derived Neurotrophic Factor As a Protection: Retinal Ganglion Cells in a Rat Glaucoma Model', *Investigative Opthalmology & Visual Science*. The Association for Research in Vision and Ophthalmology, 44(10), p. 4357. doi: 10.1167/iovs.02-1332.

Martinez-Arca, S. *et al.* (2000) 'Role of tetanus neurotoxin insensitive vesicle-associated membrane protein (TI-

VAMP) in vesicular transport mediating neurite outgrowth.', *The Journal of cell biology*. Rockefeller University Press, 149(4), pp. 889–900. doi: 10.1083/jcb.149.4.889.

Mason, M. R. J. *et al.* (2002) 'Transcriptional upregulation of SCG10 and CAP-23 is correlated with regeneration of the axons of peripheral and central neurons in vivo.', *Molecular and cellular neurosciences*, 20(4), pp. 595–615. Available at: http://www.ncbi.nlm.nih.gov/pubmed/12213442 (Accessed: 19 March 2019).

Matamoros, A. J. *et al.* (2019) 'Knockdown of Fidgetin Improves Regeneration of Injured Axons by a Microtubule-Based Mechanism.', *The Journal of neuroscience : the official journal of the Society for Neuroscience*. Society for Neuroscience, 39(11), pp. 2011–2024. doi: 10.1523/JNEUROSCI.1888-18.2018.

Matsuzaki, F. *et al.* (2011) 'Protrudin serves as an adaptor molecule that connects KIF5 and its cargoes in vesicular transport during process formation.', *Molecular biology of the cell*, 22(23), pp. 4602–20. doi: 10.1091/mbc.E11-01-0068.

McKerracher, L., Vidal-Sanz, M. and Aguayo, A. J. (1990) 'Slow transport rates of cytoskeletal proteins change during regeneration of axotomized retinal neurons in adult rats.', *The Journal of neuroscience : the official journal of the Society for Neuroscience*, 10(2), pp. 641–8. Available at: http://www.ncbi.nlm.nih.gov/pubmed/2106015 (Accessed: 4 March 2019).

McQuarrie, I. G., Brady, S. T. and Lasek, R. J. (1989) 'Retardation in the slow axonal transport of cytoskeletal elements during maturation and aging', *Neurobiology of Aging*. Elsevier, 10(4), pp. 359–365. doi: 10.1016/0197-4580(89)90049-3.

McQuarrie, I. G. and Grafstein, B. (1982) 'Protein synthesis and axonal transport in goldfish retinal ganglion cells during regeneration accelerated by a conditioning lesion.', *Brain research*, 251(1), pp. 25–37. Available at: http://www.ncbi.nlm.nih.gov/pubmed/6184129 (Accessed: 4 March 2019).

McQuarrie, I. G. and Jacob, J. M. (1991) 'Conditioning nerve crush accelerates cytoskeletal protein transport in sprouts that form after a subsequent crush', *The Journal of Comparative Neurology*, 305(1), pp. 139–147. doi: 10.1002/cne.903050113.

Mearow, K. M. *et al.* (1994) 'Expression of NGF receptor and GAP-43 mRNA in DRG neurons during collateral sprouting and regeneration of dorsal cutaneous nerves', *Journal of Neurobiology*, 25(2), pp. 127–142. doi: 10.1002/neu.480250205.

Mehta, S. T. *et al.* (2016) 'Hyperactivated Stat3 boosts axon regeneration in the CNS', *Experimental Neurology*, 280, pp. 115–120. doi: 10.1016/j.expneurol.2016.03.004.

Menei, P. *et al.* (1998) 'Schwann cells genetically modified to secrete human BDNF promote enhanced axonal regrowth across transected adult rat spinal cord.', *The European journal of neuroscience*, 10(2), pp. 607–21. Available at: http://www.ncbi.nlm.nih.gov/pubmed/9749723 (Accessed: 1 March 2019).

Meyer, R. L., Miotke, J. A. and Benowitz, L. I. (1994) 'Injury induced expression of growth-associated protein-43 in adult mouse retinal ganglion cells in vitro.', *Neuroscience*, 63(2), pp. 591–602. Available at: http://www.ncbi.nlm.nih.gov/pubmed/7891867 (Accessed: 17 March 2019).

Milde, S. *et al.* (2015) 'Axonal transport declines with age in two distinct phases separated by a period of relative stability.', *Neurobiology of aging*. Elsevier, 36(2), pp. 971–81. doi: 10.1016/j.neurobiolaging.2014.09.018.

Mladinic, M. (2007) 'Changes in Cyclic AMP Levels in the Developing Opossum Spinal Cord at the Time When Regeneration Stops Being Possible', *Cellular and Molecular Neurobiology*. Springer US, 27(7), pp. 883–888. doi: 10.1007/s10571-007-9208-3.

Mladinic, M. *et al.* (2010) 'Developmental changes of gene expression after spinal cord injury in neonatal opossums', *Brain Research*. Elsevier, 1363, pp. 20–39. doi: 10.1016/J.BRAINRES.2010.09.024.

Mladinic, M. and Wintzer, M. (2002) 'Changes in mRNA content of developing opossum spinal cord at stages when regeneration can and cannot occur after injury', *Brain Research Reviews*. Elsevier, 40(1–3), pp. 317–324. doi: 10.1016/S0165-0173(02)00214-X.

Moon, L. D. F. *et al.* (2001) 'Regeneration of CNS axons back to their target following treatment of adult rat brain with chondroitinase ABC', *Nature Neuroscience*. Nature Publishing Group, 4(5), pp. 465–466. doi: 10.1038/87415.

Moore, D. L. *et al.* (2009) 'KLF Family Members Regulate Intrinsic Axon Regeneration Ability', *Science*, 326(5950), pp. 298–301. doi: 10.1126/science.1175737.

Mori, F. *et al.* (1997) *Fetal Spinal Cord Transplants Rescue Some Axotomized Rubrospinal Neurons from Retrograde Cell Death in Adult Rats*. Available at: https://ac.els-cdn.com/S0014488696963189/1-s2.0-S0014488696963189-main.pdf?_tid=882f023e-3f76-411e-8ed6-07b8646b861f&acdnat=1551547434_751c4460ca509f8076614adf6736abe6 (Accessed: 2 March 2019).

Mortillo, S. *et al.* (2012) 'Compensatory redistribution of neuroligins and N-cadherin following deletion of synaptic β1-integrin', *The Journal of Comparative Neurology*, 520(9), pp. 2041–2052. doi: 10.1002/cne.23027.

Murray, M. *et al.* (2011) 'Peripheral nerve graft with immunosuppression modifies gene expression in axotomized CNS neurons', *The Journal of Comparative Neurology*, 519(17), pp. 3433–3455. doi: 10.1002/cne.22714.

Nadeau, S. *et al.* (2005) 'A transcriptional role for C/EBP β in the neuronal response to axonal injury', *Molecular and Cellular Neuroscience*, 29(4), pp. 525–535. doi: 10.1016/j.mcn.2005.04.004.

Nakagomi, S. *et al.* (2003) 'Expression of the activating transcription factor 3 prevents c-Jun N-terminal kinase-induced neuronal death by promoting heat shock protein 27 expression and Akt activation.', *The Journal of neuroscience : the official journal of the Society for Neuroscience*, 23(12), pp. 5187–96. Available at: http://www.ncbi.nlm.nih.gov/pubmed/12832543 (Accessed: 19 March 2019).

Nawabi, H. *et al.* (2015) 'Doublecortin-Like Kinases Promote Neuronal Survival and Induce Growth Cone Reformation via Distinct Mechanisms', *Neuron*, 88(4), pp. 704–719. doi: 10.1016/j.neuron.2015.10.005.

Neumann, S. *et al.* (2002) 'Regeneration of sensory axons within the injured spinal cord induced by intraganglionic cAMP elevation.', *Neuron*, 34(6), pp. 885–93. Available at: http://www.ncbi.nlm.nih.gov/pubmed/12086637 (Accessed: 19 March 2019).

Neumann, S. and Woolf, C. J. (1999) 'Regeneration of dorsal column fibers into and beyond the lesion site following adult spinal cord injury.', *Neuron*, 23(1), pp. 83–91. Available at: http://www.ncbi.nlm.nih.gov/pubmed/10402195 (Accessed: 1 March 2019).

Nicholls, J. and Saunders, N. (1996) 'Regeneration of immature mammalian spinal cord after injury', *Trends in Neurosciences*. Elsevier Current Trends, 19(6), pp. 229–234. doi: 10.1016/0166-2236(96)10021-7.

Nieuwenhuis, B. *et al.* (2018) 'Integrins promote axonal regeneration after injury of the nervous system', *Biological Reviews*. John Wiley & Sons, Ltd (10.1111), 93(3), pp. 1339–1362. doi: 10.1111/brv.12398.

Noh, K.-M. *et al.* (2012) 'Repressor element-1 silencing transcription factor (REST)-dependent epigenetic remodeling is critical to ischemia-induced neuronal death', *Proceedings of the National Academy of Sciences*, 109(16), pp. E962–E971. doi: 10.1073/pnas.1121568109.

Norsworthy, M. W. *et al.* (2017) 'Sox11 Expression Promotes Regeneration of Some Retinal Ganglion Cell Types but Kills Others', *Neuron*, 94(6), p. 1112–1120.e4. doi: 10.1016/j.neuron.2017.05.035.

O'Donnell, M., Chance, R. K. and Bashaw, G. J. (2009) 'Axon Growth and Guidance: Receptor Regulation and Signal Transduction', *Annual Review of Neuroscience*, 32(1), pp. 383–412. doi:

10.1146/annurev.neuro.051508.135614.

O'Sullivan, N. C. *et al.* (2012) 'Reticulon-like-1, the Drosophila orthologue of the Hereditary Spastic Paraplegia gene reticulon 2, is required for organization of endoplasmic reticulum and of distal motor axons', *Human Molecular Genetics*, 21(15), pp. 3356–3365. doi: 10.1093/hmg/dds167.

Oblinger, M. M. and Lasek, R. J. (1988) 'Axotomy-induced alterations in the synthesis and transport of neurofilaments and microtubules in dorsal root ganglion cells.', *The Journal of neuroscience : the official journal of the Society for Neuroscience*, 8(5), pp. 1747–58. Available at: http://www.ncbi.nlm.nih.gov/pubmed/3130470 (Accessed: 4 March 2019).

Oh, Y. M. *et al.* (2018) 'Epigenetic regulator UHRF1 inactivates REST and growth suppressor gene expression via DNA methylation to promote axon regeneration', *Proceedings of the National Academy of Sciences*, 115(52), pp. E12417–E12426. doi: 10.1073/pnas.1812518115.

Ohtake, Y., Hayat, U. and Li, S. (2015) 'PTEN inhibition and axon regeneration and neural repair.', *Neural regeneration research*. Wolters Kluwer -- Medknow Publications, 10(9), pp. 1363–8. doi: 10.4103/1673-5374.165496.

Osborne, A. *et al.* (2018) 'Neuroprotection of retinal ganglion cells by a novel gene therapy construct that achieves sustained enhancement of brain-derived neurotrophic factor/tropomyosin-related kinase receptor-B signaling', *Cell Death & Disease*. Nature Publishing Group, 9(10), p. 1007. doi: 10.1038/s41419-018-1041-8.

Otero, M. G. *et al.* (2014) 'Fast axonal transport of the proteasome complex depends on membrane interaction and molecular motor function', *Journal of Cell Science*, 127(7), pp. 1537–1549. doi: 10.1242/jcs.140780.

Özdinler, P. H. and Macklis, J. D. (2006) 'IGF-I specifically enhances axon outgrowth of corticospinal motor neurons', *Nature Neuroscience*, 9(11), pp. 1371–1381. doi: 10.1038/nn1789.

Pan, Y.-X. *et al.* (2007) 'Activation of the *ATF3* gene through a co-ordinated amino acid-sensing response programme that controls transcriptional regulation of responsive genes following amino acid limitation', *Biochemical Journal*, 401(1), pp. 299–307. doi: 10.1042/BJ20061261.

Pan, Y. A. *et al.* (2003) 'Effects of neurotoxic and neuroprotective agents on peripheral nerve regeneration assayed by time-lapse imaging in vivo.', *The Journal of neuroscience : the official journal of the Society for Neuroscience*, 23(36), pp. 11479–88. Available at: http://www.ncbi.nlm.nih.gov/pubmed/14673013 (Accessed: 7 March 2019).

Pantakani, D. V. K. *et al.* (2011) 'Oligomerization of ZFYVE27 (Protrudin) Is Necessary to Promote Neurite Extension', *PLoS ONE*. Edited by M. Gasset. Public Library of Science, 6(12), p. e29584. doi: 10.1371/journal.pone.0029584.

Parent, A. *et al.* (2009) 'Rab11 regulates the recycling of the beta2-adrenergic receptor through a direct interaction.', *The Biochemical journal*. Portland Press Limited, 418(1), pp. 163–72. doi: 10.1042/BJ20080867.

Park, K. K. *et al.* (2008) 'Promoting Axon Regeneration in the Adult CNS by Modulation of the PTEN/mTOR Pathway', *Science*, 322(5903), pp. 963–966. doi: 10.1126/science.1161566.

Park, K. K. *et al.* (2008) 'Promoting Axon Regeneration in the Adult CNS by Modulation of the PTEN/mTOR Pathway', *Science*, 322(5903), pp. 963–966. doi: 10.1126/science.1161566.

Park, M. *et al.* (2004) 'Recycling endosomes supply AMPA receptors for LTP.', *Science (New York, N.Y.)*. American Association for the Advancement of Science, 305(5692), pp. 1972–5. doi: 10.1126/science.1102026.

Pearson, A. G. *et al.* (2003) 'ATF3 enhances c-Jun-mediated neurite sprouting.', *Brain research. Molecular brain research*, 120(1), pp. 38–45. Available at: http://www.ncbi.nlm.nih.gov/pubmed/14667575 (Accessed: 19 March 2019).

Pearson, C. S. *et al.* (2018) 'Identification of a critical sulfation in chondroitin that inhibits axonal regeneration', *eLife*, 7. doi: 10.7554/eLife.37139.

Pease, M. E. *et al.* (2000) 'Obstructed axonal transport of BDNF and its receptor TrkB in experimental glaucoma.', *Investigative ophthalmology & visual science*, 41(3), pp. 764–74. Available at: http://www.ncbi.nlm.nih.gov/pubmed/10711692 (Accessed: 15 March 2019).

Pease, M. E. *et al.* (2009) 'Effect of CNTF on Retinal Ganglion Cell Survival in Experimental Glaucoma', *Investigative Opthalmology & Visual Science*, 50(5), p. 2194. doi: 10.1167/iovs.08-3013.

Penzes, P. and Rafalovich, I. (2012) 'Regulation of the Actin Cytoskeleton in Dendritic Spines', in *Advances in experimental medicine and biology*, pp. 81–95. doi: 10.1007/978-3-7091-0932-8_4.

Pernet, V. *et al.* (2013) 'Long-distance axonal regeneration induced by CNTF gene transfer is impaired by axonal misguidance in the injured adult optic nerve', *Neurobiology of Disease*, 51, pp. 202–213. doi: 10.1016/j.nbd.2012.11.011.

Pernet, V. *et al.* (2013) 'Misguidance and modulation of axonal regeneration by Stat3 and Rho/ROCK signaling in the transparent optic nerve', *Cell Death & Disease*. Nature Publishing Group, 4(7), pp. e734–e734. doi: 10.1038/cddis.2013.266.

Petkovic, M. *et al.* (2014) 'The SNARE Sec22b has a non-fusogenic function in plasma membrane expansion', *Nature Cell Biology*. Nature Publishing Group, 16(5), pp. 434–444. doi: 10.1038/ncb2937.

Petrova, V. and Eva, R. (2018) 'The Virtuous Cycle of Axon Growth: Axonal Transport of Growth-Promoting Machinery as an Intrinsic Determinant of Axon Regeneration', *Developmental Neurobiology*, 78(10), pp. 898–925. doi: 10.1002/dneu.22608.

Plunet, W., Kwon, B. K. and Tetzlaff, W. (2002) 'Promoting axonal regeneration in the central nervous system by enhancing the cell body response to axotomy', *Journal of Neuroscience Research*, 68(1), pp. 1–6. doi: 10.1002/jnr.10176.

des Portes, V. *et al.* (1998) 'Doublecortin Is the Major Gene Causing X-Linked Subcortical Laminar Heterotopia (SCLH)', *Human Molecular Genetics*, 7(7), pp. 1063–1070. doi: 10.1093/hmg/7.7.1063.

Powelka, A. M. *et al.* (2004) 'Stimulation-dependent recycling of integrin beta1 regulated by ARF6 and Rab11.', *Traffic (Copenhagen, Denmark)*, 5(1), pp. 20–36. Available at: http://www.ncbi.nlm.nih.gov/pubmed/14675422 (Accessed: 4 March 2019).

Prekeris, R., Foletti, D. L. and Scheller, R. H. (1999) 'Dynamics of tubulovesicular recycling endosomes in hippocampal neurons.', *The Journal of neuroscience : the official journal of the Society for Neuroscience*, 19(23), pp. 10324–37. Available at: http://www.ncbi.nlm.nih.gov/pubmed/10575030 (Accessed: 20 March 2019).

Puttagunta, R. *et al.* (2014) 'PCAF-dependent epigenetic changes promote axonal regeneration in the central nervous system', *Nature Communications*, 5(1), p. 3527. doi: 10.1038/ncomms4527.

Qiu, J. *et al.* (2002) 'Spinal axon regeneration induced by elevation of cyclic AMP.', *Neuron*, 34(6), pp. 895–903. Available at: http://www.ncbi.nlm.nih.gov/pubmed/12086638 (Accessed: 1 March 2019).

Qiu, J. *et al.* (2005) 'Development/Plasticity/Repair Conditioning Injury-Induced Spinal Axon Regeneration Requires Signal Transducer and Activator of Transcription 3 Activation'. doi: 10.1523/JNEUROSCI.3269-04.2005.

Quigley, H. A. *et al.* (2000) 'Retrograde axonal transport of BDNF in retinal ganglion cells is blocked by acute IOP elevation in rats.', *Investigative ophthalmology & visual science*, 41(11), pp. 3460–6. Available at: http://www.ncbi.nlm.nih.gov/pubmed/11006239 (Accessed: 15 March 2019).

Raiborg, C. *et al.* (2015) 'Repeated ER–endosome contacts promote endosome translocation and neurite

outgrowth', *Nature*, 520(7546), pp. 234–238. doi: 10.1038/nature14359.

Raivich, G. *et al.* (2004) 'The AP-1 Transcription Factor c-Jun Is Required for Efficient Axonal Regeneration', *Neuron*, 43(1), pp. 57–67. doi: 10.1016/j.neuron.2004.06.005.

Rajagopalan, S. *et al.* (2007) 'Use of a Constitutively Active Hypoxia-Inducible Factor-1α Transgene as a Therapeutic Strategy in No-Option Critical Limb Ischemia Patients', *Circulation*, 115(10), pp. 1234–1243. doi: 10.1161/CIRCULATIONAHA.106.607994.

Ramon y Cajal, S. (1928) *Degeneration and regeneration of the nervous system.*, *Degeneration and regeneration of the nervous system.* Oxford, England: Clarendon Press.

Rao, K. *et al.* (2016) 'Spastin, atlastin, and ER relocalization are involved in axon but not dendrite regeneration.', *Molecular biology of the cell*. American Society for Cell Biology, 27(21), pp. 3245–3256. doi: 10.1091/mbc.E16-05-0287.

Rasband, M. N. (2010) 'The axon initial segment and the maintenance of neuronal polarity', *Nature Reviews Neuroscience*. Nature Publishing Group, 11(8), pp. 552–562. doi: 10.1038/nrn2852.

Ren, M. *et al.* (1998) 'Hydrolysis of GTP on rab11 is required for the direct delivery of transferrin from the pericentriolar recycling compartment to the cell surface but not from sorting endosomes.', *Proceedings of the National Academy of Sciences of the United States of America*. National Academy of Sciences, 95(11), pp. 6187–92. doi: 10.1073/PNAS.95.11.6187.

Richardson, P. M. and Issa, V. M. (no date) 'Peripheral injury enhances central regeneration of primary sensory neurones.', *Nature*, 309(5971), pp. 791–3. Available at: http://www.ncbi.nlm.nih.gov/pubmed/6204205 (Accessed: 19 March 2019).

Richardson, P. M., Issa, V. M. and Aguayo, A. J. (1984) 'Regeneration of long spinal axons in the rat.', *Journal of neurocytology*, 13(1), pp. 165–82. Available at: http://www.ncbi.nlm.nih.gov/pubmed/6707710 (Accessed: 1 March 2019).

Richardson, P. M., McGuinness, U. M. and Aguayo, A. J. (1980) 'Axons from CNS neurones regenerate into PNS grafts', *Nature*. Nature Publishing Group, 284(5753), pp. 264–265. doi: 10.1038/284264a0.

Rodriguez, A. R., de Sevilla Müller, L. P. and Brecha, N. C. (2014) 'The RNA binding protein RBPMS is a selective marker of ganglion cells in the mammalian retina', *Journal of Comparative Neurology*, 522(6), pp. 1411–1443. doi: 10.1002/cne.23521.

Romanelli, R. J. *et al.* (2007) 'Insulin-like Growth Factor Type-I Receptor Internalization and Recycling Mediate the Sustained Phosphorylation of Akt', *Journal of Biological Chemistry*, 282(31), pp. 22513–22524. doi: 10.1074/jbc.M704309200.

Rouaux, C. and Arlotta, P. (2013) 'Direct lineage reprogramming of post-mitotic callosal neurons into corticofugal neurons in vivo', *Nature Cell Biology*. Nature Publishing Group, 15(2), pp. 214–221. doi: 10.1038/ncb2660.

Ruschel, J. *et al.* (2015) 'Systemic administration of epothilone B promotes axon regeneration after spinal cord injury', *Science*, 348(6232). doi: 10.1126/science.aaa2958.

Ruschel, J. and Bradke, F. (2018) 'Systemic administration of epothilone D improves functional recovery of walking after rat spinal cord contusion injury', *Experimental Neurology*, 306, pp. 243–249. doi: 10.1016/j.expneurol.2017.12.001.

Saita, S. *et al.* (2009) 'Promotion of Neurite Extension by Protrudin Requires Its Interaction with Vesicle-associated Membrane Protein-associated Protein', *Journal of Biological Chemistry*, 284(20), pp. 13766–13777. doi: 10.1074/jbc.M807938200.

Salminen, A. and Novick, P. J. (1987) 'A ras-like protein is required for a post-Golgi event in yeast secretion', *Cell*. Cell Press, 49(4), pp. 527–538. doi: 10.1016/0092-8674(87)90455-7.

Schindelin, J. *et al.* (2012) 'Fiji: an open-source platform for biological-image analysis.', *Nature methods*. NIH Public Access, 9(7), pp. 676–82. doi: 10.1038/nmeth.2019.

Schmitz, S. K. *et al.* (2011) 'Automated analysis of neuronal morphology, synapse number and synaptic recruitment', *Journal of Neuroscience Methods*. Elsevier, 195(2), pp. 185–193. doi: 10.1016/J.JNEUMETH.2010.12.011.

Schultz J. (2016) *Laser Treatment for Glaucoma - Independence, OH - Eye Care*. Available at: https://www.myeyedoc.com/blog/2016/05/07/laser-treatment-for-glaucoma-169933 (Accessed: 15 March 2019).

Schwab, M. E. and Bartholdi, D. (1996) 'Degeneration and regeneration of axons in the lesioned spinal cord', *Physiological Reviews*, 76(2), pp. 319–370. doi: 10.1152/physrev.1996.76.2.319.

Schwaiger, F. W. *et al.* (2000) 'Peripheral but not central axotomy induces changes in Janus kinases (JAK) and signal transducers and activators of transcription (STAT).', *The European journal of neuroscience*, 12(4), pp. 1165–76. Available at: http://www.ncbi.nlm.nih.gov/pubmed/10762348 (Accessed: 19 March 2019).

Seijffers, R., Allchorne, A. J. and Woolf, C. J. (2006) 'The transcription factor ATF-3 promotes neurite outgrowth', *Molecular and Cellular Neuroscience*, 32(1–2), pp. 143–154. doi: 10.1016/j.mcn.2006.03.005.

Seijffers, R., Mills, C. D. and Woolf, C. J. (2007) 'ATF3 Increases the Intrinsic Growth State of DRG Neurons to Enhance Peripheral Nerve Regeneration', *Journal of Neuroscience*, 27(30), pp. 7911–7920. doi: 10.1523/JNEUROSCI.5313-06.2007.

Shaw, G. and Bray, D. (1977) 'Movement and extension of isolated growth cones.', *Experimental cell research*, 104(1), pp. 55–62. Available at: http://www.ncbi.nlm.nih.gov/pubmed/556695 (Accessed: 7 March 2019).

Sheehan, D. *et al.* (1996) 'A somatodendritic distribution of Rab11 in rabbit brain neurons.', *Neuroreport*, 7(7), pp. 1297–300. Available at: http://www.ncbi.nlm.nih.gov/pubmed/8817553 (Accessed: 4 March 2019).

Shen, Y. *et al.* (2009) 'PTPsigma is a receptor for chondroitin sulfate proteoglycan, an inhibitor of neural regeneration.', *Science (New York, N.Y.)*. NIH Public Access, 326(5952), pp. 592–6. doi: 10.1126/science.1178310.

Sheppard, A. M., Hamilton, S. K. and Pearlman, A. L. (1991) 'Changes in the distribution of extracellular matrix components accompany early morphogenetic events of mammalian cortical development.', *The Journal of neuroscience : the official journal of the Society for Neuroscience*, 11(12), pp. 3928–42. Available at: http://www.ncbi.nlm.nih.gov/pubmed/1720815 (Accessed: 19 March 2019).

Shewan, D., Berry, M. and Cohen, J. (1995) 'Extensive regeneration in vitro by early embryonic neurons on immature and adult CNS tissue.', *The Journal of neuroscience : the official journal of the Society for Neuroscience*, 15(3 Pt 1), pp. 2057–62. Available at: http://www.ncbi.nlm.nih.gov/pubmed/7891152 (Accessed: 2 March 2019).

Shirane, M. *et al.* (2008) 'Regulation of apoptosis and neurite extension by FKBP38 is required for neural tube formation in the mouse', *Genes to Cells*, 13(6), pp. 635–651. doi: 10.1111/j.1365-2443.2008.01194.x.

Shirane, M. and Nakayama, K. I. (2006) 'Protrudin Induces Neurite Formation by Directional Membrane Trafficking', *Science*, 314(5800), pp. 818–821. doi: 10.1126/science.1134027.

da Silva, S. and Wang, F. (2011) 'Retrograde neural circuit specification by target-derived neurotrophins and growth factors', *Current Opinion in Neurobiology*, 21(1), pp. 61–67. doi: 10.1016/j.conb.2010.07.007.

Skene, J. H. and Willard, M. (1981) 'Axonally transported proteins associated with axon growth in rabbit central and peripheral nervous systems.', *The Journal of cell biology*, 89(1), pp. 96–103. Available at:

http://www.ncbi.nlm.nih.gov/pubmed/6164683 (Accessed: 4 March 2019).

Smith, B. N. *et al.* (2014) 'Exome-wide Rare Variant Analysis Identifies TUBA4A Mutations Associated with Familial ALS', *Neuron*, 84(2), pp. 324–331. doi: 10.1016/j.neuron.2014.09.027.

Smith, D. S. and Skene, J. H. (1997) 'A transcription-dependent switch controls competence of adult neurons for distinct modes of axon growth.', *The Journal of neuroscience : the official journal of the Society for Neuroscience*, 17(2), pp. 646–58. Available at: http://www.ncbi.nlm.nih.gov/pubmed/8987787 (Accessed: 19 March 2019).

Smith, P. D. *et al.* (2009) 'SOCS3 Deletion Promotes Optic Nerve Regeneration In Vivo', *Neuron*, 64(5), pp. 617–623. doi: 10.1016/j.neuron.2009.11.021.

Smith, R. P. *et al.* (2011) 'Transcriptional profiling of intrinsic PNS factors in the postnatal mouse', *Molecular and Cellular Neuroscience*, 46(1), pp. 32–44. doi: 10.1016/j.mcn.2010.07.015.

Song, A. *et al.* (2009) 'A Selective Filter for Cytoplasmic Transport at the Axon Initial Segment', *Cell*, 136(6), pp. 1148–1160. doi: 10.1016/j.cell.2009.01.016.

Song, M. *et al.* (2015) 'Slitrk5 Mediates BDNF-Dependent TrkB Receptor Trafficking and Signaling.', *Developmental cell*. NIH Public Access, 33(6), pp. 690–702. doi: 10.1016/j.devcel.2015.04.009.

Sosa, L. *et al.* (2006) 'IGF-1 receptor is essential for the establishment of hippocampal neuronal polarity', *Nature Neuroscience*. Nature Publishing Group, 9(8), pp. 993–995. doi: 10.1038/nn1742.

Starkey, M. L. *et al.* (2009) 'Expression of the regeneration-associated protein SPRR1A in primary sensory neurons and spinal cord of the adult mouse following peripheral and central injury', *The Journal of Comparative Neurology*, 513(1), pp. 51–68. doi: 10.1002/cne.21944.

Stenmark, H. (2009) 'Rab GTPases as coordinators of vesicle traffic', *Nature Reviews Molecular Cell Biology*. Nature Publishing Group, 10(8), pp. 513–525. doi: 10.1038/nrm2728.

Sui, W.-H. *et al.* (no date) 'Myosin Va mediates BDNF-induced postendocytic recycling of full-length TrkB and its translocation into dendritic spines', *Journal of Cell Science*. doi: 10.1242/jcs.160259.

Sun, F. *et al.* (2011) 'Sustained axon regeneration induced by co-deletion of PTEN and SOCS3.', *Nature*. NIH Public Access, 480(7377), pp. 372–5. doi: 10.1038/nature10594.

Takahashi, K. and Yamanaka, S. (2006) 'Induction of pluripotent stem cells from mouse embryonic and adult fibroblast cultures by defined factors.', *Cell*. Elsevier, 126(4), pp. 663–76. doi: 10.1016/j.cell.2006.07.024.

Tan, C. L. *et al.* (2012) 'Kindlin-1 Enhances Axon Growth on Inhibitory Chondroitin Sulfate Proteoglycans and Promotes Sensory Axon Regeneration', *Journal of Neuroscience*, 32(21), pp. 7325–7335. doi: 10.1523/JNEUROSCI.5472-11.2012.

Tang, Z. *et al.* (2011) 'An Optic Nerve Crush Injury Murine Model to Study Retinal Ganglion Cell Survival', *Journal of Visualized Experiments*, (50). doi: 10.3791/2685.

Tas, R. P. *et al.* (2017) 'Differentiation between Oppositely Oriented Microtubules Controls Polarized Neuronal Transport.', *Neuron*. Elsevier, 96(6), p. 1264–1271.e5. doi: 10.1016/j.neuron.2017.11.018.

Taylor, A. M. *et al.* (2009) 'Axonal mRNA in Uninjured and Regenerating Cortical Mammalian Axons', *Journal of Neuroscience*, 29(15), pp. 4697–4707. doi: 10.1523/JNEUROSCI.6130-08.2009.

Tedeschi, A. *et al.* (2009) 'A p53-CBP/p300 transcription module is required for GAP-43 expression, axon outgrowth and regeneration', *Cell Death & Differentiation*, 16(4), pp. 543–554. doi: 10.1038/cdd.2008.175.

Tedeschi, A. *et al.* (2016) 'The Calcium Channel Subunit Alpha2delta2 Suppresses Axon Regeneration in the Adult

CNS', *Neuron*, 92(2), pp. 419–434. doi: 10.1016/j.neuron.2016.09.026.

Tedeschi, A. and Bradke, F. (2017) 'Spatial and temporal arrangement of neuronal intrinsic and extrinsic mechanisms controlling axon regeneration', *Current Opinion in Neurobiology*. Elsevier Current Trends, 42, pp. 118–127. doi: 10.1016/J.CONB.2016.12.005.

Templeton, J. P. and Geisert, E. E. (2012) 'A practical approach to optic nerve crush in the mouse.', *Molecular vision*. Emory University, 18, pp. 2147–52. Available at: http://www.ncbi.nlm.nih.gov/pubmed/22876142 (Accessed: 15 March 2019).

Terenzio, M. *et al.* (2018) 'Locally translated mTOR controls axonal local translation in nerve injury.', *Science (New York, N.Y.)*. American Association for the Advancement of Science, 359(6382), pp. 1416–1421. doi: 10.1126/science.aan1053.

Terrado, J. *et al.* (1999) 'Expression of the genes for alpha-type and beta-type calcitonin gene-related peptide during rat embryogenesis.', *Neuroscience*, 92(2), pp. 713–27. Available at: http://www.ncbi.nlm.nih.gov/pubmed/10408620 (Accessed: 20 March 2019).

Tetzlaff, W. *et al.* (1989) 'Axonal transport and localization of B-50/GAP-43-like immunoreactivity in regenerating sciatic and facial nerves of the rat.', *The Journal of neuroscience : the official journal of the Society for Neuroscience*, 9(4), pp. 1303–13. Available at: http://www.ncbi.nlm.nih.gov/pubmed/2703878 (Accessed: 17 March 2019).

Tetzlaff, W. *et al.* (1991) 'Response of facial and rubrospinal neurons to axotomy: changes in mRNA expression for cytoskeletal proteins and GAP-43.', *The Journal of neuroscience : the official journal of the Society for Neuroscience*, 11(8), pp. 2528–44. Available at: http://www.ncbi.nlm.nih.gov/pubmed/1831228 (Accessed: 17 March 2019).

Tetzlaff, W. *et al.* (1994) 'Response of rubrospinal and corticospinal neurons to injury and neurotrophins.', *Progress in brain research*, 103, pp. 271–86. Available at: http://www.ncbi.nlm.nih.gov/pubmed/7886211 (Accessed: 19 March 2019).

Tohda, C. *et al.* (2001) 'Axonal transport of VR1 capsaicin receptor mRNA in primary afferents and its participation in inflammation-induced increase in capsaicin sensitivity.', *Journal of neurochemistry*, 76(6), pp. 1628–35. Available at: http://www.ncbi.nlm.nih.gov/pubmed/11259480 (Accessed: 8 March 2019).

Trakhtenberg, E. F. and Goldberg, J. L. (2012) 'Epigenetic regulation of axon and dendrite growth', *Frontiers in Molecular Neuroscience*, 5, p. 24. doi: 10.3389/fnmol.2012.00024.

Tsujino, H. *et al.* (2000) 'Activating Transcription Factor 3 (ATF3) Induction by Axotomy in Sensory and Motoneurons: A Novel Neuronal Marker of Nerve Injury', *Molecular and Cellular Neuroscience*, 15(2), pp. 170–182. doi: 10.1006/mcne.1999.0814.

Tuszynski, M. H. *et al.* (1996) 'Nerve Growth Factor Delivery by Gene Transfer Induces Differential Outgrowth of Sensory, Motor, and Noradrenergic Neurites after Adult Spinal Cord Injury', *Experimental Neurology*, 137(1), pp. 157–173. doi: 10.1006/exnr.1996.0016.

Tuszynski, M. H. and Steward, O. (2012) 'Primer Concepts and Methods for the Study of Axonal Regeneration in the CNS'. doi: 10.1016/j.neuron.2012.05.006.

Twiss, J. L. *et al.* (2000) 'Translational Control of Ribosomal Protein L4 mRNA Is Required for Rapid Neurite Regeneration', *Neurobiology of Disease*, 7(4), pp. 416–428. doi: 10.1006/nbdi.2000.0293.

Ullrich, O. *et al.* (1996) 'Rab11 regulates recycling through the pericentriolar recycling endosome.', *The Journal of cell biology*. Rockefeller University Press, 135(4), pp. 913–24. doi: 10.1083/JCB.135.4.913.

Varga, Z. M. *et al.* (1995) 'The critical period for repair of CNS of neonatal opossum (Monodelphis domestica) in

culture: correlation with development of glial cells, myelin and growth-inhibitory molecules.', *The European journal of neuroscience*, 7(10), pp. 2119–29. Available at: http://www.ncbi.nlm.nih.gov/pubmed/8542069 (Accessed: 2 March 2019).

Vaudry, D. *et al.* (2002) 'Signaling Pathways for PC12 Cell Differentiation: Making the Right Connections', *Science*, 296(5573), pp. 1648–1649. doi: 10.1126/science.1071552.

Venkatesh, I. *et al.* (2016) 'Epigenetic profiling reveals a developmental decrease in promoter accessibility during cortical maturation in vivo', *Neuroepigenetics*. Elsevier, 8, pp. 19–26. doi: 10.1016/J.NEPIG.2016.10.002.

Venkatesh, I. *et al.* (2018) 'Developmental Chromatin Restriction of Pro- Growth Gene Networks Acts as an Epigenetic Barrier to Axon Regeneration in Cortical Neurons', *Developmental Neurobiology*. John Wiley & Sons, Ltd, 78(10), pp. 960–977. doi: 10.1002/dneu.22605.

Venkatesh, I. and Blackmore, M. G. (2017) 'Selecting optimal combinations of transcription factors to promote axon regeneration: Why mechanisms matter', *Neuroscience Letters*, 652, pp. 64–73. doi: 10.1016/j.neulet.2016.12.032.

Verdú, E. *et al.* (2000) 'Influence of aging on peripheral nerve function and regeneration.', *Journal of the peripheral nervous system : JPNS*, 5(4), pp. 191–208. Available at: http://www.ncbi.nlm.nih.gov/pubmed/11151980 (Accessed: 2 March 2019).

Verma, P. *et al.* (2005) 'Axonal Protein Synthesis and Degradation Are Necessary for Efficient Growth Cone Regeneration', *Journal of Neuroscience*, 25(2), pp. 331–342. doi: 10.1523/JNEUROSCI.3073-04.2005.

Vidal-Sanz, M. *et al.* (1987) 'Axonal regeneration and synapse formation in the superior colliculus by retinal ganglion cells in the adult rat.', *The Journal of neuroscience : the official journal of the Society for Neuroscience*. Society for Neuroscience, 7(9), pp. 2894–909. doi: 10.1523/JNEUROSCI.07-09-02894.1987.

Voelker, D. R. (2009) 'Genetic and Biochemical Analysis of Non-Vesicular Lipid Traffic', *Annual Review of Biochemistry*. Annual Reviews , 78(1), pp. 827–856. doi: 10.1146/annurev.biochem.78.081307.112144.

Vogelaar, C. F. *et al.* (2009) 'Axonal mRNAs: characterisation and role in the growth and regeneration of dorsal root ganglion axons and growth cones.', *Molecular and cellular neurosciences*. Europe PMC Funders, 42(2), pp. 102–115. doi: 10.1016/j.mcn.2009.06.002.

Walsh, F. (no date) *Gene therapy first to 'halt' most common cause of blindness - BBC News*, *2019*. Available at: https://www.bbc.co.uk/news/health-47226987 (Accessed: 27 March 2019).

Wang, H. *et al.* (2012) 'Neurofilament proteins in axonal regeneration and neurodegenerative diseases.', *Neural regeneration research*. Wolters Kluwer -- Medknow Publications, 7(8), pp. 620–6. doi: 10.3969/j.issn.1673-5374.2012.08.010.

Wang, Z. *et al.* (2015) 'Overexpression of Sox11 Promotes Corticospinal Tract Regeneration after Spinal Injury While Interfering with Functional Recovery', *Journal of Neuroscience*, 35(7), pp. 3139–3145. doi: 10.1523/JNEUROSCI.2832-14.2015.

Wang, Z. *et al.* (2017) 'Combined chondroitinase and KLF7 expression reduce net retraction of sensory and CST axons from sites of spinal injury', *Neurobiology of Disease*, 99, pp. 24–35. doi: 10.1016/j.nbd.2016.12.010.

Welz, T., Wellbourne-Wood, J. and Kerkhoff, E. (2014) 'Orchestration of cell surface proteins by Rab11', *Trends in Cell Biology*. Elsevier Current Trends, 24(7), pp. 407–415. doi: 10.1016/J.TCB.2014.02.004.

Weng, Y.-L. *et al.* (2017) 'An Intrinsic Epigenetic Barrier for Functional Axon Regeneration', *Neuron*, 94(2), p. 337–346.e6. doi: 10.1016/j.neuron.2017.03.034.

Werner, A. *et al.* (2000) 'Impaired axonal regeneration in alpha7 integrin-deficient mice.', *The Journal of*

neuroscience : the official journal of the Society for Neuroscience, 20(5), pp. 1822–30. Available at: http://www.ncbi.nlm.nih.gov/pubmed/10684883 (Accessed: 19 March 2019).

Whalley, K. *et al.* (2009) 'Changes in progenitor populations and ongoing neurogenesis in the regenerating chick spinal cord', *Developmental Biology*, 332(2), pp. 234–245. doi: 10.1016/j.ydbio.2009.05.569.

What is spinal cord injury? | Spinal Research (no date). Available at: https://www.spinal-research.org/injury/what-spinal-cord-injury (Accessed: 28 February 2019).

Willis, D. E. *et al.* (2007) 'Extracellular stimuli specifically regulate localized levels of individual neuronal mRNAs.', *The Journal of cell biology*. The Rockefeller University Press, 178(6), pp. 965–80. doi: 10.1083/jcb.200703209.

Witte, H., Neukirchen, D. and Bradke, F. (2008) 'Microtubule stabilization specifies initial neuronal polarization', *J Cell Biol*. Rockefeller University Press, 180(3), pp. 619–632. doi: 10.1083/JCB.200707042.

Wong, W.-K. *et al.* (2014) 'Hepatocyte Growth Factor Promotes Long-Term Survival and Axonal Regeneration of Retinal Ganglion Cells after Optic Nerve Injury: Comparison with CNTF and BDNF', *CNS Neuroscience & Therapeutics*, 20(10), pp. 916–929. doi: 10.1111/cns.12304.

Wrigley, S., Arafa, D. and Tropea, D. (2017) 'Insulin-Like Growth Factor 1: At the Crossroads of Brain Development and Aging.', *Frontiers in cellular neuroscience*. Frontiers Media SA, 11, p. 14. doi: 10.3389/fncel.2017.00014.

Wu, Z. *et al.* (2007) 'Caenorhabditis elegans neuronal regeneration is influenced by life stage, ephrin signaling, and synaptic branching', *Proceedings of the National Academy of Sciences*, 104(38), pp. 15132–15137. doi: 10.1073/pnas.0707001104.

Xing, L. and Bassell, G. J. (2013) 'mRNA Localization: An Orchestration of Assembly, Traffic and Synthesis', *Traffic*. John Wiley & Sons, Ltd (10.1111), 14(1), pp. 2–14. doi: 10.1111/tra.12004.

Xue, K. *et al.* (2018) 'Beneficial effects on vision in patients undergoing retinal gene therapy for choroideremia', *Nature Medicine*. Nature Publishing Group, 24(10), pp. 1507–1512. doi: 10.1038/s41591-018-0185-5.

Yalçın, B. *et al.* (2017) 'Modeling of axonal endoplasmic reticulum network by spastic paraplegia proteins', *eLife*, 6. doi: 10.7554/eLife.23882.

Yang, Y. *et al.* (2007) 'betaIV spectrin is recruited to axon initial segments and nodes of Ranvier by ankyrinG.', *The Journal of cell biology*. The Rockefeller University Press, 176(4), pp. 509–19. doi: 10.1083/jcb.200610128.

Yao, F. *et al.* (2018) 'Did you choose appropriate tracer for retrograde tracing of retinal ganglion cells? The differences between cholera toxin subunit B and Fluorogold', *PLOS ONE*. Edited by A. S. Lewin. Public Library of Science, 13(10), p. e0205133. doi: 10.1371/journal.pone.0205133.

Yau, K. W. *et al.* (2016) 'Dendrites In Vitro and In Vivo Contain Microtubules of Opposite Polarity and Axon Formation Correlates with Uniform Plus-End-Out Microtubule Orientation', *Journal of Neuroscience*. Society for Neuroscience, 36(4), pp. 1071–1085. doi: 10.1523/JNEUROSCI.2430-15.2016.

Yiu, G. and He, Z. (2006) 'Glial inhibition of CNS axon regeneration.', *Nature reviews. Neuroscience*. NIH Public Access, 7(8), pp. 617–27. doi: 10.1038/nrn1956.

York, R. D. *et al.* (1998) 'Rap1 mediates sustained MAP kinase activation induced by nerve growth factor', *Nature*, 392(6676), pp. 622–626. doi: 10.1038/33451.

Zhang, C. *et al.* (2012) 'Role of spastin and protrudin in neurite outgrowth', *Journal of Cellular Biochemistry*, 113(7), pp. 2296–2307. doi: 10.1002/jcb.24100.

Zhang, C. *et al.* (2017) 'Fatty acid synthase cooperates with protrudin to facilitate membrane outgrowth of cellular protrusions', *Scientific Reports*. Nature Publishing Group, 7(1), p. 46569. doi: 10.1038/srep46569.

Zhang, J. Y. *et al.* (2000) 'Endogenous BDNF is required for myelination and regeneration of injured sciatic nerve in rodents.', *The European journal of neuroscience*, 12(12), pp. 4171–80. Available at: http://www.ncbi.nlm.nih.gov/pubmed/11122329 (Accessed: 1 March 2019).

Zhao, R.-R. *et al.* (2013) 'Combination treatment with anti-Nogo-A and chondroitinase ABC is more effective than single treatments at enhancing functional recovery after spinal cord injury', *European Journal of Neuroscience*. John Wiley & Sons, Ltd (10.1111), 38(6), p. n/a-n/a. doi: 10.1111/ejn.12276.

Zheng, J. Q. *et al.* (2001) 'A functional role for intra-axonal protein synthesis during axonal regeneration from adult sensory neurons.', *The Journal of neuroscience : the official journal of the Society for Neuroscience*, 21(23), pp. 9291–303. Available at: http://www.ncbi.nlm.nih.gov/pubmed/11717363 (Accessed: 7 March 2019).

Zhou, B. *et al.* (2016) 'Facilitation of axon regeneration by enhancing mitochondrial transport and rescuing energy deficits', *The Journal of Cell Biology*, 214(1), pp. 103–119. doi: 10.1083/jcb.201605101.

Zivraj, K. H. *et al.* (2010) 'Subcellular Profiling Reveals Distinct and Developmentally Regulated Repertoire of Growth Cone mRNAs', *Journal of Neuroscience*, 30(46), pp. 15464–15478. doi: 10.1523/JNEUROSCI.1800-10.2010.

Zörner, B. and Schwab, M. E. (2010) 'Anti-Nogo on the go: from animal models to a clinical trial', *Annals of the New York Academy of Sciences*. John Wiley & Sons, Ltd (10.1111), 1198, pp. E22–E34. doi: 10.1111/j.1749-6632.2010.05566.x.

Zou, H. *et al.* (2009) 'Axotomy-Induced Smad1 Activation Promotes Axonal Growth in Adult Sensory Neurons', *Journal of Neuroscience*, 29(22), pp. 7116–7123. doi: 10.1523/JNEUROSCI.5397-08.2009.